Central
Coast
Watershed
Studies

CCoWS

San Clemente Dam Removal Sediment Impacts: Year One Report

Publication No. WI-2016-10
27 September 2016

CSUMB Class ENVS 660 Fall 2016:

Kaitlyn Chow
Julia Fields
Steve Flores
Kristen Hart
Alana Kleven
Lauren Luna
Leah MacCarter
Doug Smith Ph.D. (Instructor)

The Watershed Institute

School of Natural Sciences
California State University
Monterey Bay
http://watershed.csumb.edu

100 Campus Center, Seaside, CA, 93955-8001
831 582 4696 / 4431

Contact:
dosmith@csumb.edu

Acknowledgements

We are grateful for the assistance of:

- Granite Construction (Wayne Bounds, Michael Barnhart, Bill McGowan, David Hamblin)
- Monterey Peninsula Water Management District (Greg James, Larry Hampson, Beverly Chaney, Jonathan Lear)
- NOAA Southwest Fisheries Science Center (Lee Harrison)
- USGS (Amy East, Joshua Logan)
- California American Water Company

This report primarily represents graduate student work completed within the constraints of a fixed-duration (five-week), limited-verification college class setting.

This report may be cited as:
CSUMB Class ENVS 660: Chow K, Fields J, Flores S, Hart K, Kleven A, Luna L, MacCarter L, and Smith D. 2016. San Clemente Dam Removal Sediment Impacts: Year One Report. Watershed Institute, California State University Monterey Bay, Publication No. WI-2016-10, 38 pp.

Executive Summary

This study was conducted as part of a class project by students in the Advanced Watershed Science and Policy (ENVS 660) course at California State University at Monterey Bay (CSUMB).

Many dams in the United States have outlived their designed lifespan and are no longer serving intended purposes of water storage, energy production, and flood control. Dam removal is one economically viable option for these ineffectual dams. However, resultant changes in flow intensity and sediment transport may severely affect lower reaches including damage to endangered fish species spawning grounds and degradation of water quality.

The San Clemente Dam was removed in 2015 after 94 years of impairment to natural fluvial processes on the Carmel River in Monterey County, California. We identified possible sources of sediment and estimated the total volume that accumulated downstream of the former dam. We quantified ten substantial sediment deposits by measuring spatially referenced deposit thickness with an iron rod, pocket rod, tape and pocket transit. ArcGIS was used to interpolate deposit thickness from field measurements; the interpolated thickness grid was used to determine the volume of each deposit. We estimated the dimensions and volumes of smaller deposits in the field using a meter tape and pocket rod. Sediment samples were collected from most deposits to analyze grain size distribution and shape.

We estimated approximately 4,560 cubic meters (5,900 cubic yards) of sediment were deposited in the Carmel River along 3.5 km of channel immediately below the former San Clemente Dam during the 2016 water year. The largest deposits occurred in low-gradient reaches and pools. The sediment wave tapered at the upstream and downstream ends creating an overall bell shape. Deposit particle size was highly variable spatially.

Potential sources of sediment included the Carmel Watershed above the Carmel River Reroute and Dam Removal (CRRDR) project site, the San Clemente Creek Watershed, erosion within the CRRDR, as well as colluvial processes and construction activities downstream of the former SCD. Sediment input downstream of the CRRDR appeared minimal while the contribution of the upstream sources and the CRRDR site itself could potentially contribute more than a thousand cubic meters of sediment each.

Our results serve as a baseline for evaluating the impact of the 2016 Soberanes Fire to the Carmel Watershed which could release the same magnitude of sediment as the 2016 winter.

Table of Contents

1 Introduction

1.1 Background

Dams impede natural fluvial processes of rivers both upstream and downstream of an impoundment. Built for water storage, energy, and flood control, dams have supported the growth of numerous cities worldwide. In the United States, accelerated dam construction in the twentieth century led to an inventory of roughly 79,000 dams, as listed by the US Army Corps of Engineers (FEMA 2009). Dams are now exceeding their designed lifespan, becoming less economically viable and, in some cases, detrimental to surrounding riverine ecosystems through alteration of natural flow regimes and native species habitat (Poff and Hart 2002). To mitigate these effects, resource managers plan and carry out dam removal projects.

Dam removal can have both positive and negative effects downstream by modification of flow intensity and increased sediment supply (Pizzuto 2002). Redistribution of sediment following dam removal could be favorable to aquatic species by increasing variation in grain size. On the other hand, previous studies on dam removal note an immediate negative side effect is the large downstream sediment influx following the disturbance (Bednarek 2001). Fine sediment biologically impairs rivers; in particular, they influence fish migration, food source and reproduction (Berkman and Rabeni 1987, Everest *et al.* 1987, Suttle *et al.* 2004). However, these problems are typically short-lived, as rivers eventually flush out accumulated sediment (Higgs 2002).

Many studies discuss sedimentation and sediment transport from dam removal by case studies or modelling, but have no empirical data to verify consequential impacts (Doyle *et al.* 2000, Bednarek 2001, Higgs 2002, Cui and Wilcox 2008). In this report, we quantify the accumulation of sediment downstream of a major dam removal project using field observations.

1.2 Study Area: Carmel Watershed

This study took place in the reach below the former San Clemente Dam (SCD) on the Carmel River in Monterey County, California (Fig. 1). The Carmel River is 57.9 kilometers (36 miles) long and the watershed encompasses 660 square kilometers (255 square miles). Various agencies and organization monitor and manage the watershed intensively since it is a key freshwater resource to the Monterey Peninsula.

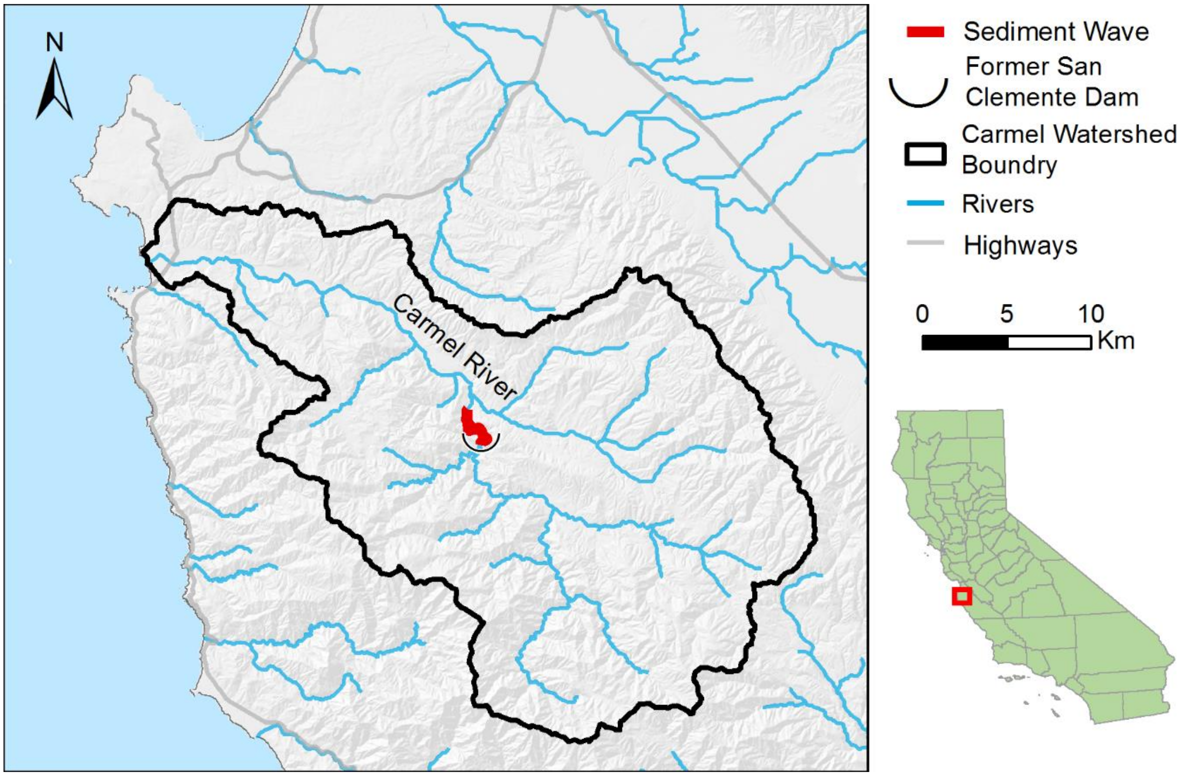

Figure 1. Location of the former San Clemente Dam and sediment impact area in the Carmel Watershed, Monterey County, CA.

1.3 Regional Geology

Active faults continuously fracture bedrock, controlling the geomorphology of the watershed (Fig. 2). Ongoing uplift of the Santa Lucia and Sierra de Salinas Ranges led to "v"-shaped canyons in the headwaters, contributing to high sediment transport rates (Smith *et al*. 2004). High transport rates generate enough gravel, sand, and silt to maintain the floodplains of the Carmel River (Rosenberg 2001). Fractured granitic rocks from the upper Carmel Watershed supply a significant source of bedload, which provides vertical channel stability. Construction of the SCD in 1921 eliminated transport of bedload downstream. Any substantial increase or decrease in bedload could cause channel morphology to change, including downcutting and development of coarse boulder armor downstream, and could reduce overall habitat quality (Dettman 1989, Kondolf and Curry 1986).

Sediment transport is inconsistent year-to-year in the Carmel River because flow depends on highly variable precipitation (Fig. 3). Precipitation in the Carmel Watershed ranges from 14 inches near the mouth of the Carmel River to 41 inches in the upper tributaries of the watershed (Rosenberg 2001). In the 2016 water year, the highest peak flow occurred in March at 1,110 cfs with a recurrence interval of 2.4 years (Tetra Tech 2016). During low to normal flow years, sediment is retained until high-flow events wash it downstream (Smith *et al.* 2004). Sediment yield can be especially high during strong El Niño winters and after intense fires. The winter of 1982 provides a good example of a very rainy wet season: 1.9 million tons of sediment were mobilized in the Carmel River, including 418,000 tons of bedload (Krebs 1983).

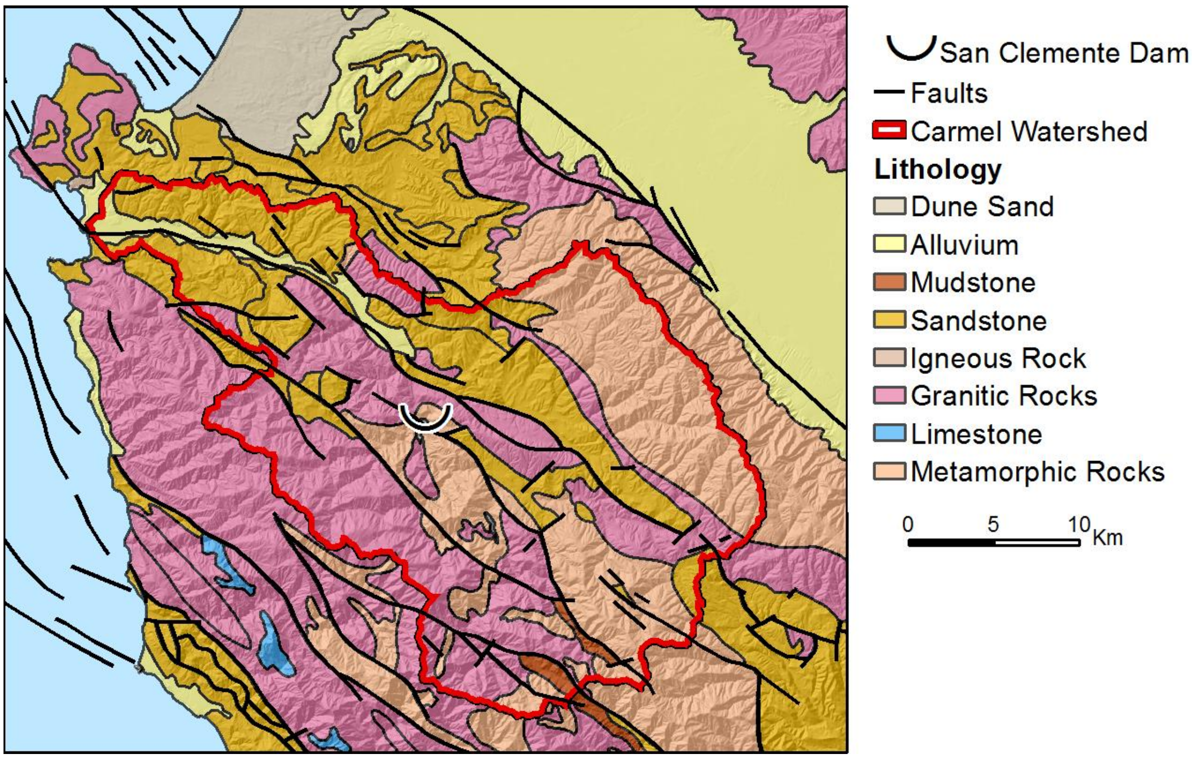

Figure 2. Carmel Watershed geologic map including dominant rock types and faults near the former San Clemente Dam in the Carmel Watershed (geologic data from Jennings *et al.* 1977).

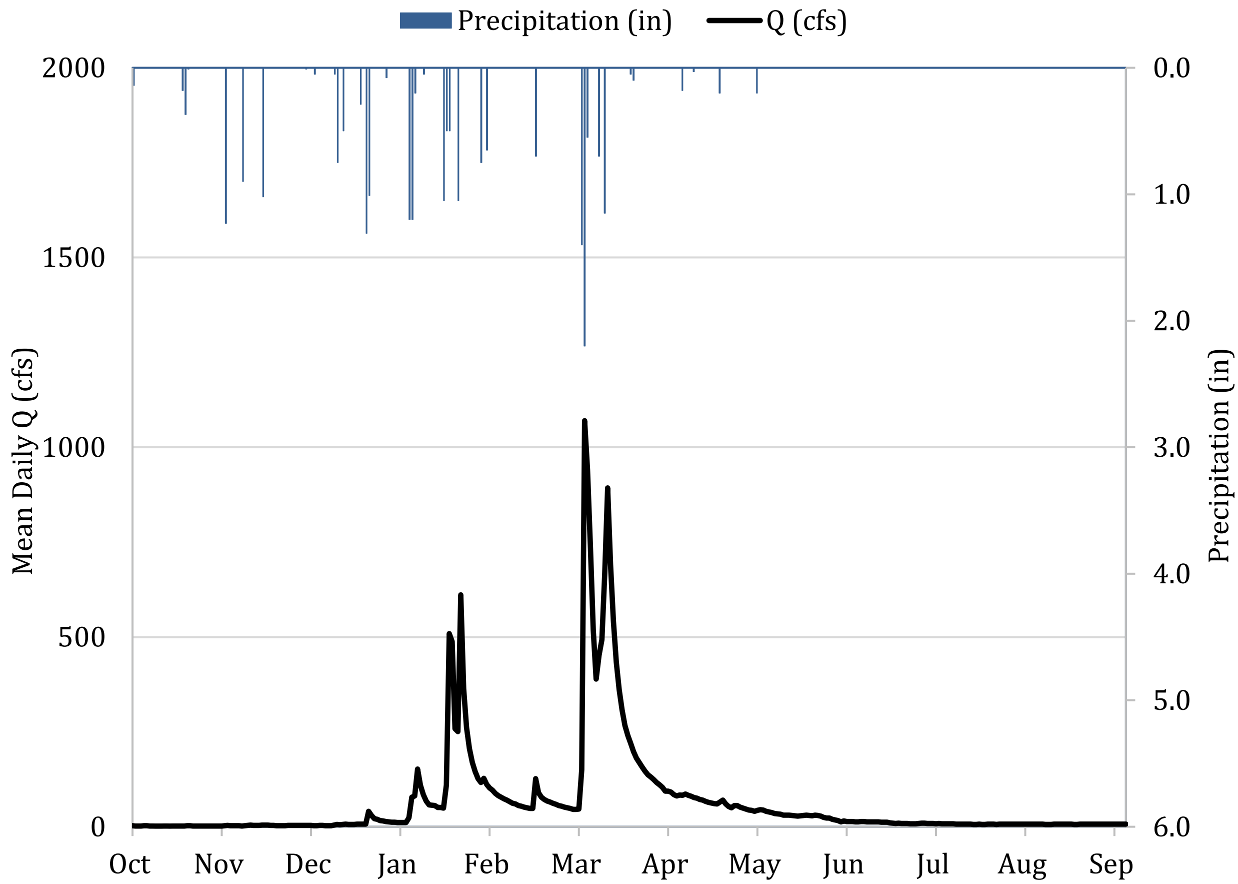

Figure 3. Water year 2016 mean daily flow from Monterey Peninsula Water Management District's Sleepy Hollow gauge and Granite Construction's daily precipitation gauge downstream of the former San Clemente Dam.

1.4 Fire History

Wildfires have played an integral role in Carmel Watershed history. Pre-1990 fire frequency was once every 21 years in the upper Carmel Watershed (Mathews 1989). Intensity of wildfires in California is projected to increase as temperatures rise and drought persists (Westerling *et al.* 2006). Wildfires act as catalysts for surface erosion and sediment transport on burned landscapes. Areas of intense burning are susceptible to landslides and debris flows during post-fire rain events.

Two historic fires in Monterey County show variability in fire-related sediment yield: the Marble Cone Fire (1977) and Basin Complex Fire (2008). The Basin Complex Fire had virtually no sediment impacts (Richmond 2009), but intense rains following the Marble

Cone Fire caused a sediment wave to move through the Carmel River (Hecht 1981). Habitats affected by the increase in sediment recovered after three years (Hecht 1981).

The Basin Complex Fire burned approximately 28,664 acres of the upper Carmel Watershed, of which 13,700 acres were considered moderate to high burn severity (Smith *et al.* 2009) and were at high risk of generating significant debris flows, but they did not materialize because the following winter did not produce any intense rain events (Kelly 2012).

The Soberanes Fire was first reported on July 22, 2016. The fire was started by an unattended campfire on Soberanes Canyon Trail in Garrapata State Park. The fire approached the upper Carmel Watershed on August 5, 2016 (Fig. 4). The Soberanes Fire continues to burn actively as of September 23, 2016. The fire has consumed approximately 121,000 acres to date, including 2,085 acres in the upper Carmel Watershed (USDA-FS 2016).

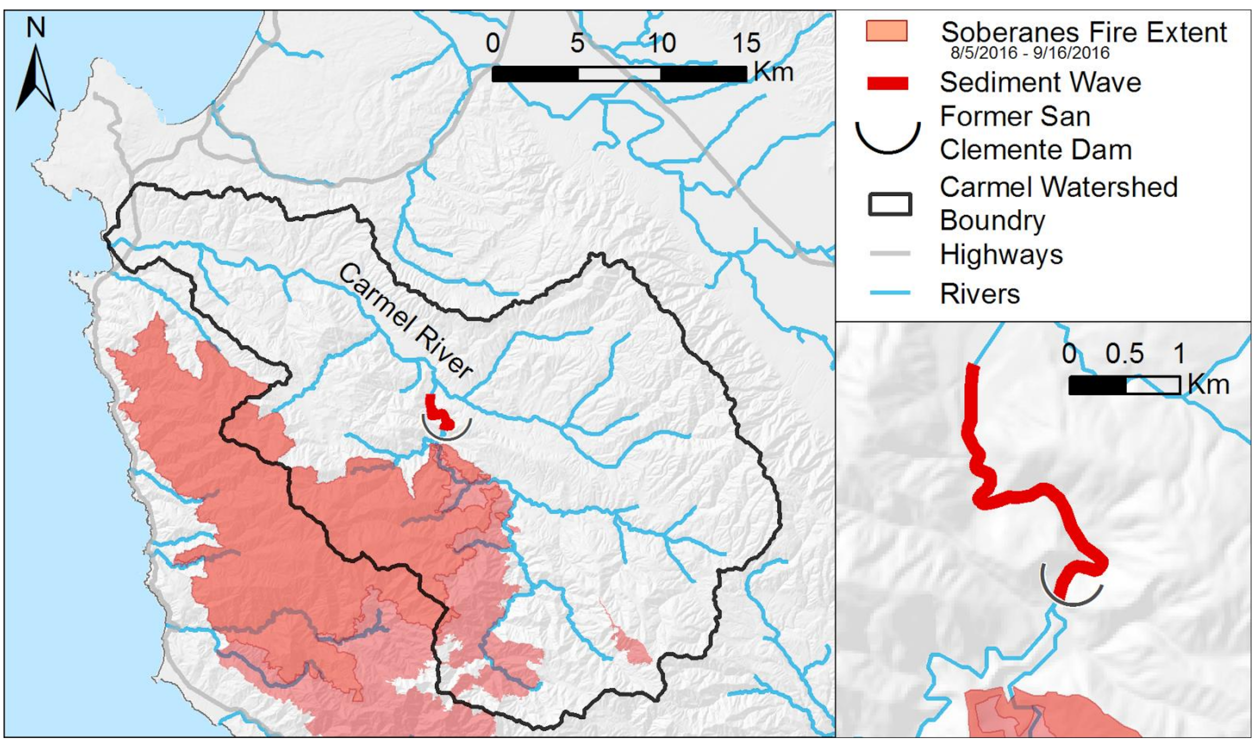

Figure 4. Extent of the Soberanes Fire in Carmel Watershed when it approached the San Clemente Dam Removal site on 8/5/16, and 9/16/2016 (data provided by the U.S. Forest Service).

1.5 San Clemente Dam Removal

The SCD impacted the flows, habitats, and geomorphology of the Carmel River from 1921to 2015 (Boughton *et al.* 2016). The dam rose 106 feet from the river floor and had an initial water capacity of 1,425 acre-feet. The combination of highly erodible bedrock in the upper watershed and a history of high-intensity fires led to a build-up of over 2.5 million cubic yards of sediment behind the dam, reducing reservoir capacity by 95% prior to its removal (EIR 2008).

The Carmel River Reroute and San Clemente Dam Removal Project (CRRDR) in 2011 included rerouting the river through San Clemente Creek and stabilizing the accumulated sediment in the older channel (EIR 2008). The CRRDR is the first project to attempt to stabilize the stockpile of sediment, rather than destroying the dam and allowing the sediment to move downstream. Stabilizing the sediment decreased possible downstream impacts (EIR 2008).

The Carmel River reroute channel design is divided into three general reaches (Fig. 5). The Upper Carmel Reach, located upstream of the reservoir, is a 960-foot long section of the river excavated through relatively unconsolidated sediments. Downstream of the Upper Carmel Reach, the Reroute Reach cut through a mountain ridge previously separating the Carmel River from the San Clemente Creek. The Reroute Reach connected the Upper Carmel Reach to the Combined Flow Reach, a junction where flows from the upper Carmel River merged with the San Clemente Creek and flowed to the main channel below the former SCD site (Tetra Tech 2016).

Planners selected the CRRDR design because it would protect downstream residence from the seismically unsafe SCD, allow unimpaired steelhead migration, provide riparian habitat for native species, restore the natural sediment flow of the Carmel River, and replenish beach erosion. The other alternatives included no action, dam notching, and dam strengthening. While the long-term positive results of dam removal might take time to achieve, the anticipated short-term impacts of the CRRDR included degradation to the downstream habitat, reduction in water quality, increased traffic around the construction site, increased sedimentation, and higher flooding frequency (EIR 2008). We evaluated the downstream sediment impacts on the Carmel River following the first post-dam runoff events of the 2016 water year.

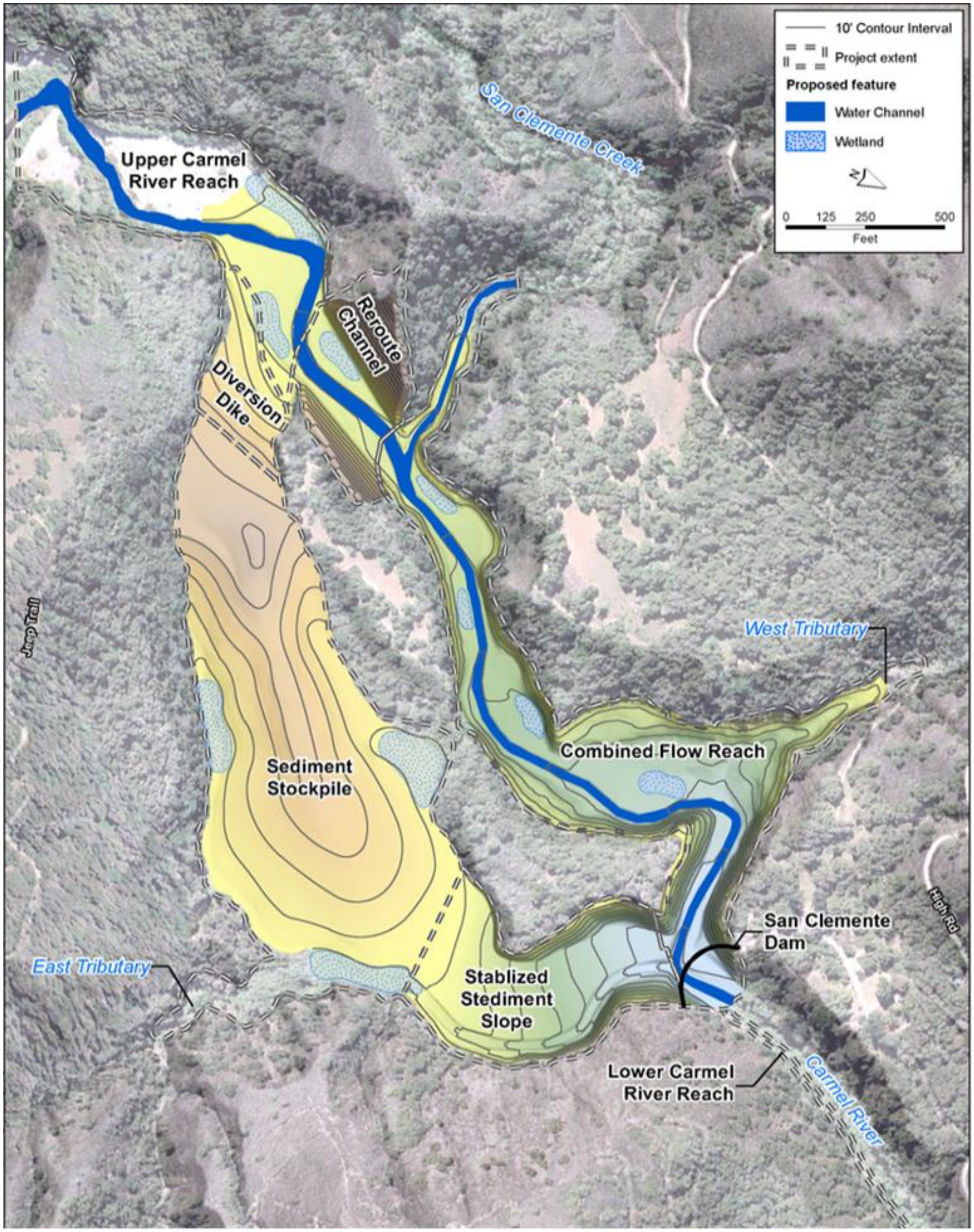

Figure 5. Map of the Carmel River Dam Removal and Reroute Project shows the Upper Carmel Reach, Reroute Reach, and Combined Flow Reach (URS 2012).

1.6 Project Goals

The purpose of this study was to quantify total volume and grain size parameters of sediment accumulated downstream from the former SCD, identify possible sources of sediment, and provide a timeline for any post-dam impacts we found. This study provides a baseline of in-channel sediment storage in advance of potential Soberanes Fire impacts.

2 Methods

2.1 Sediment Volume Quantification

2.1.1 Data Collection

We evaluated sediment located directly downstream of the former SCD that was deposited in water year 2016, the first runoff season immediately following dam removal. During reconnaissance work, we recorded locations of sediment deposits with a handheld GPS, and qualitatively described the deposit size and grain size. Sediment deposit volumes of less 20 m^3 were estimated by measuring the length and width with a tape measure and approximating the thickness with a pocket rod. We determined the full extent of the sediment wave by noting the point at which deeper, low gradient reaches of channel (pools and runs) were no longer storing post-dam removal sand and gravel. Post-dam sediment deposited in water year 2016 was easily identified because the pre-dam removal Carmel River channel along the same reach was armored with large cobble and boulders.

We quantified ten substantial sediment deposits by taking thickness measurements with a calibrated iron rod driven vertically into the deposit. The rod was hammered into the deposit until a change in resistance indicated the top of the pre-existing boulder substrate. We determined thickness measurement positions by recording polar coordinates from an arbitrary center point in each sediment deposit. Polar coordinates for each thickness measurement and boundary point were determined with a Brunton pocket transit and meter tape. We took thickness measurements at sporadic positions along the tape in a radial pattern until there were enough points to accurately model the volume of the deposit. We recorded an average of 58 thickness measurements for each deposit. We converted polar coordinates for each measurement to Cartesian coordinates through the following equation:

$$E = d \times \sin(\theta)$$

$$N = d \times \cos(\theta)$$

where d is the distance from an arbitrary center point in meters, θ is the compass bearing (true north) in degrees, E is easting, and N is northing. We used precise local positions for modeling volume. We shifted the local coordinates to approximate NAD83 UTM meters for general mapping illustration in ArcGIS.

One large deposit (Deposit 7) was in a construction zone; therefore, we were unable to quantify the sediment volume using the above methods. Instead, we obtained cross-sectional elevation data from the Monterey Peninsula Water Management District. Northwest Hydraulic Consultants surveyed the cross sections for the Federal Emergency Management Agency (FEMA) in 2006. Three cross sections from the data set had been surveyed at Deposit 7, located at the former Old Carmel River dam. Dr. Lee Harrison (NOAA) visually estimated that the sediment deposit at this site was one meter thick on average (personal communication). We calculated the cross-sectional area of the three cross sections at an average depth of one meter and multiplied the average area by the estimated length of the deposit (30 m) to derive an approximate volume of the sediment deposit.

2.1.2 Data Analysis

Thickness data for each pool were imported and interpolated in ArcGIS using the kriging spatial analyst tool. Kriging is a multistep process including exploratory statistical analysis, variogram modeling, and surface creation. The tool fits a mathematical function to nearby data points at each location to determine cell values. We used a field sketch and boundary points from the field survey to create a mask denoting the perimeter of the sediment deposit, which defined the analysis area. Rasters of each deposit were interpolated using ordinary kriging with a gaussian semivariogram model, default search radius settings, and a spatial resolution of one meter. To calculate volume, we created a constant raster with a thickness of zero, and used the cut and fit tool to calculate net volume between two surfaces.

2.2 Sediment Grain Size Analysis

2.2.1 Sample Collection and Processing

We collected representative samples of both large and smaller deposits. Smaller deposits were sampled at the tail end of the sediment wave. Samples included at least one estimate of fill material and one estimate of pavement, if present. Samples were oven-dried for 24 hours and then poured through a stack of nine brass sieves with a range of mesh sizes to develop grain size percentiles. The largest mesh (37.5 mm) was selected to be slightly smaller than that largest particles present in the samples. The smallest sieve (2 mm) was selected for sand and finer particles to be weighed as one grain size category. We shook the copper stack for 30 seconds to encourage particles to pass through the smallest possible perforation. The base pan collected particles smaller than 2 mm. Each sieve was weighed before (empty) and after (with collected sediment) to calculate a difference in mass. We then calculated the grain size percentiles of each sample, including the D50.

2.2.2 Data Analysis

Grain size percentiles for each deposit that included gravel were determined using Microsoft Excel and R Statistical package (R Core Team 2015). We generated histograms for each deposit to visually analyze grain size as a function of distance from the former SCD.

For sand only samples, we qualitatively described the overall sand size category and typical grain shape (angular or rounded) using a grain size comparator. We recorded the most common grain size and shape for each sample.

3 Results

3.1 Sediment Volume

Approximately 4,560 cubic meters (5,900 cubic yards) of sediment were deposited downstream of the former SCD (Fig. 6, Table 1). Very small deposits were found throughout the 3.5 km impact extent, but were not estimated due to their relatively low contribution to the overall sediment wave. The average gradient of the Carmel River underlying the sand wave was 1.7%; the gradient for the first 900 m below the former SCD was 4.4% and the rest of the reach was 0.7% (Fig. 7). The largest deposits occurred in reaches with both low gradient and large sediment accommodation space (pools and runs). Riffles were universally free of new deposits, except for sporadic thin patches of floodplain-mantling sand. Generally, a bell-shaped trend of deposit volume occurred with increased distance from the former SCD (Fig. 6). The largest deposits were in the first substantial pool downstream of the restoration site (Deposit 7) and upstream of the Sleepy Hollow ford (Deposit 16), and consisted of 21% and 34% of the total volume respectively (Fig. 7).

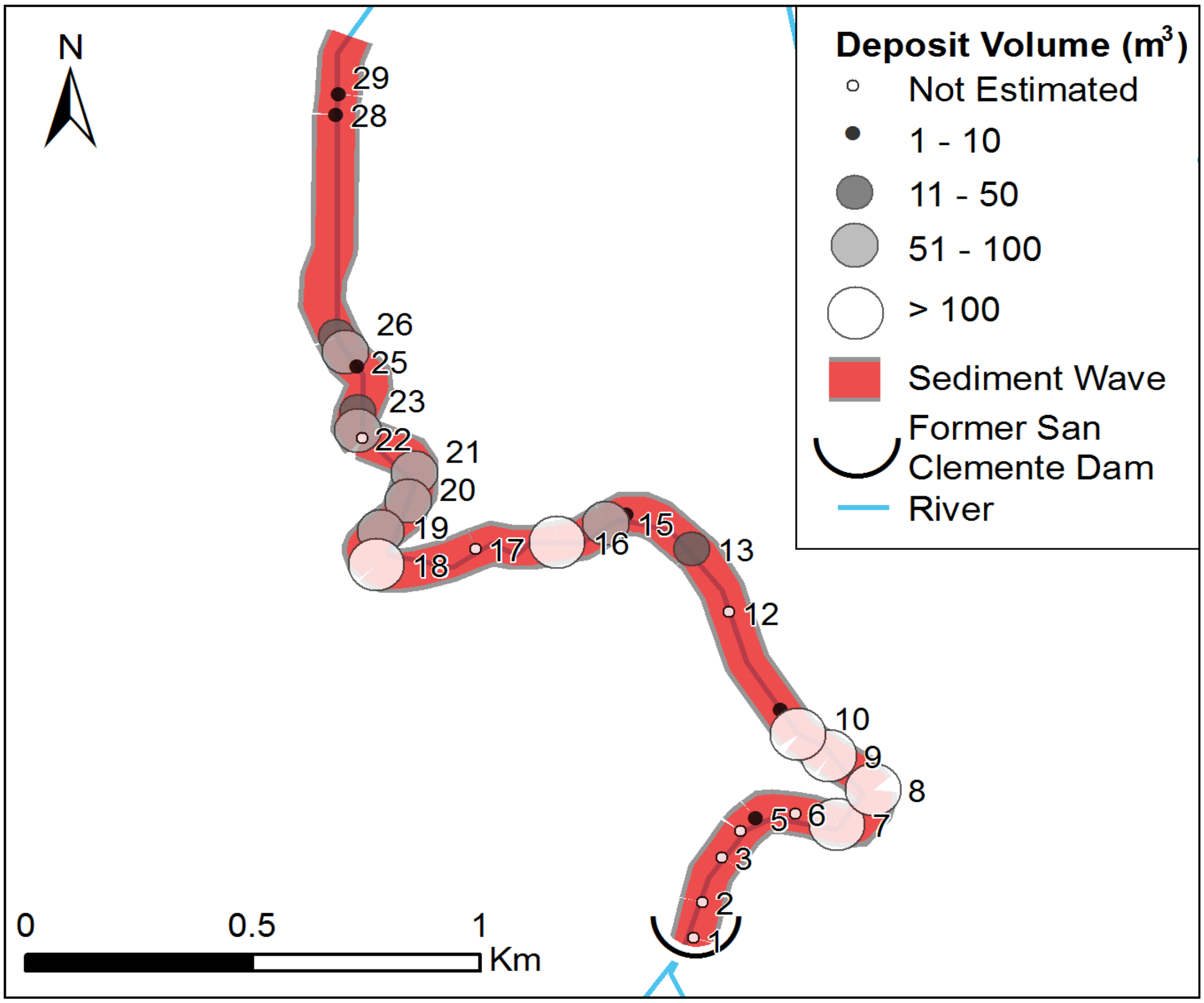

Figure 6. Sediment deposit extent, location, and volume downstream of the former San Clemente Dam.

Table 1. Sediment deposit summary downstream from the former San Clemente Dam including Deposit ID number, distance from the former SCD, approximate area, approximate volume, mean thickness, percentage of the entire deposit, and approximate UTM coordinates. An asterisk (*) next to the volume indicates a volume estimate rather than modeled volume. A dash (---) indicates the deposit volume was small and not estimated.

Deposit #	Distance from Dam (km)	Area (m^2)	Volume (m^3)	Avg Thickness (m)	Percentage	E	N
1	0.02	---	---			615764	4033129
2	0.11	---	---			615785	4033213
3	0.22	---	---			615827	4033318
4	0.30	---	---			615868	4033381
5	0.34	18	10 *	0.6	0.2%	615900	4033411
6	0.44	---	---			615989	4033421
7	0.53	970	970	1.0	21.3%	616081	4033396
8	0.67	357	140	0.4	3.1%	616159	4033478
9	0.79	324	190	1.0	4.2%	616063	4033559
10	0.88	663	400	0.6	8.8%	615995	4033609
11	0.95	---	< 3 *		0.0%	615956	4033667
12	1.21	---	---			615843	4033896
13	1.38	42	11 *	0.3	0.2%	615760	4034046
14	1.55	---	1 *		0.0%	615616	4034127
15	1.60	217	85	0.4	1.9%	615572	4034104
16	1.72	1,916	1570	0.7	34.4%	615466	4034060
17	1.90	---	---			615286	4034045
18	2.13	670	740	1.1	16.2%	615068	4034008
19	2.23	200	90	0.5	2.0%	615077	4034087
20	2.33	274	85	0.8	1.9%	615137	4034158
21	2.40	134	110	0.8	2.4%	615152	4034223
22	2.55	---	---			615037	4034307
23	2.57	148	80	0.5	1.8%	615026	4034323
24	2.62	27	11 *	0.4	0.2%	615026	4034368
25	2.75	---	15 *		0.3%	615024	4034475
26	2.79	---	20 *		0.4%	614999	4034509
27	2.83	150	30 *	0.2	0.7%	614981	4034546
28	3.36	0.5	0.25 *	0.5	0.0%	614979	4035067
29	3.41	0.5	0.08 *	0.2	0.0%	614984	4035117
Total		**6,111**	**4,560**		**100%**		

3.2 Grain Size

Grain size was spatially variable (Fig. 7, Fig. 8). There was channel pavement at four of the upstream deposits including Deposits 16 and 18. The sample with the largest median grain size (d_{50} = 16 mm) was from a volumetrically smaller deposit (Deposit 5), located closest to the former SCD (Fig. 7). The downstream tail of the sediment wave comprised five ancillary sand deposits (Fig. 8). The farthest downstream deposit was 0.5 m wide, 1 m long and 0.15 m thick.

Sand particles were angular due to being first cycle sediment derived directly from granitic and metamorphic sources. Pebble-sized particles were mostly granitic and metamorphic, with a small percent derived from the Tertiary Monterey Formation. The five most downstream sediment samples consisted of gravel-free sand (Fig. 8).

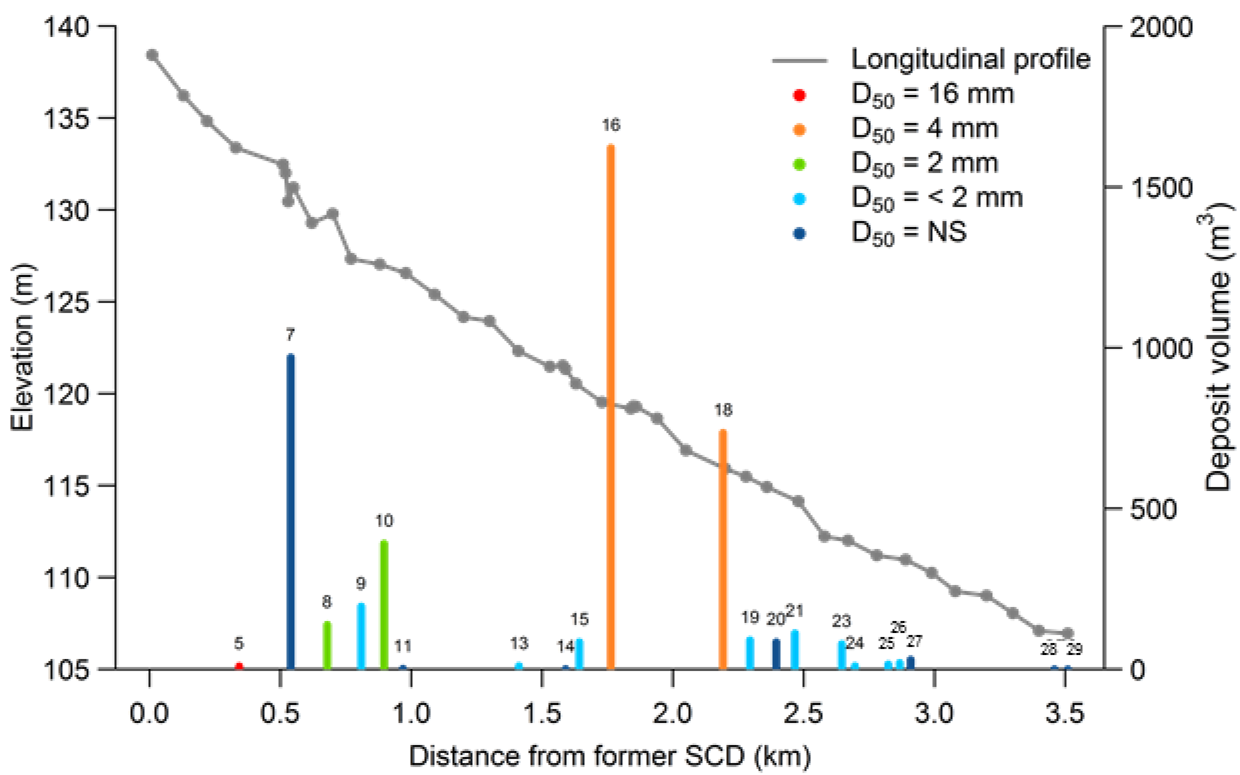

Figure 7. Longitudinal profile of the study area on the Carmel River, CA, derived from FEMA cross sections (2006), including location, volume, and D_{50} for significant sediment deposits; NS indicates that the deposits were not sampled for sediment size.

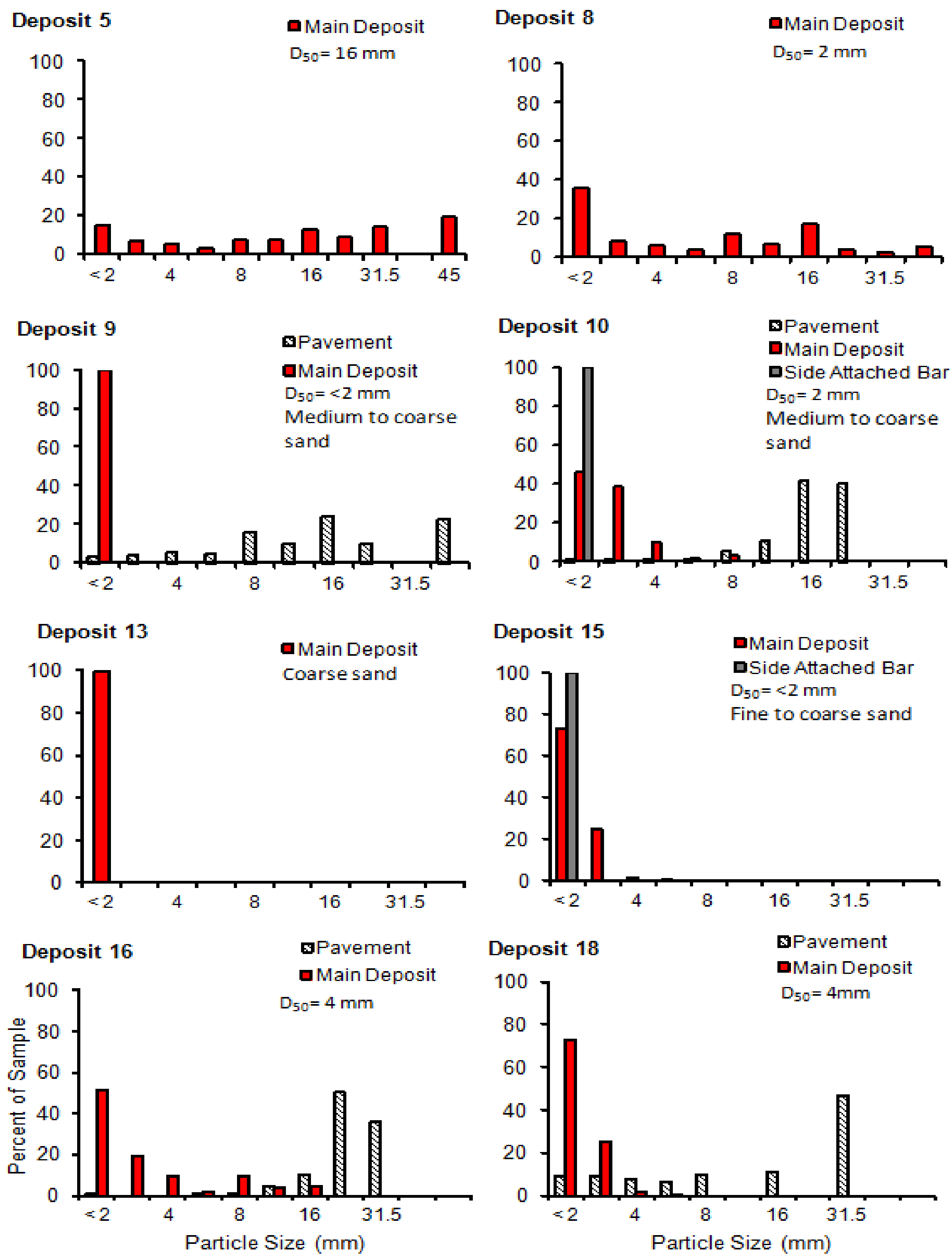

Figure 8. Particle size distribution histograms and sample descriptions for sampled deposits, continued on next page.

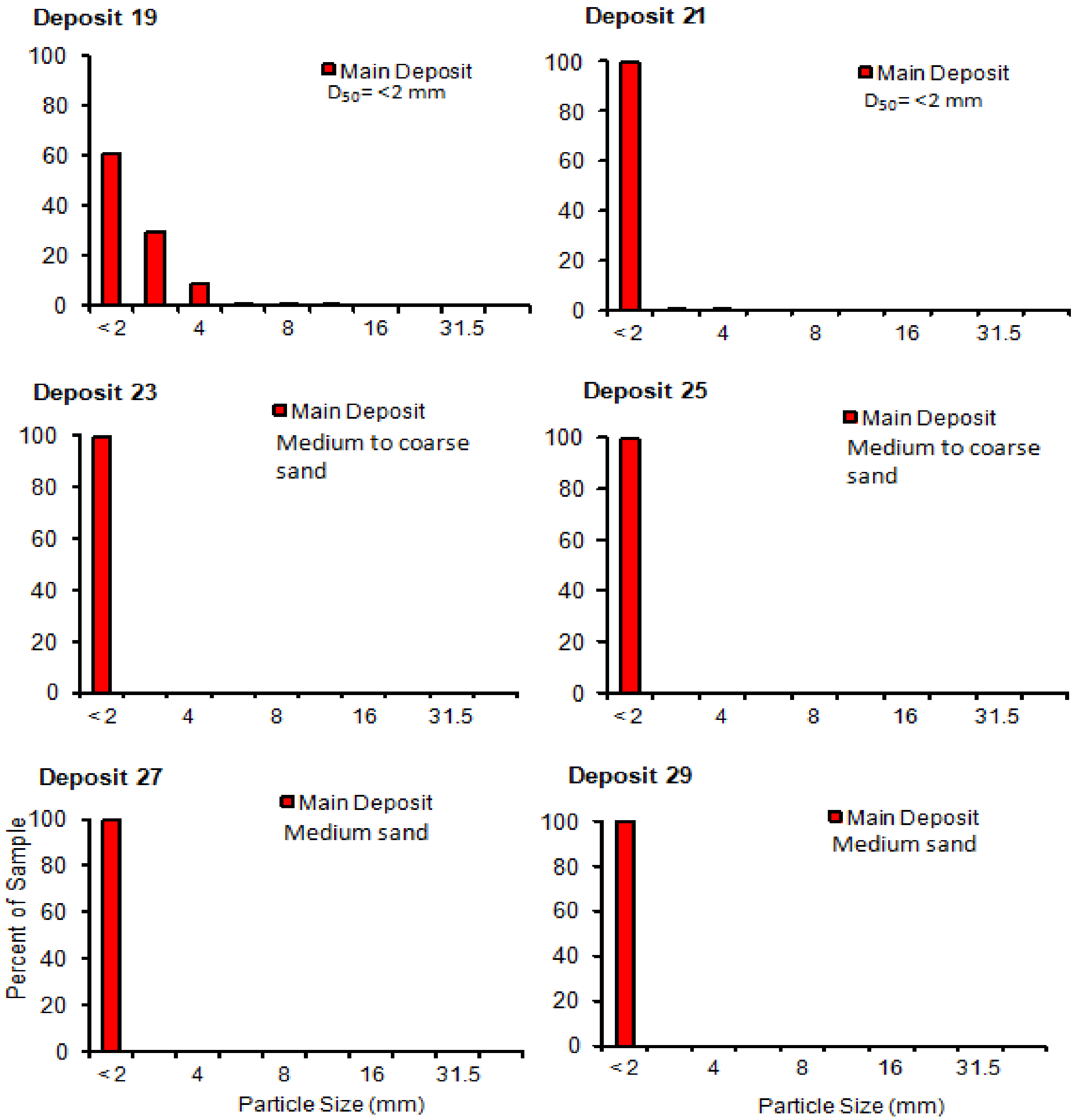

Figure 8 (continued). Particle size distribution histograms and sample descriptions for sampled deposits.

4 Discussion

We attempted to quantify post-dam-removal sediment impacts and provide pre-fire baseline conditions for future studies. A 3.5 km-long, 4,560 m^3 sand and gravel sediment wave was deposited in lower gradient reaches below the former SCD. The deposit is discontinuous with long reaches of steeper, sediment-free channel separating both minor and major sediment deposits. The wave tapers at both upstream and downstream ends, and gradually diminishes in grain size and volume within the downstream tail. Deposits farther downstream from the former SCD dwindled in size and filled gaps between large cobbles, but did not completely cover pre-existing substrate. Our volume estimate is almost certainly an underestimate, given that we did not measure 8 small mapped deposits that we estimate did not exceed 4 m^3 each (80 m^3 total volume), and discontinuous, thin sandy floodplain deposits that were not estimated.

The sediment wave progressed past the former SCD during the largest flow events occurring in January and March 2016, when the highest mean daily discharges reached 611 cfs (cubic-feet per second) and 1070 cfs, respectively. Smaller flow events occurred but did not exceed 152 cfs. Granite Construction staff working in the study area recalled that sand began to fill major pools following major storm events (David Hamblin, personal communication 2016).

4.1 Sediment Sources

Sediment deposits in the 3.5 km stretch of river directly below the former SCD were new deposits attributable to sediment transport following dam removal. Potential major sources of sediment included the Carmel Watershed above the CRRDR, San Clemente Creek, erosion within the CRRDR, colluvial processes and construction activities downstream of the former SCD.

Annual bedload rates from the Carmel Watershed are only poorly constrained, even for water years like 2016 when there were no fire impacts, landslides or extreme floods. By averaging reservoir capacity changes during unexceptional time-periods, upper and lower estimates of bedload during water year 2016 could be as high as five acre-feet per year (AFY) and as low as one AFY. Upper estimates were derived and from reservoir sedimentation rates and storage capacity measurements recorded in 1960 and 1970 and averaged (MPWMD 1995). A similar methodology was used to estimate the lower annual bedload yield calculated between 1984 and 1993 (MPWMD 1995). Therefore, the bedload contribution from the upper Carmel Watershed could account for between 1,200 to 6,200 m^3 of sediment. San Clemente Creek may have contributed 1,200 to 2,500 m^3 of sediment (Matthews 1989). Particle sizes from the upper Carmel Watershed are primarily cobble and gravel, with minimal sand input from Pine and Cachagua Creeks (ASCE 1992). This grain size is incompatible with the deposits we found below the former SCD.

Erosion from within the CRRDR was documented, but not quantified by Marson *et al.* (2016). Tetra Tech (2016) estimated the volume of sediment eroded from the unconfined Upper Carmel Reach of the CRRDR to be approximately 4,000 m^3. This estimate was comparable in scale to the total sediment volume (4,560 m^3) we measured below the former SCD. The grain size distribution in the deposits (generally gravelly sand and sandy gravel) is similar to the material eroded from the Upper Carmel Reach as well.

Visual assessment indicated that there were no significant contributions from colluvial processes downstream of the former SCD. Construction activities were well constrained behind silt fence installations, and thus did not provide excess sediment to the channel.

The total available source sediment ranged from 6,400 m^3 to 12,700 m^3 (Table 2). However, the only directly estimated source was 4,000 m^3 from the CRRDR (Tetra Tech 2016), leaving only approximately 560 m^3 of the sediment wave to have come either from other erosion sites within the CRRDR (Marson *et al.* 2016) or from very sparse inputs from the Carmel Watershed and San Clemente Creek.

Table 2. Sediment source location and annual volume estimates for the Carmel River up and downstream of the CRRDR.

Location from CRRDR	Source	Acre-feet	Cubic meters	Literature Source
Upstream	Carmel Watershed	1 – 5	1200 – 6200	MPWMD 1995
	San Clemente Creek	1 – 2	1200 – 2500	MPWMD 1995
CRRDR	CRRDR erosion	3	4000	Tetra Tech 2016
Downstream	Colluvial processes	0	0	Field Recon
	Construction	Minimal	Minimal	Field Recon

4.2 Biological Impacts

The sediment wave will likely have a complex impact on local biological conditions, where a short-term negative impact is followed by general improvement over pre-SCD removal conditions. Heterogeneity in streambed particle size is critical for maintaining trophic stability and providing prey base and life cycle habitat for many species found in the Carmel River (Merz and Chan 2005; USFWS 2002; Everest *et al.* 1987). Historically, fine grains and cobbles were absent from SCD to Tularcitos Creek resulting in an armored streambed (MPWMD 2004).

Sudden influx of sand and gravel to the study reach could affect the benthic macroinvertebrate (BMI) populations of the surveyed reach. Increased abundance of fine sediments in the channel commonly depletes taxonomic diversity and impedes BMI productivity by accumulating in interstitial spaces of the streambed where BMI's are most abundant (Cover *et al.* 2008). Conversely, high gradient armored streambeds, like those present before the sediment wave arrived, increase BMI drift propensity resulting in reduced taxonomic richness (Wilcox *et al.* 2008).

Annual Carmel River BMI surveys completed by Monterey Peninsula Water Management District (MPWMD) suggest substrate size is only a single factor contributing to healthy BMI populations. Sediment deprivation and streambed armoring resulted in less diverse and abundant BMI populations from the SCD to the confluence with Tularcitos Creek. However, BMI populations improved downstream near Robinson Canyon Road (MPWMD 2010) likely through the addition of mobile sediment.

Recent sandy-gravel deposits downstream of the former SCD may continue to degrade BMI productivity in the near term, but impacts are likely to attenuate over time. Once the sand fraction is flushed downstream, the remaining gravel will enhance habitat for BMI, and productivity might rise above pre dam-removal conditions. This is important as two federally threatened species in the Carmel River, south-central California coast steelhead (Oncorhynchus mykiss) and California red-legged frogs (Rana draytonii) depend on BMI populations as a major food source (NMFS 2013; USFWS 2002).

Steelhead utilize pool habitat for both summer refuge and spawning grounds (Nielsen and Lisle 1994; Spina 2005). Deep pools retain cooler temperatures and provide habitat through prolonged hot, dry summers. The sediment wave accumulated in areas of the channel with low stream flow velocity, such as deep pools, that were historically maintained because the SCD prevented bedload from reaching the site. The accretion of sediments in pools dramatically reduced the cool water habitat available to steelhead and eliminated a major source of sustained cold-water flows to the lower Carmel River. Salmonids prefer medium fist sized particles (25-150mm) for red nest formation, typically found in pool glides (Merz and Chan 2005). We observed fine sand substrates dominating pool glides with a pavement veneer. Prior to dam removal riffle and pool habitat demonstrated minimal variability in substrate size and armoring resulted in virtually unsuitable steelhead spawning habitat (MPWMD 2004). Therefore sand wave sediments accumulated in glides are unlikely to degrade spawning habitat beyond pre-existing conditions.

Over time, improved sediment transport resulting from the CRRDR project will benefit the lower Carmel River ecosystem by encouraging establishment of riparian vegetation and reconnecting the river to the historic floodplain. Stratified layering of sand and clay deposits carried downstream will accrete in eddies and slow water formed by large woody debris accumulations. These deposits are hotspots for plant growth and will propagate riparian vegetation along the streambanks, reducing bank erosion and channel incision (URS 2012).

4.3 Fire Impacts

Increased sediment transport downstream of the former SCD is anticipated during the subsequent rainy seasons as a result of the 2016 Soberanes Fire. Sediment liberated by the fire and mobilized by runoff causes concern for Carmel Watershed. The fire approached the former SCD on 8/5/16 (Cal-Am 2016; Fig. 4). Predicted effects of the fire on the Carmel River include increased sediment flow and sedimentation. The Soberanes Phase I Burned-Area Report estimated sediment contribution from the fire to Carmel River to be 2-7 tons/acre from 2-10 year storms. We estimate that anywhere from 2,400 – 8,500 m^3 of sediment could be released from the Carmel Watershed from the Soberanes Fire by multiplying the amount of burned area (2,085 acres as of September 2016), the estimated sediment yield (2 – 7 tons/ acre), converting to mass (2,650 kg/ m^3 for quartzo-feldspathic material), and accounting for 35% porosity. The estimated fire impact in the 2017 winter might be similar in magnitude to the 2016 sediment wave.

4.4 Comparison to Other Dam Removals

Past studies of dam removals highlighted the short-term ecological impacts of dam removal such as sediment releases (Pizzuto 2002). After removal, it took a week to flush the contents of the former Lewiston dams on the Clearwater River in Idaho 6.5 km downstream to the confluence of the Snake River (Winter 1990). The Muskegon River is expected to take anywhere from 50-80 years to transport formerly detained sediment (Simons and Simons 1991). Following the phased removal of two dams on the Elwha River in Washington, 7.1 million cubic meters of sediment was released. Despite the sand wave, the Elwha River's morphology did not change in the first year post dam removal. In the second year, sand deposited on riffle crests creating a shift from pool-riffle to braided morphology (East *et al.* 2015), supporting the idea that river morphology shifts to a new equilibrium to transport supplied sediment (Schumm 1981). The scale at which a sediment wave impact lasts depends on the volume of sediment, river velocity, channel gradient, distance to the river mouth, and the technique of dam removal (Bendarek 2001).

Given the flashy nature of the Carmel River flows, most of the sand wave propagated during the winter storms. In a single, slightly above average winter flow the centroid of the sediment wave was transported approximately 1.7 km downstream. Future studies on the movement of this sand wave will provide more insight to the rate and magnitude of sand transport after a dam removal with minimal expected downstream impact such as the CRRDR project.

5 References

[ASCE] American Society of Civil Engineers Task Committee on Sediment Transport and Aquatic Habitat. 1992. Sediment and aquatic habitat in river systems. Journal of Hydraulic Engineering 118(5): 669-687.

Bednarek AT. 2001. Undamming rivers: A review of the ecological impacts of dam removal. Environmental Management 27(6): 803 – 814.

Berkman HE. And Rabeni CF. 1987. Effects of siltation on stream fish communities. Environmental Biology of Fishes 18:285-294

Bowie C. 2012. San Clemente Dam Removal Project [Internet]. California American Water. Available from: http://www.sanclementedamremoval.org/

[Cal-Am] California American Water. 2016. Upper Carmel River Basin daily reservoir storage values: August 2016.

Cover MR, May CL, Dietrich WE, Resh VH. 2008. Quantitative linkages among sediment supply, streambed fine sediment, and benthic macroinvertebrates in northern california streams. Journal of the North American Benthological Society 27:135-149.

Cui Y, Wilcox A. 2008. Development and application of numerical models of sediment transport associated with dam removal. Sedimentation Engineering: pp. 995-1020

Dettman DH. 1989. The quantity of Steelhead spawning habitat inundated or blocked by alternative water supply projects in the carmel river basin: MPWMD Technical Memorandum 89-03, 15 pp.

East AE, Pess GR, Bountry JA, Magirl CS, Ritchie AC, Logan JB, Randle TJ, Mastin MC, Minear JT, Duda JJ., Liermann MC., McHenry ML., Beechie TJ., Shafroth PB. 2015. Large-scale dam removal on the Elwha River, Washington, USA: River channel and floodplain geomorphic change. Geomorphology 246: 687-708.

[EIR] Environmental Impact Report. 2008. Final Environmental Impact Report/ Statement, San Clemente Dam Seismic Safety Project. Prepared for: California Department of Water Resources and U.S. Army Corps of Engineers. SCH #997042007. pp. 563.

Everest FH., Beschta RL, Scrivener JC., Koski KV., Sedell JR., Cederholm CJ. 1987. Fine sediment and salmonid production: a paradox. Pages 98-142 in E. O. Salo and T. W. Cundy (editors). Streamside management: forestry and fishery interactions. Contribution No. 57. Institute of Forest Resources, University of Washington, Seattle.

[FEMA] Federal Emergency Management Agency. 2009. Dam Safety in the United States: A Progress Report on the National Dam Safety Program. Fiscal years 2006 and 2007. FEMA P-759, Washington, DC.

[FEMA] Federal Emergency Management Agency. 2006. Hydrologic and hydraulic analyses (cross-sectional data) performed by Northwest Hydraulic Consultants for FEMA under contract no. EMF-2001-CO-0015.

Hecht B. 1981. Sequential changes in bed habitat conditions in the upper Carmel River following the marble-cone fire of august 1977: California Riparian Systems Conference University of California, Davis, September, 17-19, p.134-141.

Higgs S, Maclin E, Bowman M, Bednarek A. 2002. The ecology of dam removal a summary of benefits. American Rivers pp. 15.

Jennings CW, Strand RG, Rogers TH. 1977. Geologic map of California: California Division of Mines and Geology, scale 1:750,000.

Kelly SA. 2012. Geomorphic change in the upper Carmel River, CA: Effects of the 2008 Basin Complex Fire. Senior Capstone Research Project at California State University Monterey Bay.

Kondolf MG, Curry RR. 1986. Channel erosion along the Carmel River, Monterey County, California. Earth Surface Processes and Landforms v. 11, p. 307-319.

Krebs F. 1983. Computation of Total Sediment Load of the Carmel River, CA: Report to the Monterey Peninsula Water Management District.

Marson L, Besson J, Biordi C, Conlen A, DeWolf K, Gravelle M, Hubbard H, MacSween L, Santos R, Sosa M, Thompson K, Trejo-Arce J, Smith D. 2016. First Year Assessment of the Carmel River Reroute and Dam Removal Project. Division of Science and Environmental Policy. Senior Thesis Report, 101 pp.

Matthews G. 1989. Evaluation of reservoir sedimentation rates in the upper Carmel River Watershed. Monterey Peninsula Water Management District, Technical Memorandum 88-03.

Merz JE, Ochikubi Chan LK. 2005. Effects of gravel augmentation on macroinvertebrate assemblages in a regulated california river. River Research and Applications 21: 61-74.

[MPWMD] Monterey Peninsula Water Management District. 1995. Hydrologic evaluation of the Carmel River at the Los Padres Reservoir reference site and at the San Clemente reservoir mitigation site: Technical Memorandum 95-01, 30 pp.

[MPWMD] Monterey Peninsula Water Management District. 2004. Environmental and biological assessment of portions of the Carmel River Watershed, Monterey California.

[MPWMD] Monterey Peninsula Water Management District. 2010. Ten-year summary of the Monterey peninsula water management district's bioassessment program on the Carmel River.

Nicol CL, Smith DP, Watson FGR. 2015. Exploring particle density effects on partial mobility of steelhead spawning gravels. River Res. Appl. 31:62-69.

Nielsen JL, Lisle TE. 1994, Thermally stratified pools and their use by steelhead in northern California streams. Transactions of the American Fisheries Society 123: 613-626.

[NMFS] National Marine Fisheries Service. 2013. South-central california coast steelhead recovery plan. West Coast Region, california coastal area office, Long Beach, California.

Pizzuto J. 2002. Effects of dam removal on river form and process. BioScience 52(8): 683-691.

Poff NL, Hart DD. 2002. How dams vary and why it matters for the emerging science of dam removal. BioScience 52: 659-668.

R Core Team.2015. R: A language and environment for statistical computing. R Foundation for Statistical Computing, Vienna, Austria. ISBN 3-900051-07-0, URL http://www.R-project.org/

Richmond S. 2009. Post-fire channel response: A comparison between the 1977 Marble Cone Fire and 2008 Basin Complex Fire on the upper Carmel River. Master's Thesis Dissertation

Rosenberg L. 2001. Geologic resources and constraints, Monterey County, California: A technical report for the Monterey County 21st Century general plan update program. Prepared for County of Monterey Environmental Resource Policy Department. pp. 91.

Schumm, S.A., 1981. Evolution and Response of the Fluvial System, Sedimentologic Implications. Society of Economic Paleontologists and Mineralogists Special Publication 31:19-29.

Simons RK and DB Simons. 1991. Sediment problems associated with dam removal-Muskegon River, Michigan. Pages 680-685 in Hydraulic engineering, Proceedings of the 1991 national conference of the American Society of Civil Engineers, 29 July-2 August. American Society of Civil Engineers, Nashville, Tennessee.

Smith DP, Newman WB, Watson FGR, Hameister J. 2004. Physical and hydrologic assessment of the Carmel River watershed, California. The Watershed Institute, California State University Monterey Bay, Publication No. WI-2004-05/2 88 pp.

Smith DP, Kvitek R, Aiello I, Iampietro P, Quan C, Paddock E, Endris C, and Gomez K, 2009. Fall 2008 Stage-Volume Relationship for Los Padres Reservoir, Carmel Valley, California: Prepared for the Monterey Peninsula Water Management District. The Watershed Institute, California State University Monterey Bay, Publication no. WI-2009-2, 30 pp.

Spina AP. 2005. Downstream migration, rearing abundance, and pool habitat associations of juvenile steelhead in the lower main stem of a south-central California stream. North American Journal of Fisheries Management 25: 919- 930.

Suttle KB, Power ME, Levine JM, McNeely C. 2004. How fine sediment in riverbeds impairs growth and survival of juvenile salmonids. Ecological Applications 14:969-974.

Tetra Tech. 2016. Post-Construction CRRRDR Weir Boulder Movement Analysis Based Upon Surveys/Visual Observations and Remedial Recommendations.

Tetra Tech. 2015. Initial design report for the Carmel River reroute and San Clemente Dam Removal (CRRDR) project.

[URS] United Research Services. 2012. Final supplement to the EIR, No. 2. Old Carmel River dam removal.

[URS] United Research Services. 2012. Project number 26818107. Project base map. http://www.sanclementedamremoval.org/wp-content/uploads/2011/08/CRRDRProposed-Project.jpg. Last accessed: May 19, 2016.

[USDA-FS] United States Department of Agriculture-Forest Service. 2016. Soberanes Phase I Burned-Area Report. Reference FSH 2509.13.

[USFWS] United States Fish and Wildlife Service. 2002. Recovery Plan for the California Red-legged Frog (Rana aurora draytonii). U.S. Fish and Wildlife Service, Portland, Oregon. Viii. 173 pp.

Westerling AL, Hidalgo HG, Cayan DR, Swetman TW. 2006. Warming and earlier spring increase Western U.S forest wildfire activity. Science 313(5789): 940 – 943.

Wilcox AC, Peckarsky BL, Taylor BW, Encalada AC. 2008. Hydraulic and geomorphic effects on mayfly drift in high-gradient streams at moderate discharges. Ecohydrology 1(2): 176-186.

Winter BD. 1990. A brief review of dam removal efforts in Washington, Oregon, Idaho, and California. US Department of Commerce, NOAA Tech. Memo. NMFS F/NWR-28, 13 pp.

6 Appendix

6.1 Appendix A: Pool Images

Below is each pools spatially interpolated deposit thicknesses and their manually measured points.

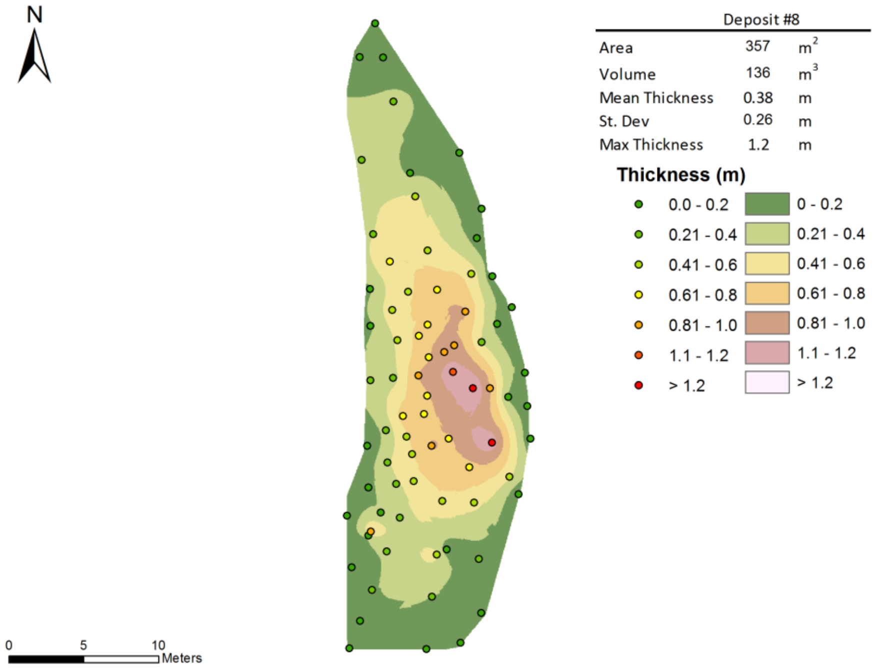

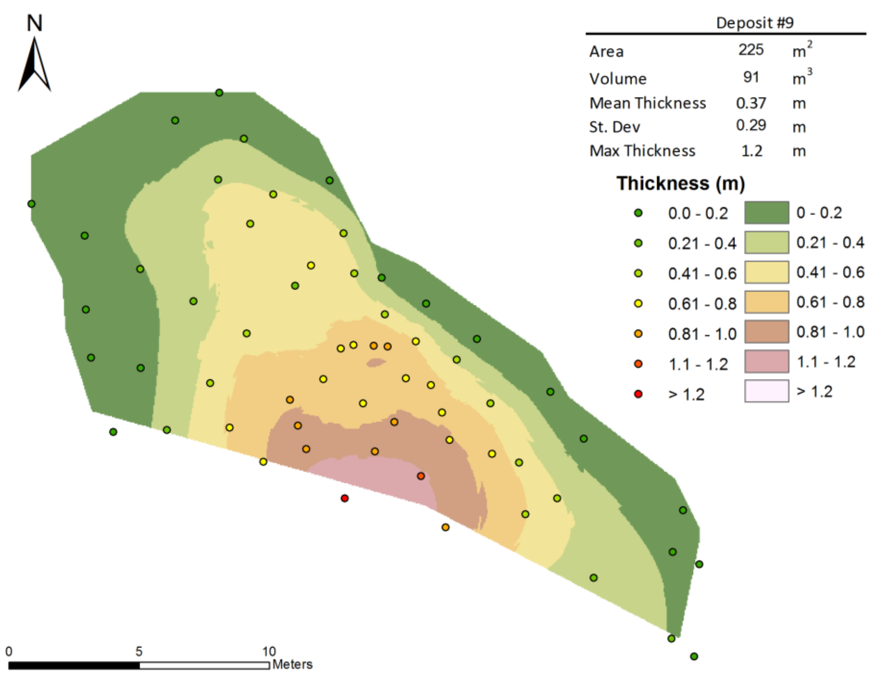

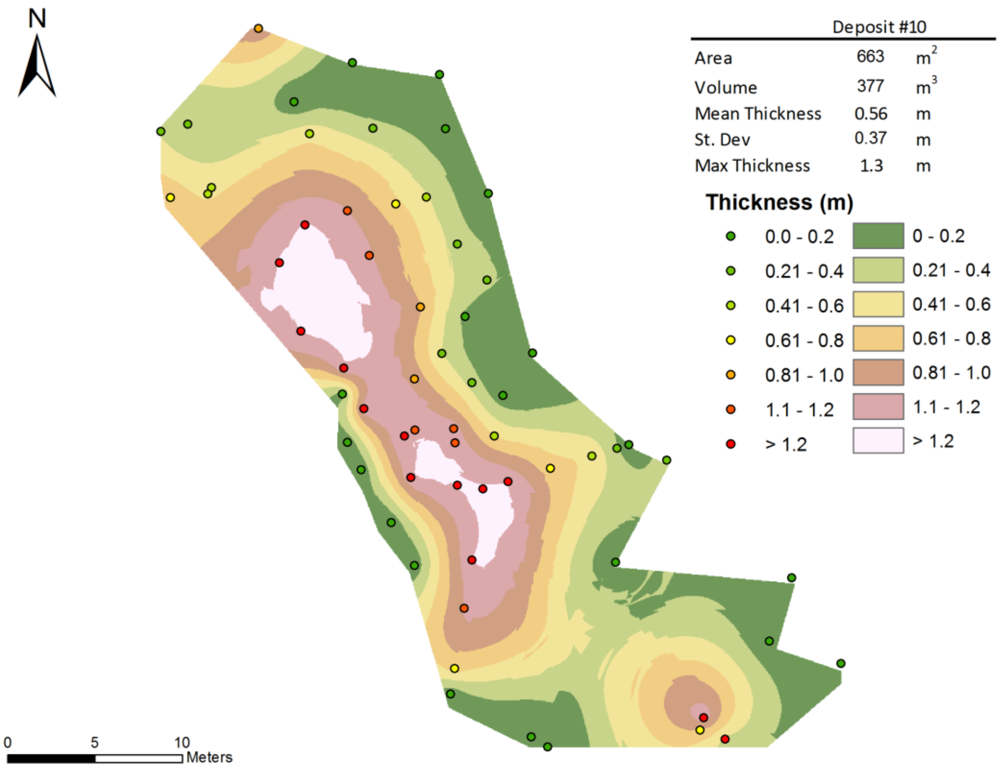
N
Deposit #10
Area 663 m2
Volume 377 m3
Mean Thickness 0.56 m
St. Dev 0.37 m
Max Thickness 1.3 m
Thickness (m)
0.0 - 0.2
0.21 - 0.4
0.41 - 0.6
0.61 - 0.8
0.81 - 1.0
1.1 - 1.2
> 1.2
0 - 0.2
0.21 - 0.4
0.41 - 0.6
0.61 - 0.8
0.81 - 1.0
1.1 - 1.2
> 1.2
0 5 10 Meters

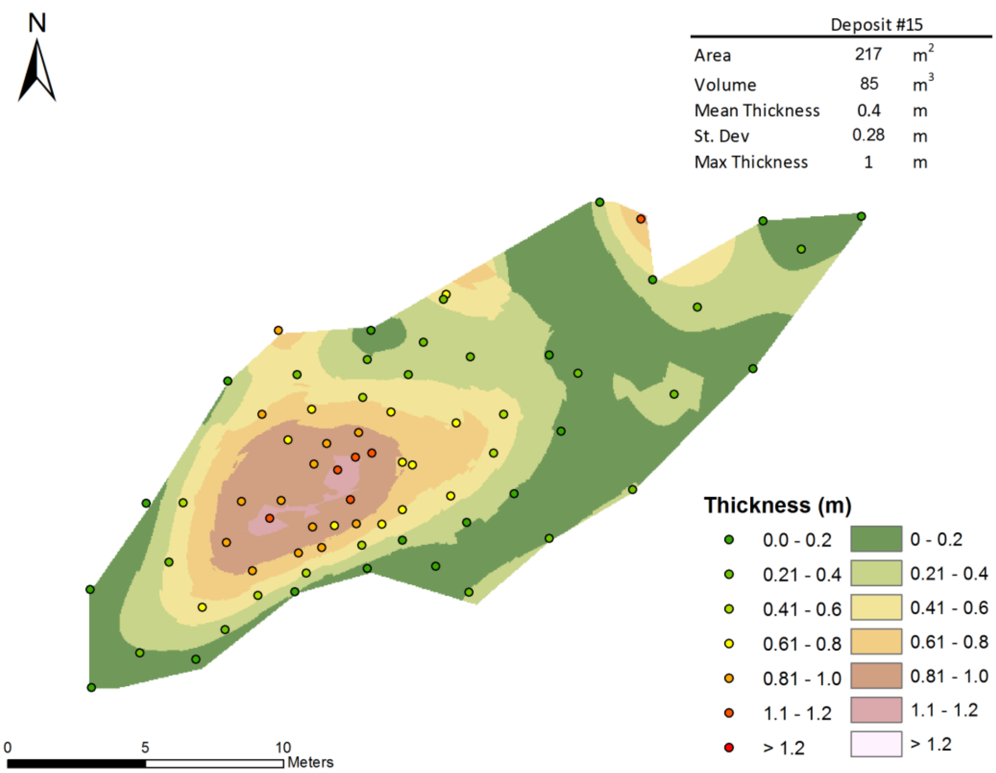
N
Deposit #15
Area 217 m2
Volume 85 m3
Mean Thickness 0.4 m
St. Dev 0.28 m
Max Thickness 1 m
Thickness (m)
0.0 - 0.2
0.21 - 0.4
0.41 - 0.6
0.61 - 0.8
0.81 - 1.0
1.1 - 1.2
> 1.2
0 - 0.2
0.21 - 0.4
0.41 - 0.6
0.61 - 0.8
0.81 - 1.0
1.1 - 1.2
> 1.2
0 5 10 Meters

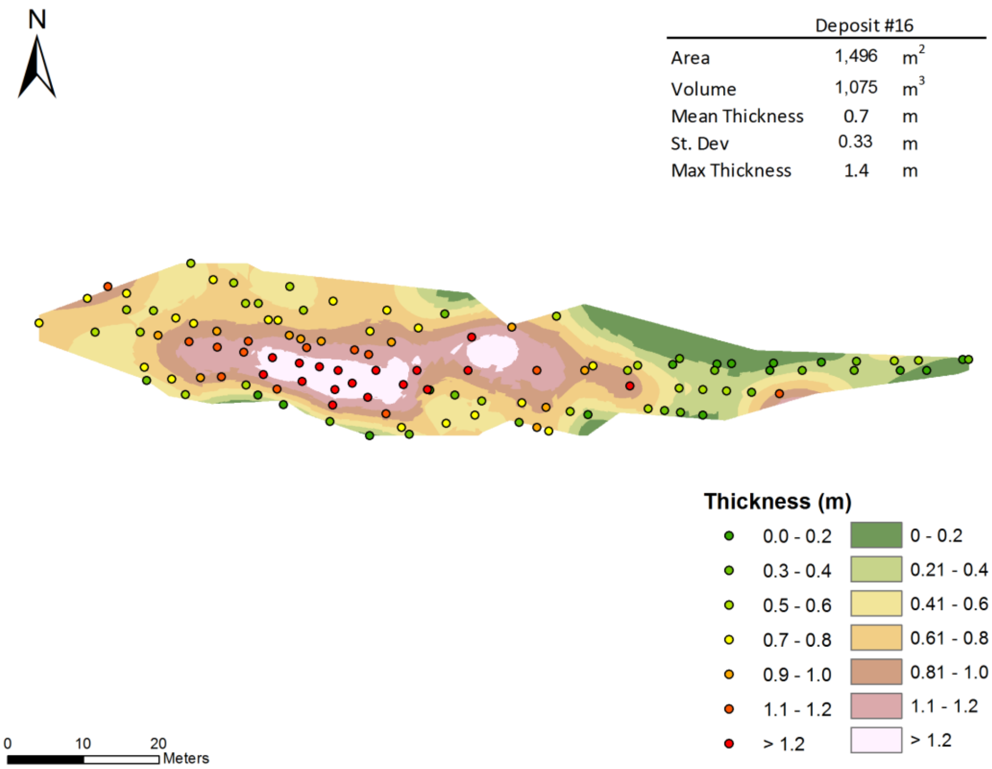
N
Deposit #16
Area 1,496 m2
Volume 1,075 m3
Mean Thickness 0.7 m
St. Dev 0.33 m
Max Thickness 1.4 m
Thickness (m)
0.0 - 0.2
0.3 - 0.4
0.5 - 0.6
0.7 - 0.8
0.9 - 1.0
1.1 - 1.2
> 1.2
0 - 0.2
0.21 - 0.4
0.41 - 0.6
0.61 - 0.8
0.81 - 1.0
1.1 - 1.2
> 1.2
0 10 20
Meters

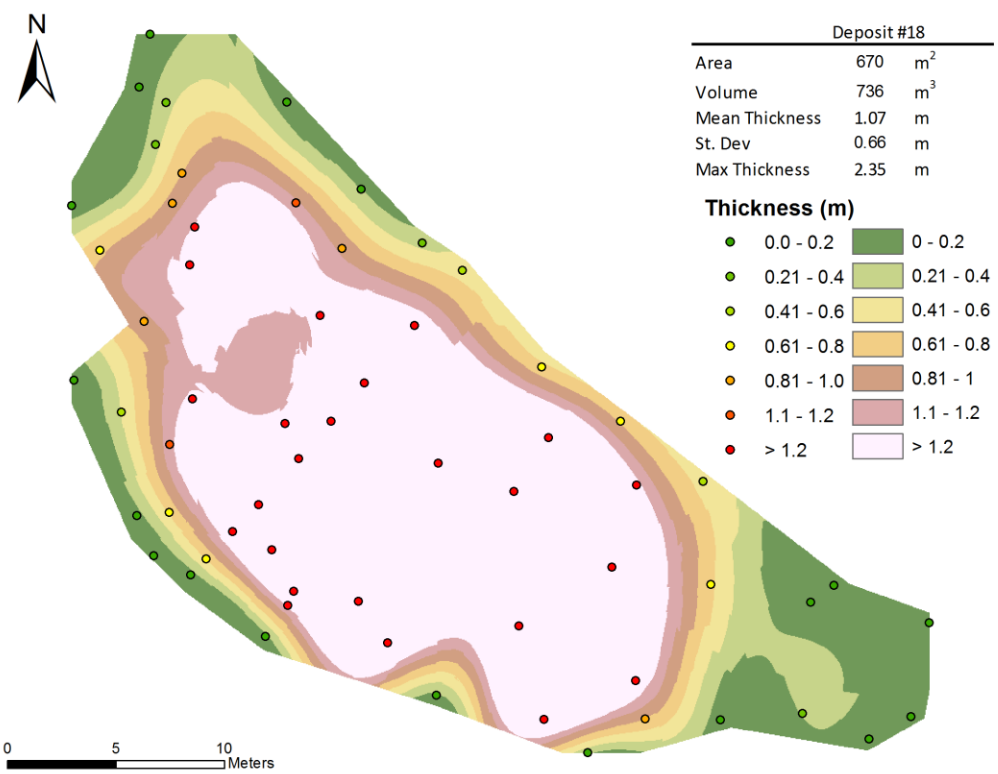
N
Deposit #18
Area 670 m2
Volume 736 m3
Mean Thickness 1.07 m
St. Dev 0.66 m
Max Thickness 2.35 m
Thickness (m)
0.0 - 0.2
0.21 - 0.4
0.41 - 0.6
0.61 - 0.8
0.81 - 1.0
1.1 - 1.2
> 1.2
0 - 0.2
0.21 - 0.4
0.41 - 0.6
0.61 - 0.8
0.81 - 1
1.1 - 1.2
> 1.2
0 5 10
Meters

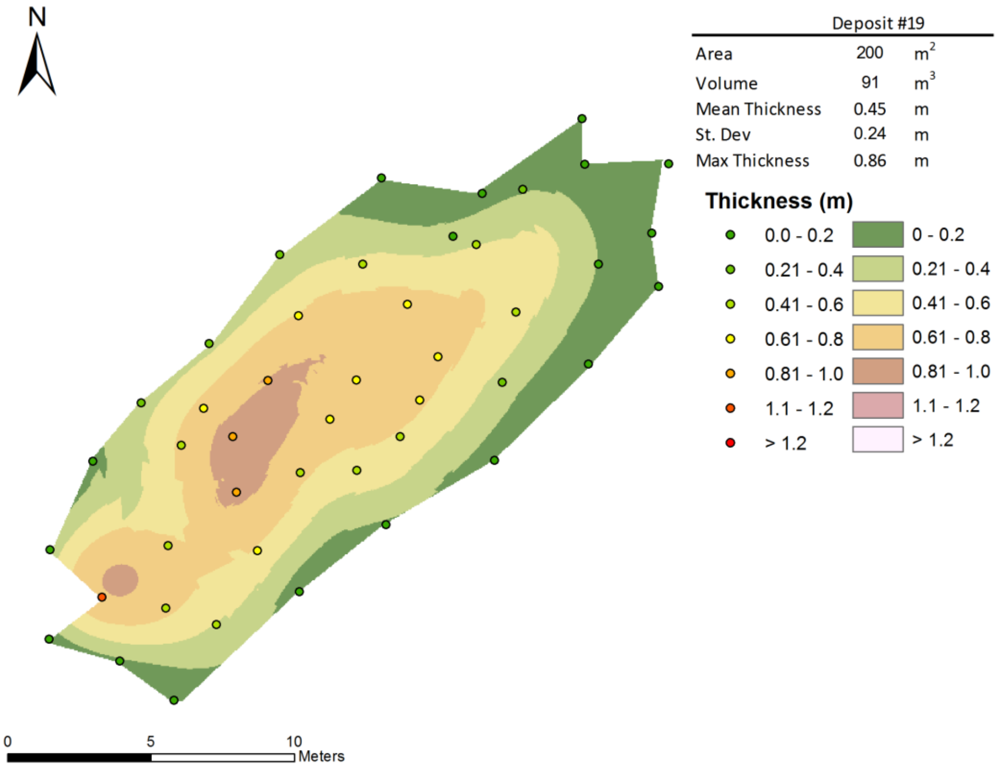
N
Deposit #19
Area 200 m²
Volume 91 m³
Mean Thickness 0.45 m
St. Dev 0.24 m
Max Thickness 0.86 m
Thickness (m)
0.0 - 0.2
0.21 - 0.4
0.41 - 0.6
0.61 - 0.8
0.81 - 1.0
1.1 - 1.2
> 1.2
0 - 0.2
0.21 - 0.4
0.41 - 0.6
0.61 - 0.8
0.81 - 1.0
1.1 - 1.2
> 1.2
0
5
10
Meters

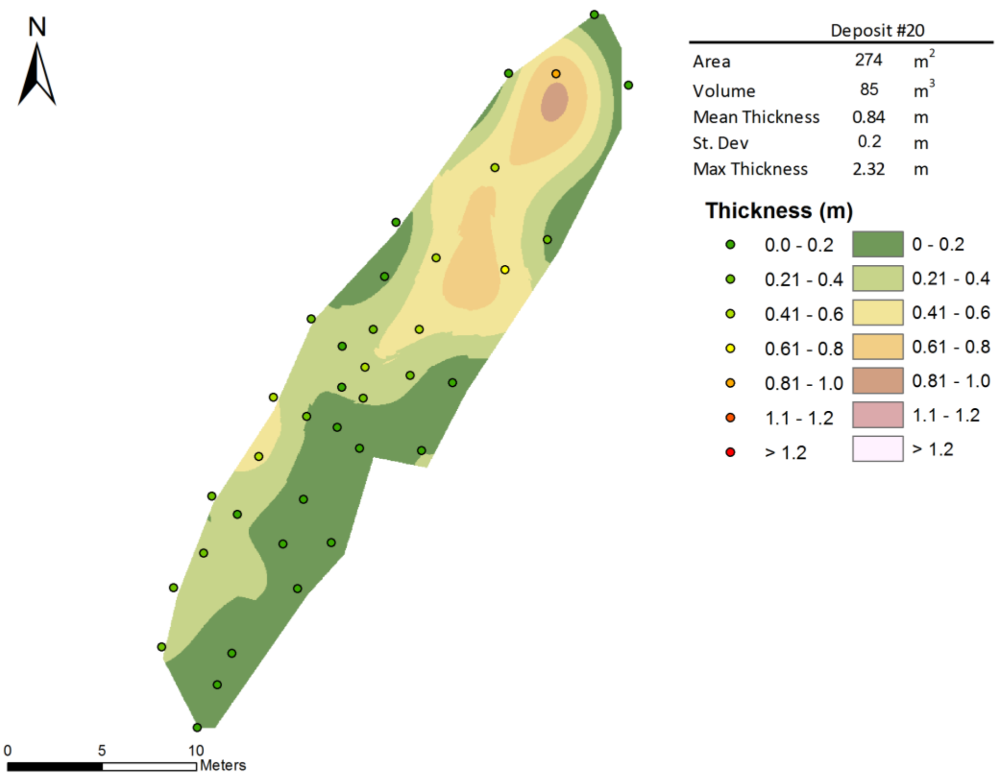
N
Deposit #20
Area 274 m²
Volume 85 m³
Mean Thickness 0.84 m
St. Dev 0.2 m
Max Thickness 2.32 m
Thickness (m)
0.0 - 0.2
0.21 - 0.4
0.41 - 0.6
0.61 - 0.8
0.81 - 1.0
1.1 - 1.2
> 1.2
0 - 0.2
0.21 - 0.4
0.41 - 0.6
0.61 - 0.8
0.81 - 1.0
1.1 - 1.2
> 1.2
0
5
10
Meters

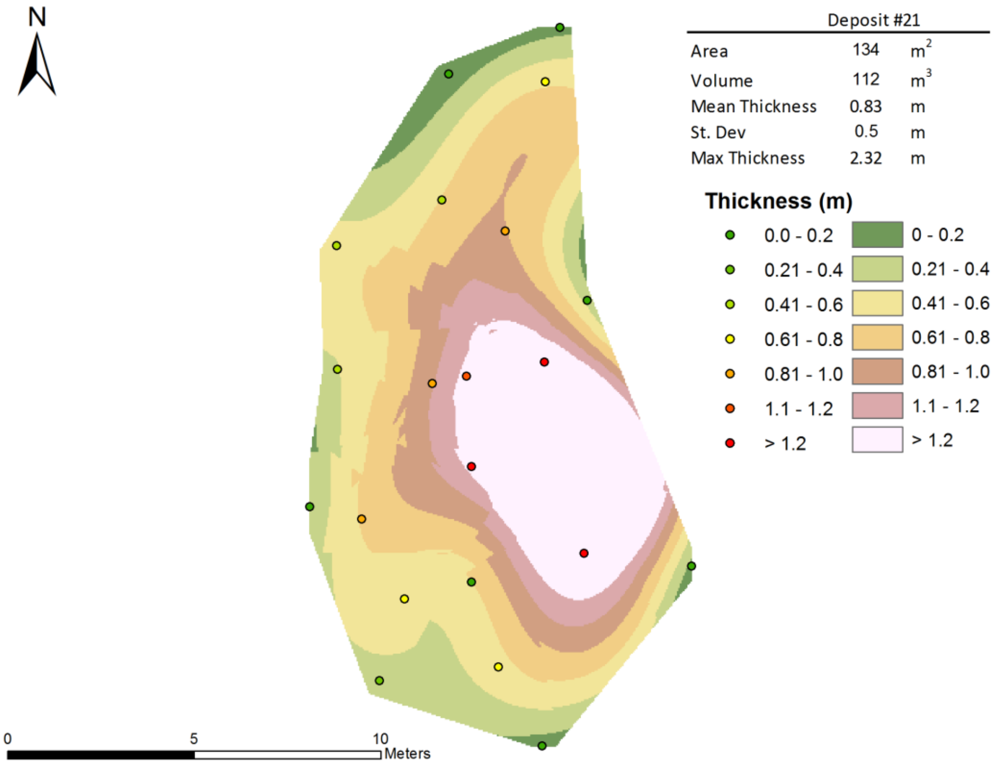
N
Deposit #21
Area 134 m2
Volume 112 m3
Mean Thickness 0.83 m
St. Dev 0.5 m
Max Thickness 2.32 m
Thickness (m)
0.0 - 0.2
0.21 - 0.4
0.41 - 0.6
0.61 - 0.8
0.81 - 1.0
1.1 - 1.2
> 1.2
0 - 0.2
0.21 - 0.4
0.41 - 0.6
0.61 - 0.8
0.81 - 1.0
1.1 - 1.2
> 1.2
0
5
10
Meters

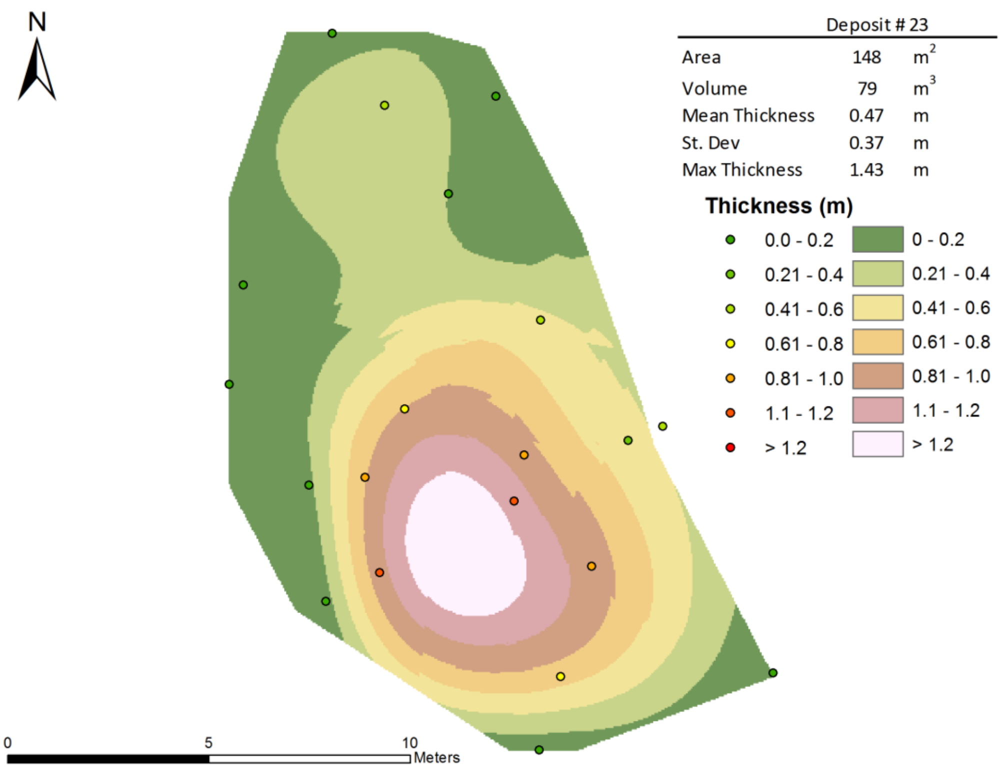
N
Deposit # 23
Area 148 m2
Volume 79 m3
Mean Thickness 0.47 m
St. Dev 0.37 m
Max Thickness 1.43 m
Thickness (m)
0.0 - 0.2
0.21 - 0.4
0.41 - 0.6
0.61 - 0.8
0.81 - 1.0
1.1 - 1.2
> 1.2
0 - 0.2
0.21 - 0.4
0.41 - 0.6
0.61 - 0.8
0.81 - 1.0
1.1 - 1.2
> 1.2
0
5
10
Meters

6.2 Appendix B: Sediment Images

Images of sand, pavement, and general pool fill sediment samples. Labels represent the deposit identification number and the location of each sample within the deposit.

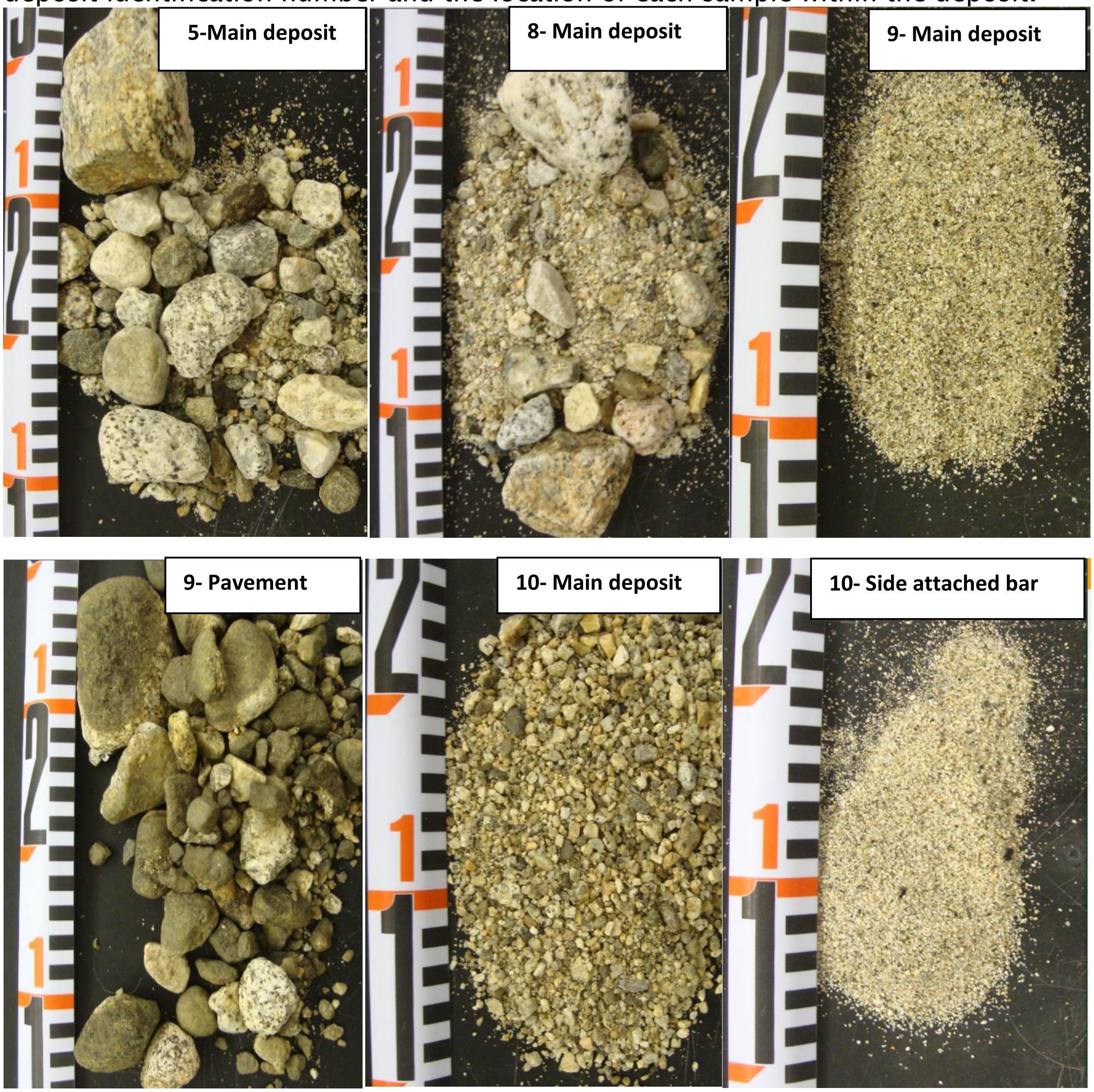


15- Main deposit


15- Side attached bar


16- Main deposit


16- Pavement


18- Pavement


18- Main deposit


19- Main deposit


21- Main deposit


23- Main deposit


25- Main deposit


27- Main deposit


29- Main deposit

SC_7

EARTH SURFACE PROCESSES AND LANDFORMS, VOL. 11, 307–319 (1986)

CHANNEL EROSION ALONG THE CARMEL RIVER, MONTEREY COUNTY, CALIFORNIA

G. MATHIAS KONDOLF

Department of Geography and Environmental Engineering, Johns Hopkins University, Baltimore, MD 21218, U.S.A.

AND

ROBERT R. CURRY

Board of Environmental Sciences, University of California, Santa Cruz, CA 95064, U.S.A.

Received 30 November 1984
Revised 5 March 1985

ABSTRACT

Historic maps, photographs, and channel cross-sections show that the channel of the Carmel River underwent massive bank erosion, channel migration, and aggradation in a major flood in 1911, then narrowed and incised by 1939. The channel was stable until 1978 and 1980, when bank erosion affected some reaches but not others. The narrowing and incision were in response to a lack of major floods after 1914 and construction in 1921 of a dam that cut off sediment supply from the most actively eroding half of the basin. Localized erosion in 1978 and 1980 occurred during low magnitude events along reaches whose bank strength had been reduced by devegetation. These events illustrate that the stability of a fluvial system can be disrupted either by application of a large erosive force in a high magnitude event (the 1911 flood) or in a low magnitude event, by reducing the resistance to erosion (bank devegetation).

The Carmel River is a potentially unstable system. Its discharge and slope characteristics place it near the threshold between meandering and braided. On the Lower Carmel, the presence of bank vegetation can make the difference between a narrow, stable meandering channel and a wide shifting channel with braided reaches.

KEY WORDS Channel instability Degradation below dams Groundwater withdrawal Riparian vegetation

INTRODUCTION

The role of vegetation in channel stability and as a determinant of stream width has been discussed by many authors, including Hadley (1961), Schumm and Lichty (1963), Turmanina (1963), Brice (1964), Zimmerman *et al.* (1967), Orme and Bailey (1970), Daniel (1971), Smith (1976), Graf (1978, 1981), and Charlton *et al.* (1978). Engineers have recognized the bank stabilizing properties of plants, especially willows, and have used them to control erosion and 'train' channels (Parsons, 1963; Seibert, 1968; Nevins, 1969). In general, one can observe that the relative importance of vegetation is greater for smaller streams, less for larger rivers (M. G. Wolman, personal communication, 1983).

The Lower Carmel River, Monterey County, California, is an example of a fluvial system in which loss of bank vegetation produced local widening at relatively low magnitude events in reaches that previously had responded mainly to high magnitude events. The potential instability of this system is illustrated by comparing its slope and discharge characteristics to those of other rivers. Using the event with a recurrence interval of 1·5 years (annual maxima) as bankfull, the Lower Carmel plots near the line separating braided from meandering channels on the plot of Leopold *et al.* (1964, p. 293) (Figure 4). Although this plot is generalized and must be applied with caution to a specific site, it suggests that the channel is metastable and is vulnerable to disruption if the balance between forces inducing and resisting erosion is upset.

0197–9337/86/030307–13$06.50

AIMS AND METHODS

Description of study area

The Carmel River rises in the rugged Santa Lucia and Sierra De Salinas Mountains in coastal Monterey County, California, and drains an area of about 660 km^2 (Figure 1). The upper 34 km of the river pass through steep canyons with only modest accumulations of alluvium; the lower 24 km traverse an alluvial valley (the 'Carmel Valley') before reaching the Pacific Ocean at Carmel. The alluvial fill is typically 15–20 m thick and consists of sands and gravels, with some silt and clay interbeds. The valley is generally up to a kilometre wide, but about 15 km from the mouth the valley narrows at a bedrock constriction (the 'Narrows') which divides the alluvial reach into the 'Middle' and 'Lower' Carmel River (Figure 2). In its upper reaches, the Carmel River is perennial, but in the alluvial valley, flow is intermittent, typically drying up in late summer.

The upper watershed is sparsely settled. Extensive commercial and residential development has occurred in the last three decades in the Carmel Valley, especially near the river mouth. Much of it is on lowland adjacent to the river and is clearly vulnerable to flooding.

The Carmel Basin has a Mediterranean climate typical of coastal central California, with moderate year-round temperatures. Virtually all precipitation (rain) falls between November and April, with 60 per cent falling between December to February. Rainfall decreases from an average annual total of 1040 mm in the high mountains of the southern part of the basin, to 360 mm near the valley mouth (R. Renard, U.S. Naval Postgraduate School, unpublished report to MPWMD).

Study objectives

Recent bank erosion along the Carmel River has caused property losses in excess of \$1·5 million. Because of local concern, this study was undertaken to establish the causes of the erosion and to place this recent channel instability in the context of historic channel changes, natural and human-induced. Using data from a variety of sources, the history of floods, dam construction, and land use was developed and related to changes in

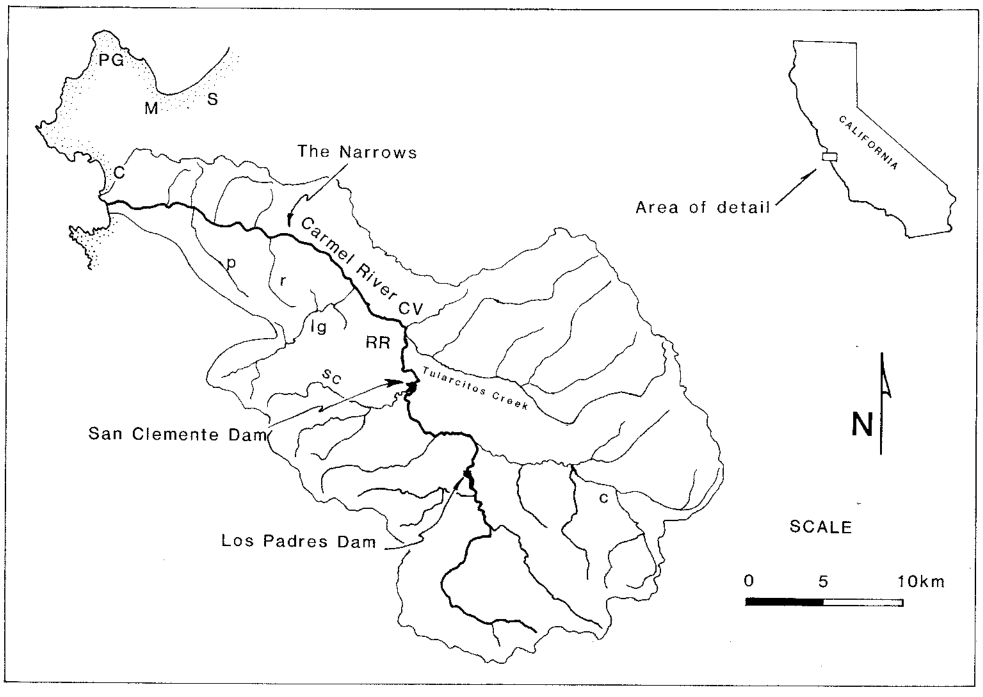

Figure 1. Basin and location map, Carmel River. Towns indicated by capital letters: S = Seaside, M = Monterey, PG = Pacific Grove, C = Carmel, CV = Carmel Valley Village, RR = Robles del Rio. Selected tributaries indicated by lower case letters: p = Potrero Creek, r = Robinson Canyon, lg = Las Garzas Creek, sc = San Clemente Creek, c = Cachagua Creek

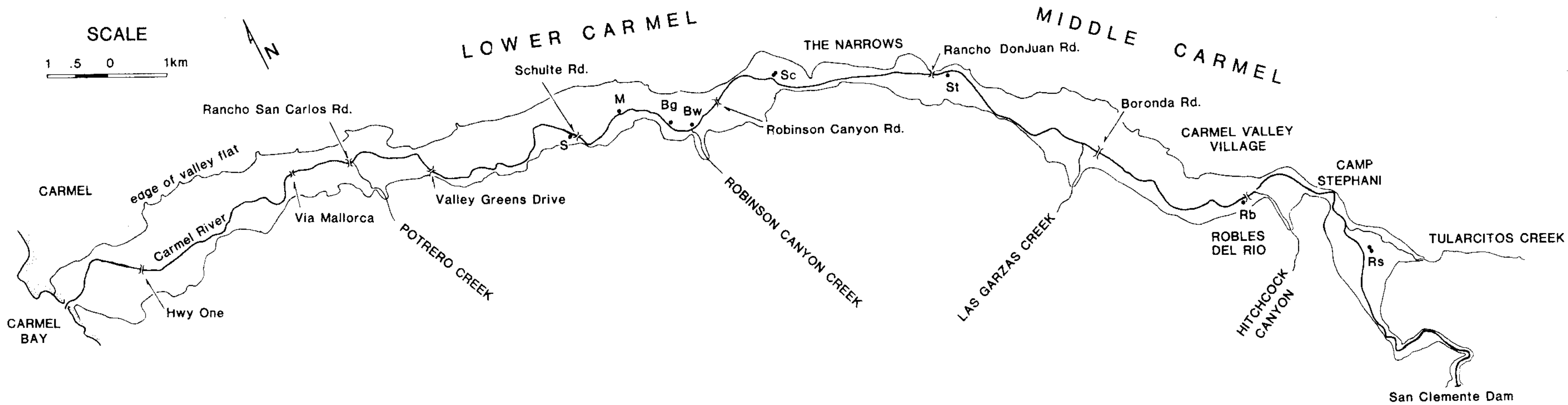

Figure 2. Location map, Middle and Lower Carmel River (Base from USGS Monterey, Seaside, and Carmel Valley 7·5′ quadrangles). Locations of Cal–Am producing wells: S = Schulte, M = Manor, Bg = Begonia, Bw = Berwick, Sc = Scarlett, St = Stanton, Rb = Robles

channel course, pattern, geometry and bed elevation. The results of these analyses were used to evaluate several hypothesized explanations for the recent bank erosion, including decreased bank resistance from loss of vegetation, degradation from closure of San Clemente Dam, and downstream variation in bank material size.

Sources of data and methods of analysis

Historic changes in channel course were plotted from boundary surveys conducted in 1858 and 1882 for Spanish land grants, and topographic maps (USGS Monterey 15′ sheet, 1913 edition; Monterey and Seaside 7·5′ sheets, 1947 and 1968 editions). Sequential aerial photographs taken in 1939, 1965, 1977, and 1980 from the collection of the Monterey County Food Control and Water Conservation District (MCFC) were studied to document changes in channel pattern and width. In addition, aerial photographs taken in other years (from the USGS, Fairchild Collection, and Map Collection at the University of California at Santa Cruz) were consulted at a reconnaissance level. Further documentation of old channel conditions was provided by ground photographs, *ca.* 1918 in the Slevin Collection, Bancroft Library, University of California, Berkeley, *ca.* the 1930s in the Pat Hathaway Collection, Pacific Grove, California, and *ca.* the 1960s in collections of Ed Lee, Carmel, Ca., and the *Carmel Pine Cone*. Other sources consulted included reports of testimony in court cases, newspaper accounts in *The Monterey Cypress*, and recollections of long-time residents (notably Roy Meadows, Meadows Lane, Carmel Valley).

Changes in channel geometry and bed elevation were documented by relocating 30 channel cross-sections surveyed in 1965 by the U.S. Army Corps of Engineers (unpublished data, U.S.A.C.A. San Francisco District). Relocation of cross-sections under bridges was straightforward and quite exact; however other cross-sections were not monumented and their relocation was not precise. Where the plotted changes were large, this imprecision was regarded as insignificant; where the plotted changes were small, the channel was regarded as essentially unchanged. At some bridges, the record could be extended back by using older cross-sections (unpublished data in files of Monterey County Surveyers and Monterey County Department of Public Works).

A flood chronology was developed from records of USGS gauges established in 1958 and 1963 (Nos. 11143200 and 11143250), and from a less reliable gauge maintained at San Clemente Dam by California–American Water Company (Cal–Am) since 1938. A pre-1938 flood history was developed from sources described above. Flood frequency plots and hydraulic geometry plots were developed from gauging station data. Drillers logs, observation well data, and pumping records were obtained from MCFC and Cal–Am. Bed and bank sediments, where exposed, were observed and sampled, and channel gradient was measured from topographic maps and field surveys. As the analysis proceeded, reaches of the river were classified as to slope, grainsize, and degree of stability in different time periods.

CHANNEL CHANGES TO 1965

Major floods occurred on the Carmel River in 1862, 1911, and possibly 1914. Little is recorded of the 1862 flood, but effects of the 1911 flood are documented. Newspaper accounts report that entire orchards were lost to bank erosion (*Monterey Cypress*, 11 March 1911), and old maps show that the course of the river shifted as much as 0·5 km during the flood (Kondolf, 1982). The peak discharge has been estimated at over 570 m^3s^{-1} at San Clemente Dam, on the order of a 100-year flood (U.S. Army Corps of Engineers, 1967). In 1914 another major flood occurred, but there is little evidence of its magnitude and none that it produced marked changes in course. It may have been much smaller than the 1911 event, or it may have caused less disruption simply because it flowed through a channel already enlarged by the 1911 flow. No major floods have occurred since.

In the decades that followed, the Lower Carmel and the Middle Carmel exhibited different changes. On the Lower Carmel, photographs taken in 1918 show a wide unvegetated channel, as yet unrecovered from the 1911 (and 1914) flooding (Slevin Collection, Bancroft Library, U.C. Berkeley). By 1939 (date of the first comprehensive aerial photography), the channel had narrowed, incised, and developed a dense riparian forest, and the channel bed from the 1911 flood stood 4 m above the incised stream as a fill terrace that can be clearly followed for 9 km (Figure 3). By 1965, the date of the first systematic channel surveys (U.S. Army

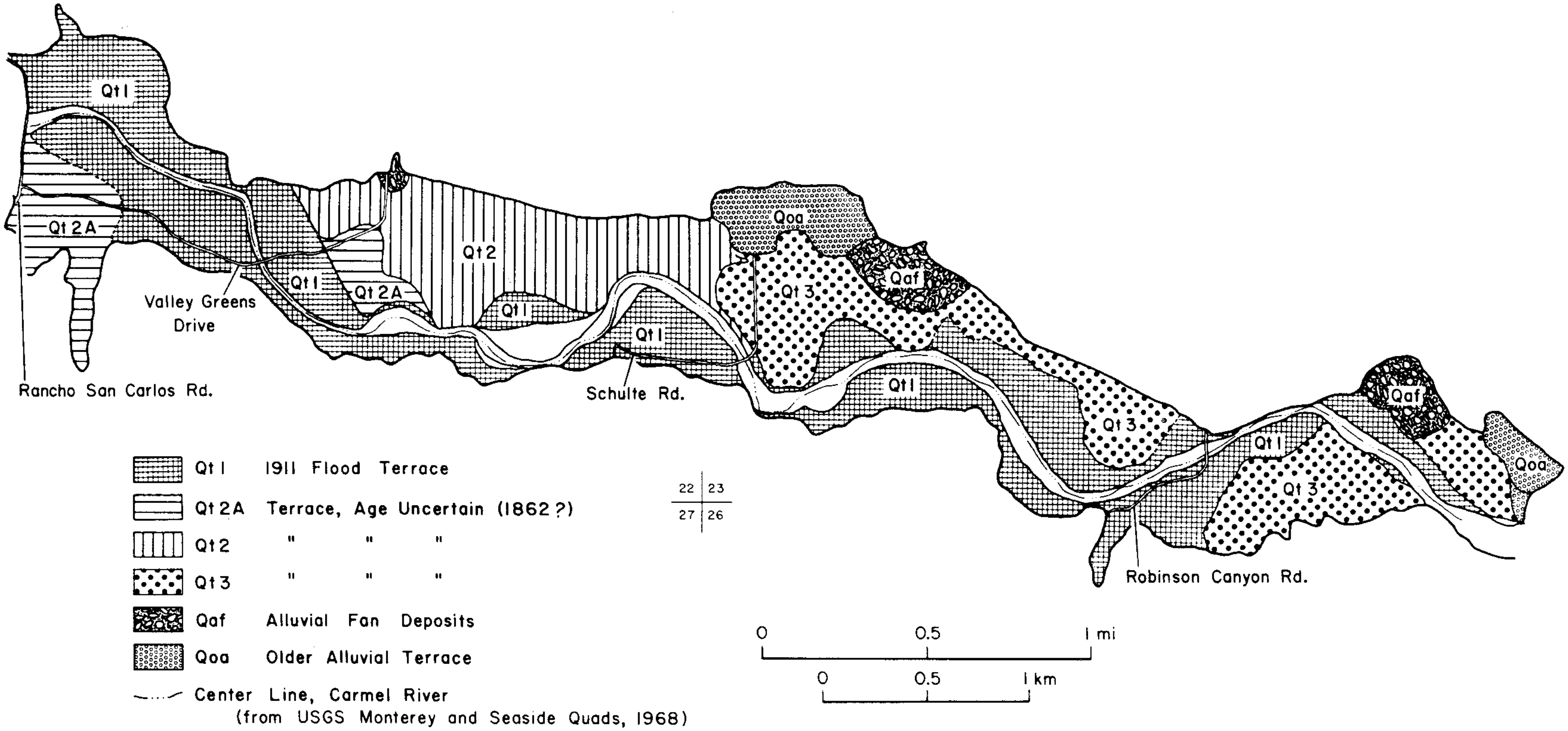

Figure 3. 1911 Flood Terrace and other Quaternary deposits of the Lower Carmel Valley, from the Narrows to San Carlos Road. Based on reconnaissance-level study of aerial photographs and field observations

Corps of Engineers, unpublished data), the channel incision and narrowing were complete. In fact, comparison of aerial photographs from 1939 with those of later years shows that the Lower Carmel changed little until the recent bank erosion.

In contrast, the Middle Carmel showed continued change from 1939 to 1965, and 1965 to the present. The channel became less braided from 1939 to 1965. From 1965 to 1982 the channel continued to incise and migrated laterally in many locations. Some specific causes contributing to the incision and lateral erosion can be identified (such as local straightening of the river for highway improvement) but much of the change may be due to the inherent instability of this steeper reach of the river. The overall gradient of the Middle Carmel is 0·005 compared to 0·003 for the Lower Carmel. The Middle Carmel plots in the braided portion of the graph defining channel pattern for streams on the slope vs. discharge plot of Leopold *et al.* (1964, p. 293; Figure 4).

Channel narrowing and incision are typically observed on rivers as they recover from major aggradational floods (Wolman and Gerson, 1978), so it is reasonable to regard the changes on the Carmel River as elements in recovery from the floods. However, the story is complicated by another event whose effects would be similar: dam construction.

In 1921, San Clemente Dam was constructed 29 km upstream from the mouth (Figure 1); in 1946 Los Padres Dam was constructed 11 km farther upsteam. Both reservoirs are small (2·65 million m^3 and 3·95 million m^3, respectively at closure) and have little effect on flood flows. However, the supply of bedload-sized sediment was cut off from the watershed upstream of San Clemente Dam. The basin upstream of the dam encompasses nearly 50 per cent of the total drainage and includes the areas of steepest relief and highest rainfall, so it was probably a major source of bedload to downstream reaches.

Sediment yields from the areas upstream of the dams, computed from reservoir sedimentation data, indicate minimum average sediment yields of about 160 tonnes/km^2/y for San Clemente Reservoir and 1050 tonnes/km^2/y for Los Padres Reservoir. The sediment yield value for San Clemente is low, in part, because sediment from half its drainage area has been trapped in Los Padres Reservoir for 39 of the last 64 years. The sediment yield for Los Padres is high because of the high erosion rates resulting from a major fire in the drainage basin in 1977 (Hecht, 1984). However, tree ring studies at a nearby site indicate natural fire frequencies from 1640–1907 averaged once per 21 years (Griffen and Talley, 1981), so fire-augmented, high sediment loads were probably typical for the Carmel in recent centuries before dam construction.

By reducing the supply of bedload to downstream reaches, dam construction on the Carmel River could be expected to induce channel narrowing, incision, and increase in sinuosity, changes that have been documented on many rivers following upstream dam construction (Williams and Wolman, 1984). Because recovery from a major aggradational flood and response to upstream dam construction induce similar responses, and because both occurred at about the same time on the Carmel River, it is difficult to separate their relative impacts in this case.

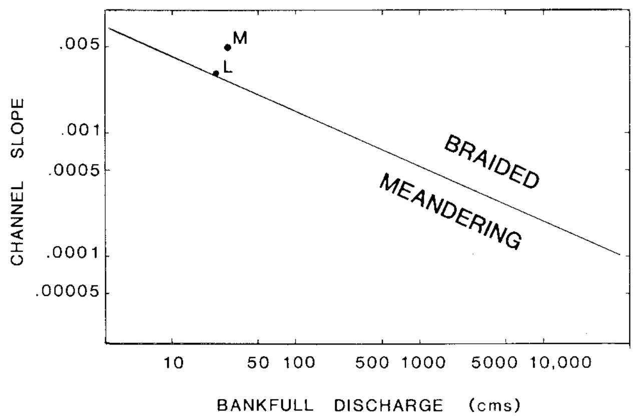

Figure 4. Channel patterns plotted by slope and bankfull discharge, with Middle (M) and Lower (L) Carmel plotted on graph. Original figure from Leopold *et al.* (1964, p. 293)

CHANNEL CHANGES SINCE 1965

Although the Middle Carmel was still undergoing adjustments from 1939 to 1978, the Lower Carmel was essentially stable over those four decades. Since 1978, however, the 15 km long Lower Carmel exhibited two distinctly different behaviour patterns: the downstream half remained stable, while the upstream half experienced extensive bank erosion. Bank erosion began in 1978 and increased in 1980. The most extensive bank erosion occurred in the reach upstream of Schulte Road bridge, where relocation of a U.S. Army Corps of Engineers cross-section site 30 m upstream of Schulte Bridge shows an increase in width from 25 to 65 m between 1965 and 1982 (Figure 5). The degradation apparent in this section occurred after 1980, and was subsequent to, not a cause of, bank erosion.

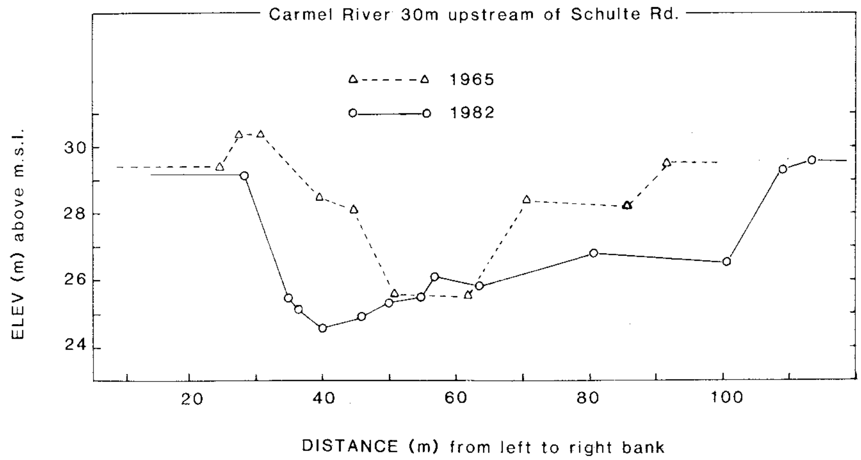

Figure 5. Sequential changes in channel cross-section of the Carmel River 30 m upstream of Schulte Road bridge. 1965 data from U.S. Army Corps of Engineers, San Francisco Office. 1965 section was not documented, so location may not be precise

The magnitude of this erosion is visible on sequential aerial photographs. Between 1977 and 1980, active channel width increased dramatically over a 0·6 km reach from Schulte Road to Manor Well (Figure 6C–D). The massive bank erosion resulted in aggradation in the eroding reach. Subsequent flows of 1982 were not as high and resulted in less bank erosion, but served to remove some of the aggraded sediment from the eroded reach, while high flows in 1983 produced further channel widening in the unstable reaches.

Altogether about 490,000 m^3 of bank material were eroded on the Lower and Middle Carmel in 1978,and 1980 (Fred Geiger, Monterey County Flood Control, personal communication, 1982), with an estimated 100,000 m^3 eroded from the 0·6 km reach from Schulte Road to the Manor Well. This sediment has, for the most part, been transported downstream to the lagoon and offshore canyon. Although residents report that some downstream pools have filled with sediment, sequential cross-sections at and near bridges show no significant changes in bed elevation. If the eroded material were evenly distributed over the channel bed downstream of Schulte Road, aggradation of about 1·9 m would be expected.

It is notable that the bank erosion occurred only upstream of Valley Greens Drive. Not only was the lowermost 8 km reach free of unusual bank erosion, but this narrow, vegetated channel remained stable despite passage of this increased load of sediment from the eroded reach. Some change in hydraulic parameters must have occurred for the downstream reach to accommodate its increased sediment load. Since no overall change in width and depth is evident, reduction of roughness through filling pools and burying riffles by finer sediment is likely.

The flows that produced the bank erosion were not unusual events. The peak flow of 1978, 208 m^3s^{-1}, was an eight year event (annual maxima), the peak flow of 1980, 166 m^3s^{-1}, a six year event. Any explanation for the bank erosion must account for its localized nature and its lack of precedent given the low magnitude of the events that produced it.

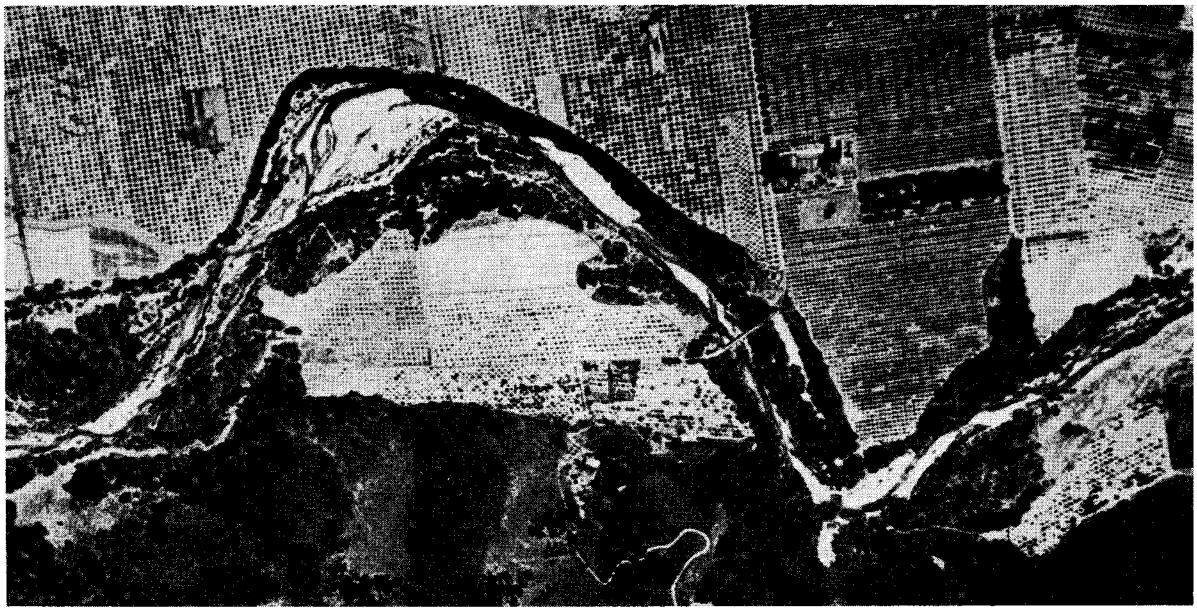

Figure 6A

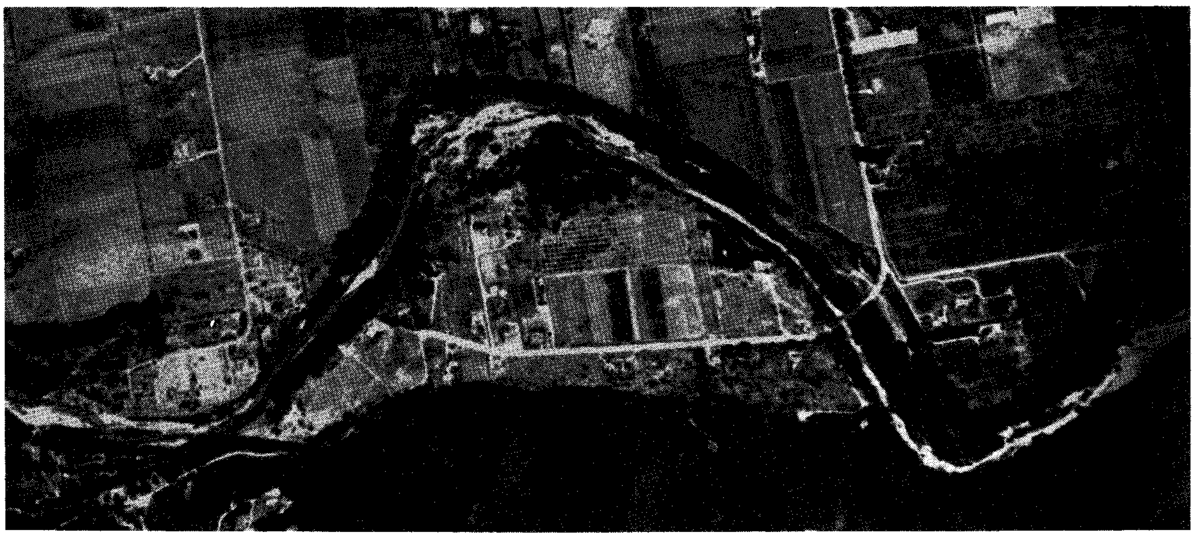

Figure 6B

BANK DEVEGETATION

The timing and distribution of bank erosion on the Carmel River are best explained by reference to bank devegetation caused by a lowered water table near municipal supply wells.

The Carmel River supplies most of the water for the Monterey Peninsula, and demand for water has increased as population has grown. The reservoirs were small when built, and sedimentation reduced their capacity further. Shrinking reservoir capacity and increasing demand over the past two decades led California–American Water Company (Cal–Am), a private utility, to draw increasingly upon water supply wells in the alluvium along the Lower and Middle Carmel. One of the first wells pumped heavily was the Berwick Well (Figure 2). By the late 1960s residents were complaining that trees were dying around the well

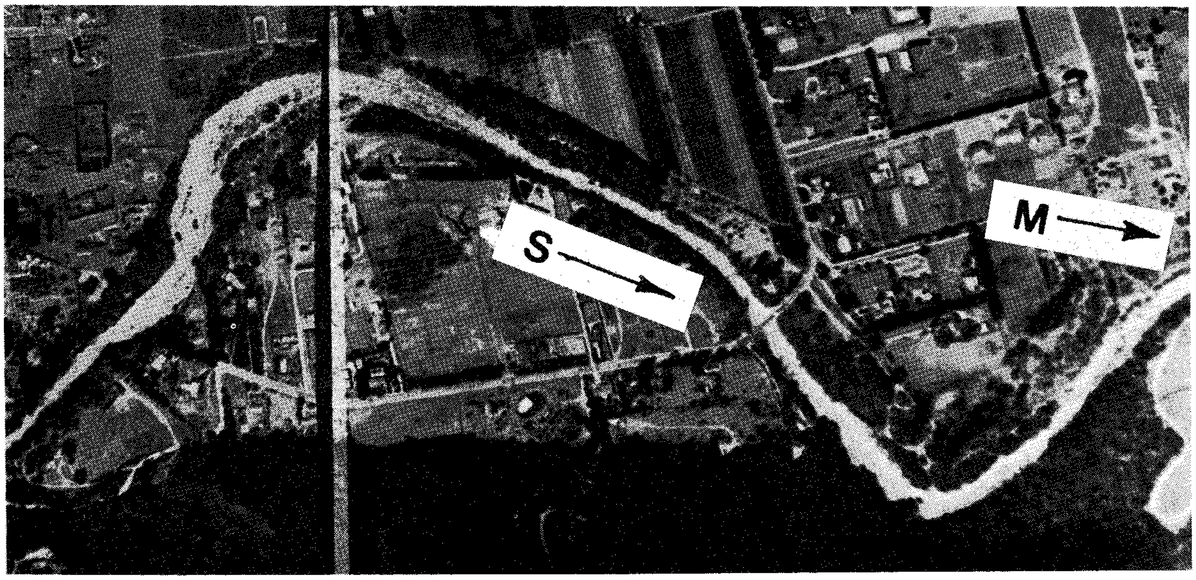

Figure 6C

Figure 6D

Figure 6. Aerial photographs, Schulte Road reach, 1939–1980. (A) 1939. A healthy but not uniformly dense riparian zone is visible. The channel had experienced a 20-year flood the previous year. (B) 1965. Riparian vegetation has grown more uniform, and encroached on formerly bare channel floor, narrowing active channel slightly. No major change apparent since 1939. (C) 1977. The riparian forest has visibly thinned. Clearing accounts for some of this thinning, but near the Manor Well, the once-live forest now consists of dead trees. Arrows point to locations of Manor Well (M) and Schulte Well (S). Some bank erosion has occurred, primarily on the outside of the large meander bed downstream of Schulte Road bridge (left side of photograph). (D) 1980. Massive bank erosion over most of reach, notably at bend upstream of Schulte Road bridge. Between Schulte Road bridge and Manor Well, approximately 100 m^3 of bank material was eroded in 1978 and 1980. Flow is from right to left. Source: Monterey County Flood Control and Water Conservation District air photo collection

(Lee, 1974), and a report by Zinke (1971) concluded that lowered water tables near the wells killed the vegetation.

As the demand for water increased, more wells were drilled and pumping increased, especially during the severe drought of 1976–1977 (Figure 7). Production from the wells reached a peak in 1976 and then decreased in 1977 because the aquifer (unconfined alluvium about 30 m thick and 0·5 km wide) was locally depleted.

Runoff in the Carmel basin is in response to rainfall and reflects the seasonal pattern of wet winters and dry

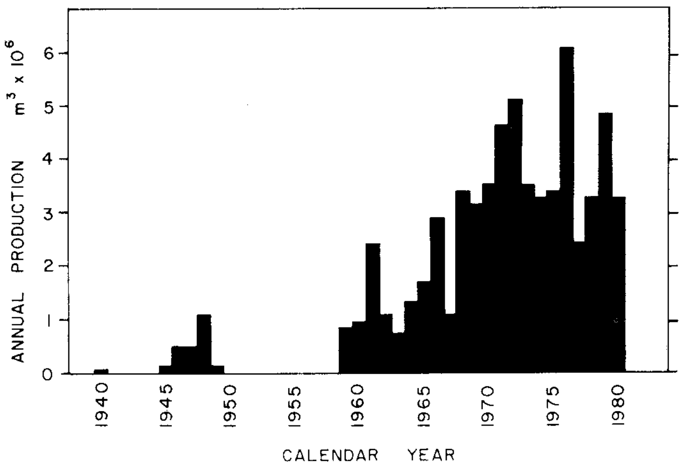

Figure 7. Annual production, Mid-Valley wells through 1980. Values are cumulative annual production for Scarlett, Berwick, Manor, Schulte, Dollar, Thacker, and Begonia wells. With exception of Dollar and Thacker, all wells located on Figure 1. Source: Cal–Am production records

summers. In normal years, the alluvium of the Carmel Valley undergoes a seasonal cycle of recharge by early winter flows, loss of water from bank storage in late spring, and drawdown of the unconfined alluvial aquifer by pumping. The pumping occurs year-round, but the drawdown is most pronounced in summer and early fall, when streamflow is not adequate to recharge the aquifer (Maloney, 1984).

During the two years of drought, the aquifer received almost none of its usual annual recharge from river flow. The lack of recharge combined with heavy pumping produced unprecedented drawdowns, exceeding 10 m over 4 km of the river. Downstream of the pumped reaches drawdown was minimal. Figure 8 compares autumn drawdown in a normal flow year (1980) and the extreme drawdown of the second drought year (1977) with the normal recharged level of the water table after a normal winter flow season (1978). The concentration of drawdown in the zone of most intense pumping supports the interpretation that the wells were primarily responsible for the depletion of the aquifer. Moreover, Kapple and Johnson (1980) report that drawdown in the pumped reach was so large that the hydraulic gradient was in the upvalley direction for much of the aquifer downstream of the Schulte Well.

Phreatophytes in the pumped reach were deprived of water for much of the two-year drought; as a result, many died. Although no one measured willow stress during the drought, Woodhouse (1983) has since found that willows are stressed near pumping wells in the Carmel Valley. Downstream of the pumped reach, phreatophytes remained healthy.

The reaches of the Carmel suffering severe drawdown and die-off of phreatophytes over the 1976–1977 drought were sites of bank erosion in 1978 and 1980. In Figure 8, the association of bank erosion (measured from cross-sections and aerial photographs) and drawdown is shown with bank erosion as measured on an arbitrary scale of *severe* (typically 30 m), *moderate* (locally variable; many reaches unaffected, many reaches with erosion, typically 10–20 m, but locally more or less), or *none* (typically no erosion, but local erosion of generally 10 m or less).

Sequential aerial photographs for the most severely eroded reach, upstream of Schulte Road, (Figure 6A–D) show the channel form essentially unchanged from 1939 to 1977. However, changes in the riparian vegetation are apparent: from 1939 to 1965, the riparian cover increased somewhat (Figure 6A–B); from 1965 to 1977 it had noticeably thinned around the Manor Well (Figure 6C). Following the flows of 1978 and 1980, active channel width had increased dramatically over the reach (Figure 6D), from 40 to 110 m at one section.

Most of the erosion occurred in 1980, despite a higher peak discharge in 1978. This is attributable to two factors: (1) The 1980 flow was of longer duration than the 1978 flow. The average daily discharge at Carmel exceeded 57 m^3s^{-1} for 6 days in 1980, but only two days in 1978. (These flows and durations were equalled or

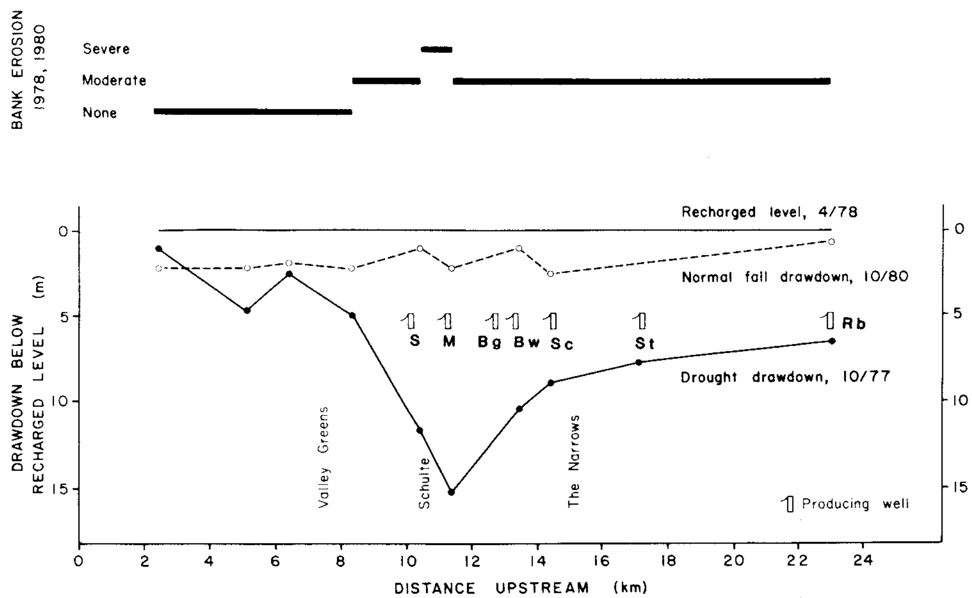

Figure 8. Water table drawdown and occurrence of bank erosion, Carmel Valley. See text for explanation. Sources of data: Monterey County Flood Control Records, Cal–Am, and field observations. Wells identified as in Figure 1

exceeded many times in the preceding decades with no comparable erosion.) (2) The roots of the willows killed in 1976–77 had decayed for another two years. Studies conducted on other species show that roots less than 17 mm in diameter are most effective in binding soil, and roots of this size generally decay within a few years after the death of the tree (Ziemer, 1981a, 1981b; O'Loughlin and Watson, 1979).

OTHER HYPOTHESES

Other hypotheses have been advanced to explain the bank erosion of 1978 and 1980. Carlson and Rozelle (1978) concluded that bed degradation, caused primarily by construction of the San Clemente Dam, was the 'underlying cause of enhanced bank erosion . . .' (p. 7.1). They also cited differences in bank material size as determinants of the distribution of bank erosion.

The historical record demonstrates that indeed the channel of the Lower Carmel incised after closure of San Clemente Dam, but the incision was essentially complete by 1939. This is consistent with published observations that degradation below dams proceeds rapidly at first, then slows as a new equilibrium profile is achieved, typically after a period of 20 years or less (Williams and Wolman, 1984; Leopold *et al.*, 1964, pp. 454–457). Given that channel incision preceded the bank erosion by four decades, it is unlikely that the one is cause of the other.

There is no evidence that the grain size of bank material differs between the unstable reach near Schulte Road and the stable reaches downstream. Drillers' logs show essentially the same heterogeneous mix of sand, gravel, and silt underlying both reaches (Cal–Am, unpublished data; MCFC, unpublished data). As shown in Figure 3, the Carmel is flanked by the same fill terrace from the 1911 flood at least from Rancho San Carlos Road to the Narrows. Where exposed in cut banks along the eroding reach, these deposits are seen to be non-cohesive interbedded sands, gravels, and silts, sediments that offer little resistance to erosion when exposed. Along the stable reaches, however, these bank sediments are not exposed. Instead, the channels are fringed by a dense wall of trees, and, most importantly, the toes of the banks are armoured with a mat of fine roots, which must be breached before the underlying bank materials are exposed to flow. Thus, even if differences existed in bank material size, the river would not be influenced by them until the stabilizing armour of vegetation had been pierced. Photographs of what is now the unstable reach show that it too had a mat of willow roots exposed along the bank toe before the effects of pumping were manifest.

CONCLUSIONS

The channel disruptions resulting from the 1911 flood and the bank destabilization of 1978 and 1980 provide a sharp contrast. The 1911 flood was a high magnitude event, with erosive forces vastly exceeding bank resistance. Massive channel widening resulted along the entire Lower and Middle Carmel. The 1978 and 1980 flows were low magnitude events, but channel widening occurred in local reaches where resistance of banks had been reduced by pumping, drawdown, and die-off of phreatophytes. For the severely eroded reach upstream of Schulte Road, the bank erosion of 1978 and 1980 was comparable to the channel widening effected by the 1911 flood. Downstream reaches, unaffected by pumping, maintained healthy bank vegetation, and experienced no major erosion. Clearly, the flows of 1978 and 1980 were not inherently more erosive than other low-magnitude events, but the banks were more erodible in a limited part of the river.

Channel stability in a system like the Carmel, so near the threshold between meandering and braided, is a precarious condition, subject to disruption by large flows or by local decreases in bank resistance. In banks composed of unconsolidated sands and gravels, willows are an important contributor to a bank's ability to resist erosion. Willows may be adversely affected by clearing of riparian forests for development, by phreatophyte elimination programmes, or by dropping the water table. It is encouraging that the well-vegetated narrow channel downstream of the unstable reaches remained stable, despite the enormous increase in bedload from the bank erosion. This implies that instability need not translate downstream, provided bank resistance is not otherwise affected.

ACKNOWLEDGEMENTS

This study was supported by a contract with the Monterey Peninsula Water Management District. For many helpful suggestions and criticisms, the authors are indebted to many, most notably John Williams, Luna Leopold, Barry Hecht, Gary Griggs, Bob Garrison and Gerry Weber. Mitch Swanson, Paul Boison, Graham Matthews, Larry Turner and others helped in the field and with ideas. Critical reviews of this manuscript by John Williams, John Cady, Robb Jacobson, Keith Richards, M. Gordon Wolman, and anonymous reviewers are gratefully acknowledged.

REFERENCES

Brice, J. C. 1964. 'Channel patterns and terraces of the Loup Rivers in Nebraska', *USGS Prof. Paper*, **422–D**, 41 pp.
Carlson, F. R. and Rozelle, K. D. 1978. *Carmel Valley Vegetation Study*, CH2M Hill, Inc., rept. of Monterey County Flood Control and Water Conservation District.
Charlton, F. G., Brown, P. M., and Benson, R. W. 1978. 'The hydraulic geometry of some gravel rivers in Britain', *Hydraulics Res. Sta. Rept. No. IT 180*, 48 pp.
Daniel, J. P. 1971. 'Channel movement of meandering Indiana streams', *USGS Prof. Paper*, **732–A**.
Graf, W. L. 1978. 'Fluvial adjustments to the spread of tamarisk in the Colorado Plateau region', *Geol. Soc. Am. Bull.*, **89**, 1491–1501.
Graf, W. L. 1981. 'Channel instability in a braided, sand bed river', *Water Res. Research*, **17**, 1087–1094.
Griffen, J. R. and Talley, T. 1981. 'Fire history, Junipero Serra Peak, Central Coastal California', in *Proc. Fire History Workshop. U.S. For. Serv. Gen. Tech. Rept.*, **RM–81**, 82–84.
Hadley, R. F. 1961. 'Influence of riparian vegetation on channel shape, northeastern Arizona', *USGS Prof. Paper*, **424–C**, 30–31.
Hecht, B. 1984. 'Sequential changes in bed habitat condition in the upper Carmel River following the Marble-Cone fire of August 1977', *Prof. Calif. Riparian Systems Conf., Univ. Calif., Davis.*
Kapple, G. W. and Johnson, M. T. 1980. *Digital simulation model for Carmel Valley groundwater basin* (Draft), USGS unpub. report to Monterey Peninsula Water Management District.
Kondolf, G. W. 1982. *Recent channel instability and historic channel changes of the Carmel River, Monterey County, California*, unpublished MS thesis, Univ. of California, Santa Cruz, 141 pp.
Lee, E. G. 1974. *A summary report of facts, analyses, and conclusions relating to the Monterey Peninsula water supply problems, PUC Case 9530*, unpublished report submitted to the California P.U.C., 10 Dec. 1974.
Leopold, L. B., Wolman, M. G., and Miller, J. P. 1964. *Fluvial Processes in Geomorphology*, San Francisco, Freeman & Co., 522 pp.
Maloney, L. M. 1984. *Aquifer–stream interaction in the lower Carmel Valley, July 1983–January 1984*, unpublished report to Monterey Peninsula Water Management District, 122 pp.

Nevins, R. H. F. 1969. 'River-training—the single thread channel', *New Zealand Engineering, December*, 367–373.

O'Loughlin, C. and Watson, A. 1979. 'Root-wood strength deterioration in Radiata Pine after clearfelling', *New Zealand Jour. Forestry Sci.*, **9**, 284–293.

Orme, A. R. and Bailey, R. G. 1970. 'Effect of vegetation conversion and flood discharge on stream channel geometry: the case of Southern California watersheds', *Proc. A.A.G.*, **2**, 101–106.

Parsons, D. A. 1963. *Vegetative control of stream bank erosion*, USDA Misc. pub. 970, paper no. 20, 130–136.

Schumm, S. A. and Lichty, R. W. 1963. 'Channel widening and flood-plain construction along Cimmarron River in Southwestern Kansas', *U.S.G.S. Prof. Paper*, **352–D**, 71–88.

Seibert, P. 1968. 'Importance of natural vegetation for the protection of the banks of streams, rivers, and canals', in *Freshwater: 3 studies*, Nature and Environmental series, Council of Europe, Strasbourg, 35–64.

Smith, D. G. 1976. 'Effect of vegetation of lateral migration of anastomosed channels of a glacier meltwater river', *Geol. Soc. Am. Bull.*, **87**, 857–860.

Turmanina, V. I. 1963. 'The magnitude of the reinforcing role of tree roots', *Moscow Univ. Herald Scientific Journal*, series V, No. 4, 78–80, translation by Dorothy Hiestrand, U.S. Forest Service, Arcata, California.

U.S. Army Corps of Engineers 1967. *Flood plain information on Carmel River, Monterey County, California*, 36 pp.

U.S. Army Corps of Engineers 1981. *Feasibility report on water resource development, Carmel River, Monterey County, California*, 13 pp.

Vanoni, V. A. (Ed.), 1975. *Sedimentation Engineering*, Am. Soc. Civil Eng., N.Y.

Williams, G. P. and Wolman, M. G. 1984. 'Downstream effects of dams on alluvial rivers', *USGS Prof. Paper*, **1286**.

Wolman, M. G. and Gerson, R. 1978. 'Relative scales of time and effectiveness in watershed geomorphology', *Earth Surface Processes*, **3**, 189–208.

Woodhouse, R. 1983. *Baseline analysis of riparian vegetation, lower Carmel Valley*, unpublished report to Monterey Peninsula Water Management District.

Ziemer, R. R. 1981a. 'Roots and stability of forested slopes', in *Erosion and Sediment Transport in Pacific Rim Steeplands. Int. Ass. Sci. Hydr. Publ.*, **132**, 343–361.

Ziemer, R. R. 1981b. 'The role of vegetation in the stability of forested slopes', *Proc. Int. Union of Forestry Res. Orgn. XVII World Congress, Kyoto*, **1981**, 297–308.

Zimmerman, R. C., Goodlett, J. C., and Comer, G. H. 1967. 'Influence of vegetation on channel form of small streams', *Symp. on River Morphology. Int. Ass. Sci. Hydr. publ. no. 75*, 255–275.

Zinke, P. J. 1971. *The effect of water well operation on riparian and phreatophyte vegetation in middle Carmel Valley*, unpubished report to Carmel Valley Property Owners Association, Reb. 1971.

Analysis of Potential Dam Removal/Retrofit Impacts to Habitat, Flooding and Channel Stability in the Carmel Valley, California

R.A. Mussetter[1] and S.C. Trabant[2]

[1,2]Mussetter Engineering, Inc., 1730 South College Avenue, Fort Collins, CO 80525; PH (970) 224-4612; FAX (970) 472-6062; Email bobm@mussei.com, stuartt@mussei.com

Abstract

The California Department of Water Resources, Division of Safety of Dams (DWR-DSD), has determined that San Clemente Dam on the Carmel River in Monterey County, California, does not meet seismic safety standards. Several alternatives are being considered to bring the dam to a safe condition. These alternatives include thickening of the approximately 22-m-high, concrete arch dam, lowering of the dam to the extent necessary to meet seismic standards, and complete removal. At the present time, the reservoir upstream from the dam, which had an original storage capacity of about 1.76M m^3, is nearly filled with sediment. An additional alternative has recently been suggested that would divert the Carmel River into San Clemente Creek near the head of the reservoir in a manner that would isolate about 80 percent of the sediment that is stored in the reservoir. The 31-km reach of the Carmel River downstream from the dam passes through urbanized areas within the Carmel Valley; thus, flooding and channel stability are matters of significant concern. In addition, the Carmel River contains habitat for the endangered steelhead and red-legged frog that could potentially be affected in both positive and negative ways by removal or lowering of the dam. Sediment-routing studies were conducted using the HEC-6T model to evaluate the response of the river to elevated sediment loads associated with the various removal/retrofit alternatives. The results are being used by the owners of the dam and the resource agencies to evaluate potential public safety impacts due to increased flooding and channel instability, as well as the potential for habitat restoration as the river recovers from the increased sediment loading. The modeling was performed in an interactive manner that allowed for management of complexities associated with the size-range and spatial distribution of the reservoir deposits and changes in the dam configuration. Results obtained from the modeling studies are believed to realistically describe the magnitude, and temporal and spatial distribution of erosion within the reservoir, and deposition and subsequent erosion in the river as the elevated sediment loads pass downstream.

Introduction

The California Department of Water Resources, Division of Safety of Dams (DWR-DSD), has determined that San Clemente Dam, an approximately 22-m-high, concrete arch dam located in Monterey County, California, does not meet seismic safety standards. Several alternatives are being considered to bring the dam to a safe-condition. These alternatives include thickening the dam, lowering the dam by about 6 m to increase its seismic stability, and complete removal. An additional alternative has recently been suggested that would divert the Carmel River into San Clemente Creek near the head of the reservoir in a manner that would isolate about 80 percent of the sediment that is stored in the reservoir, thereby allowing removal of dam without the attendant downstream sedimentation impacts. The dam removal option would restore aquatic and in-channel habitat through and upstream of the reservoir, including spawning habitat and rearing areas for steelhead, which was listed as an endangered species by the National Marine Fisheries Service (NMFS) in 1997. Since construction of San Clemente Dam in 1921, approximately 1.85M m^3 of primarily sand-sized sediment has deposited in the reservoir upstream from the dam, leaving less than 185,000 m^3 of the original 1.76M m^3 water-storage capacity of the reservoir sediment-free (Figure 1). Due to the relatively large volume of sediment that would be released, the originally-proposed dam removal alternative would likely be undertaken in phases, with progressive notching of the dam, followed by periods of sediment evacuation from the reservoir and downstream recovery.

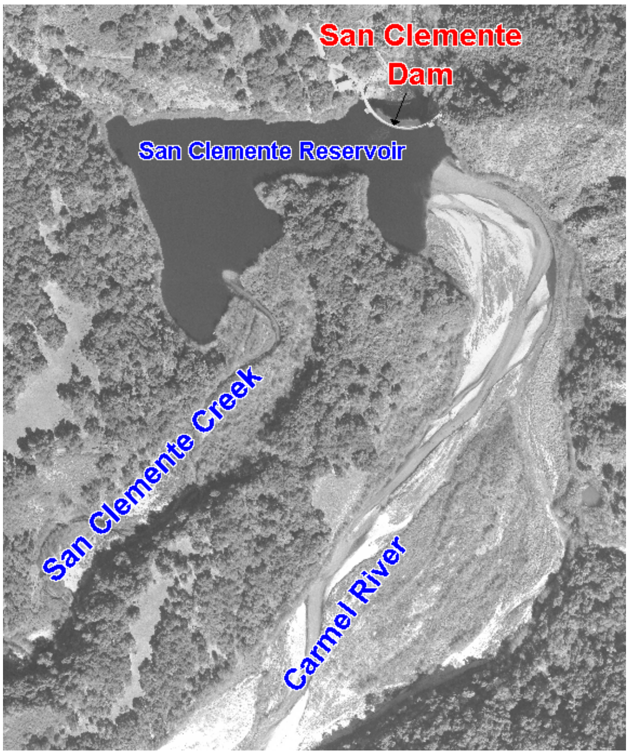

Figure 1. San Clemente Dam and San Clemente Reservoir.

Modeling Effects of Dam Removal

The decision-making process for dam removal involves not only an evaluation of the fiscal costs and benefits of removal, but also the costs and benefits to public safety and to the environment (EWRI, 2003; Graf, 2003). The most potentially detrimental aspect of dam removal involves the evacuation of reservoir sediments that were trapped throughout the lifetime of the dam (Heinz Center, 2002). Dam removal may have adverse effects on channel stability and flooding that can significantly affect public safety in urbanized areas, and on the health of in-channel habitat along the downstream channel, because of increased sediment loads (Doyle et al., 2003, Graf, 2003).

The use of sediment-routing models to evaluate the effects of dam removal on the downstream river provides a useful tool in the decision making process (ASCE, 1997). Modeling evacuation of deposited sediments from reservoirs requires knowledge of the size and distribution of the sediments (Cui et al., in press), since sediment size affects the rate of delta erosion and downstream movement of the eroded material (Doyle, 2003). Sediment-transport relationships used in the modeling should be carefully selected based on the size of sediment in the reservoir and the expected range of possible hydraulic conditions in the downstream river. Special care is warranted for channels where the existing bed material downstream from the dam is relatively coarse, but primarily fine sediments are stored in the reservoir (Cui et al., in press). Models should correctly address the deposition and subsequent erosion of sediments in the downstream reaches, especially where sediments deposit in the overbanks, causing floodplain accretion (Graf, 2003).

Modeling Approach Used for this Study

Consistent with the discussion in the previous section, the primary concerns about removal of San Clemente Dam are related to the effects of the evacuated reservoir sediments on flooding, channel stability, and in-channel habitat in the 31-km long reach of the Carmel River downstream from the dam that passes through the Carmel Valley where varying degrees of urbanization have occurred. Sediment-routing studies of erosion into the delta deposits in the reservoir during phased removal of the dam, and the subsequent movement of the released sediment through the downstream reach of the river between the dam and the Pacific Coast, were performed to assist the owners of the dam and the resource agencies evaluate the potential public safety impacts due to increased flooding and channel instability, as well as the potential for habitat restoration as the river recovers from the increased sediment loading. The studies were performed using the HEC-6T computer code (Thomas, 2003). Models were developed for both the reservoir and the downstream reach, and these models were executed over a 41-year period of simulated mean daily flows for a range of scenarios, including continued operation of the dam in its current configuration (i.e., baseline scenario) and several dam retrofit/removal scenarios (Table 1).

The rate of erosion of the reservoir sediments, and the temporal and longitudinal response of the downstream river to the increased sediment supply, will depend on the hydrologic sequence that occurs after the dam is lowered. Because of the uncertainty in the sequence that will actually occur, a sensitivity analysis was performed during the initial phases of the modeling to identify natural flow sequences that would cause the worst-case responses. The sensitivity analysis indicated that a wet period followed by an extended dry period, and a dry period followed by an extended wet period, caused to the greatest response at different locations along the reach. As a result, the key scenarios were ultimately modeled using two different hydrologic sequences that from the natural record that matched these two end-member conditions.

Table 1. Summary of sediment-routing model runs.

Scenario		Initial Hydrologic Condition	
		Wet	Dry
0	Baseline (dam reinforced and left in place)	X	X
1	Initial 5.8-m notch only	X	X
2	Initial 5.8-m notch, additional 4.6-meter notches in 5-year increments until dam removal	X	X
3	Initial 5.8-m notch, additional 4.6-m notches in 10-year increments until dam removal	X	X
4	Same as Scenario 2, except excavate overbank sediment before each 4.6-m notch	X	
5	Same as Scenario 1 with increased lateral inflows within reservoir	X	

Results obtained from the models were evaluated to estimate the impacts of each scenario on flooding, channel stability, and habitat conditions in the river downstream from the dam. The effects on flooding were evaluated by comparing maximum water-surface elevations and extents of inundation that would be experienced if the 100-year event occurred during each year of the simulation, based on modeled conditions on April 1. Damage-index values that provided a basis for evaluating the relative change in damages among alternatives for the worst-case year were also developed using standard depth-damage curves (Grigg and Helweg, 1975). Potential channel stability impacts were evaluated by comparing the predicted volumes of sediment deposited in the channel and the changes in bed elevation from each simulation with the baseline condition results. Impacts to in-channel habitat were evaluated by comparing changes in bed-material size, suspended-sediment load, and the effect of deposition on minimum flow depth thresholds for fish passage.

Reservoir Erosion Model

The reservoir portion of the sediment-routing model was developed to investigate the rate of erosion of reservoir sediments under the various dam retrofit/removal scenarios. The topographic data used in the model were derived from mapping of the existing deposits that was developed using aerial photogrammetry and hydrographic surveys of San Clemente Reservoir that were conducted in 2002.

Sediment data were derived from an extensive subsurface investigation of the sediment deposits in the reservoir that involved drilling, logging, and sampling of 17 soil borings and excavation, logging, and sampling of 13 test pits (Kleinfelder, 2002). The borings were conducted in the downstream, finer-grained portion of the reservoir deposits and they extended to refusal of the auger, which generally corresponded to the bedrock beneath the pre-dam alluvium. The test pits were excavated using a track hoe in the upstream portion of the reservoir, where the deposits were shallower and coarse-grained, and they extended to depths up to 5 m, subject to stability of the pit walls during excavation. Laboratory sieve analysis and hydrometer tests were performed on 152 samples that were obtained from the borings and test pits, and the results were used in conjunction with the existing and historic topographic mapping to evaluate the distribution of sediments in the reservoir. For purposes of the modeling, the stratigraphic sections were simplified to eliminate the discontinuous and interbedded layers that represent a relatively small percentage of the total quantity of material in the reservoir deposits (Figure 2), and composite gradations were developed for each of the stratigraphic intervals based on the volume-weighted average of the samples contained within the interval.

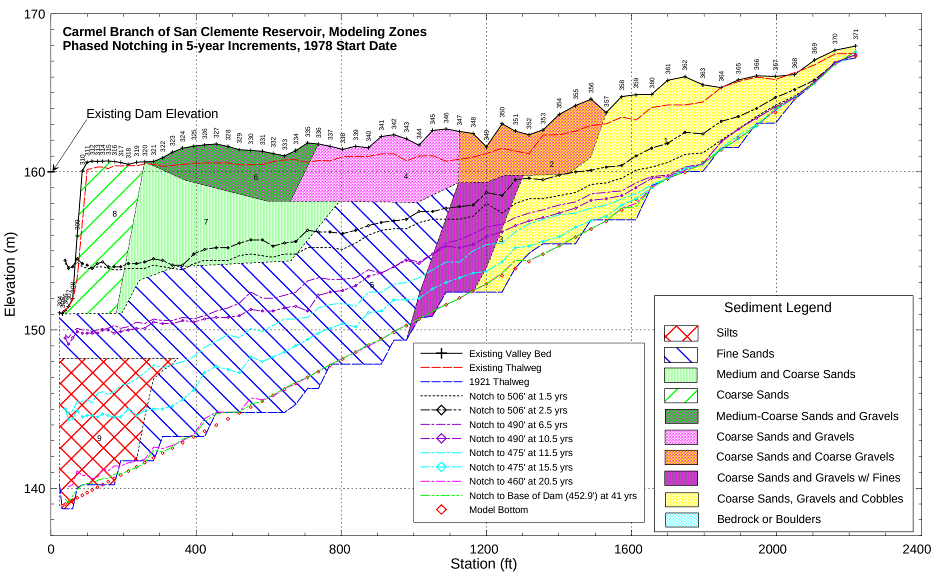

Figure 2. Longitudinal profile showing the sediment-size boundaries used in the model runs and the predicted bed profiles during the simulation for the Carmel Branch of San Clemente Reservoir.

The background sediment supply to the reservoir was specified using a sediment-rating curve that reproduced the estimated long-term sediment load to the reservoir. Annual background loads varied from 123.5 m^3/yr to about 117,200 m^3/yr, and averaged about 20,350 m^3/yr. Sediment transport capacities were computed in the both the reservoir and river portions of the model using the Toffaleti (1969)/Meyer-Peter-Müller (1948) relationship.

Flows are input to the HEC-6T model as a series of steady-state discharges. To achieve numerical stability, it was necessary to vary the time-step length as a function of discharge, with smaller time steps generally required for larger flows. A series of preliminary simulations were used to establish a relationship between the maximum stable time-step length and discharge, with the resulting lengths varying from 0.1 days (2.4 hours) at low discharges to less than 1 minute at higher discharges. In general, it was found that the rapid changes in the channel geometry near the headcut in the reservoir deposits controlled the time-step length. As a result, it was possible to use larger time steps in the baseline-conditions model than for the various dam removal scenarios. In addition, because changes in channel geometry are most significant following a notching event, smaller time steps were used immediately after notching of the dam, and time steps were lengthened later in the simulation to conserve computational time.

Because the HEC-6T code does not provide a mechanism to automatically change the configuration of the dam to reflect the phased notching associated with the dam removal scenarios, it was necessary to stop the model at the point in the simulation when the notch was to be constructed, manually change the cross section to represent the modified dam configuration, and then restart the model.

A significant complication in modeling the dam-notching scenarios arises because HEC-6T does not provide a direct mechanism for varying the gradation of the bed sediment reservoir with depth, and the vertical variation in grain size throughout the reservoir is significant (Figure 2). This problem was resolved by specifying the gradation of the upper stratigraphic layers in the initial phases of the model runs, and then comparing the simulated bed profile with the interval boundaries as the model progressed. When a significant portion of the bed profile crossed an interval boundary, the model was stopped, the bed-sediment reservoir gradation was manually changed, and the model was restarted from that point using the new gradation.

Under each of the dam removal scenarios, rapid erosion of the reservoir sediments occurred immediately after the notching events, followed by a more gradual flattening of the reservoir bed profile as the slope adjusted to the notch elevation (Figure 2). As expected, periods of significant reservoir erosion corresponded to high flow periods in the hydrologic record (Figure 3). For the scenario illustrated in Figure 3, the bulk of reservoir deposits stabilize about 2 years after the dam is notched to within about 2 m of the base, and a total of about 1.2M m^3 of the existing 1.85M m^3 of deposited sediment is removed from the reservoir over the duration of the simulation. The amount of sediment eroded from the reservoir for the other modeled scenarios ranged from about 240,000 m^3 if only a single 5.8 m notch is constructed to 1.2M m^3 if the dam is completely removed (Figure 4).

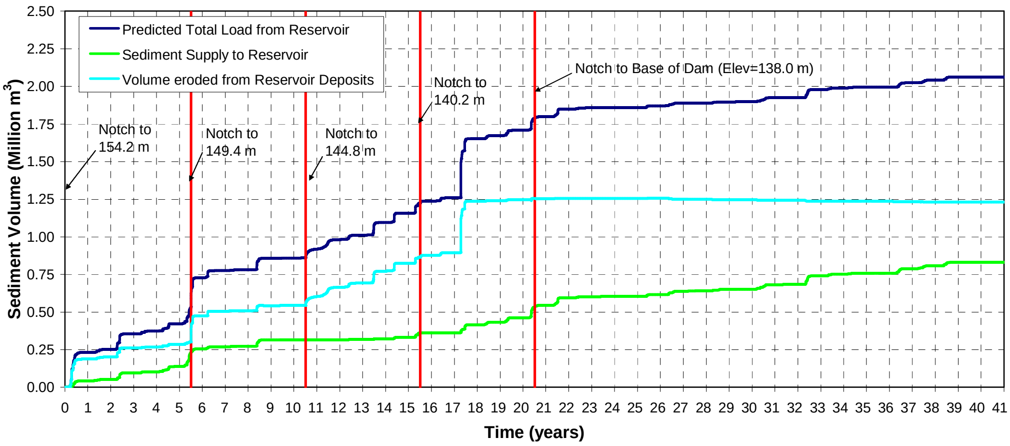

Figure 3. Example plot showing the sediment supply, predicted total load and volume of eroded reservoir deposits for Scenario 2, wet hydrologic conditions start.

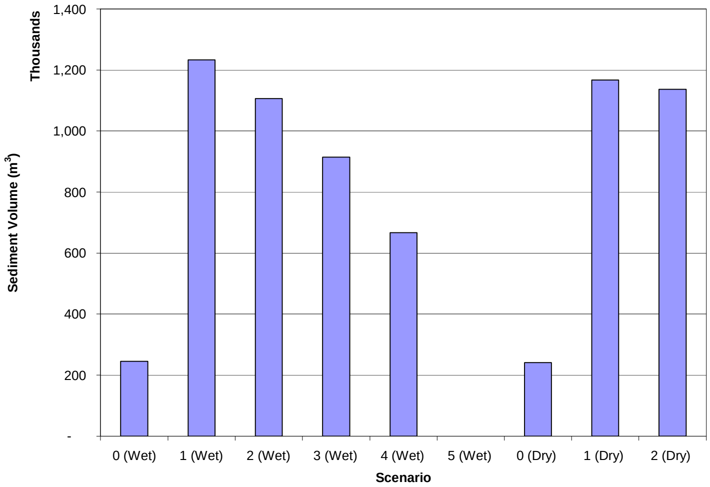

Figure 4. Volume of sediment eroded from reservoir deposits for each modeled scenario.

Modeling Effects on Downstream River

Results from the reservoir model were used to develop the inflowing sediment load (both rate and size gradation versus time) to the downstream river portion of the model. The geometric data used in the river model consisted of 234 cross sections and geometry for the numerous bridges along the reach that were developed from aerial mapping and field surveys. Under existing conditions, the channel roughness is significantly influenced by the size of the bed material, with coarser materials generally having greater roughness. Channel roughness (Manning's *n*) values used in the existing conditions model, and validated by comparing model results with rating curves for four gages along the reach, ranged from 0.035 in the sand-bed portions of the reach to 0.049 in the gravel and cobble-bed portions of the reach.

Under the dam retrofit/removal scenarios where significant quantities of sand-sized sediment are released into the downstream river, the larger particles will be covered with sand, resulting in a decrease in roughness. To account for this process, a modification to the HEC-6T code was implemented to vary the Manning's *n*-value as a function of the deposition depth predicted by the model. In applying this method, it was assumed that the bed roughness would decrease from the relatively high values used for the existing gravel- and cobble-bed portions of the reach to a lower-limit value of 0.035 when the bed is completely covered with sand. The depth of sediment required to cover the original bed sediments was estimated from measured maximum grain sizes.

Lateral sediment inflows from the five most significant tributaries along the reach were estimated using available data and information about the watershed and channel characteristics. Limits on the portion of the channel in which erosion or deposition could occur were specified in the input files so that deposition could occur at any point across the cross section, including the overbanks, but only erosion could occur within the active channel limits, resulting in permanent storage of sediments in the overbank areas to simulate typical floodplain accretion processes.

A significant complication in the modeling arises from the large size-difference between the existing bed material in the upstream approximately 25-km reach of the reach and the reservoir deposits that would be eroded and released into the downstream river under the various dam-removal scenarios. During periods when moderately high sediment loads are being released from the reservoir, the bed material will have a strongly bi-modal size distribution, and the sediment-transport relationships that are available in HEC-6T are not strictly applicable to this condition. During periods of high sediment releases, however, the existing coarse-grained bed will be covered with the sand-sized material that is released from the reservoir. The effects of these releases were, therefore, modeled by treating the existing bed as a nonerodible boundary on which the finer sediment can deposit, but into which erosion cannot occur. Although this assumption is a significant simplification, the model results are believed to adequately represent the deposition and re-entrainment processes that would actually occur during the dam removal process.

To evaluate the potential flooding impacts due to sediment storage associated with the different dam-removal scenarios, the modified cross sections from the sediment-routing model were exported to a step-backwater model that included detailed bridge geometry that cannot be used in the HEC-6T model, and this model was used to determine water-surface profiles for the 100-year flood peak.

The model results for the dam-notching scenarios generally indicated that a wave of sediment would build near the upstream end of the downstream river reach soon after the notch is constructed, and this sediment wave would translate and attenuate in the downstream direction. The specific timing of the translation depended strongly on the hydrologic sequence that occurred during the few years immediately after the notch, and the amount of attenuation of the wave was affected by both the hydrologic sequence, the geometric characteristics of the channel, and the presence of constrictions that cause backwater and upstream sediment storage. The total volume that remained in storage within the active channel at the end of the 41-year simulation period ranged from about 80,000 m^3 with only a single 5.8-m notch and initially dry conditions to over 720,000 m^3 with complete dam removal and initially wet conditions, and the amount of sediment stored in the overbanks ranged from about 60,000 m^3 to 170,000 m^3 (Figure 5).

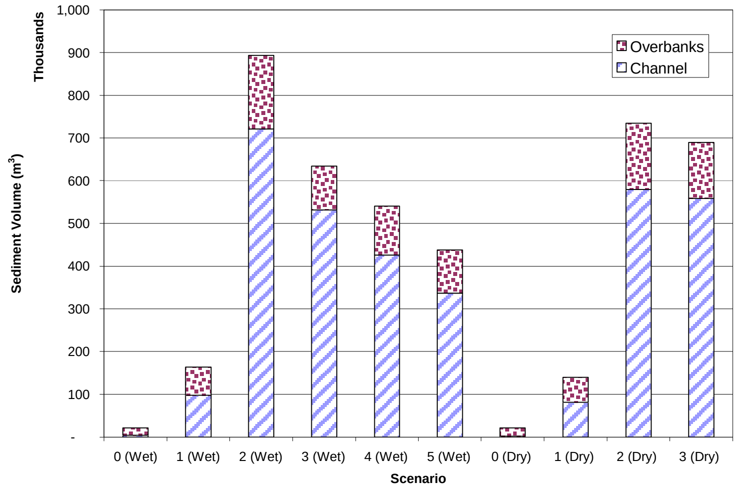

Figure 5. Volume of sediment stored in the channel bed and overbanks at the end of the simulation for each modeled scenario.

The model results for the various scenarios that were considered provided a means of quantifying the expected changes in a range of in-channel conditions, including average aggradation depth, changes in bed-material gradation during the high sediment-loading period, changes in occurrence of shallow areas where fish passage would be hindered during low-flow periods, and changes in the suspended-sediment concentration that could impact the health of fish that are passing through the reach. Impacts to overbank areas along the reach primarily focused on changes in flood damage potential. The flood-damage analysis generally indicated that the most significant effects occur upstream from channel constrictions where the most in-channel sediment storage would occur during the passage of the sediment wave. The relative change in damages from baseline conditions to the conditions that would occur under the various dam-notching/removal scenarios varied throughout the downstream reach. At some locations, developed areas that would not be subject to inundation during the 100-year flood peak under existing conditions would be inundated. In other areas, the depth of inundation increased from shallow flooding, where simple floodproofing measures such as low berms or minor grading changes that would cut off a particular flow path, are feasible to flooding of sufficient depth to cause extensive damages. At many locations, however, the incremental increase in damage potential was relatively small because most of the affected property improvements would be flooded to substantial depth during the 100-year event, even under existing conditions.

Conclusions

This HEC-6T sediment-routing study of San Clemente Reservoir and the downstream approximately 31-km reach of the Carmel River in Monterey County, California, assisted the dam owners and resource agencies to quantify the erosional response of the existing reservoir deposits and the commensurate response of the downstream river to elevated sediment loads associated with several scenarios for lowering or complete removal of San Clemente Dam. In general, the results showed that the magnitude and duration of the downstream river's response depends strongly on both the total amount of sediment that is exposed to erosion during the dam-lowering and removal process and on the specific hydrologic sequence that occurs during periods after the dam is lowered. The study also illustrated that, despite the significant challenges that must be met in modeling the complex erosional and depositional behavior of the reservoir deposits and downstream river, this type of modeling effort can provide valuable information to assist dam owners and resource agencies in making sound decisions regarding the most beneficial and cost-effective methods for solving public safety and environmental issues associated with our aging inventory of dams.

Acknowledgements

The studies that form the basis for this work were funded by American Water Works Company (AWWC) and the California Department of Water Resources (CDWR). The authors gratefully acknowledge AWWC's assistance and permission to use the study results provided by AWWC. We also wish to acknowledge assistance that was provided by CDWR staff, including John Shelton, Kevin Faulkenberry and Paul Romero.

References

American Society of Civil Engineers (1997). Guidelines for Retirement of Dams and Hydroelectric Facilities: Task Committee on Guidelines for Retirement of Dams and Hydroelectric Facilities. New York, New York, pp. 71-94.

Ayres Associates (2002). Mapping Report for San Clemente Reservoir.

Cui, Y. and Wilcox, A. (in press). Development and Application of Numerical Modeling of Sediment Transport Associated with Dam Removal. Appendix A, Stillwater Sciences, Berkeley, California, 65 p.

Doyle, M.W., Stanley, E.H. and Harbor, J.M. (2003). Channel adjustments following two dam removals in Wisconsin. Water Resources Research, v. 39, no. 1, 1011, pp. ESG2.1-ESG2.15.

EWRI Task Force on Dam Removal (2003). White Paper on Removal of Functioning Dams. 3 p.

Graf, W.L. (ed) (2003). *Dam Removal Research: Status and Prospects*. The H. John Heinz III Center for Science Economics and the Environment, Washington, D.C., 151 p.

Griemann, B. and Klumpp, C. (date unknown). Numerical Modeling of Sediment Migration during Dam Removal. U.S. Bureau of Reclamation, Denver Federal Center, Denver, Colorado, 6 p.

Grigg, N.S. and Helweg, O.T. (1975). State-of-the-art of estimating flood damage in urban areas. Water Resources Bulletin, American Water Resources Association, v. 11, no.2.

Heinz Center (2002). *Dam Removal: Science and Decision Making*. The H. John Heinz III Center for Science, Economics and the Environment, Washington, D.C., pp. 109-115.

Kleinfelder, Inc. (2002). Sediment Characterization Study, San Clemente Reservoir, Monterey County, California. Prepared for Mussetter Engineering, Inc. and American Water Works Service Company, November.

Meyer-Peter, E. and Müller, R. (1948). Formulas for bed-load transport. *In* Proceedings of the 2nd Congress of the International Association for Hydraulic Research, Stockholm, 2: Paper No. 2, pp 39-64.

Thomas, W.A. (2001). Sedimentation in Stream Networks (HEC-6T), User Manual.

U.S. Army Corps of Engineers (1990). HEC-2, Water Surface Profiles, User's Manual, Hydrologic Engineering Center, Davis, California.

MINES AND MINERAL RESOURCES OF MONTEREY COUNTY, CALIFORNIA

BY

EARL W. HART

California Division of Mines and Geology

COUNTY REPORT 5

California Division of Mines and Geology

1966

south (for descriptions of that deposit and recent plant operations see *Del Monte Properties Company—Fan Shell Beach deposit*).

The southern part of the Moss Beach deposit was leased to Owens-Illinois, who has produced large amounts of glass sand from the deposit continuously since 1943. This sand has been used to supply the feldspathic raw material necessary in the company's production of flint and colored glass, with the exception that a minor amount of biotite-rich heavy minerals has been sold for roofing and other purposes. The sand produced by Owens-Illinois is similar to other dune sand of the north Moss Beach and Fan Shell Beach deposits, being nearly white, medium grained, and well sorted. It is composed mainly of quartz and feldspar in subequal parts, with a small amount of biotite and other heavy minerals. The raw sand contains 0.12-0.15 percent iron oxide, about half of which is stains on the quartz and feldspar.

The sand is obtained from dunes covering an area some tens of acres in size and rising as high as 40 feet above the weathered granitic rock of a wave-cut terrace. Dune sand is bulldozed a maximum of 100 yards to a conical surge pile, at the base of which is a reclaiming tunnel. A vibrating hopper feeds the sand to a 24-inch conveyor belt which moves the material 2,400 feet northeast to a storage pile at the processing plant. Every 2 or 3 years, when the sand deposit is locally depleted, the reclaiming tunnel, hopper, and part of the conveyor system are removed to another part of the sand deposit. When visited in July 1959, the bulldozer operator was able to supply the plant with sufficient sand by working half a day for 5 days a week.

At the processing plant, raw sand from the storage pile is passed through a 1¼-inch mesh screen to remove occasional rocks and trash, and is stored at a surge pile. At a drawpoint, sand is reclaimed from the base of the surge pile as needed for processing in the enclosed washing section. The present washing section was installed in 1952 to replace an earlier installation. The sand first is washed in a trommel with a 12-mesh screen where water is added, and oversize (mostly pine needles) is removed. Next, the sand goes to a rake classifier where organic material and silt are removed, the water and fines flowing to a thickener nearby. A horizontal vacuum filter then dewaters the sand to 5½ percent water at a capacity of about 50 tons per hour and the sand is stored for subsequent drying. Some of the water used in this section is obtained from the municipal water system, but much of the water is reclaimed from the thickener. Sludge from the thickener is wasted.

After washing and classification, the sand is conveyed to the drying section where it passes through a rotary drier and rotary cooler. Fine sand from the drier exhaust is collected in a cyclone separator and recombined with the dried sand, which is elevated to a storage silo in the magnetic cleaning section of the plant.

Most of the sand stored in the magnetic cleaning section is processed by a battery of 14 Dings induced-roll, magnetic separators which remove the iron-bearing minerals from the sand. The magnetic fraction, which consists mainly of biotite with small amounts of ilmenite, garnet, monazite and other heavy minerals, is stored for possible future sale. Small tonnages of this material have been sold to manufacturers of roofing paper in the past. All of the magnetically cleaned sand and the sand not processed by magnetic separation are shipped by rail to the Oakland, Portland, and Tracy glass container plants of Owens-Illinois. Both products are used for their aluminous content (feldspars) and are admixed with silica sand from the company's Ione, California, plant. The company refers to the magnetically-cleaned sand as "flint" sand, which has an average iron oxide content of about 0.07 percent. The flint sand is used in the manufacture of clear glass. Sand not processed by magnetic separation contains 0.11-0.12 percent iron oxide and is used to make colored glass. Chemical and screen analyses of "flint" sand sampled April 1959 are given in Table 6. The processing plant operates 5 days a week and 8 hours per day, except for the magnetic cleaning section which is operated two shifts a day. Seven men were employed in July 1959.

Quaternary Stream Deposits

Reported production of sand and gravel from stream deposits has averaged nearly 500,000 short tons per year from 1959 to 1964. This is about twice the aver-

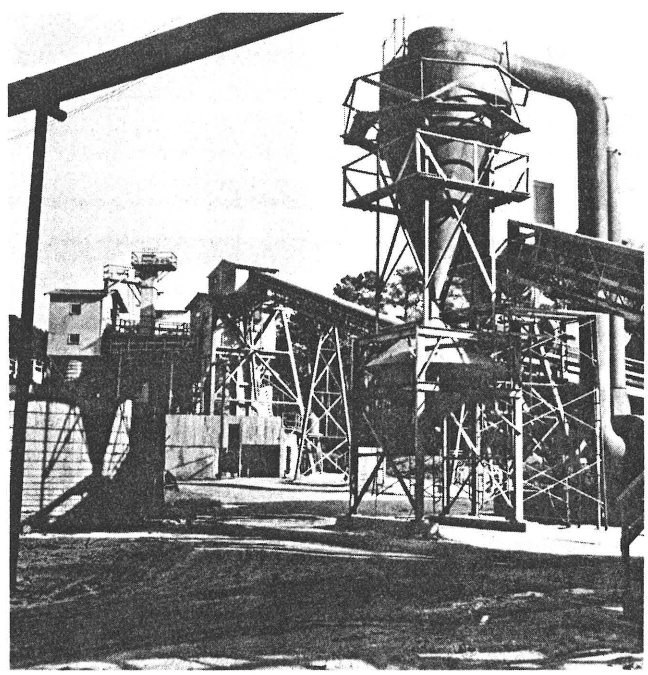

Photo 38. Owens-Illinois sand plant. Moss Beach dune sand, after screening and washing, is dried (right) and magnetically cleaned (background tower). Thickener tank (left) enables operator to reclaim water.

*Table 6. Chemical and screen analysis of Moss Beach "flint" sand produced by Owens-Illinois.**

Chemical analysis		Screen analysis	
Oxide	Percentage	U.S. sieve size	Percent retained on
SiO_2	80.44	20	0.0
Al_2O_3	11.68	30	0.6
Fe_2O_3	0.069	40	7.7
TiO_2	0.011	50	40.2
Na_2O	3.11	60	28.4
K_2O	2.79	70	16.4
CaO	1.66	80	5.9
Ignition loss	0.24	100	0.7
		140	Tr
Total	100.00%	−140	Tr
		Percent heavy minerals	0.013

* Sample collected by Owens-Illinois April 1959 and analyzed by S. F. Taylor, Chemist.

age production for the preceding 6 years and was due largely to increased highway construction.

Except for a few more or less continuous operations located near population centers in Monterey County, most of the sand and gravel is produced with portable equipment at pits located close to large construction projects. Upon completion of these projects, pit operations generally cease and the equipment is moved to another project. By far the largest use of stream sand and gravel is for crusher run base, concrete treated base, plant mix surfacing (i.e., asphalt concrete), and imported borrow in road construction. Only a few of the developed deposits provide materials of high enough quality for use in concrete. Other uses of sand and gravel include backfill, drain rock, filtration gravel, and roofing, landscaping and driveway gravel.

Stream deposits generally can be classified according to how they are formed and their present position within a given stream drainage. The following nomenclature is used for deposits described herein:

Stream channel—the present bed where a natural stream of water runs. The dry bed of an intermittent stream is called a *dry wash.*

Flood plain—that portion of a stream valley which is built of sediments as a result of periodic overflow of the present stream channel. The flood plain sediments are usually fine grained, but they may include coarser material of former stream channels.

Terrace or alluvial terrace—erosion remnants of an older flood plain which lie above the present flood plain.

Alluvial fan—a low fan-shaped feature formed by the deposition of sediments at the mouth of a stream valley where the stream leaves the mountains and enters an adjacent valley or plain.

Because the various deposits within a given stream valley are composed of similar rock material, the best quality and most easily developed deposits are usually developed first. In a great majority of cases, the shallow stream channel (or dry wash) deposits are less weathered and more accessible than the older and often thicker flood plain, terrace and alluvial fan deposits. They also require less beneficiation and are nearer to water supplies. Another advantage of channel deposits is that the aggregate resource is at least partly renewable as a result of periodic flooding. Monterey County is no exception to these generalities, and virtually all of the better quality material (i.e. other than that used for fill or imported borrow) has come from present stream channels or the younger portions of flood plains and alluvial fans adjacent to the present stream channels.

In addition to the variations existing between the different types of deposits of a given stream valley, there are very important variations that exist among the different drainages of the county. Variations in the composition of sand and gravel directly affects the physical and chemical quality of the aggregate. As can be seen on the Geologic Map (Plate I), a wide variety of formations supply the numerous stream drainages with many different kinds of rocks. The effects of weathering, stream transportation, and other factors further modify the composition, shape and size-distribution of the rock debris so that the final stream deposit is unlike any other deposit, either in the same stream valley or in other drainages.

The most important stream deposits in the county are tabulated in Table 7, where the type, description, and past development of the deposits are summarized according to stream drainages. An effort is also made to assess the potential value of the deposits and drainages with regard to possible future sources of aggregate material. The tabulation is necessarily arbitrary and incomplete. Much of the basic data used to draw conclusions were made available by the California Division of Highways (San Luis Obispo District, Materials Testing Section) in late 1959.

To 1962 the most important sources of stream sand and gravel have been the lower Carmel River and dry wash part of the Arroyo Seco. Although neither source contains material of outstanding quality, they are the best sources of structurally sound gravel in the northern and central parts of the county. The Salinas River deposits (channel, floodplain and terraces) are by far the largest in the county, but with few possible exceptions the coarse aggregate is considered unsuitable for use in portland cement and asphalt concretes and other structural uses where high quality is desired. Some of the terraces (Qt) shown on the geologic map (Plate I) are actually alluvial fans, in part, and are composed almost solely of material derived from adjacent tributary streams. As such, some of these fans, particularly along the front of the Gabilan Range, may contain material of good structural quality. Probably the best quality aggregate occurring in substantially large deposits are found in the lower course of the Sur River and in the middle and upper portions of the Nacimiento River. Unfortunately, these little-used sources are difficult to develop because of their relatively remote locations and because of recreational or military restrictions.

During 1960, at least 6 pits were active in Monterey County. Two of the operations (Valley Rock and Adobe Co. and South Counties Sand and Gravel Co.) were small and designed to meet a variety of local commercial needs. A third pit (Odello) supplied only minor amounts of filtration gravel on an intermittent basis. Two pits, (Haber and Wolter) provided road material under both private and public contracts. A sixth operation (Zabala deposit) was completing a large state contract for road construction materials. The deposits operated in 1960 are described below. With one major exception, the sand and gravel needs of the county are supplied by local deposits: coarse aggregate for portland cement concrete in roads and large structures is generally imported from Hollister (San Benito River gravel) and Logan Siding (crushed hornblende diorite) both in San Benito County. Other imported sand and gravel products also are used in marginal areas of the county as a matter of economics.

Haber deposit. Location: SW¼ sec. 16, T. 16 S., R. 1 E., M.D., on Carmel River east of bridge access to San Carlos Ranch. Ownership: E. H. Haber, leased to Granite Construction Company, Watsonville, in 1960.

The Haber deposit consists of Recent sand and gravel of the Carmel River channel which at this point is about 100 feet wide. The material is mainly of granitic derivation, but siliceous Monterey shale and metamorphic rock debris are present in small amounts. The early development history of this deposit is not known. Immediately prior to October 1959, the deposit was operated by Fisher and Stokes, Contractors. After that, Granite Construction Company worked the deposit as a source of road construction material for the nearby Carmel Hill housing subdivision. It is reported that the California Division of Highways used this same material for crusher run base, subbase and concrete-treated base in constructing State Highway 1 near Carmel Hill.

When visited in July 1960, the present operator was dismantling a 1,200-ton per day capacity portable plant. Sufficient crushed gravel (about minus one inch) was stockpiled to complete the company's contract. It is reported that the sand and gravel was crushed, screened to two size fractions and recombined according to specifications. The material was not washed. By October 1961, a small stockpile of processed material remained on the south bank of the river and this was drawn from only intermittently. The sand and gravel was obtained from the present stream channel north of the plant site. No pit was observed in the area and it is probable that the company stripped the stream gravels to a maximum depth of 5–10 feet for some distance along the stream course.

Odello deposit. Location: SE¼ sec. 13 (proj.), T. 16 S., R. 1 W., M.D., on south levee of Carmel River just east of State Highway 1. Ownership: Bruno Odello, Carmel, leased to Monterey Sand Company, Box 928, Monterey, 1959.

This deposit was worked about 1927–1933 by a man named Machado, who obtained sand and gravel from the river channel. The present operation was initiated in 1950 when Monterey Sand Company constructed a washing-screening tower on the south levee (Bruno Odello, personal communication, 1959).

Sand and gravel are obtained from a relatively narrow stream channel (less than 100 feet wide) confined between two levees and flanked by extensive flood plains. The gravel is mostly well rounded and of granitic origin, but metamorphic rocks and siliceous and diatomaceous shale are present. Mechanical analyses are not available, but the sand appears to comprise well over 50 percent of the deposit. Water is obtained from a shallow well near the plant.

As far as is known, the present operation has been small and intermittent and in recent years the plant has been operated only infrequently. When the plant is operating, material is dredged by dragline scraper from a 6-foot-deep pond in the stream channel and stored at a surge pile adjacent to the washing-screening tower. The sand and gravel are washed and screened to 6 size-fractions ranging from coarse sand to 2-inch gravel. Undersize sand and silt are returned to the river and the oversize cobbles are discarded at a nearby waste pile. The sand and gravel products are stored in drain bins for subsequent loading and trucking to Monterey Sand Company's Sand City sand plant (described under Quaternary Beach and Dune Deposits sub-section). The material is reportedly used mainly for filtration purposes. When visited in October 1961, the dredging equipment was inoperative and vegetation was growing in the bottom of the dry stream bed.

South Counties Sand and Gravel Co. (Cazin) deposit. Location: NE¼ sec. 21, T. 18 S., R. 7 E., M.D., ½ mile south of Metz. Ownership: South Counties Sand and Gravel Co. (A. B. Woodward, owner), Metz Road, King City, owns 67 acres.

The deposit, located at the mouth of Chalone Creek just west of the Metz Road, was operated at least as early as 1949 or 1950 by Max Cazin and since 1958 by the present operator. Production has been continuous, but small, since 1950.

This dry channel deposit is several hundred feet wide, and about 15 feet deep. It consists of about 80 percent sand and 20 percent gravel, almost all of the latter being of minus 2-inch size. (The following data, although based primarily on sand and gravel just east of the Metz Road, are believed to be as applicable to the South Counties deposit as it is to the Metz Aggre-

Table 7. Summary of geology and development of important Quaternary stream deposits, Monterey County

Deposits (Stream drainages)	Geology of deposits: Type and extent	Geology of deposits: Description of materials present[1]	Development of deposits: Utilization	Development of deposits: Name and location of pits (see text or tabulation at end of report for details)	Remarks (Potential use, restrictions, etc.)
Arroyo Seco	Stream channel (dry wash) deposit; extends from confluence with Salinas Riv. upstream 20 miles; lower 10 miles of braided channels average ½ mile wide and over 15′ deep; upper course averages about 100′ wide. Little or no overburden; replenished during infrequent floods. Additional deposits may occur in the flood plain and alluvial fan in the lower course of the Arroyo Seco.	Mainly granitic with lesser Monterey shale, Sur Series rocks, and Tertiary sandstone; at Zabala pit 30–50% is sand and 10–12% is +3″; one mile from confluence with Salinas River size and percentage of gravel diminishes and percentage of shale increases; upper course of deposit has abundance of cobbles and boulders. Material is marginal quality for portland cement concrete; shale more common in gravel sizes than in sand.	Important source of asphalt concrete aggregate and base materials in road construction in recent years. No commercial development.	Zabala (W½ 35-18S-6E) Clark (SE¼ 23-18S-6E)	Large reserves make this important source of structural aggregate for Salinas Valley area. Strong afternoon wind causes dust and is major drawback to commercial development.
Carmel River (lower)	Stream channel deposit; extends 15 miles from mouth to junction Tularcitos Cr.; channel relatively narrow, averaging 100′ wide and over 15′ deep; little or no overburden. Partial replenishment during floods. Extensive flood plain on lower reaches may also contain gravel deposits under silty veneer.	Mainly granitic with some Sur Series and Monterey shale type rocks; maximum gravel size about 8″ at head of valley; diminishes to 4″ maximum near State Highway 1 where it is excessively sandy. Some unsound and potentially reactive gravel makes deposit marginal for portland cement concrete.	Constant exploitation since 1920. Commercial production small—used for portland cement concrete, roofing gravel, drain rock. Non-commercial production large, intermittent—used for asphalt concrete and base materials in road construction.	Valley Rock & Adobe Co. (SE¼ 24-16S-1E) Haber (SW¼ 16-16S-1E) Wolter (NE¼ 21-16S-1E) Morse (SE¼ 29-16S-2E) Odello (SE¼ 13-16S-1W) Otey (W½ 13-16S-1W)	Channel deposit reserves probably moderate; rate of replenishment during flood is small compared to mining. Flood plain deposits may be large but not developed.
Carmel River (upper) and tributaries (includes Chupines, Tularcitos, San Clemente, and Cachagua Creeks)	Stream channel deposits locally developed, but generally narrow and shallow. Also, locally extensive flood plains and terraces.	Probably mainly granitic with Sur Series and minor Tertiary sedimentary types. Considerable variations expected among the different deposits (i.e. lithology, size-distribution, soundness, etc.).	Stream channel deposits supplied concrete aggregate to construct dams and spillway; also probably used for road construction.	California Water & Telephone Co. (NE¼ 8-18S-3E) and (SW¼ 24-17S-2E)	Deposits of limited accessibility, but potential source of road and dam construction materials for local projects.
Chalone Creek	Stream channel (dry wash) deposit; extends 3 miles upstream from confluence Salinas River; averages 150′ wide, widening near mouth where it is at least 15′ deep. Partial replenishment is effected during occasional floods.	Gravel consists mainly of acid volcanic rock (85%) with some granitic rocks and minor amounts of metamorphic rocks, serpentine, sandstone and shale; sand is mainly granitic with some volcanic fragments; at South Counties' pit, sand is 80% of deposit. Small percentage of plus 1½″ at confluence increase to about 10% plus 2″ 2–3 miles upstream.	Modest past production. Material used since 1910–1920 for portland cement concrete, bituminous aggregate, drain rock. Sand used with imported gravel for state projects.	South Counties (NE¼ 21-18S-7E) Metz (NE¼ 21-18S-7E)	Tests made by California Div. of Highways indicate gravel is sound and durable, but possibly reactive with high alkali cement.
Nacimiento River	Stream channel and flood plain deposits; extends from south county boundary upstream 20 miles; lower 11 miles as much as 1,000′ wide; upper reaches average 50–100′ wide. Additional deposits extend from Nacimiento Dam in San Luis Obispo Co. to confluence Salinas River in Monterey Co.	Mainly granitic and Sur Series rocks with less Franciscan type rocks and younger sandstone; gravel is coarse with abundant 3–6″ gravel near San Miguel Creek and abundant 3–4″ 7 miles downstream near U.S. Army pit.	Deposits utilized by Hunter-Liggett Military Reservation, but uses unknown. Deposits downstream from Nacimiento Dam (San Luis Obispo Co.) used to construct earthfill dam and concrete spillway.	U.S. Army (E½ 32-23S-7E)	Probably one of best quality deposits in county, but remoteness and military control prevents commercial development.
Northern Gabilan Range (includes Gabilan, Alisal, Quail and Natividad Creeks, and Chualar, Johnson and Henry Sands Canyons)	Stream channels (dry washes) and alluvial fans; channel deposits are mostly small; fans at stream mouths more extensive and locally lie on or interfinger with Salinas River alluvium.	Mainly derived from granitic rock and some Sur Series rock types; physical properties variable; fans probably are predominantly sandy.	Production entirely non-commercial; use mainly for road construction as plant mix surfacing, imported base, concrete treated base. Sand at Bardin Estate deposit possibly used for portland cement concrete.	Bardin Estate (S½ 2-15S-3E) Bardin Ranch (20-14S-4E) Hurt Ranch (SE¼ 12-15S-4E) La Macchia (NW¼ 29-16S-6E)	Channel deposits may be useful locally, but are small; fans potentially useful for road construction; dry streams present water problem; but groundwater may be available at depth.
Northern Sierra de Salinas (includes Toro Creek, San Benancio Gulch, Watson Creek and Calera Canyon)	Stream channels; mostly narrow and shallow.	Mainly granitic debris in sand and fine gravel sizes.	Used by county and state for base materials and plant mix aggregate in road construction.	Ferrini (NW¼ 17-16S-3E)	Probably limited to use as local source of road construction material.
Pancho Rico Creek	Stream channel (dry wash) deposits; extends several miles upstream from Salinas River; maximum width 100′; probably shallow.	In NE¼ 16-22S-10E gravel composed of sandstone, acid volcanic, granitic, Sur Series, Franciscan rocks, and siliceous and clay shales; sand mainly quartz and feldspar with rock fragments and mica; maximum gravel size 3″ or 4″; gravel comprised about 50% of sample examined.	Used by state for borrow and possibly base materials in highway construction.	Brennan (NW¼ 15-22S-10E)	Gravel contains soft or flat fragments of sandstone and shale; siliceous shale and some volcanics possibly reactive with high alkali cement.
Salinas River	Stream channel, flood plain, and terrace deposits; extends entire length of county; valley many miles wide, and channel locally one mile wide.	Mainly granitic and Tertiary sedimentary rocks including significant amount of clay shale and opaline shale; sand predominates over gravel except for local gravel lenses.	Some intermittent past production of stream bars and terrace gravels for road construction. No recent production except possibly for borrow. When used as portland cement aggregate in road, pavement deteriorated due to alkali reaction with siliceous shale.	Unnamed (SW¼ 24-20S-8E) State pits (near Bradley)	High proportion of unsound and reactive material restrict the use of this deposit mainly to imported subbase and borrow for roads.

Table 7. Summary of geology and development of important Quaternary stream deposits, Monterey County—Continued

Deposits (Stream drainages)	Geology of deposits		Development of deposits		Remarks (Potential use, restrictions, etc.)
	Type and extent	Description of materials present[1]	Utilization	Name and location of pits (see text or tabulation at end of report for details)	
San Antonio River	Stream channel deposit; extends about 40 miles upstream from confluence Salinas River; maximum width about 1,000′; upper 10–15 miles much narrower. Reserves in lower portion of river undoubtedly large.	Lower course of river is excessively sandy and gravel reported to be composed of abundant soft Tertiary sediments. However, U.S. Army pit 30 miles upstream from Salinas River consists of 50% gravel with abundant +1½″ sizes; gravel subrounded and mainly granitic and metamorphic with lesser amounts of sandstone and shale.	Local use at Hunter-Liggett Military Reservation.	U.S. Army (SW¼ 29-22S-7E)	Highest use of downstream portion of deposit probably restricted to imported sub-base and fill. Better quality deposits occur in upper course of river and possibly in tributaries.
San Lorenzo Creek-Lewis Creek	Stream channel deposits; extends many miles upstream from confluence Salinas River; at Boyd pit deposit is 100-200′ wide and over 10′ thick; at Eade pit near confluence Lewis Creek deposit is about 100′ wide and probably shallow. Gravel deposits in flood plain and stream terraces may be extensive downstream (e.g. at Monterey County pit), but have thin soil overburden.	Near mouth at Boyd pit, gravel consists of Franciscan types with lesser granitic, Tertiary sedimentary and volcanic rocks and comprises about 20% of deposit. Upstream at Eade pit, gravels are 50% of deposit. Terrace deposit at Monterey County pit is over 50% gravel with abundant sizes to 4″; gravel has similar lithology to channel gravel but is more weathered.	Intermittent production of channel deposits for many years; main use is for bituminous aggregate and imported base materials for county and state roads; county pit in terrace deposit also supplied plant mix and crusher run base material.	Eade (N¼ 14-19S-9E) Boyd (4-20S-8E) Monterey County (?) (SE¼ 33-19S-8E)	
Sur River	Stream channel deposit; extends upstream 1 mile from ocean; maximum width about 500 feet and average about 200 feet; at least 10′ deep. No overburden; replenished in flood stages. Additional deposits may occur in adjacent flood plain.	Mainly granitic rocks with lesser Sur Series and Franciscan type rocks; gravel comprises over 50% of deposit one mile upstream where 10–20% is +3″ and boulders are common. Gravel is subrounded and appears to be sound and durable.	Used by State Div. of Highways for structural backfill and by U.S. Navy for housing development; commercial use spotty and small.	Molera Ranch (NW¼ 15-19S-1E)	Limited test data indicate material to be excellent for portland cement concrete and all road construction uses. Development possibly restricted by residents or county.

[1] *Sur Series* rocks consist of gneiss, schist, crystalline limestone, quartzite and contact metamorphic rocks; *Franciscan type* rocks—includes indurated sandstone, chert, greenstone, serpentine, and vein quartz mainly; *Monterey shale*—mainly opaline shale with some clay shale and diatomaceous rocks.

gate Co. deposit.) According to an unpublished report of the California Division of Highways by H. D. Woods (1952), a sample of gravel from Metz Aggregate Company's raw materials stockpile, located immediately upstream, consisted of 85 percent volcanic rocks (mainly rhyolitic) and small amounts of quartzite, limestone, sandstone, schist and siliceous shale. Sand from the same place was composed of 85.6 percent granitic particles, quartz and feldspar; 9.3 percent volcanics; 3.9 percent mica; 0.6 percent siliceous shale; and 0.6 percent miscellaneous (mostly heavy minerals). Because partly-glassy volcanic rock and siliceous shale are present, the aggregate of Chalone Creek is considered to be potentially reactive with the alkali in portland cement, and preliminary tests seemed to bear this out in part. However, the material has been used successfully in concrete structures dating back more than 40 years. In addition, Chalone Creek sand was used with imported crushed granitic rock to make concrete for the State Prison at Soledad and for pavements and culverts in highway construction. After one to three years of service, none of the structures showed deleterious effects, according to Woods. This is too short a period to be conclusive and, unless proved otherwise, Chalone Creek aggregate (especially the gravel) should be used with low-alkali cement in making concrete. According to the results of several tests made by the California Division of Highways, Chalone Creek material has met all state specifications (as of 1952) for the physical quality of concrete aggregate. The continued local use of the gravel for concrete would seem to indicate the material can be used satisfactorily for concrete purposes. In addition, sand produced by South Counties was acceptable by the State Division of Highways for use with imported aggregate in portland cement concrete pavement for construction of U. S. Highway 101 in 1960–61.

South Counties Sand and Gravel Company purchased the deposit west of Metz Road in 1958 from Max Cazin, who produced only unwashed material for local use. (For additional data on the deposit east of Metz Road, see Metz Aggregate Co. in Tabulation at end of report.) The present pit is worked with two front-end loaders and dump trucks. The raw material is processed at an adjacent plant where it is washed and screened to four size-fractions—plus 1½-inch oversize, 1½-inch x ⅜-inch, ⅜-inch x ⅛-inch and minus ⅛-inch sand. The sand is classified by a 12-foot long screw. Maximum capacity of the plant is 50 tons per hour. Groundwater, obtained from a 120-foot well is reported to be ample. Oversize gravel is sold for drain rock. Most of the rest of the products are used for various local purposes, including concrete. The owner operates 4 transit mix trucks to supply local concrete needs. When specifications require it, crushed hornblende diorite from the Granite Rock Company quarry at Logan Siding, San Benito County, or gravel from the San Benito River near Hollister are used as the coarse concrete aggregate.

Insufficient data are available to determine the reserves of the South Counties Sand and Gravel Co.

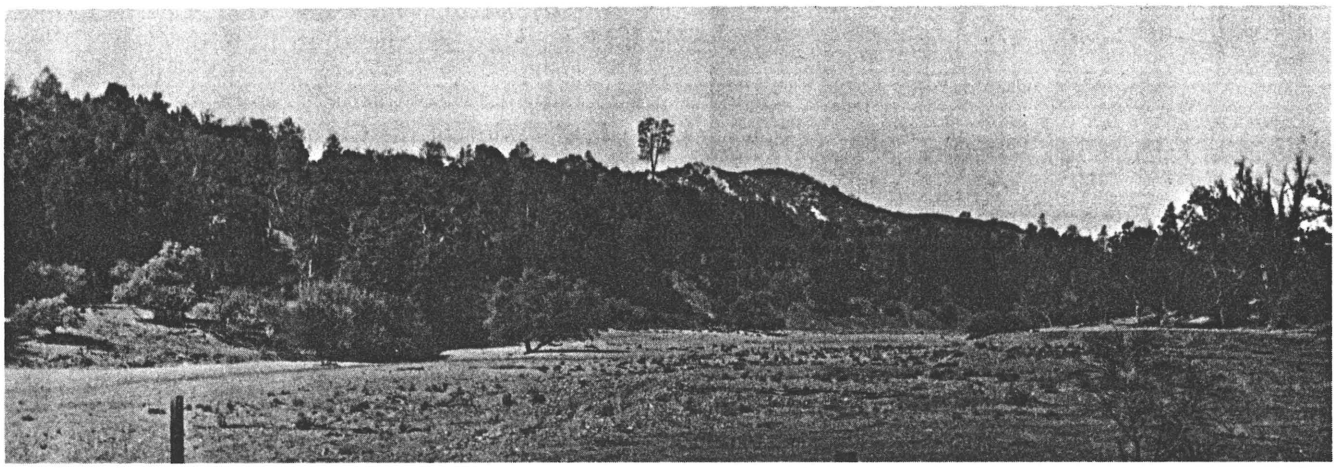

Photo 39. Nacimiento River channel and flood plain deposit in sec. 32-23S-7E. This deposit is 100 yards wide and 1 mile long and is composed of good quality aggregate. This and other deposits along the Nacimiento River are mostly undeveloped due to distance from market and current military ownership.

deposit, but the presence of fine sand at a depth of about 15 feet at one point indicates sand and gravel reserves to be rather small. However, additional reserves are exposed in the channel for a distance of 3 miles upstream. Some material may also be present in the floodplain near the mouth of the Creek. The resources are partly renewed during infrequent floods (last one, winter 1957–58).

Valley Rock and Adobe Co. (Murphy) deposit. Location: SE¼ sec. 24, T. 16 S., R. 1 E., M.D., on Carmel River immediately east of Farm Center. Ownership: Valley Rock and Adobe Company (John B. Simpson, owner), P.O. Box 64, Carmel Valley.

Sand and gravel are obtained commercially from the present stream channel of the Carmel River by the Valley Rock and Adobe Co. who purchased the property from M. J. Murphy in 1955. The former owner first obtained material from the Carmel River about 1920, and established the present plant in 1928. The plant has been operated continuously ever since then on a small scale. The small, permanent, crushing-screening plant is located adjacent to the main pit.

The gravel, most of which is smaller than 2 or 3 inches, appears to comprise about 30–40 percent of the excavated material. It consists mainly of granitic rock with some metamorphic rocks of the Sur Series and a small amount of siliceous shale of the Monterey Formation (the owner estimates 3 percent siliceous shale). The gravel is rounded to subrounded. The sand is derived mainly from granitic rock and is subangular.

Sand and gravel are obtained from the stream channel within one-quarter of a mile of the plant. The material is partly replenished during occasional flood stages of the river. However, additional sand and gravel have been obtained from other points in the river channel within a distance of one mile from the plant. The material is excavated by a bulldozer and a small-capacity front end loader. A dump truck is used to transport some of the material to the plant.

At the plant, the gravel is crushed to minus 1½ inches and part of this goes to a bunker without washing. This product is sold locally, mainly as concrete aggregate. The rest of the material is washed in a re-

Photo 40. South Counties Sand and Gravel Co. pit at the mouth of Chalone Creek. Although wide near the mouth, this dry wash deposit narrows to 150 feet wide less than 1 mile upstream. The deposit is excessively sandy at this location.

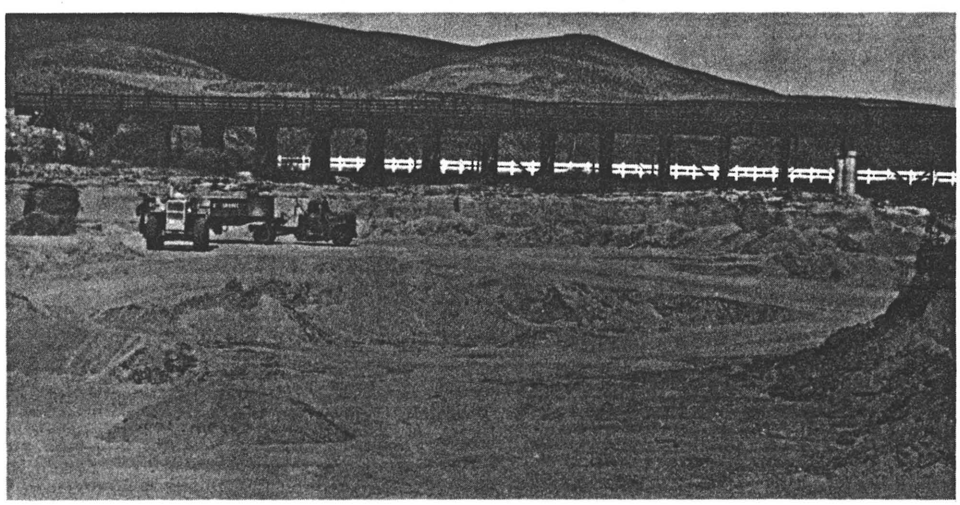

Photo 41. Valley Rock and Adobe Company's sand and gravel pit. This Carmel River stream channel deposit is narrow, being confined by levees over a distance of 15 miles upstream from the mouth. The stream normally flows most of the year, but after three successive "dry" winters the channel was completely dry in October 1961.

volving trommel and sized by screens having ¾-inch, ⅜-inch and 4-mesh openings, the separate fractions being stored in individual bunkers. Sand (minus 4-mesh) is sold mainly to nearby Valley Transit Mix Co. for use in ready mix concrete; pea gravel (⅜-inch x 4 mesh) is sold mostly as driveway and roofing gravel; ¾-inch x ⅜-inch gravel is sold for concrete and 1½-inch x ¾-inch material is used by the owner for drain rock in the construction of septic tanks. Capacity of the plant is reported to be 100 tons per day.

Wolter Deposit: Location: NE¼ sec. 21, T. 16 S., R. 1 E., M.D., on the north levee of Carmel River. Ownership: Luis F. Wolter, Carmel Valley, leased to Phil Calabrese (contractor), Sand City, 1961.

This portion of the Carmel River channel has been worked intermittently for 10 years by Monterey County as a source of road construction material. The sand and gravel appears similar in size-gradation and composition to other nearby channel deposits (see under Haber and Valley Rock and Adobe Co.), being mainly of granitic origin. The channel deposit is about 100 feet wide, but the depth is not known. This property was leased early in 1960 by Phil Calabrese, who installed a portable crushing-screening plant of substantial capacity.

When visited in July 1960, sand and gravel was bulldozed from a shallow pond in the river channel into a surge pile. From there the material was conveyed to the portable plant where it was crushed to minus 1½-inches. Part of this was stockpiled directly and part screened to plus ⅜-inch and minus ⅜-inch fractions. The material was not washed. Most of the output was used by the operator to construct streets at a nearby residential subdivision, but some was sold to Monterey County for road construction material. The plant had been removed when last visited in October 1961 and only a small stockpile of crushed material remained. At that time, the river was not flowing.

Zabala deposit: Location: W½ sec. 35, T. 18 S., R. 6 E., M.D., 2 miles west of Greenfield. Ownership: Walter Zabala, Greenfield, leased to Delphia-Early Co. operating under a contract with the California Division of Highways, 1960.

The Zabala deposit has not been investigated sufficiently to determine its exact nature, but brief obser-

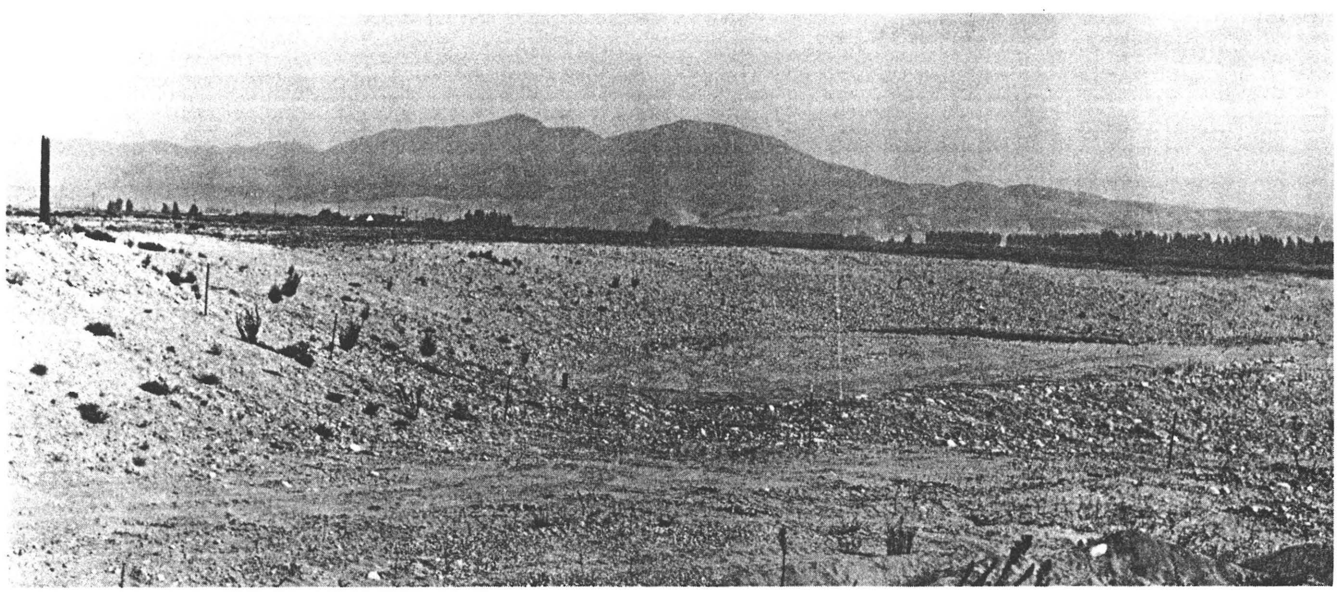

Photo 42. Zabala sand and gravel pit near Greenfield was used as an important source of base materials and asphalt concrete aggregate in construction of U.S. Highway 101 in 1958–61. Pit is developed in Arroyo Seco dry wash. The deposit is one of the largest in Monterey County, having a length of 10 miles and average width of about ½ mile.

SAND & GRAVEL—Continued

Map No.	Name of claim, mine, or group	Location	Owner (Name, address)	Geology	Remarks and references
116	Del Monte Properties Co. — Fan Shell Beach	Near SE cor. sec. 33, T. 15 S., R. 1 W., M.D., 4 miles southwest of Pacific Grove.	Del Monte Properties Co., Sand Dept., 620 Market St., San Francisco (1961)	Recent sand dune deposit.	Important source of glass sand and other specialty sands since 1955. Dune sand from Moss Beach supplied sand prior to that. Plant located 1 mile south of Pacific Grove. Pacific Improvement Co. was predecessor of present operator. (Aubury 06:278; Waring and Bradley 19:614; Boalich 21:157; Laizure 25:54–55; Sampson and Tucker 31:440; Wright 48:44–45; Lenhart 52:100–103; Utley 53:90–92; Messner 54:5–8; Gay 57:547, 548, 560; herein under Quaternary Beach and Dune Deposits).
117	Del Monte Properties Co.—Sawmill Gulch	Sec. 26, T. 15 S., R. 1 W., M.D., 2 miles southeast of Pacific Grove.	Del Monte Properties Co., 620 Market St., San Francisco (1963)	Quaternary deposit of dune sand and granitic wash.	Developed by prospect pit and drill holes. Potential source of specialty sand. (Herein, under Quaternary Beach and Dune Deposits, Monterey Peninsula Area).
118	Eade..............	N½ sec. 14, T. 19 S., R. 9 E., M.D., 10 miles northeast of King City.	H. T. Eade, Lonoak (1960)	Recent stream channel deposit in San Lorenzo Creek. Consists of 50% gravel to 3 inches and 7% minus 200-mesh where developed.	Deposit operated intermittently in recent years and on small scale. Material is crushed and screened in portable plants by various contractors. Used mainly by state as imported base and road mix aggregate.
119	Ferrini.............	NW¼ sec. 17, T. 16 S., R. 3 E., M.D., 9 miles south of Salinas.	Not determined.........	Sand and fine gravel from small stream channel deposit on north fork of Watson Creek.	Material screened and used as base material and plant mix aggregate for county roads.
120	Gould............	SW¼ sec. 15, T. 19 S., R. 6 E., M.D., 4½ miles southwest of Greenfield.	E. C. and F. E. Gould, Greenfield (1960)	Moderate-sized deposit of sand and gravel mapped as Paso Robles Formation, but may be younger stream terrace deposit. Gravel comprises about ½ of deposit and consists mainly of granitic and metamorphic rocks with some siliceous and diatomaceous shale and sandstone in the finer sizes. The sand is mainly quartz, feldspar and granitic fragments.	Developed by hillside pit 100 feet by 200 feet with maximum face of 50 feet. Used intermittently in recent years by County as road fill, but probably could be used for higher road construction purposes. Oversize boulders scalped from gravel are stockpiled and could be used as a small source of crushed rock. Pit was inactive in June 1960.
121	Granite Construction Co.	SW¼ sec. 15, T. 15 S., R. 1 E., M.D., in Sand City.	Granite Construction Co., Watsonville (1961)	Recent beach and dune sand.	Deposit operated since late 1940's as source of fine aggregate used in adjacent concrete and asphalt plants. Active 1961. (Herein, under Quaternary Beach and Dune Deposits).
122	Haber.............	SW¼ sec. 16, T. 16 S., R. 1 E., M.D., 3 miles southwest of Carmel.	E. H. Haber, Leased by Granite Construction Co., Watsonville (1960)	Sand and gravel from stream channel deposit, Carmel River.	Moderately large production 1959–1960. Supplied base materials in state highway and subdivision road construction. (Herein, under Quaternary Stream Deposits).
123	Hurt Ranch.........	SE¼ sec. 12, T. 15 S., R. 4 E., M.D., 5 miles northwest of Chualar.	Hazel Hurt, Salinas (1960)	Stream channel deposit of Quail Creek. Consists of 50% gravel, including 15% plus 3-inches. Pit not visited, but channel deposits just below appear insignificant in size.	Granite Construction Co., Watsonville, crushed material to minus ¾-inch for use as asphalt concrete aggregate in State highway construction 1951. Inactive 1961.
124	La Macchia.........	NW¼ sec. 29, T. 16 S., R. 6 E., M.D., 5½ miles east of Gonzales.	La Macchia Ranch (1960)	Sand and gravel from dry wash. Composed mainly of granitic debris. Channel deposit narrow and probably shallow.	County reportedly used as road mix aggregate.
	Lake Majella........	....	....	....	Previous name for sand dune deposits near Moss Beach; formerly utilized by Del Monte Properties Co. (which see) and since 1943 by Owens-Illinois (which see).
	Lapis..............	....	....	....	See Pacific Cement and Aggregates, Inc.—Lapis.
	Machado..........	....	....	....	See Odello.
125	Metz..............	NE¼ sec. 21, T. 18 S., R. 7 E., M.D., at Metz	Samuel T. Mathews, Metz (1961)	Sand and gravel deposit in dry channel of Chalone Creek, east of Metz Rd. The percentage and sizes of gravel not determined, but probably slightly coarser than adjacent pit of South Counties Sand and Gravel Co. (which see for geology).	Pit operated by Metz Aggregate Co., a subsidiary of Granite Construction Co. of Watsonville, for 10 years prior to early 1959 when the operation was abandoned. The sand and gravel was washed, screened, scrubbed in a trommel, and crushed to minus one-inch. The sand was ground in a ball mill and classified to meet grading specifications. Material mainly used in local transit mix operation. When higher specifications required, crushed granitic rock from Logan was substituted for the coarse aggregate (e.g. in construction of Soledad Prison). The plant was active about 2 months per year and production was probably modest. Inactive and plant equipment removed.
126	Molera Ranch.......	NW¼ sec. 15 and NE¼ sec. 16, T. 19 S., R. 1 E., M.D., 4 miles northwest of Big Sur.	Mrs. Frank Molera, Big Sur (1961)	Stream channel and floodplain deposit on the Sur River. Coarse aggregate comprises a substantial part of the deposit which was derived from granitic and metamorphic rocks and some Franciscan type rocks. The aggregate appears to be sound	Developed by several pits and trenches as much as 15 feet deep. The excavations were made by Paul Woof in 1957, Granite Construction Co. in 1959–1960, and possibly others. The material used for the Point Sur Navy housing development was processed by portable equipment, but the details of this were not determined. Some of the sand and gravel also was used, without processing, as struc-

SAND & GRAVEL—Continued

Map No.	Name of claim, mine, or group	Location	Owner (Name, address)	Geology	Remarks and references
	Molera Ranch —Continued			and durable. Deposit in channel and banks average about 150 feet wide, one mile long, and more than 15 feet thick. Additional deposits may exist in wide floodplain near mouth of river.	tural backfill behind concrete cribbing along State Highway 1.
127	Monterey County (?).	SE¼ sec. 33, T. 19 S., R. 8 E., M.D., 2 miles northeast of King City.	Not determined (leased by Monterey County?) (1960)	Sand and gravel from terrace deposit of San Lorenzo Creek. Where developed, it consists of 40% gravel and 4% minus 200-mesh. Thin soil overburden. Gravel is rounded to subrounded and consist of Franciscan type rocks with lesser granitic, volcanic and Tertiary sedimentary rocks, including some soft and siliceous shales.	Developed by trench 300 x 50 x 15 feet. Used by county as source of subbase, crusher run base, and plant mix aggregate in construction of Bitterwater Road, 1948. Not active (?).
128	Monterey Sand Co. —Marina	Center sec. 24, R. 14 S., T. 1 E., M.D., 1 mile northwest of Marina.	Monterey Sand Co., Box 928, Monterey (1961)	....	Beach sand deposit and plant; operated continuously since about 1944. (Herein under Quaternary Beach and Dune Deposits).
129	Monterey Sand Co.— Sand City	SW¼ sec. 15, T. 15 S., R. 1 E., M.D., in Sand City.	Monterey Sand Co., Box 928, Monterey (1961)	....	Beach and dune sand deposit worked at least as early as 1931 by Sydney Ruthven. The present owner operated deposit and sand plant since 1946. (Pit and Quarry 49: 83–84; Gay 57:517; herein, under Quaternary Beach and Dune Deposits).
130	Monterey Sand Co.— San Jose Creek	SE¼ sec. 23 T. 16 S., R. 1 W., M.D., 2 miles south of Carmel.	State of California (1960)	Beach and dune sand deposit at mouth of San Jose Creek. Deposit consists of very coarse grains of quartz, feldspar, and granitic debris piled in drifts as much as 15–20 feet high.	Developed to a minor extent in the early 1950's by Monterey Sand Co. for use as filtration sand. The sand was processed at the company's Sand City plant. Deposit is inactive and now part of the Carmel River Beach State Park and Bird Sanctuary.
131	Morse.............	SE¼ sec. 29, T. 16 S., R. 2 E., M.D., 9 miles east of Carmel in Carmel Valley.	Morse property (1960)	Stream channel deposit of Carmel River. Sand and gravel mainly of granitic composition; contains 45% gravel and 3% minus 200-mesh.	Pit located ½ mile west of Los Laurelles Grade Rd.; developed by Madonna Construction Co. under state contract. Material crushed and used as imported base and asphalt concrete aggregate in construction of Los Laurelles Grade Road, 1959–1960. Some material also stockpiled for county use as base material and road mix aggregate 1959–1960. Inactive late 1960.
	Murphy...........	....	....	....	See Valley Rock and Adobe Co.
132	Odello............	SE¼ sec. 13, T. 16 S., R. 1 W., M.D., 1 mile southeast of Carmel.	Bruno Odello, Carmel, leases to Monterey Sand Co., Box 928, Monterey (1960)	Sand and gravel in stream channel of Carmel River.	Deposit worked intermittantly since 1927, first by a man named Machado and most recently by Monterey Sand Co. (Herein, under Quaternary Stream Deposits).
133	Otey..............	SW¼ sec. 13, T. 16 S., R. 1 W., M.D., one mile south of Carmel.	Not determined.........	Sand from channel or floodplain of Carmel River.	Albert Otey produced plaster sand from pit near mouth of river in the 1920's. The sand was not processed, but was shovelled directly into trucks for marketing. (Laizure 25:57; Sampson and Tucker 31:441).
134	Owens-Illinois— Moss Beach (Lake Majella)	SE¼ sec. 22, T. 15 S., R. 1 W., M.D., 2 miles southwest of Pacific Grove.	Owens-Illinois 350 Sansome Street, San Francisco (1961)	Recent dune sand.............	Used since 1943 as source of feldspathic glass sand. Company processes at a nearby sand plant for shipments to Oakland factory. (Wright 48:44; Gay 57:548, 562; herein, under Quaternary Beach and Dune Deposits). North part of deposit worked by Pacific Improvement Co. 1903–1920 and Del Monte Properties Co. (which see) 1921–1955 until depleted (Aubury 06:278; Waring and Bradley 19:614; Boalich 21:157; Laizure 25:54–55; Sampson and Tucker 31:440).
135	Pacific Cement and Aggregates, Inc.— Lapis	E½ sec. 13, T. 14 S., R. 1 E., M.D. 2 miles north of Marina.	Pacific Cement and Aggregates, Inc., 400 Alabama St., San Francisco (1961)	....	Beach and dune sand deposits worked by E. B. and A. L. Stone (1906–1918); Bay Development Co. (1918–1928); and present owner (since 1928). Material is processed at nearby plant. (Waring and Bradley 19:614–615; Laizure 25:55; Sampson and Tucker 31:441; Wright 48:45–46; Gay 57:548, 553; herein, under Quaternary Beach and Dune Deposits).
136	Pacific Cement and Aggregates, Inc. —Prattco	N½ sec. 15, T. 15 S., R. 1 E., M.D., 1 mile north of Seaside.	Pacific Cement and Aggregates, Inc., 400 Alabama St., San Francisco (1961)		Beach and dune sand deposit operated by Pratt Building Materials Co. since 1921 and by the present owner since 1929. (Laizure 25:55–56; Sampson and Tucker 31:441; Gay 57:548; herein, under Quaternary Beach and Dune Deposits).
	Pacific Improvement Co.	....	....	....	See Del Monte Properties Co. and Owens-Illinois.
	Pratt Building Materials Co. (Prattco)	....	....	....	See Pacific Cement and Aggregates, Inc.—Prattco.
	Prattco Sand Pit No. 4	....	....	....	See Pacific Cement and Aggregates, Inc.—Prattco.
137	Seaforth Corp.......	W½ sec. 25, T. 14 S., R. 1 E., M.D., one mile southwest of Marina.	Seaforth Corp., Dewitt Rucker, Pres., Box 314, Pebble Beach (1960)	Large Recent dune deposit......	Company owns 200 acres of dunes just north of Fort Ord. A moderate amount of sand was produced in 1959 and 1960 mainly for use as fill. The owner reports land is to be subdivided for housing development.

SAND & GRAVEL—Continued

Map No.	Name of claim, mine, or group	Location	Owner (Name, address)	Geology	Remarks and references
138	Seaside Sand and Gravel Co.	NW¼ sec. 24, T. 14 S., R. 1 E., M.D., one mile northwest of Marina.	Seaside Sand and Gravel Co., Inc., P.O. Box 513, Marina (1961)	....	Beach sand obtained and processed at nearby plant since 1957. (Calif. Div. Mines 58: 11–12; herein, under Quaternary Beach and Dune Deposits.)
139	South Counties Sand & Gravel Co. (Cazin)	NE¼ sec. 21, T. 18 S., R. 7 E., M.D., ½ mile south of Metz	South Counties Sand & Gravel Co., (A. B. Woodward, owner), Metz (1961)	....	Small sand and gravel operation at mouth of Chalone Creek. Formerly owned by Max Cazin. (Herein, under Quaternary Stream Deposits.)
140	Titus..............	NE¼ sec. 2, T. 16 S., 2 E., M.D., 7 miles southwest of Salinas	T. W. Titus, 240 Benancio Rd., Salinas (1960)	Poorly-consolidated conglomerate (fanglomerate?) of the Paso Robles Formation. Consists of angular debris derived from granitic and metamorphic rocks. The material is mainly sand.	Pit developed 1945–1955 by several contractors who used material as subbase in state road construction. Two other inactive pits in similar material located nearby to the east and southeast. (Also see herein under Older Formations.)
141	Turkey Flat.........	S¼ cor., sec. 32, T. 23 S., R. 15 E., M.D., 3 miles southeast of Parkfield	Not determined.........	Stream terrace deposit consisting of interbeds of sand and gravel. At the pit, the gravel comprises about 50% of the material and consists of serpentine, silica-carbonate rock and Franciscan rock types.	Developed by a pit 50 feet by 100 feet by 12–14 feet. Although no equipment was at pit when visited April 1960, it is apparent pit was operated recently. The use of the material is not known, but it would appear to be restricted to use as fill or subbase material.
142	U.S. Army (Nacimiento River)	E½ sec. 32, T. 23 S., R. 7 E., M.D., 6½ miles southwest of Jolon	U.S. Army, Hunter-Liggett Military Reservation (1961)	Sand and gravel deposit in stream channel and floodplain of Nacimiento River. Deposit is large, being at least 100 yards wide and a mile long. Gravel comprises about 50% of material at pit and consists of granitic and metamorphic rocks with minor sandstone and some Franciscan rock types. The material appears to be of good quality and probably suitable for use as concrete aggregate. Similar material occurs over a distance of 20 miles upstream from the county boundary.	Developed by small pit 8–10 feet deep in floodplain. Material used by U.S. Army for unknown purposes.
143	U.S. Army (San Antonio River)	SW¼ sec. 29, T. 22 S., R. 7 E., M.D., 4 miles west of Jolon	U.S. Army, Hunter-Liggett Military Reservation (1961)	Sand and gravel in stream channel of San Antonio River. Deposit is about 100 feet wide, over 10 feet thick and more than ½ mile long. It contains 50% gravel to a maximum size of 3 or 4 inches. Gravel is predominantly composed of granitic and metamorphic rocks, with lesser sandstone and siliceous and soft shales.	Developed extensively in vicinity of bridge for use at military reservation. No equipment at excavation site, but active in recent years.
144	Valley Rock and Adobe Co. (Murphy)	SE¼ sec. 24, T. 16 S., R. 1 E., M.D., 6 miles east of Carmel	Valley Rock and Adobe Co. (John B. Simpson, owner), P.O. Box 64, Carmel Valley (1961)	....	Sand and gravel obtained from stream channel of Carmel River from about 1920 to 1955 by M. J. Murphy and since 1955 by present owner. (Herein, under Quaternary Stream Deposits.)
145	Wolter............	NE¼ sec. 21, T. 16 S., R. 1 E., M.D., 4 miles southeast of Carmel	Luis F. Wolter, Carmel Valley, leases to Phil Calabrese, Contractor, Sand City (1961)	....	Stream channel deposit on Carmel River, worked intermittently since about 1950 as source of road materials. (Herein, under Quaternary Stream Deposits.)
146	Zabala............	W½ sec. 35, T. 18 S., R. 6 E., M.D., 2 miles west of Greenfield	Walter Zabala, Greenfield (1960)	....	Large dry wash channel deposit in Arroyo Seco; developed 1959–1960 by Delphia-Early under a contract with the State Division of Highways. (Pacific Roadbuilder and Engrg. Rev. 59:15–16; herein under Quaternary Stream Deposits.)

SILVER

	Alisal.............	Not determined. (Possibly W½ sec. 9, T. 14 S., R. 4 E., M.D.)	Not determined. (Sec. 9 owned by D. F. Davies, 1029 Old Stage Rd., Salinas) (1966)	....	Early silver prospect. (Duflot de Mofras 1844; Trask 1854:18, 55-56; Blake 1858:295, 301, 303; Bancroft 1886:144, 176; Waring and Bradley 19:615; Laizure 25:23, 56; Goodwin 57:571, herein).

STONE—CRUSHED & BROKEN

147	Arroyo Seco.......	NE¼ sec. 2, T. 20 S., R. 4 E., M.D., 16 miles southwest of Greenfield	U.S. Forest Service (1960)	Decomposed granite, reportedly..	Reportedly developed by several pits which provide base materials and plant mix aggregate for road construction in and around the Arroyo Seco campground of the U.S. Forest Service. Active 1960 (?).

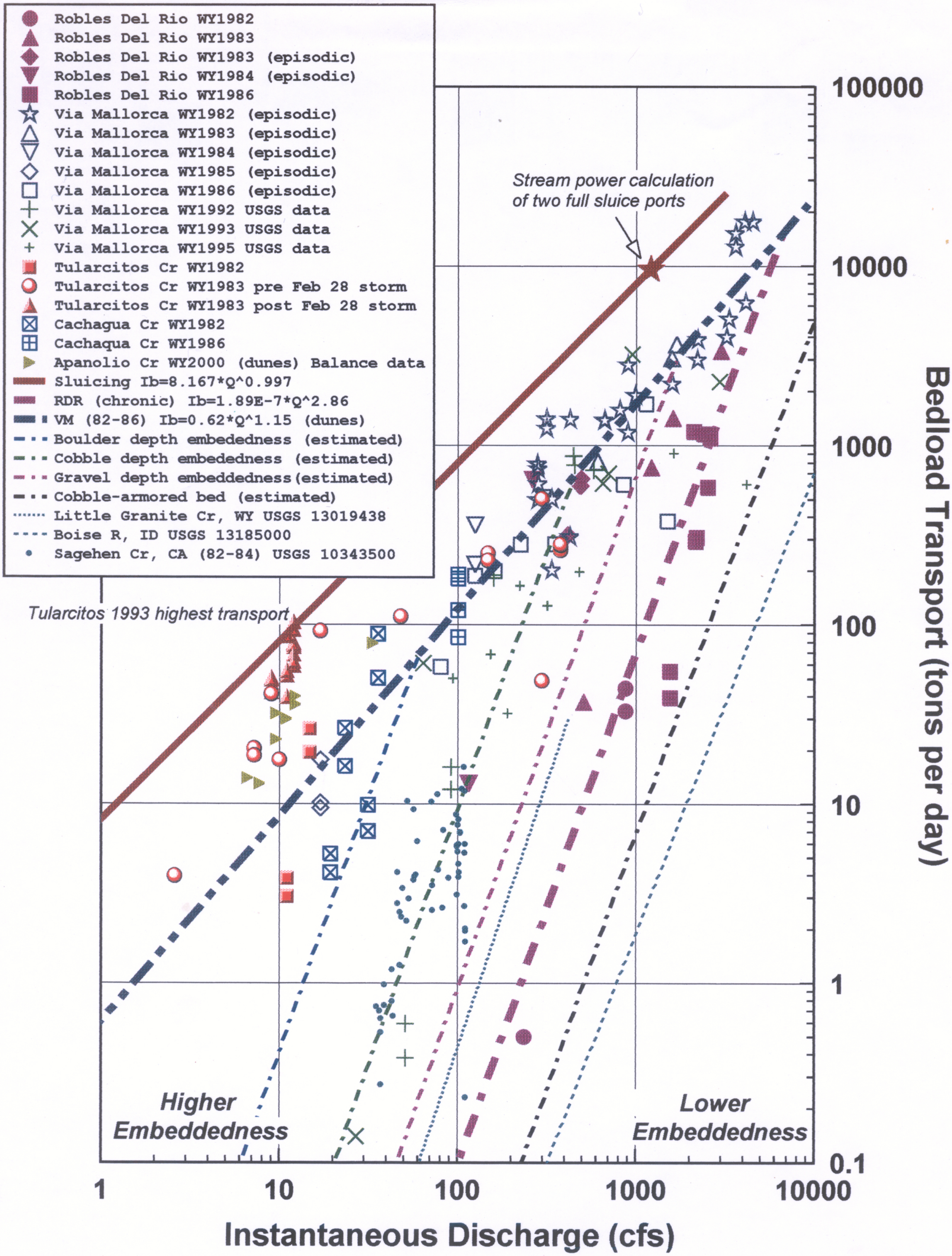

Balance Hydrologics, Inc.

Figure 1. Bedload transport rates in Carmel River. For comparison rates are also shown for other streams originating on granitic watersheds.

Central
Coast
Watershed
Studies

CCoWS

2015 Pre-San Clemente Dam Removal Morphological Monitoring of the Carmel River Channel in Monterey County, California

Publication No. WI-2016-01

28 January 2016

Kaitlyn Chow
Lauren Luna
August Delforge
Douglas Smith (Ph.D.)

The Watershed Institute

Division of Science and Environmental Policy
California State University Monterey Bay
http://watershed.csumb.edu

100 Campus Center, Seaside, CA, 93955-8001
831 582 4696 / 4431

Contact:
dosmith@csumb.edu

Executive Summary

San Clemente Dam was removed from the Carmel River in fall 2015. A study of dam-removal impacts on the Carmel River will compare channel shape and substrate measurements from before-and-after dam removal. In 2013 several sites were selected for monitoring, both downstream of the dam (impact sites) and upstream of the dam (control sites). Subsets of the study sites were established by CSUMB and collaborating partners with the USGS and NOAA. This report presents a resurvey of the 2013 sites that were established by CSUMB. It also presents the first measurements of a new impact site and a new control site.

The resurvey of previous sites indicates that we will be able to determine vertical geomorphic changes greater than approximately 3 cm in the future before-after survey comparisons. The resurveys also showed that there has no substantial geomorphic change between 2013 and 2015. Substrate grain size analysis shows considerable change in sample percentiles during the span from 2013 to 2015 at some sites. The presence of high variability in the "before removal" era, suggests that only large changes will be detectable in the "before-after" comparison, to be attempted in future studies. The lack of geomorphically altering flows between 2013 and 2015 shows that grain size distributions can change with little forcing.

This report can be cited as:

Chow K., Luna L., Delforge A. and Smith D. 2016. 2015 Pre-San Clemente Dam Removal Morphological Monitoring of the Carmel River Channel in Monterey County, California. The Watershed Institute, California State University Monterey Bay, Publication No. WI-2016-01, 50 pp.

Acknowledgements

Funding and support for this project was provided by U.C. Santa Cruz and NOAA Fisheries Service's Southwest Fisheries Science Center and by CSUMB Undergraduate Research Opportunity Center.

We are grateful for the assistance and collaboration of:

- David Boughton, Lee Harrison, Colin Nicol, and Lea Bond (NOAA Fisheries)
- Amy East and Josh Logan (USGS)
- John Silveus, Alana Kleven, Steve Flores, and Leah MacCarter (CSUMB)

Table of Contents

1 Introduction

The 32 m tall San Clemente Dam, located in the northern Santa Lucia Mountains of Central California, was removed from the Carmel River in fall of 2015 (Figure 1). The dam was decommissioned because the 1425 acre feet reservoir was more than 95% filled with sediment, the dam was located near a seismically active fault zone, and there was uncertainty about the dam's ability to withstand a major flood (CCOWS 2012 for summary). Unlike all previous dam removal projects, this project was designed to minimize downstream impacts to fish habitat and flood frequency by sequestering all the stored sediment on site (SCDRP 2015). Sediment transport modeling of the dam removal project indicated that the river would not be significantly altered by the project (Mussetter 2005).

In collaboration with the U.S. Geological Survey and NOAA Fisheries Service, we established several study reaches in 2013 to monitor the actual downstream impacts of the dam removal project (Leiker et al. 2014). The study reaches include "impact" reaches located downstream of the dam, and "control" reaches located upstream of the dam. At each study reach surveyed in 2013, Leiker et al. (2014), or collaborators, surveyed benchmarked channel cross sections and performed particle counts to establish a baseline for documenting changes related to the dam removal. Our study resurveyed the Leiker et al. (2014) reaches to document between-survey precision, investigate natural annual variability, and to create a "before dam removal" data set that immediately preceded dam removal. We also added another "impact" study reach downstream of the dam and a "control" reach upstream of the dam removal project.

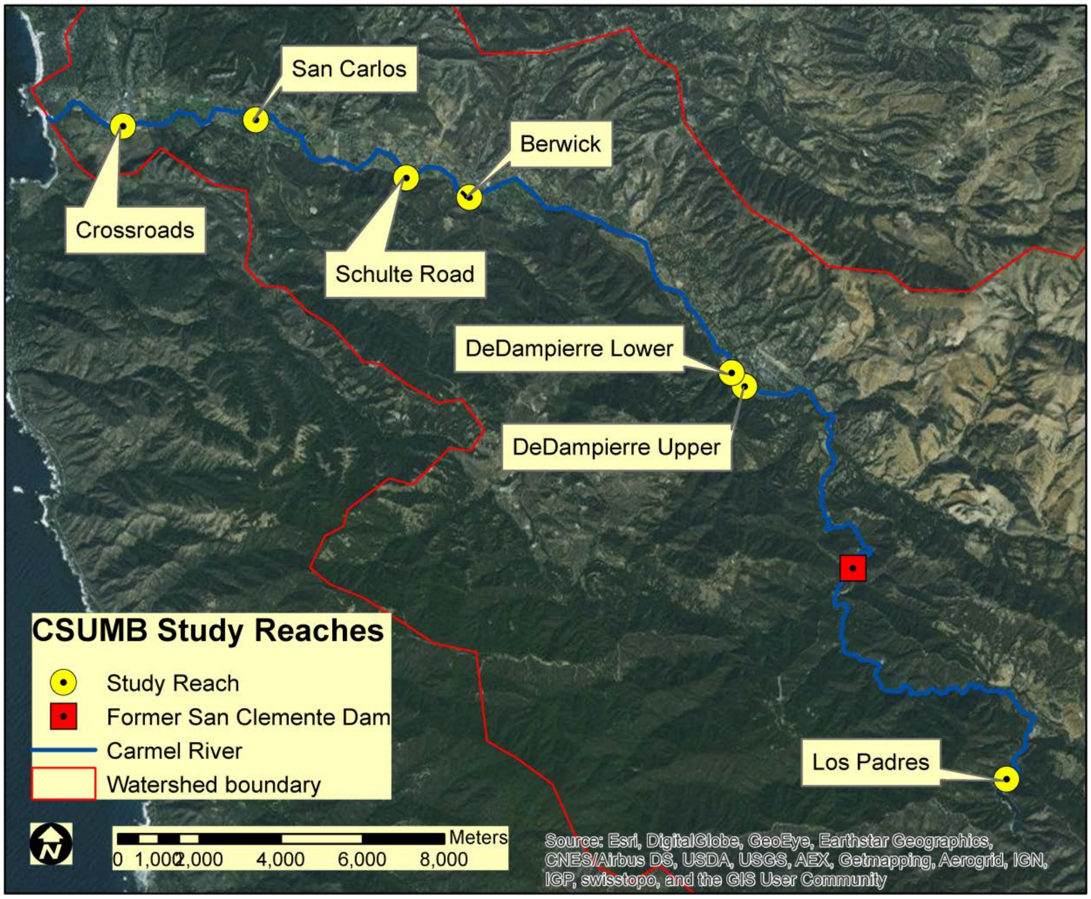

Figure 1. Location of study reaches upstream and downstream of the San Clemente Dam on the Carmel River.

2 Methods

Following the methods of the initial 2013 study (Leiker et al. 2014), we conducted geomorphic measurements of the Carmel River before the San Clemente Dam (SCD) reroute and removal at six diverse and representative reaches of the river that could change character following dam removal. The geomorphology of each reach was studied in the dry season when there were low flows and easy access to the channel. Data were collected in the fall of 2015. Five reaches established in 2013 were resurveyed and an additional "impact" reach was added downstream of the dam

(Berwick in Figure 1). An additional “control” reach was added to the study upstream of the San Clemente dam to better understand morphological change that was not influenced by the dam removal (Las Padres in Figure 1). Each study reach is described below:

- **Los Padres (LP)**: Located directly downstream from the Los Padres Dam, this reach is the most upstream reach established in 2015.
- **DeDampierre Upper (DDU)**: Located in the upper portion DeDampierre Park, the reach extends from the footbridge past the baseball fields. This reach contains several pieces of large wood installed for a restoration project by the Monterey Peninsula Water Management district (MPWMD).
- **DeDampierre Lower (DDL)**: This reach begins at the lower end of DeDampierre park and extends to the Carmel Valley Trail and Saddle Club downstream of the park.
- **Berwick (BW)**: Established in 2015, this reach is located on California American Water (CalAm) property.
- **Schulte Road (SR)**: Located upstream of the Schulte Road Bridge. This reach begins in land owned by the Big Sur Land Trust and extends to 100m upstream of the Schulte Bridge.
- **San Carlos (SC)**: Located just downstream of the San Carlos Road Bridge. The reach extends from the bridge to the California American Water (CalAm) San Carlos production well.
- **Crossroads (CR)**: Located adjacent to the Crossroads Shopping Center at the mouth of Carmel Valley. This is the most downstream reach included in this study.

Each reach was approximately 300 m in length and contained four to six transects evenly spaced at 60 m. Cross sections occurred in a variety of hydraulic settings, including riffles, glides, runs, and pools. Using the previous benchmarks established in 2013, we resurveyed each cross section using an autolevel, leveling rod, and 30 meter tape (Harrelson et al. 1994). At each cross section, a taut tape was set between the left and right benchmarks to facilitate a precise resurvey of each transect and guide shot distances. Points along transect were shot at one meter increments with additional shots to record breaks in slope. Surveys were closed at the end of every cross section using the left benchmark. Cross section data were plotted and visually compared with the 2013 surveys. At the two new reaches (Los Padres and Berwick), new cross section benchmarks were set and georeferenced using methods similar to those of Leiker et al. (2014) before autolevel surveys were performed.

In addition to topographic surveys, pebble counts were performed along each cross section to determine average particle size distribution. Pebble counts included only particles within the active low flow channel as indicated by recent substrate activity. We employed a sampling technique from Bunte and Abt (2001) that uses a 60 x 60 cm sampling quadrat. This method reduces serial correlation by adjusting the spacing between intersections on the frame to equal the dominant large particle size (≈D95). The 60 x 60 cm square sampling frame was constructed from 1" PVC pipe with notches every 10 cm. Elastic bands were then attached to notches according to the dominant large particle size of each transect.

The sampling grid was moved repeatedly across the estimated low flow channel at fixed intervals to achieve a sample size of ≥ 100.   A gravelometer was used to measure particle sizes for pebble counts. Particle size percentiles were determined in R

(R Core Team, 2012). Particle size histograms and cumulative frequency graphs were generated for each cross section for comparison with the 2013 measurements.

3 Results

3.1 Los Padres Reach

The Los Padres reach is located directly downstream of the Los Padres Dam (Figure 1). This reach is upstream of the San Clemente Dam reroute site and serves as a control reach to be compared with the downstream reaches (Figure 2).

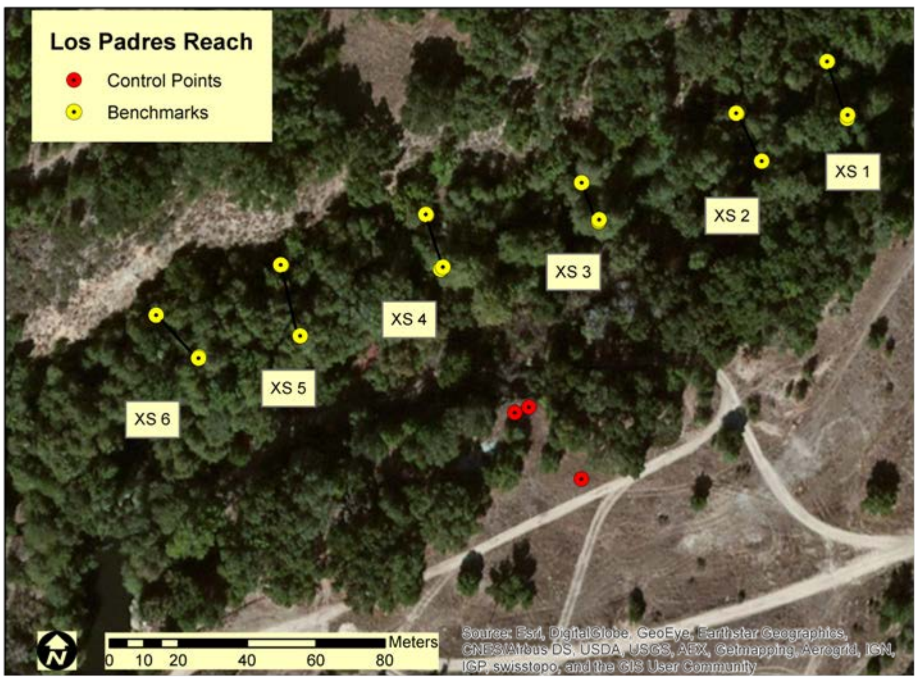

Figure 2. Location of georeferenced control points and cross sections within the Los Padres Reach.

The median grain size of this reach (D50) ranged from coarse pebbles to boulders (22.6 - 300 mm) among transects (Table 1). The 84th and 90th percentiles (D84 and D90) were mostly boulders with the exception of transect 1 (LP 1) which ranged from very coarse pebbles to cobbles (Figure 3). Cross sections located in pools tended to have smaller particle sizes while riffles tended to have larger particle sizes. Grain size distribution analysis revealed similar distributions of smaller particles, but higher variability in the larger particles between transects where large boulders were present. The width of cross sections in this reach covered the active channel and potions of floodplain when possible. Cross section widths ranged from 12 – 22 m and the average low-flow active channel observed in the field was between 10 – 12 m. The channel geometry and pebble count distribution of each surveyed cross section is in the Appendix.

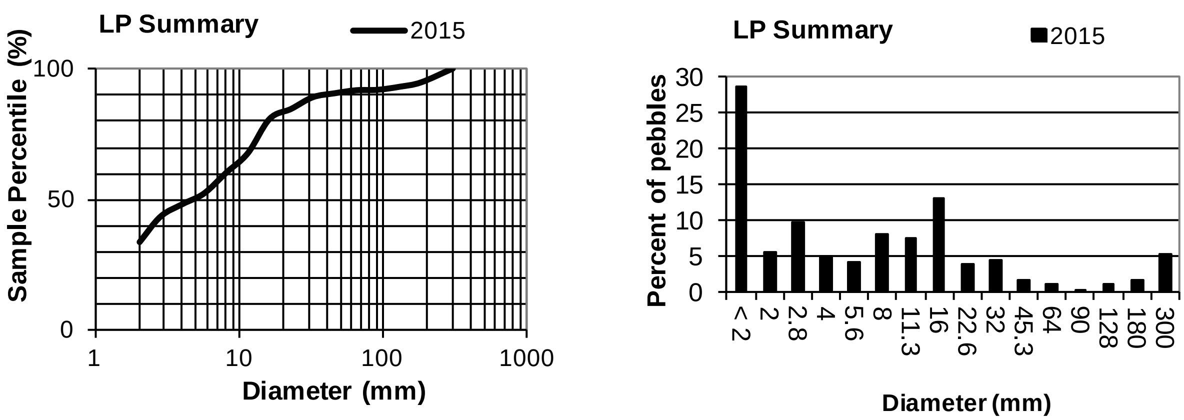

Figure 3. Summary pebble count distribution (LP 1 – LP 6) for the Los Padres reach displayed as cumulative percentiles (left) and individual bins (right) for 2015.

Table 1. Grain size distribution and cumulative finer than graphs among cross-sectional transects within the Los Padres Reach for 2013 & 2015. Runs like LP6 tended to have smaller particles.

	2015				
Los Padres	**D_{16}**	**D_{35}**	**D_{50}**	**D_{84}**	**D_{95}**
LP 1	16.0	32.0	64.0	300.0	300.0
LP 2	22.6	32.0	45.3	300.0	300.0
LP 3	11.3	38.7	90.0	300.0	300.0
LP 4	64.0	180.0	300.0	300.0	300.0
LP 5	13.7	45.3	128.0	300.0	300.0
LP 6	2.0	11.3	22.6	45.3	90.0

3.2 DeDampierre Upper Reach

The DeDampierre Upper Reach (Figure 4) is the most upstream reach monitored by CSUMB that will see impacts of the San Clemente Dam reroute. This reach included four large wood installments constructed by MPWMD. The large wood installments have created large, deep scour pools.

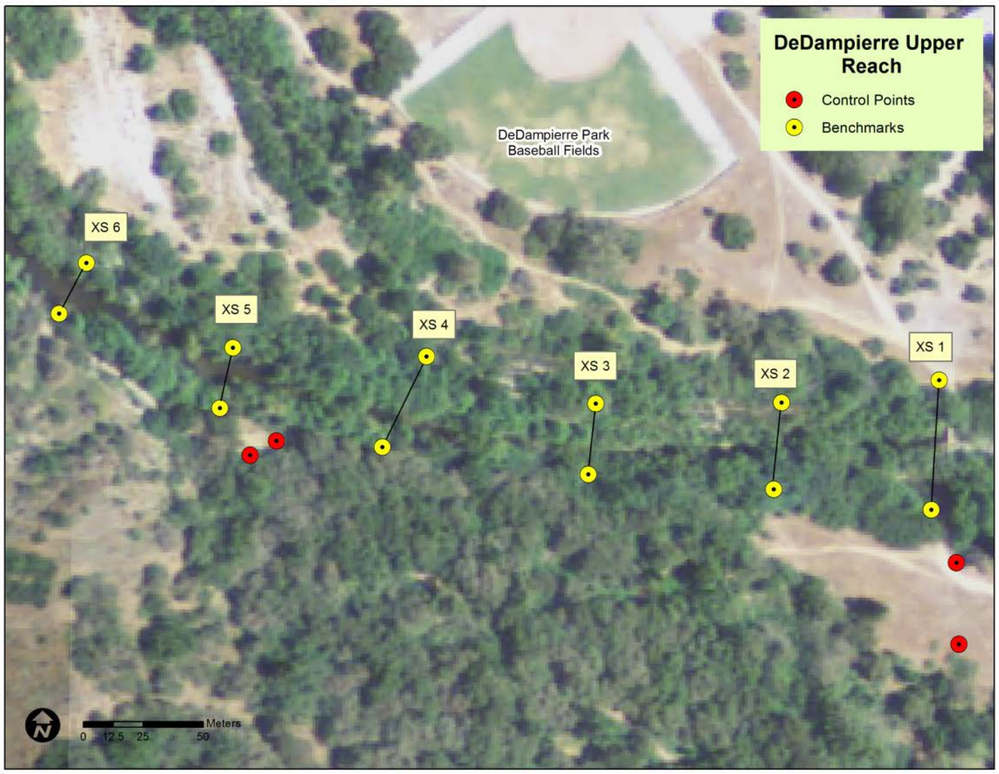

Figure 4. Location of georeferenced control points and cross sections within the DeDampierre Upper Reach.

The D50 of this reach ranged from fine pebbles to cobbles (5.6 – 90 mm) among transects (Table 2). Since 2013, grain size has increased overall, in large part because the < 2 mm fraction was removed (Figure 5). The 85th and 90th percentiles (D85 and D90) included a range of particle sizes from medium gravel and to small boulders (Table 2). Cross sections located in pools tended to have smaller particle sizes while riffles tended to have larger particle sizes. The pools formed by the large wood installments in this reach had much smaller particle sizes than other sections of the reach. The width of cross sections in this reach covered the active channel and potions of floodplain when possible. Two of the six cross sections (DDU2 & 3) were extended in 2015 by approximately 10 m. There are no noteworthy changes in channel shape at this reach.

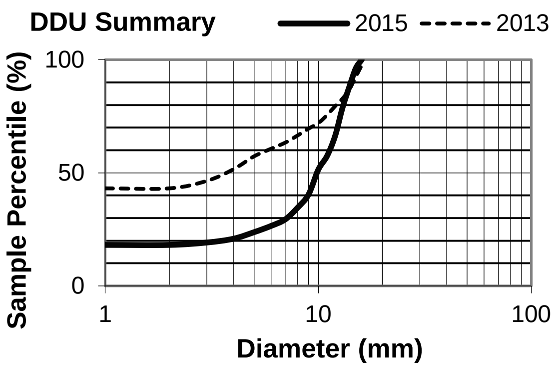

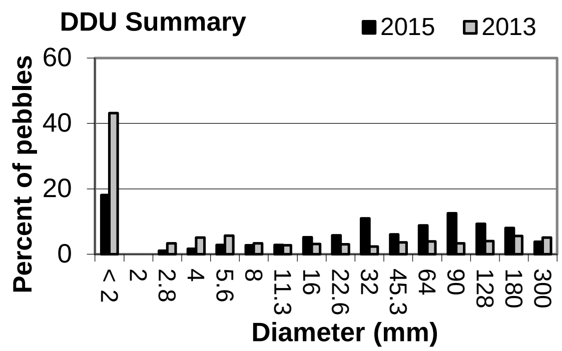

Figure 5. Summary pebble count distribution (DDU 1 – DDU 6) for the DeDampierre Upper reach displayed as cumulative percentiles (left) and individual bins (right) for 2015 and 2013.

Table 2. Grain size distribution and cumulative finer than graph among cross-sectional transects within the DeDampierre Upper Reach. Riffles such as DDU 3, tended to have larger particles than pools, such as DDU 1.

	2013					2015				
DeDampierre Upper	D_{16}	D_{35}	D_{50}	D_{84}	D_{95}	D_{16}	D_{35}	D_{50}	D_{84}	D_{95}
DDU 1	2.0	2.0	2.0	16.0	54.7	2.0	2.0	5.6	16.0	32.0
DDU 2	2.0	2.0	2.0	64.0	300.0	2.0	2.5	32.0	128.0	180.0
DDU 3	2.0	2.0	8.0	128.0	300.0	22.6	64.0	90.0	180.0	300.0
DDU 4	2.0	2.0	19.3	240.0	300.0	22.6	45.3	64.0	128.0	300.0
DDU 5	2.0	2.0	4.0	180.0	240.0	2.0	16.0	32.0	90.0	128.0
DDU 6	2.0	4.0	4.0	32.0	300.0	11.3	54.7	64.0	128.0	180.0

3.3 DeDampierre Lower Reach

This reach is located directly downstream of the DeDampierre Upper Reach. The upstream portion of the reach is a wide and open channel with a pool and long run. The reach narrows after cross section 3 (XS 3 of Figure 6) and has a steeper gradient than Upper DeDampierre.

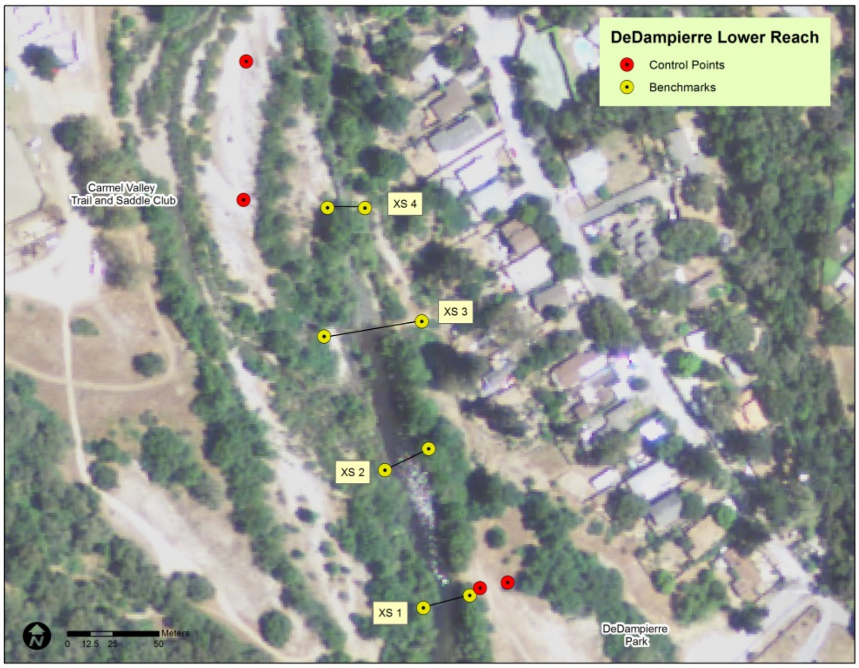

Figure 6. Location of georeferenced control points and cross sections within the DeDampierre Lower Reach.

The D50 ranged from medium- to very coarse-pebbles. (13.65 – 64 mm) among transects (Table 3). The D84 and D90 contained only cobbles. 2015 results reveal a less diverse distribution of particles and an increase in fine to very coarse pebbles (Figure 7). The width of cross sections in this reach covered the active channel and portions of floodplain when possible. Cross section widths ranged from 16 – 44 m and the average low-flow active channel observed in the field was between 10 – 20 m.

There has been no topographic change over all cross sections within this reach (Appendix).

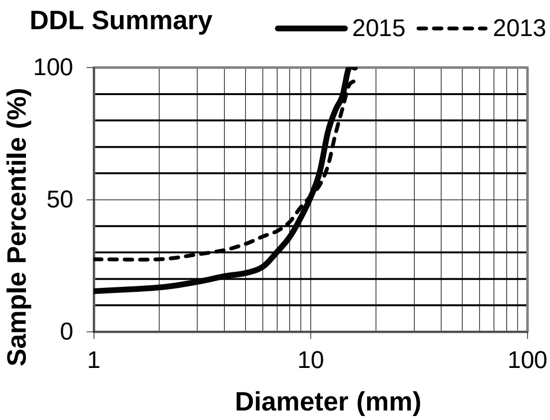

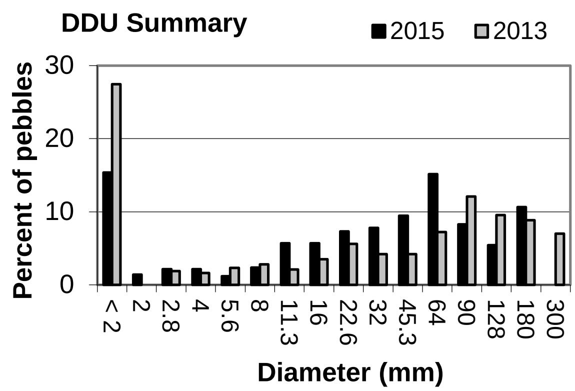

Figure 7. Summary pebble count distribution (DDL 1 - DDL 4) for the DeDampierre Lower reach displayed as cumulative percentiles (left) and individual bins (right) for 2015 and 2013.

Table 3. Grain size distribution and cumulative finer than graph among cross-sectional transects within the DeDampierre Lower Reach. DDL 1 has the largest pool (Appendix) and the largest decrease in grain size between 2013 and 2015.

	2013					2015				
DeDampierre Lower	D_{16}	D_{35}	D_{50}	D_{84}	D_{95}	D_{16}	D_{35}	D_{50}	D_{84}	D_{95}
DDL 1	2.0	2.0	11.3	180.0	300.0	2.0	2.0	13.7	90.0	180.0
DDL 2	2.0	8.0	45.3	128.0	180.0	9.7	32.0	45.3	90.0	128.0
DDL 3	2.0	11.3	22.6	128.0	300.0	8.0	16.0	22.6	64.0	128.0
DDL 4	2.0	22.6	64.0	180.0	300.0	2.0	32.0	64.0	180.0	180.0

3.4 Berwick Reach

Established in 2015, this site is located on California American Water (CalAm) property (Figure 8).

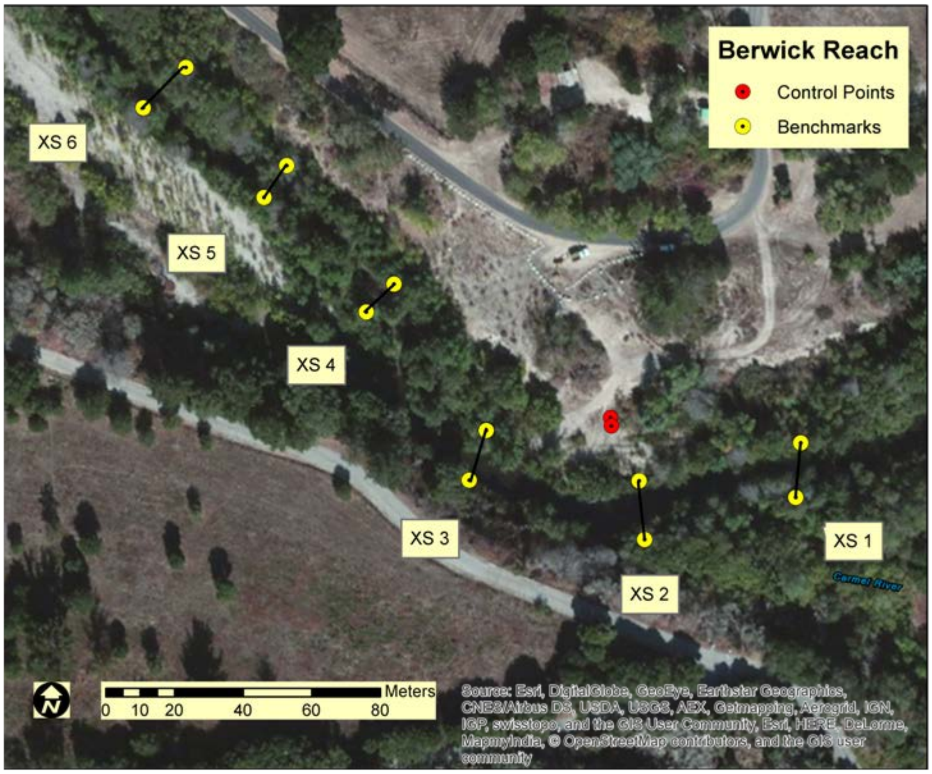

Figure 8. Location of georeferenced control points and cross sections within the Berwick Reach.

The median D50 ranged from coarse sand to very coarse pebbles (1-64 mm) (Table 4). The D84 and D90 contained coarse pebbles to boulders (Figure 9). The cross sections in this reach continue the trend of pools having a smaller particle size, such as BW 4 & BW 5. Cross section widths ranged from 11 to 16 m and the average low-flow active channel observed in the field was between 5-15 m (Appendix).

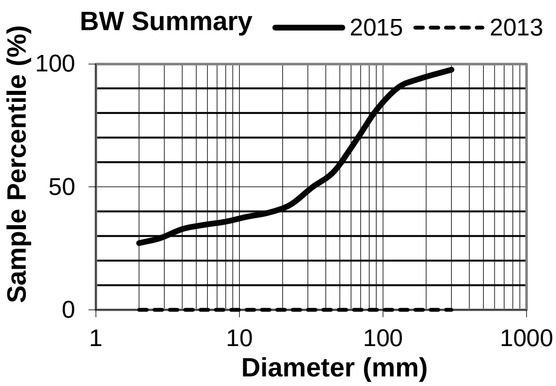

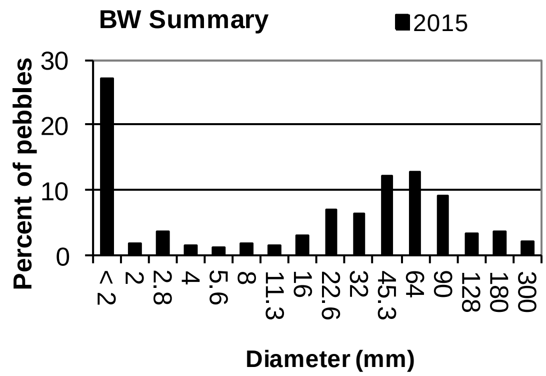

Figure 9. Summary pebble count distribution (BW 1 – BW 6) for the Berwick reach displayed as cumulative percentiles (left) and individual bins (right) for 2015.

Table 4. Grain size distribution and cumulative finer than graph among cross sectional transects within the Berwick Reach.

	2015				
Berwick	D_{16}	D_{35}	D_{50}	D_{84}	D_{95}
BW 1	19.3	32.0	64.0	90.0	128.0
BW 2	2.0	45.3	64.0	180.0	300.0
BW 3	2.0	4.0	22.6	64.0	90.0
BW 4	2.0	2.0	2.0	22.6	45.3
BW 5	2.0	5.6	22.6	64.0	64.0
BW 6	2.0	4.0	32.0	90.0	180.0

3.5 Schulte Reach

The Schulte reach is located approximately 200 m upstream of the Schulte Bridge and extends above the 'Steinbeck Pool' which is located between cross sections 2 and 3 (Figure 10).

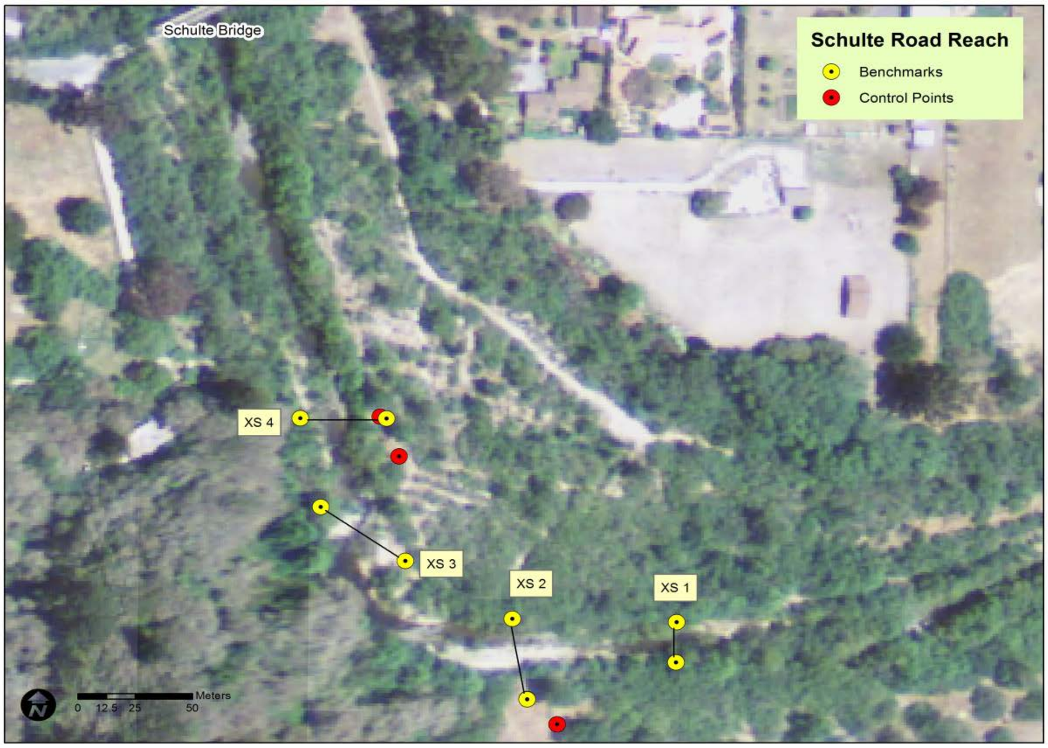

Figure 10. Locations of georeferenced control points and cross sections within the Schulte Road Reach.

The D50 ranged from granules to coarse pebbles (2-32 mm) among transects approximately the same as 2013 (Table 5). The D84 and D90 contained a wide range of particle sizes from coarse pebbles to boulders. The variability of sand and granules to cobbles and boulders is highest in pools, evident by cross section 1 (D50= 2 mm, D84= 45.3 mm).

Particle size distribution has not changed since 2013 (Figure 11). The channel width of cross sections in this reach covered the active channel and portions of floodplain when possible. Cross section widths ranged from 15-35 m and the average low-flow active channel observed in the field was between 10-15 m (Appendix).

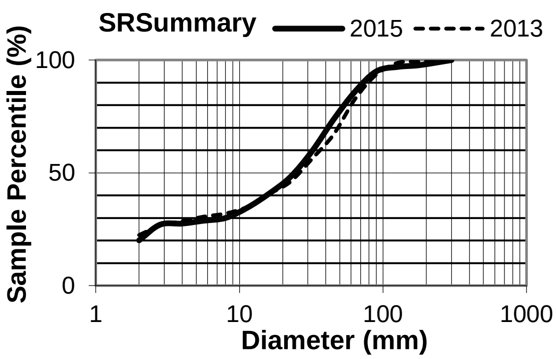

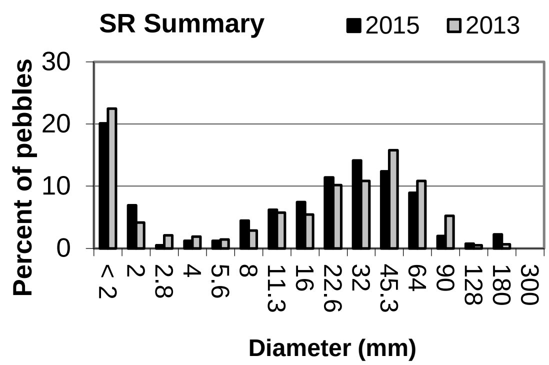

Figure 11. Summary pebble count distribution (SR 1 - SR 4) for the Schulte Road reach displayed as cumulative percentiles (left) and individual bins (right) for 2015 and 2013.

Table 5. Grain size distribution and cumulative finer than graph among cross-sectional transects within the Schulte Road Reach. SR1 has the deepest pool and smallest grain size.

	2013					2015				
Schulte Road	D_{16}	D_{35}	D_{50}	D_{84}	D_{95}	D_{16}	D_{35}	D_{50}	D_{84}	D_{95}
SR 1	2.0	2.0	2.0	45.3	180.0	2.0	2.0	2.0	45.3	180.0
SR 2	8.0	16.0	22.6	45.3	64.0	8.0	16.0	22.6	45.3	64.0
SR 3	16.0	22.6	32.0	45.3	64.0	16.0	22.6	32.0	45.3	64.0
SR 4	2.0	8.0	27.3	64.0	64.0	2.0	8.0	27.3	64.0	64.0

3.6 San Carlos Reach

The D50 ranged from very coarse sand to coarse pebbles (1.9-32 mm) among transects with a more frequent occurrence of sand and fine pebbles (Table 6). The D84 and D90 ranged from very coarse pebbles to boulders with not much variation. Not much changed since 2013 (Figure 12). Large boulders were less frequent this far downstream. The channel width of cross sections in this reach covered the active channel and portions of floodplain when possible (Figure 13). Cross section widths ranged from 19-47 m and the average low-flow active channel observed in the field was between 10-15 m. Channel shape also has not significantly changed since 2013 (Appendix).

Table 6. Grain size distribution and cumulative finer than graph among cross-sectional transects within the San Carlos Reach.

	2013					**2015**				
San Carlos	**D_{16}**	**D_{35}**	**D_{50}**	**D_{84}**	**D_{95}**	**D_{16}**	**D_{35}**	**D_{50}**	**D_{84}**	**D_{95}**
SC 1	9.7	16.0	16.0	45.3	122.0	5.6	27.3	45.3	90.0	128.0
SC 2	11.3	22.6	32.0	45.3	64.0	11.3	32.0	45.3	90.0	109.0
SC 3	2.0	5.6	11.3	32.0	45.3	2.0	2.0	2.8	45.3	300.0
SC 4	2.0	2.0	2.8	45.3	64.0	2.0	2.0	2.0	45.3	90.0
SC 5	2.0	5.6	11.3	32.0	45.3	2.0	16.0	32.0	54.7	64.0
SC 6	2.0	2.0	1.9	32.0	45.3	2.0	2.0	2.8	32.0	64.0

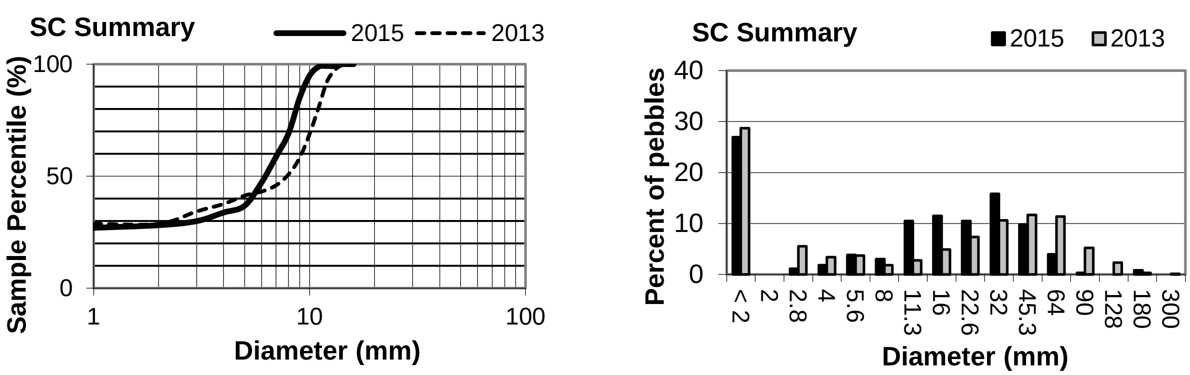

Figure 12. Summary pebble count distribution (SC 1 - SC 6) for the San Carlos reach displayed as cumulative percentiles (left) and individual bins (right) for 2015 and 2013.

Figure 13. Locations of georeferenced control points and cross sections within the San Carlos Reach.

3.7 Crossroads Reach

Crossroads is the lowermost reach monitored, and is located adjacent to the Crossroads shopping center near the mouth of Carmel Valley (Figure 14). The D50 ranged from medium pebbles to coarse pebbles (11.3-22.6 mm) among transects (Table 7). The D84 and D90 contained coarse to very coarse pebbles. Particle size distributions between cross sections were very consistent (Figure 15). The channel width of cross sections in this reach covered the active channel and portions of floodplain when possible. Cross section widths ranged from approximately 16 - 25 m and the average low-flow active channel observed in the field was between 10 - 15 m. There has not been significant topographic change at this reach since 2013 (Appendix).

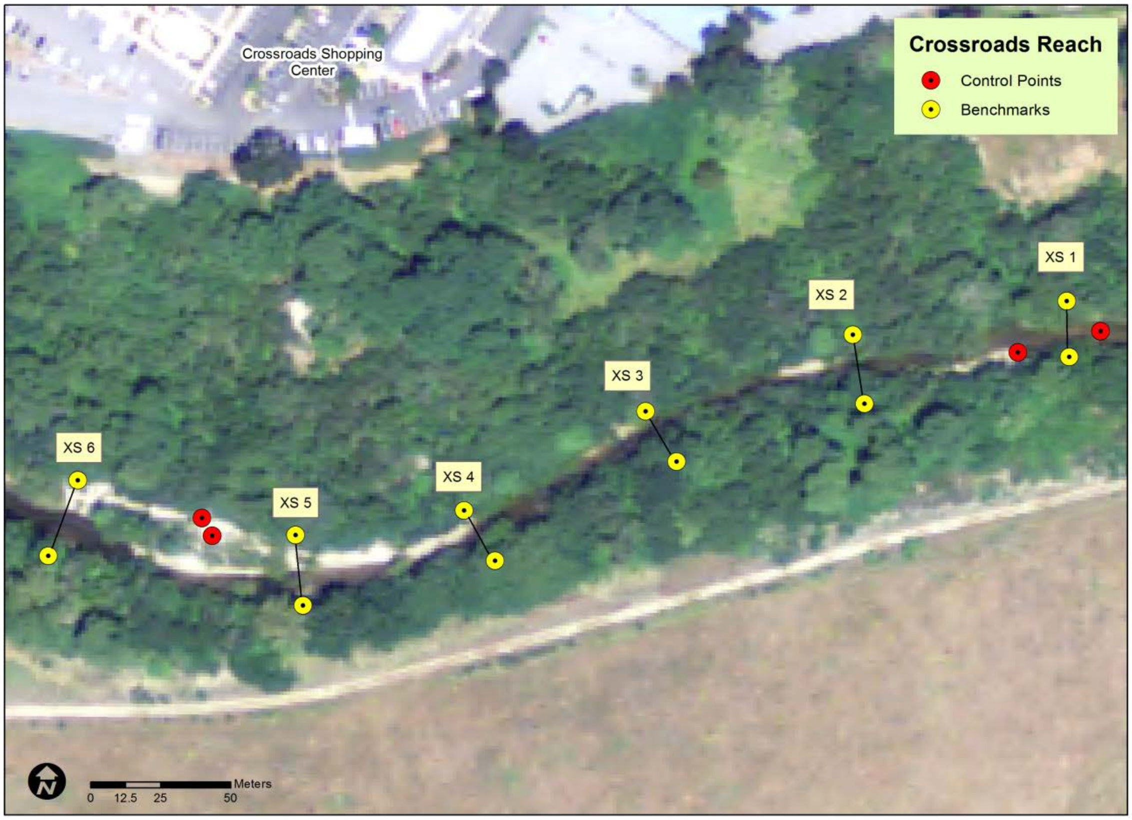

Figure 14. Locations of georeferenced control points and cross sections within the Crossroads Reach.

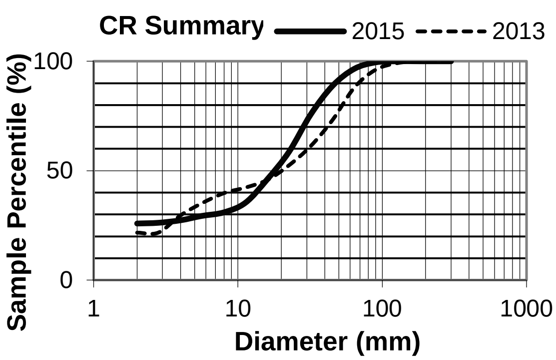

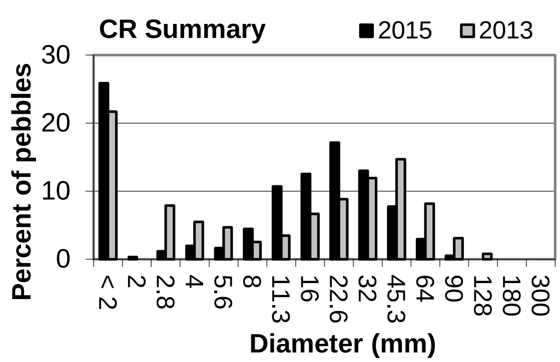

Figure 15. Summary pebble count distribution (CR 1 – CR 6) for the Crossroads reach displayed as cumulative percentiles (left) and individual bins (right) for 2015 and 2013.

Table 7. Grain size distribution and cumulative finer than graph among cross-sectional transects within the Crossroads Reach. This reach is dominated by sand. It is the furthest downstream and has the smallest average grain size.

	2013					2015				
Crossroads	D_{16}	D_{35}	D_{50}	D_{84}	D_{95}	D_{16}	D_{35}	D_{50}	D_{84}	D_{95}
CR 1	8.0	16.0	16.0	32.0	45.3	3.4	16.0	22.6	38.7	45.3
CR 2	2.0	2.0	11.3	32.0	45.3	2.0	2.8	9.7	32.0	45.3
CR 3	2.0	2.0	11.3	32.0	45.3	2.0	2.0	2.8	32.0	45.3
CR 4	2.0	8.0	16.0	32.0	64.0	2.0	4.0	11.3	32.0	54.7
CR 5	6.8	16.0	22.6	32.0	54.7	2.0	11.3	16.0	45.3	64.0
CR 6	1.5	8.0	11.3	32.0	45.3	2.0	4.0	8.0	32.0	45.3

4 Discussion

The cross section plots indicate little geomorphic change has occurred between the 2013 and 2015 surveys (Appendix), despite flows of 700 cfs and 1000 cfs during that time span. Likewise, the plots indicate that between-survey error is acceptably low, giving confidence in our ability to document even minor geomorphic changes in the post-dam removal era. In general, future surveys should be able to capture vertical changes in the bed exceeding approximately 3 cm.

Particle distribution appears to be bimodal with a large amount of sand and cobbles, but sparse intermediate sizes (Appendix). Upstream reaches have a larger abundance of small cobbles, coarse gravel and sand this year (Figure 16).

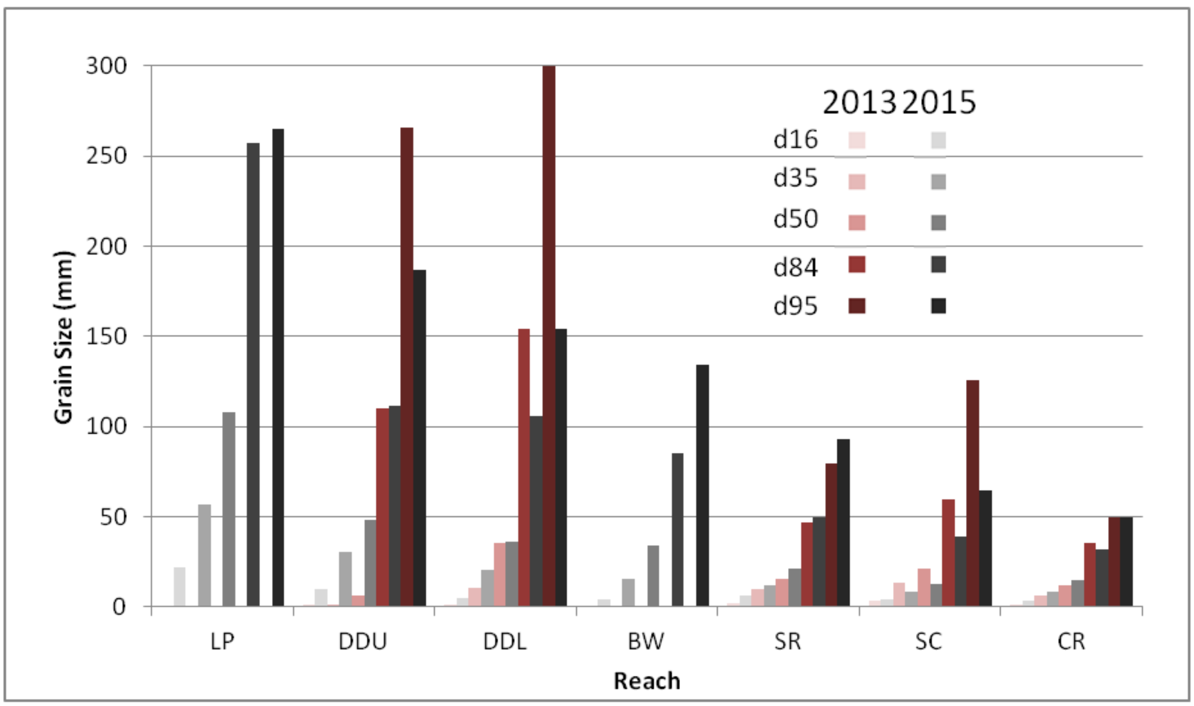

Figure 16. Particle size percentiles averaged within reaches and arranged by year from upstream (LP) to downstream (CR). Symbols are Los Padres (LP), upper DeDampierre (DDU), lower DeDampierre (DDL), San Carlos Road (SC), and Crossroads (CR). 2013 data from Leiker et al. (2014). Locations in Figure 1.

Particle size percentiles monotonically decreased downstream in 2015, as expected for a river system with downstream decreasing slope (Figure 16). Grain size percentiles in upstream sites (DDU and DDL) have decreased in size and variation between 2013 and 2015. Downstream reaches (SR, SC, and CR) did not show as much change (Figure 16). Given the considerable grain size changes that occurred between 2013 and 2015 in the “before” dam removal era, future studies that compare “before” and “after” dam conditions will only be able to assign very large changes in grain size distribution to the dam removal impact.

5 References

Bunte K., Abt S. 2001. Sampling Frame for Improving Pebble Count Accuracy in Coarse Gravel-bed Streams. Journal of the American Water Resources Association. Vol. 37, No. 4:1001-1014.

[CCOWS] Central Coast Watershed Studies. 2012. San Clemente Dam Removal and Carmel River Reroute Monitoring Plan: Carmel, CA. The Watershed Institute, Seaside, CA. Available from: http://ccows.csumb.edu/pubs/proj_pubs/2012/ENVS660_Carmel_Monitoring/CSUMB_ENVS660_ClassReport_DamRemovalMonitoring_121024.pdf

Harrelson C. Rawlins C. Potyondy J. 1994. Stream channel reference sites: an illustrated guide to field technique. Gem Tech. Per. RM-245. Fort Collins, CA: U.S. Department of Agriculture, Forest Service, Rocky Mountain Forest and Range Experiment Station, 61 pp.

Leiker S. Delforge A. Geisler E. Smith D. 2014. Pre-San Clemente Dam Removal Morphological Monitoring of the Carmel River Channel in Monterey County, California. The Watershed Institute, California State University Monterey Bay, Publication No. WI-2014-07, 32 pp.

Mussetter Engineering, Inc., 2005. Hydraulic and Sediment-transport Analysis of the Carmel River Bypass Option, California. Prepared for California American Water. April 25, 2005. 74pp.

[NOAA] National Oceanic and Atmospheric Administration. Fisheries Staff and Collaborators. Nov 2012. DRAFT Conceptual Model of the Carmel River System. SW Fisheries Science Center, Santa Cruz, CA.

R Core Team (2012). R: A language and environment for statistical computing. R Foundation for Statistical Computing, Vienna, Austria. ISBN 3-900051-07-0, URL http://www.R-project.org/

[SCDRP] San Clemente Dam Removal Project. 2014. Project Overview. Available from: http://www.sanclementedamremoval.org/

6 Appendix

6.1 Cross sections

Channel geometry for each cross section surveyed within each reach. Cross sections are denoted by their reach abbreviation (LP, DDU, DDL, BW, SR, SC, and CR) and transect number descending from upstream to downstream (1 to 4 or 6).

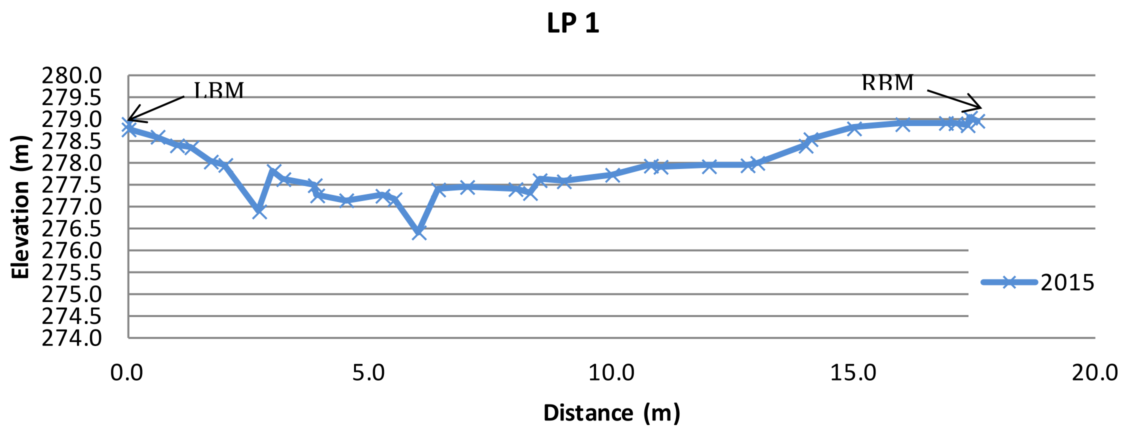

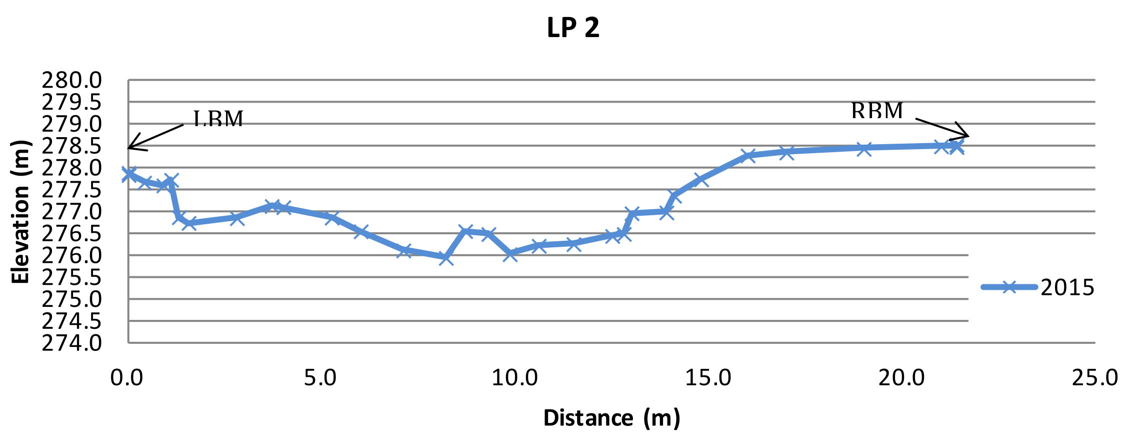

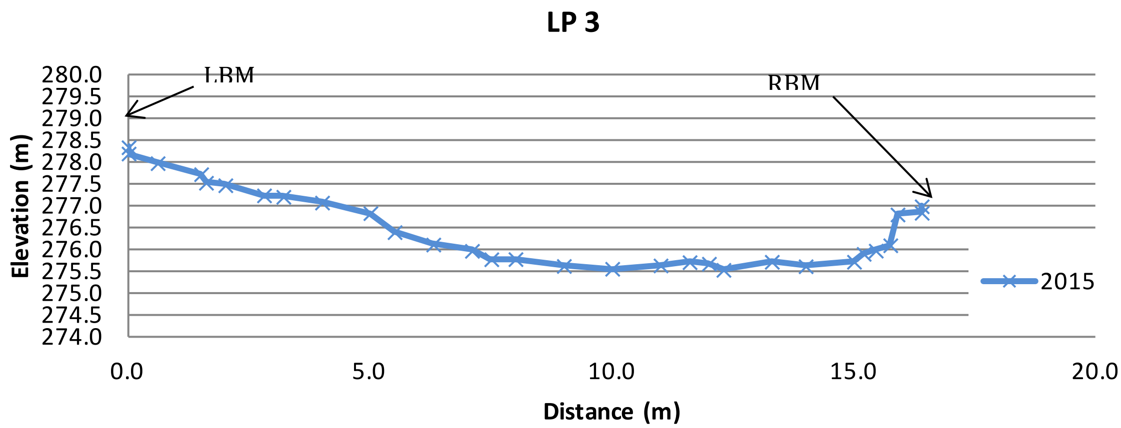
LP 3
LBM
RBM
Elevation (m)
280.0
279.5
279.0
278.5
278.0
277.5
277.0
276.5
276.0
275.5
275.0
274.5
274.0
0.0
5.0
10.0
15.0
20.0
Distance (m)
2015

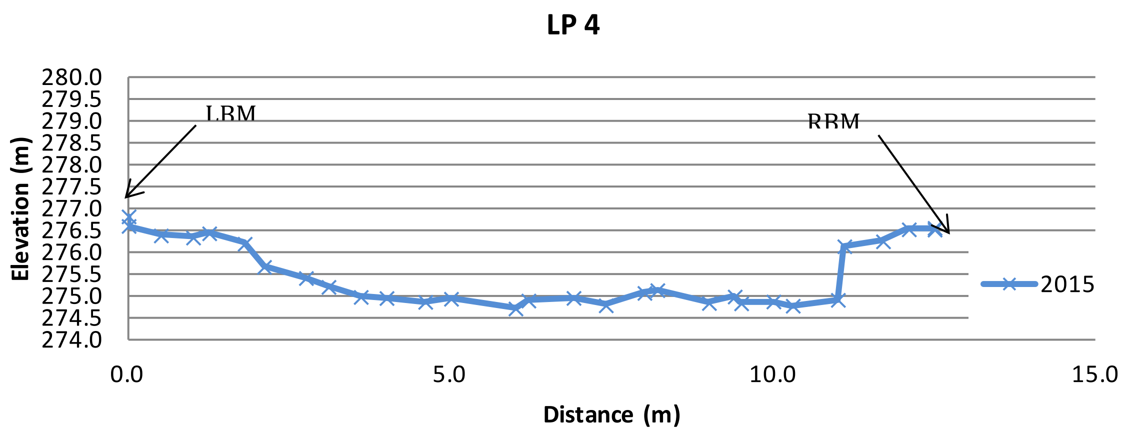
LP 4
LBM
RBM
Elevation (m)
280.0
279.5
279.0
278.5
278.0
277.5
277.0
276.5
276.0
275.5
275.0
274.5
274.0
0.0
5.0
10.0
15.0
Distance (m)
2015

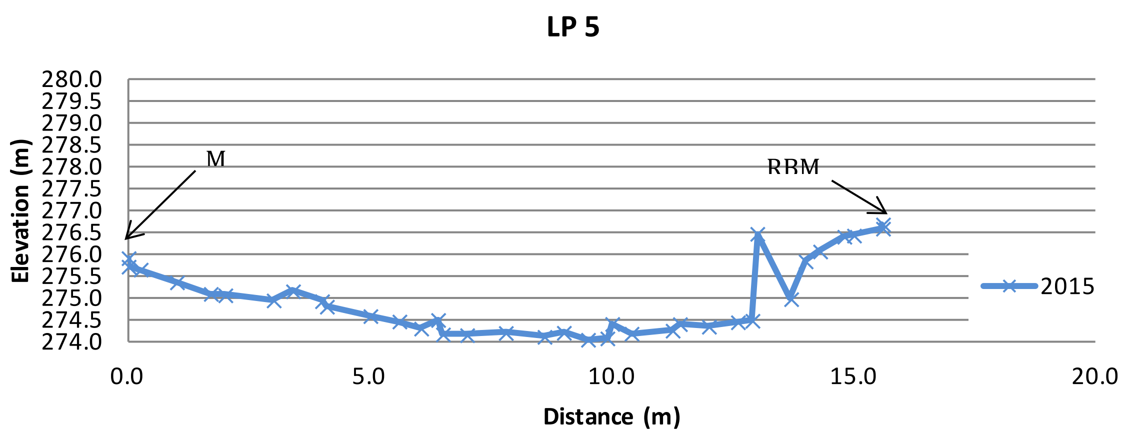
LP 5
M
RBM
Elevation (m)
280.0
279.5
279.0
278.5
278.0
277.5
277.0
276.5
276.0
275.5
275.0
274.5
274.0
0.0
5.0
10.0
15.0
20.0
Distance (m)
2015

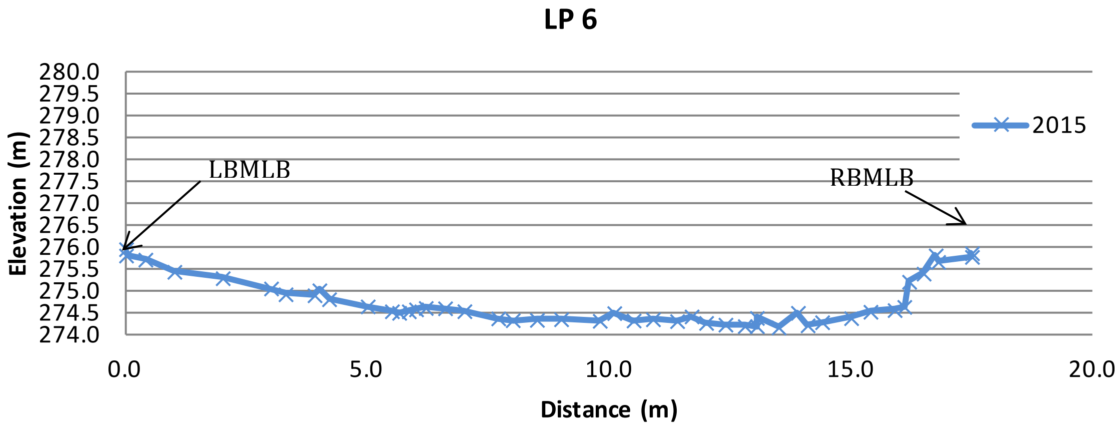
LP 6
280.0
279.5
279.0
278.5
278.0
277.5
277.0
276.5
276.0
275.5
275.0
274.5
274.0
Elevation (m)
LBMLB
RBMLB
2015
0.0
5.0
10.0
15.0
20.0
Distance (m)

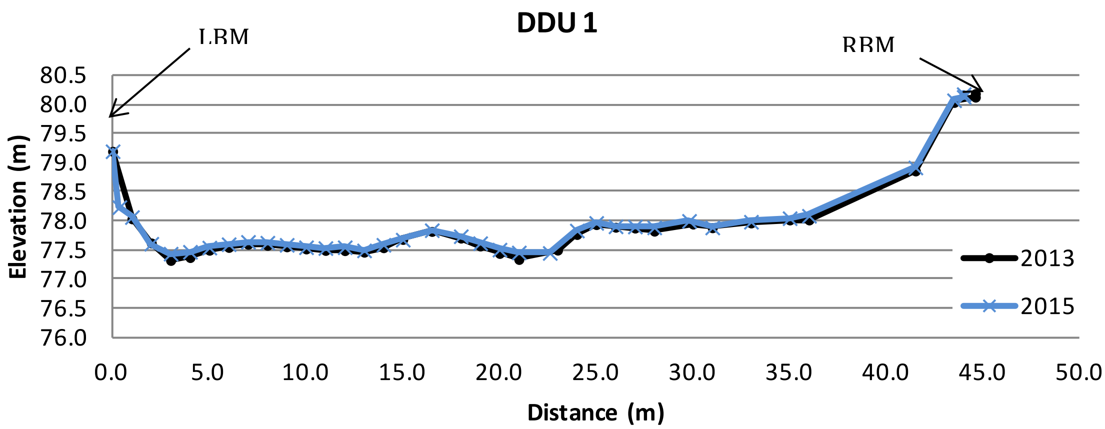
DDU 1
LBM
RBM
80.5
80.0
79.5
79.0
78.5
78.0
77.5
77.0
76.5
76.0
Elevation (m)
2013
2015
0.0
5.0
10.0
15.0
20.0
25.0
30.0
35.0
40.0
45.0
50.0
Distance (m)

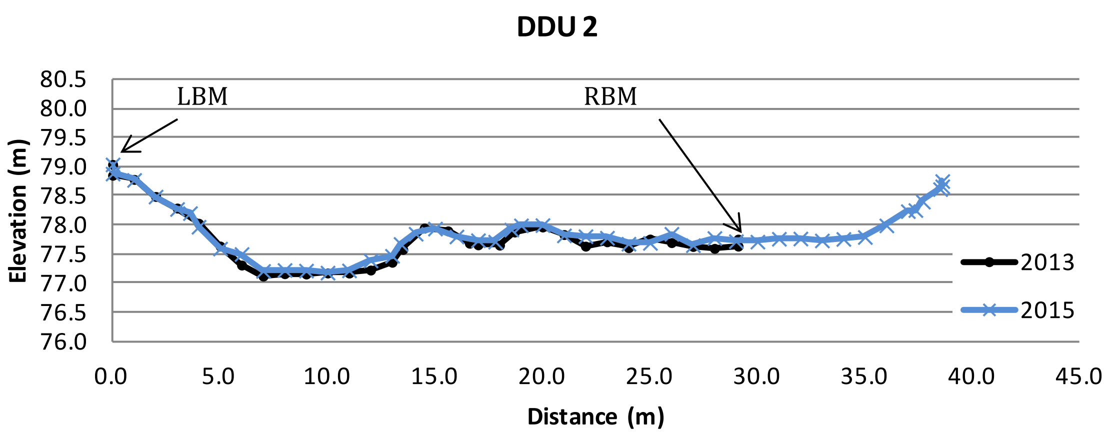
DDU 2
80.5
80.0
79.5
79.0
78.5
78.0
77.5
77.0
76.5
76.0
Elevation (m)
LBM
RBM
2013
2015
0.0
5.0
10.0
15.0
20.0
25.0
30.0
35.0
40.0
45.0
Distance (m)

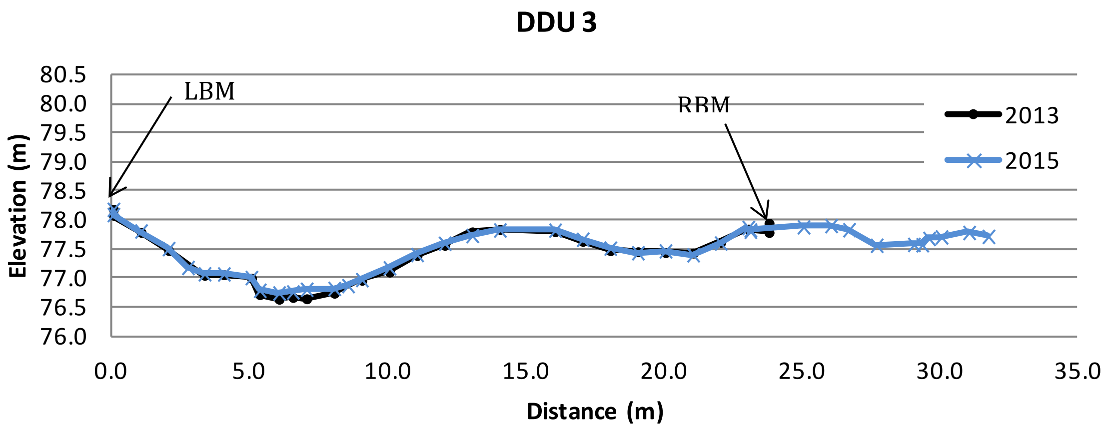
DDU 3
LBM
RBM
2013
2015
Elevation (m)
Distance (m)
80.5
80.0
79.5
79.0
78.5
78.0
77.5
77.0
76.5
76.0
0.0
5.0
10.0
15.0
20.0
25.0
30.0
35.0

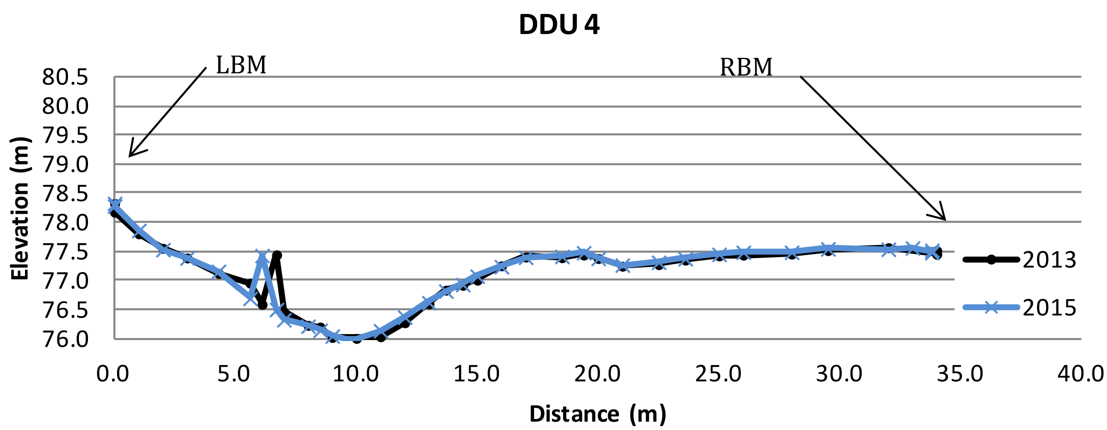
DDU 4
LBM
RBM
2013
2015
Elevation (m)
Distance (m)
80.5
80.0
79.5
79.0
78.5
78.0
77.5
77.0
76.5
76.0
0.0
5.0
10.0
15.0
20.0
25.0
30.0
35.0
40.0

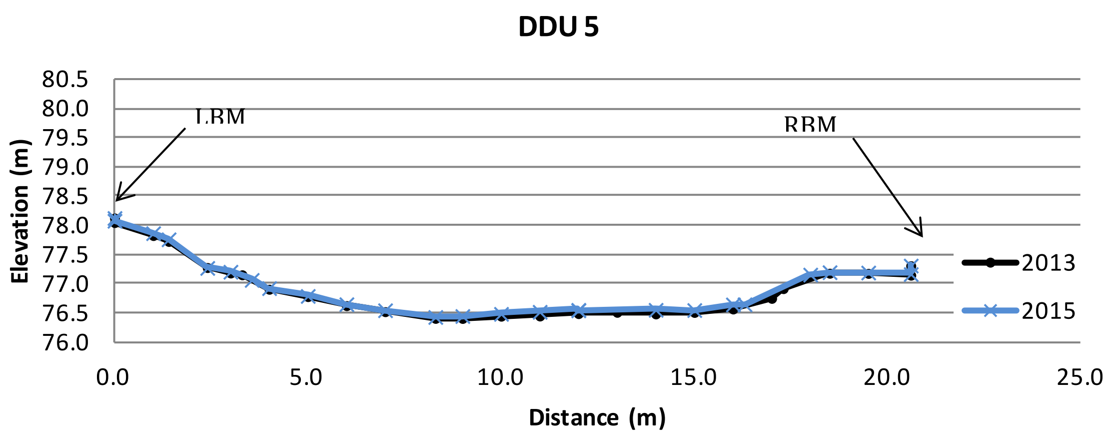
DDU 5
LBM
RBM
2013
2015
Elevation (m)
Distance (m)
80.5
80.0
79.5
79.0
78.5
78.0
77.5
77.0
76.5
76.0
0.0
5.0
10.0
15.0
20.0
25.0

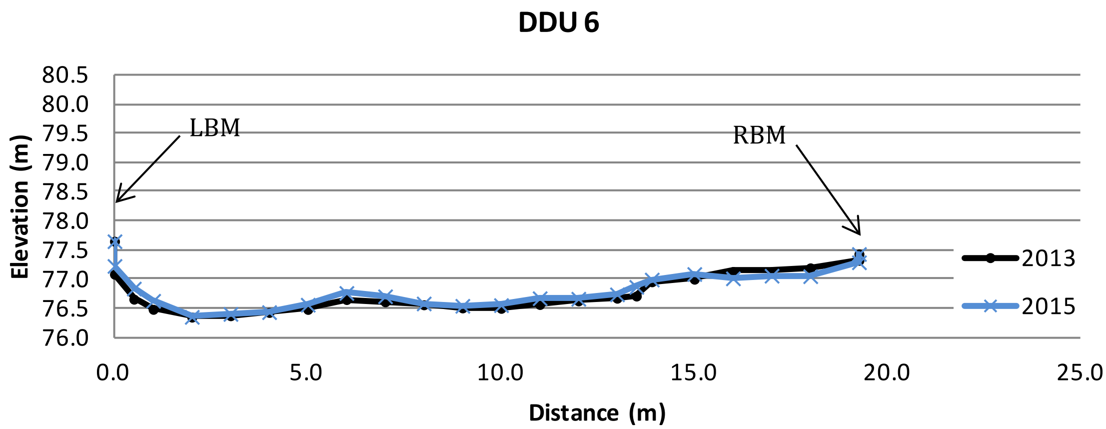
DDU 6
Elevation (m)
80.5
80.0
79.5
79.0
78.5
78.0
77.5
77.0
76.5
76.0
0.0
5.0
10.0
15.0
20.0
25.0
Distance (m)
LBM
RBM
2013
2015

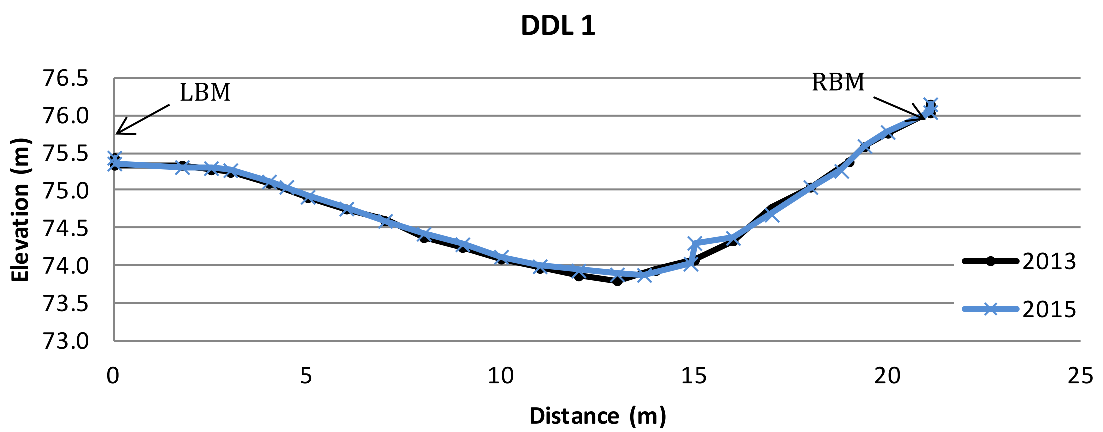
DDL 1
Elevation (m)
76.5
76.0
75.5
75.0
74.5
74.0
73.5
73.0
0
5
10
15
20
25
Distance (m)
LBM
RBM
2013
2015

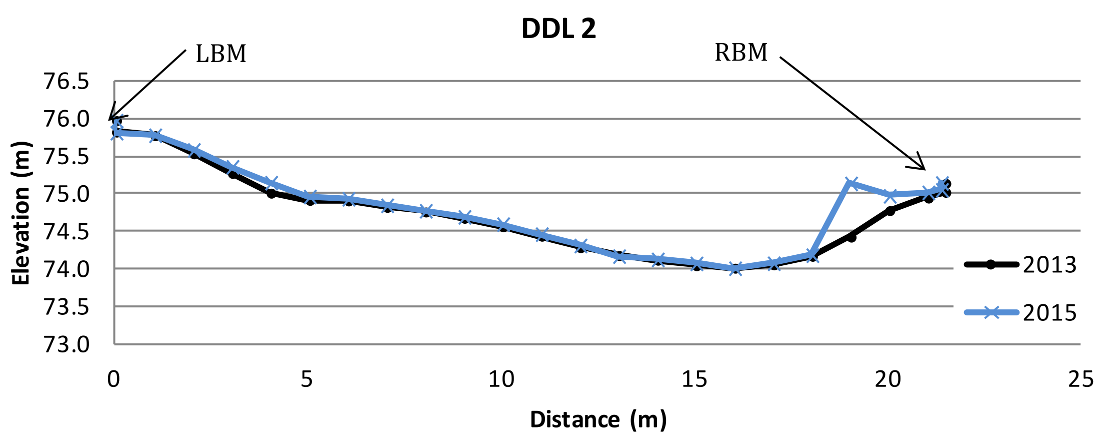
DDL 2
Elevation (m)
76.5
76.0
75.5
75.0
74.5
74.0
73.5
73.0
0
5
10
15
20
25
Distance (m)
LBM
RBM
2013
2015

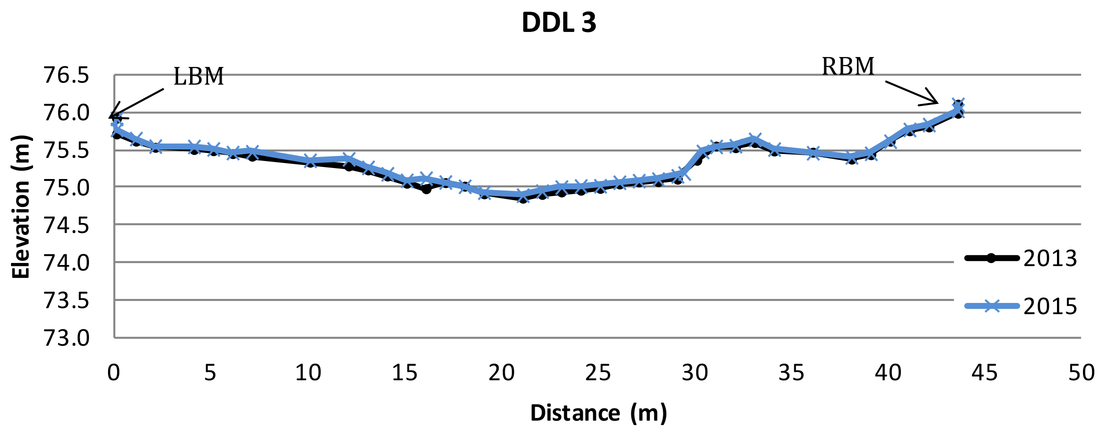
DDL 3
LBM
RBM
Elevation (m)
76.5
76.0
75.5
75.0
74.5
74.0
73.5
73.0
0
5
10
15
20
25
30
35
40
45
50
Distance (m)
2013
2015

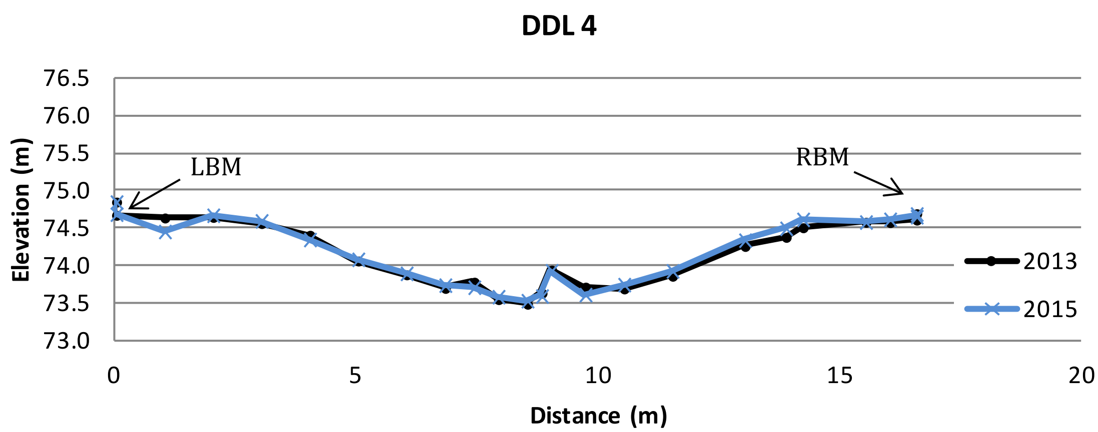
DDL 4
LBM
RBM
Elevation (m)
76.5
76.0
75.5
75.0
74.5
74.0
73.5
73.0
0
5
10
15
20
Distance (m)
2013
2015

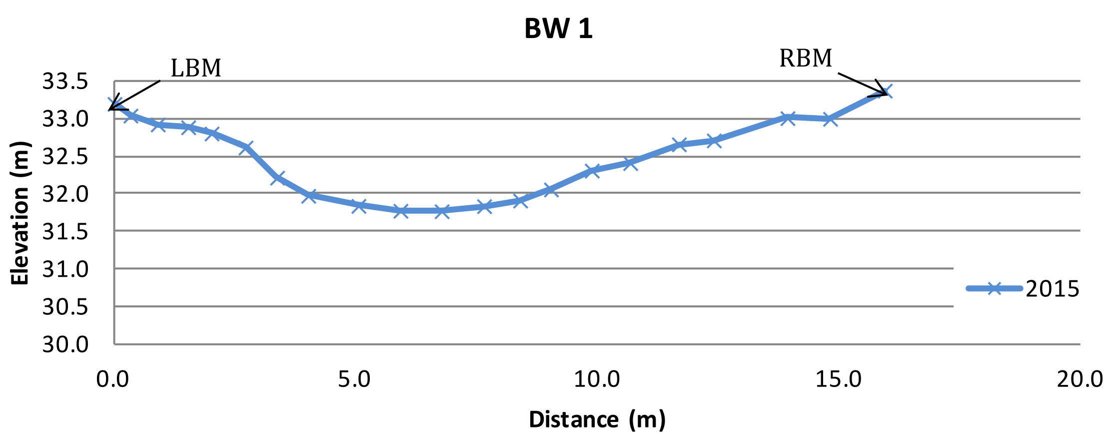
BW 1
LBM
RBM
Elevation (m)
33.5
33.0
32.5
32.0
31.5
31.0
30.5
30.0
0.0
5.0
10.0
15.0
20.0
Distance (m)
2015

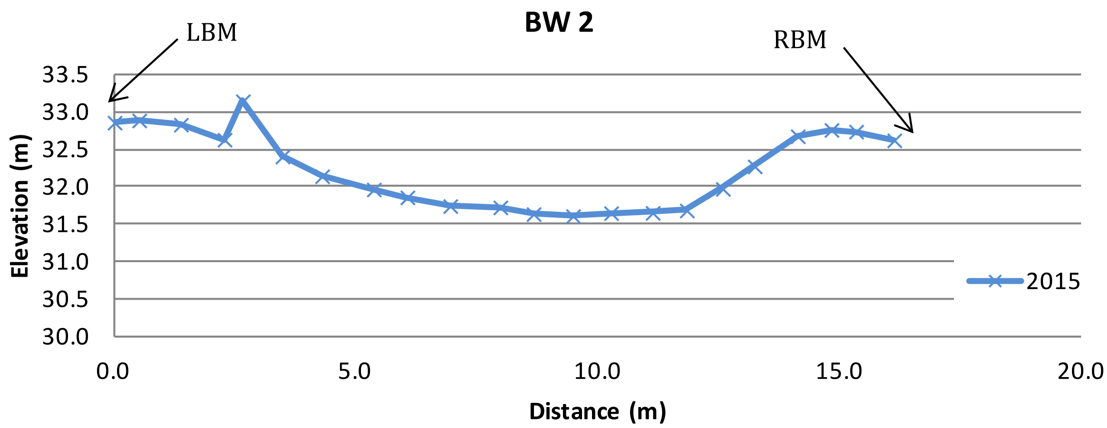
BW 2
LBM
RBM
Elevation (m)
33.5
33.0
32.5
32.0
31.5
31.0
30.5
30.0
0.0
5.0
10.0
15.0
20.0
Distance (m)
2015

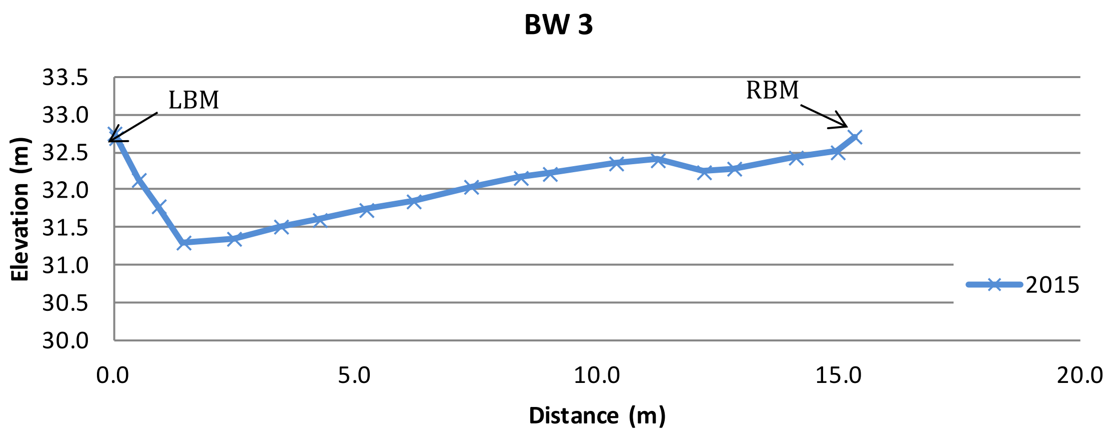
BW 3
LBM
RBM
Elevation (m)
33.5
33.0
32.5
32.0
31.5
31.0
30.5
30.0
0.0
5.0
10.0
15.0
20.0
Distance (m)
2015

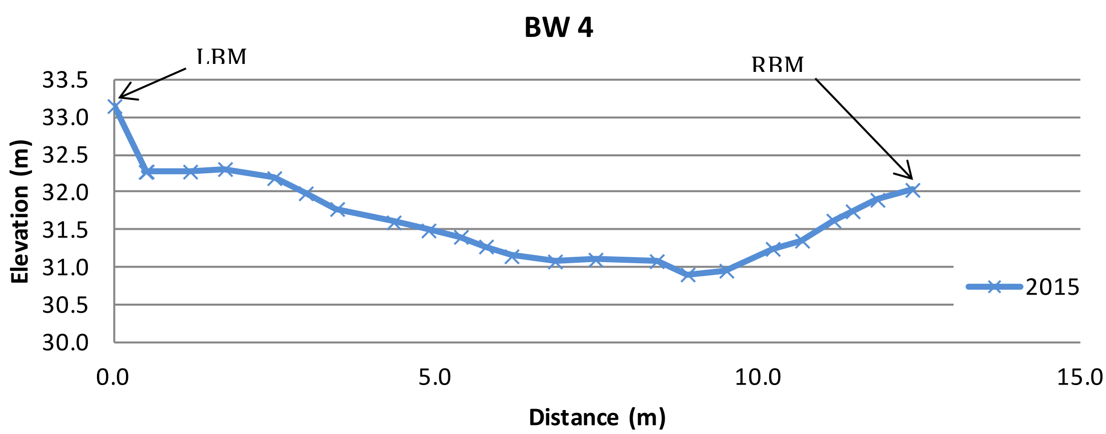
BW 4
LBM
RBM
Elevation (m)
33.5
33.0
32.5
32.0
31.5
31.0
30.5
30.0
0.0
5.0
10.0
15.0
Distance (m)
2015

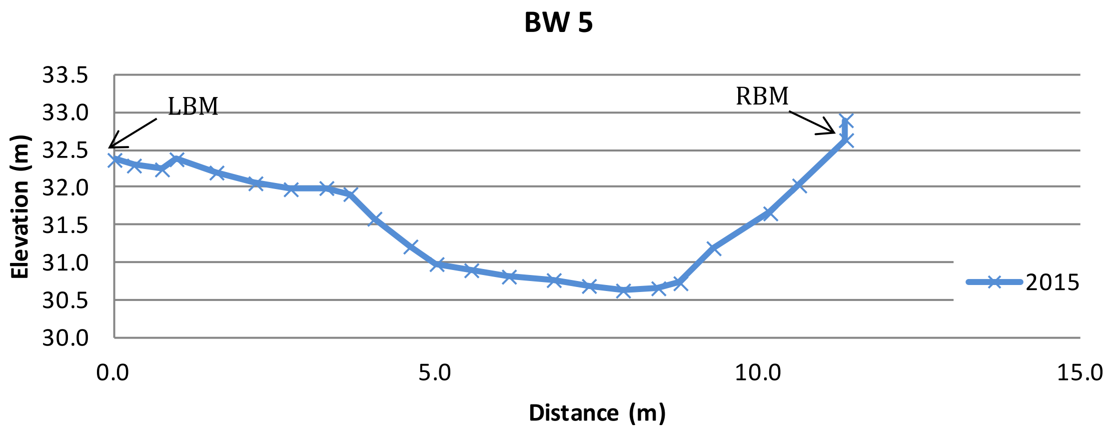
BW 5
33.5
33.0
32.5
32.0
31.5
31.0
30.5
30.0
Elevation (m)
LBM
RBM
2015
0.0
5.0
10.0
15.0
Distance (m)

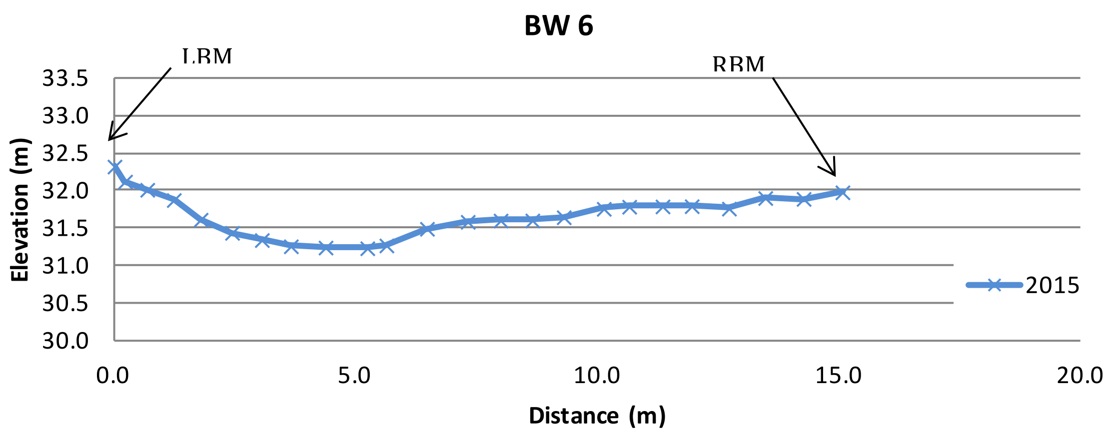
BW 6
33.5
33.0
32.5
32.0
31.5
31.0
30.5
30.0
Elevation (m)
LBM
RBM
2015
0.0
5.0
10.0
15.0
20.0
Distance (m)

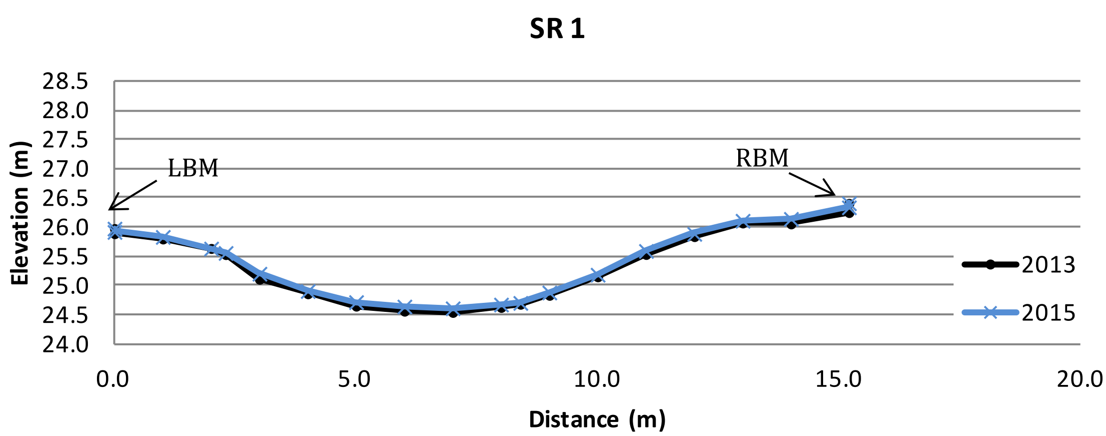
SR 1
28.5
28.0
27.5
27.0
26.5
26.0
25.5
25.0
24.5
24.0
Elevation (m)
LBM
RBM
2013
2015
0.0
5.0
10.0
15.0
20.0
Distance (m)

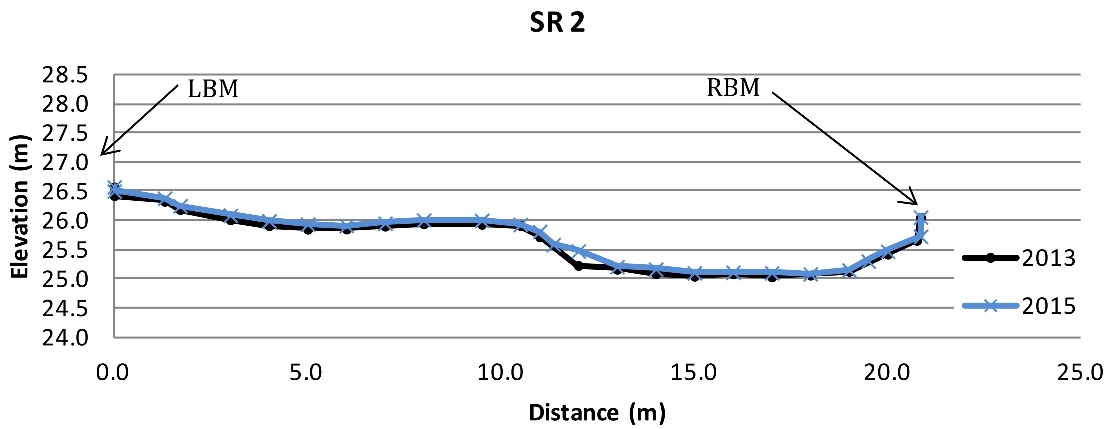
SR 2
LBM
RBM
Elevation (m)
Distance (m)
2013
2015

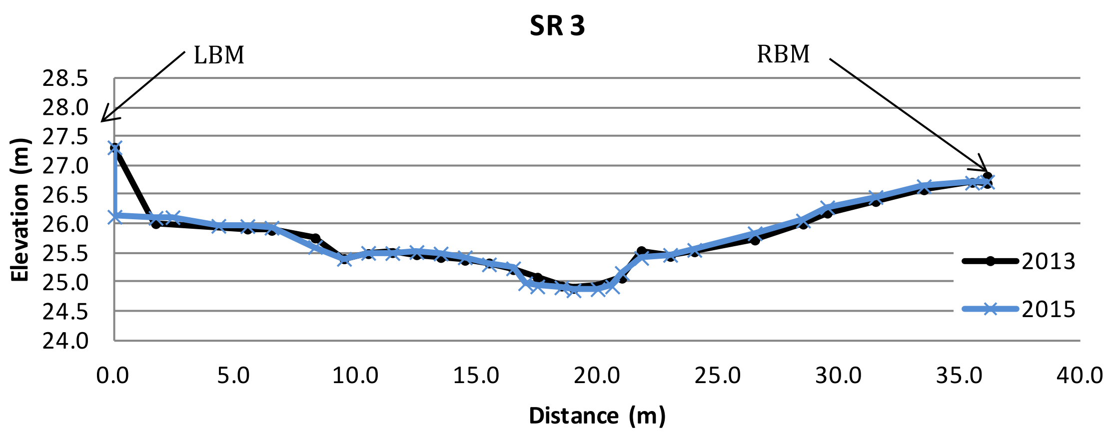
SR 3
LBM
RBM
Elevation (m)
Distance (m)
2013
2015

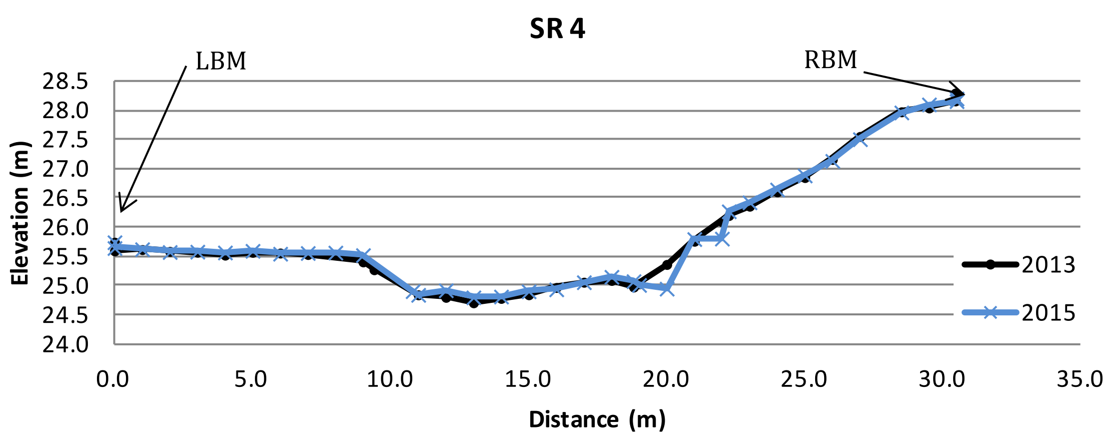
SR 4
LBM
RBM
Elevation (m)
Distance (m)
2013
2015

SC 1

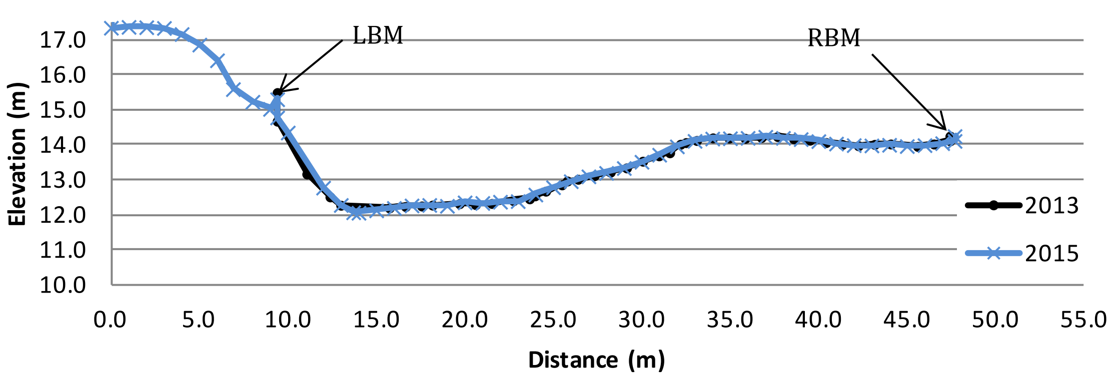

LBM
RBM
17.0
16.0
15.0
14.0
13.0
12.0
11.0
10.0
Elevation (m)
0.0
5.0
10.0
15.0
20.0
25.0
30.0
35.0
40.0
45.0
50.0
55.0
Distance (m)
2013
2015

SC 2

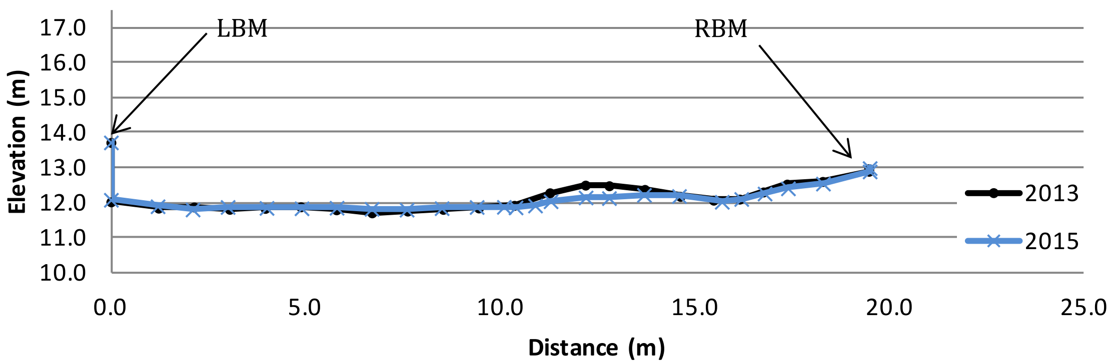

LBM
RBM
17.0
16.0
15.0
14.0
13.0
12.0
11.0
10.0
Elevation (m)
0.0
5.0
10.0
15.0
20.0
25.0
Distance (m)
2013
2015

SC 3

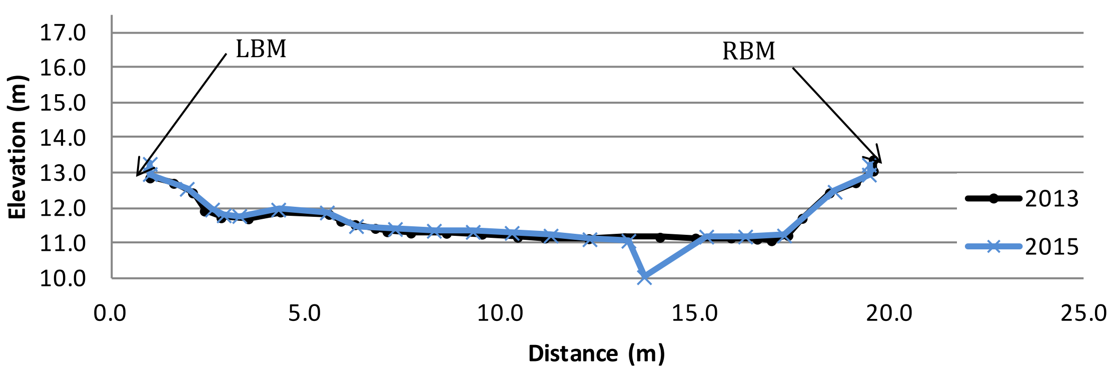

LBM
RBM
17.0
16.0
15.0
14.0
13.0
12.0
11.0
10.0
Elevation (m)
0.0
5.0
10.0
15.0
20.0
25.0
Distance (m)
2013
2015

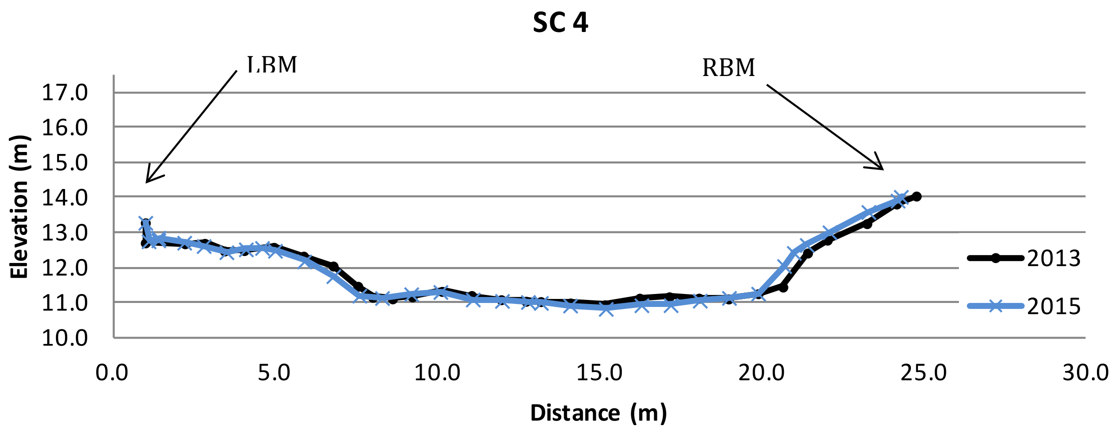
SC 4
LBM
RBM
17.0
16.0
15.0
14.0
13.0
12.0
11.0
10.0
Elevation (m)
0.0
5.0
10.0
15.0
20.0
25.0
30.0
Distance (m)
2013
2015

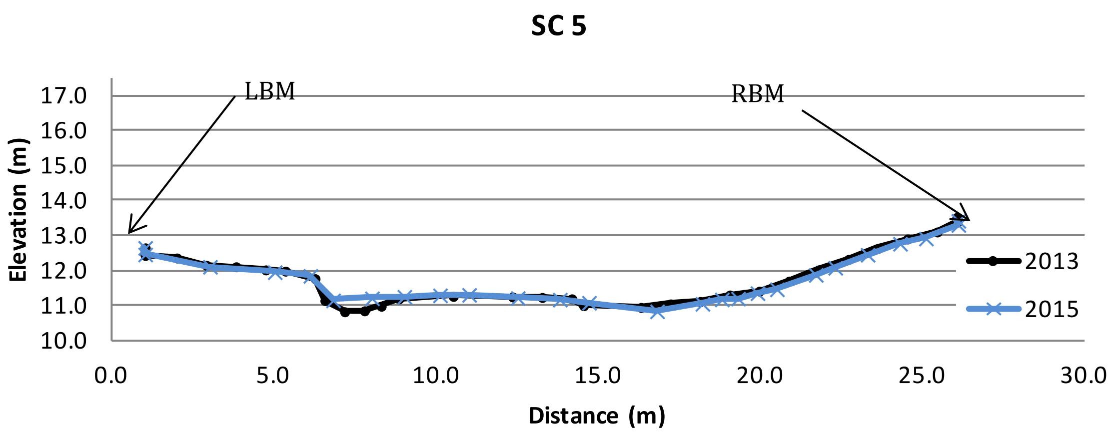
SC 5
LBM
RBM
17.0
16.0
15.0
14.0
13.0
12.0
11.0
10.0
Elevation (m)
0.0
5.0
10.0
15.0
20.0
25.0
30.0
Distance (m)
2013
2015

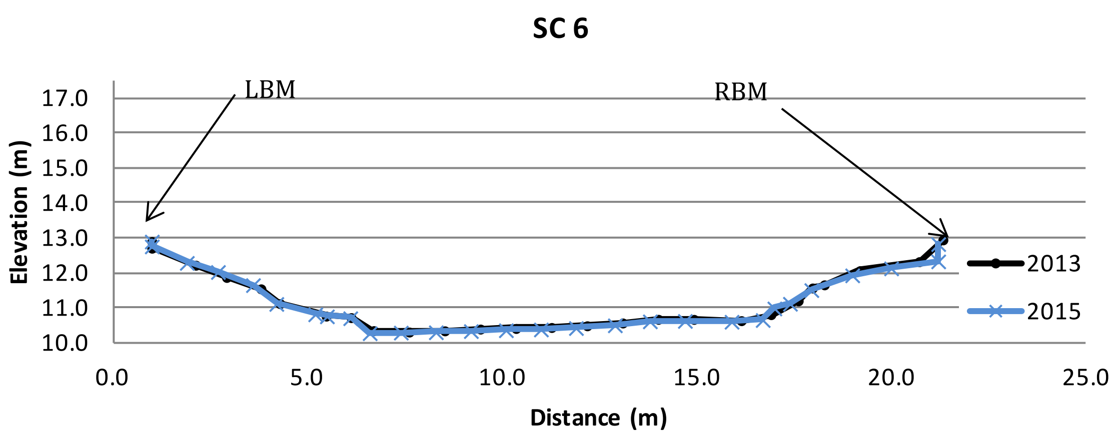
SC 6
LBM
RBM
17.0
16.0
15.0
14.0
13.0
12.0
11.0
10.0
Elevation (m)
0.0
5.0
10.0
15.0
20.0
25.0
Distance (m)
2013
2015

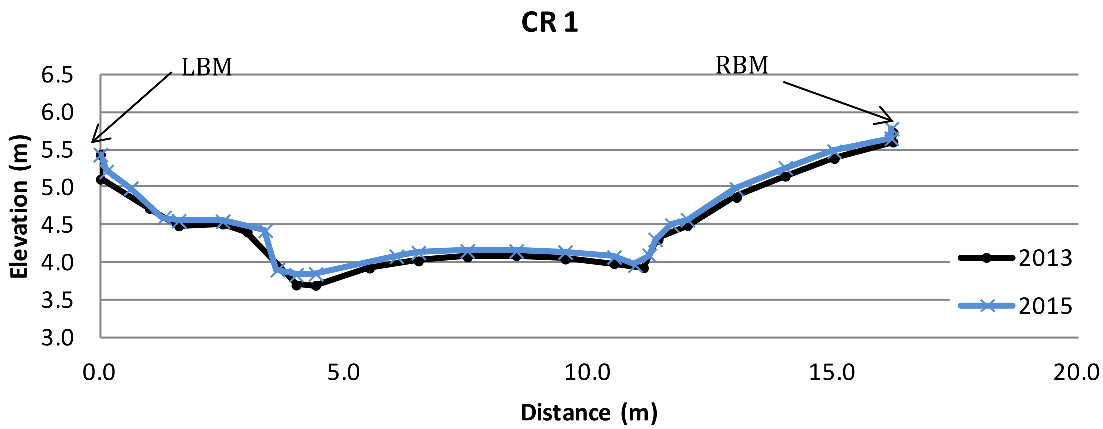
CR 1
LBM
RBM
Elevation (m)
6.5
6.0
5.5
5.0
4.5
4.0
3.5
3.0
0.0
5.0
10.0
15.0
20.0
Distance (m)
2013
2015

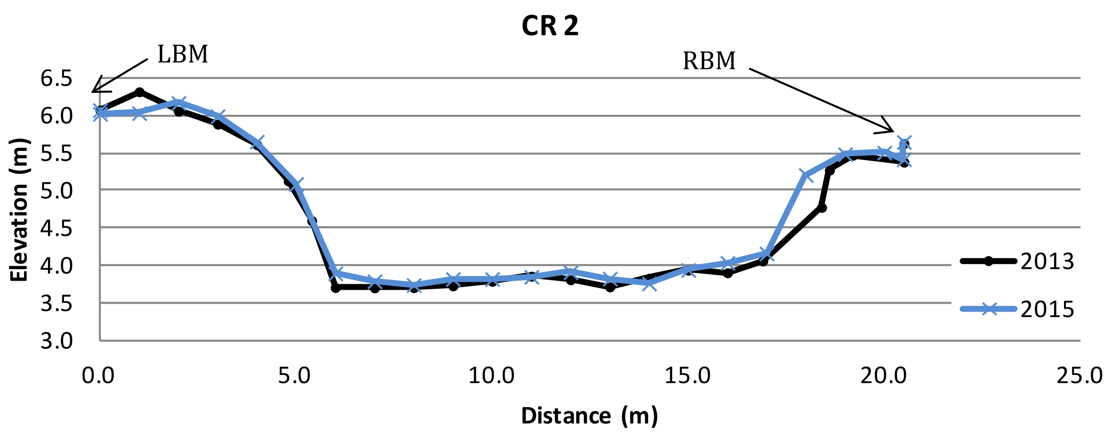
CR 2
LBM
RBM
Elevation (m)
6.5
6.0
5.5
5.0
4.5
4.0
3.5
3.0
0.0
5.0
10.0
15.0
20.0
25.0
Distance (m)
2013
2015

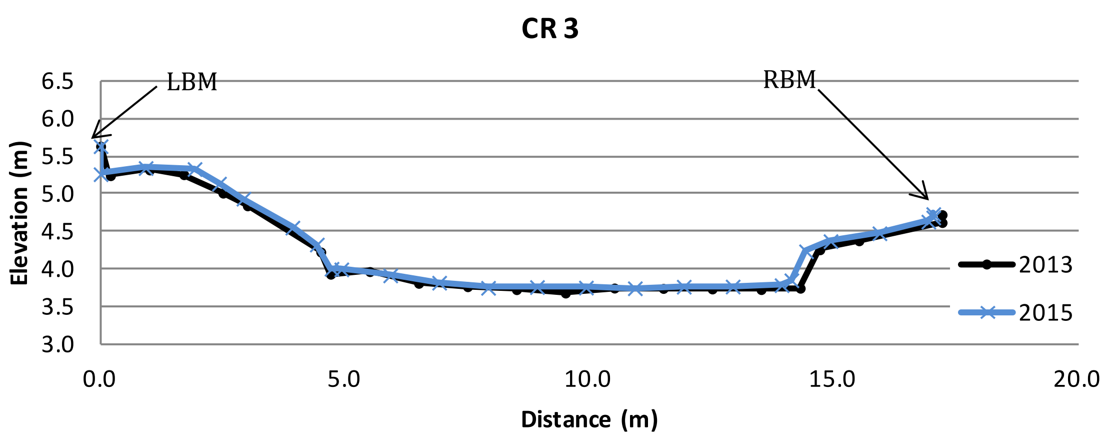
CR 3
LBM
RBM
Elevation (m)
6.5
6.0
5.5
5.0
4.5
4.0
3.5
3.0
0.0
5.0
10.0
15.0
20.0
Distance (m)
2013
2015

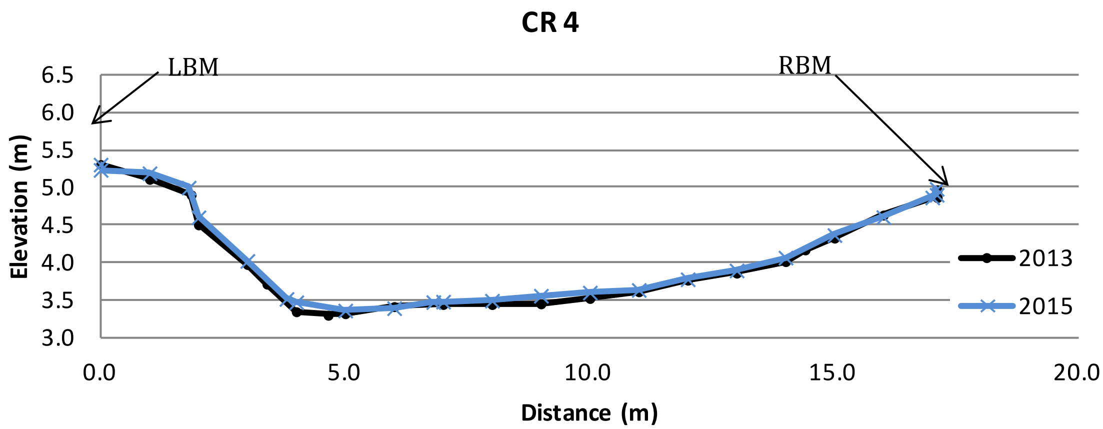
CR 4
LBM
RBM
Elevation (m)
Distance (m)
2013
2015
6.5
6.0
5.5
5.0
4.5
4.0
3.5
3.0
0.0
5.0
10.0
15.0
20.0

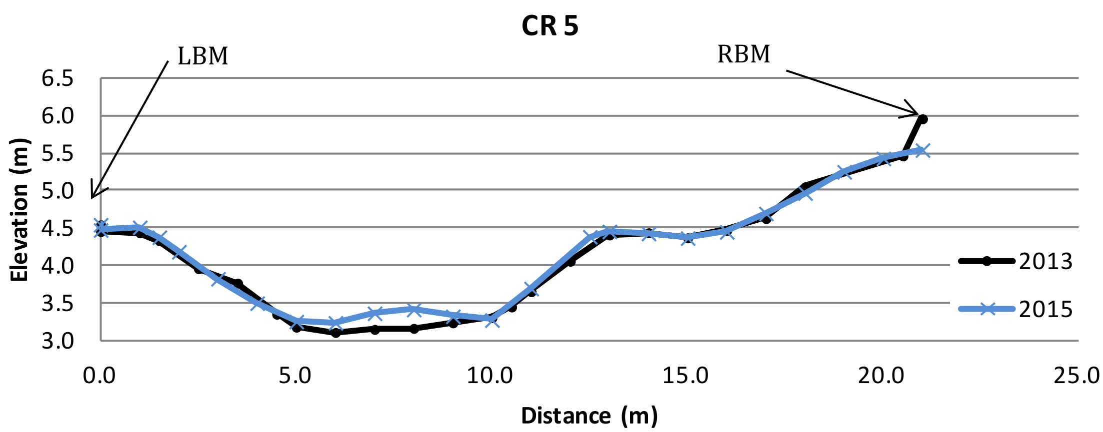
CR 5
LBM
RBM
Elevation (m)
Distance (m)
2013
2015
6.5
6.0
5.5
5.0
4.5
4.0
3.5
3.0
0.0
5.0
10.0
15.0
20.0
25.0

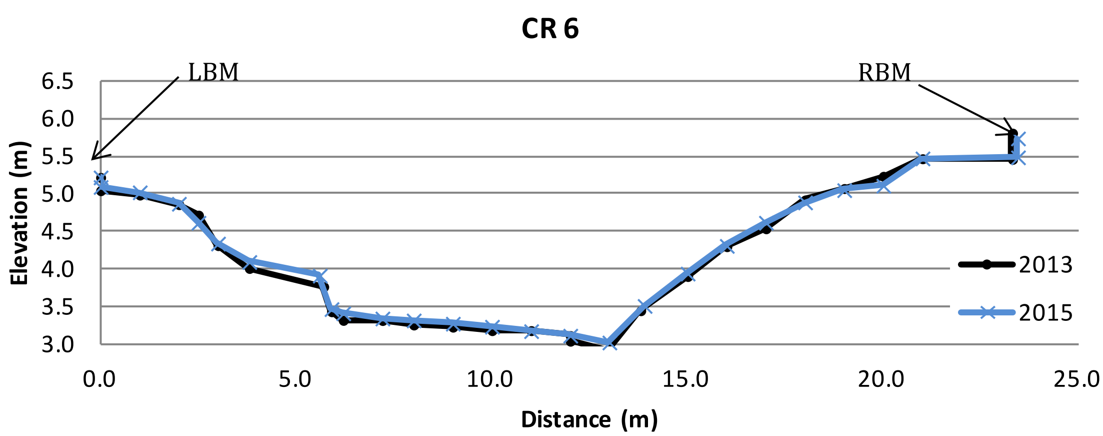
CR 6
LBM
RBM
Elevation (m)
Distance (m)
2013
2015
6.5
6.0
5.5
5.0
4.5
4.0
3.5
3.0
0.0
5.0
10.0
15.0
20.0
25.0

6.2 Pebble Counts

Channel pebble counts for each cross section within each reach. Reaches are denoted by their reach abbreviation (LP, DDU, DDL, BW, SR, SC, and CR) and transect number descending from upstream to downstream (1 to 4 or 6).

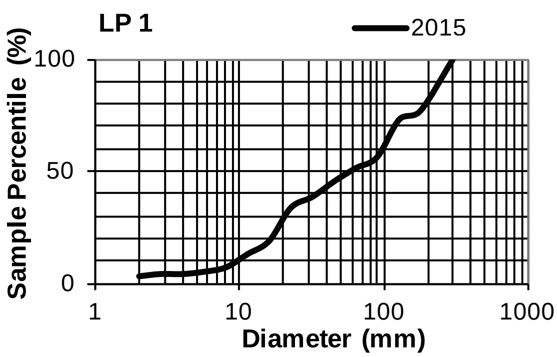

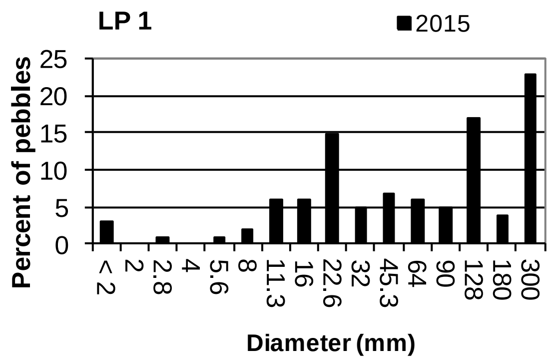

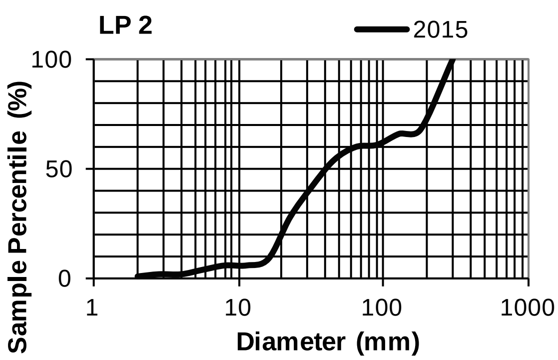

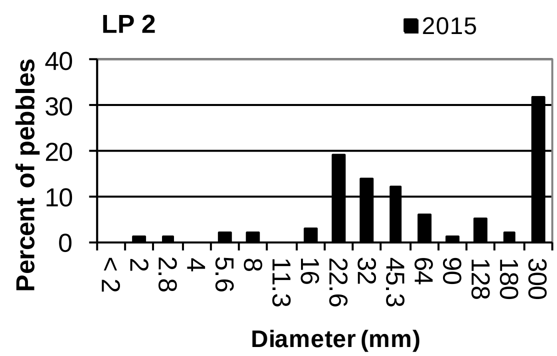

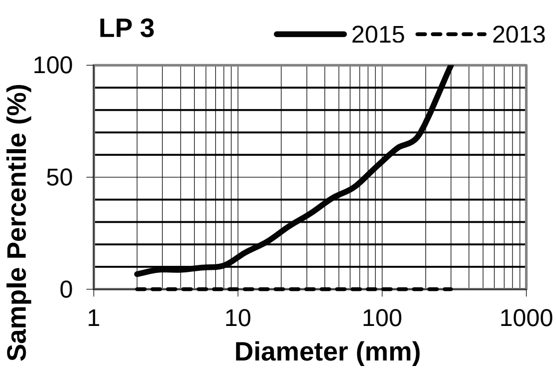

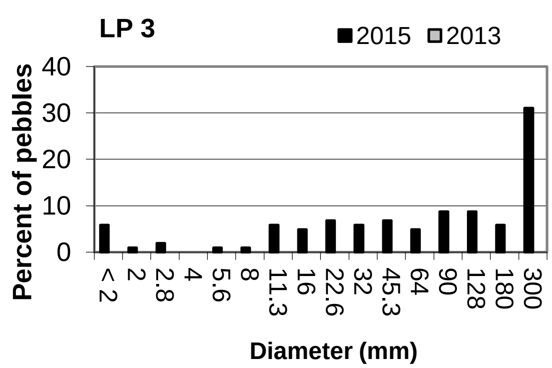

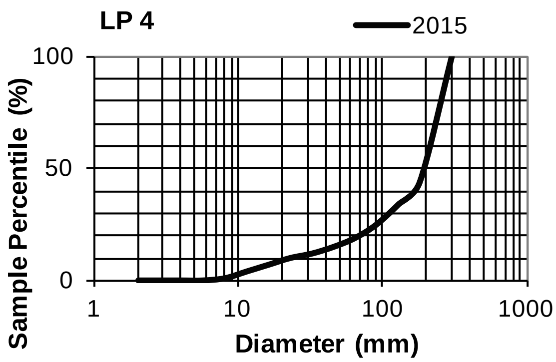
LP 4
2015
Sample Percentile (%)
100
50
0
1
10
100
1000
Diameter (mm)

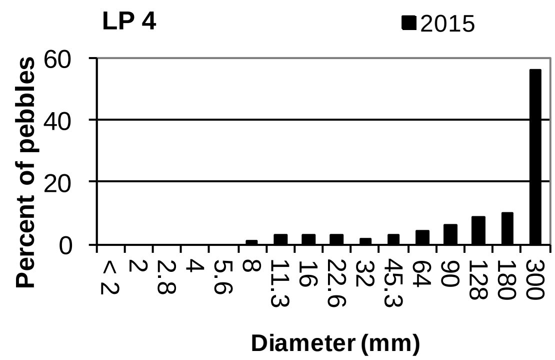
LP 4
2015
Percent of pebbles
60
40
20
0
< 2
2
2.8
4
5.6
8
11.3
16
22.6
32
45.3
64
90
128
180
300
Diameter (mm)

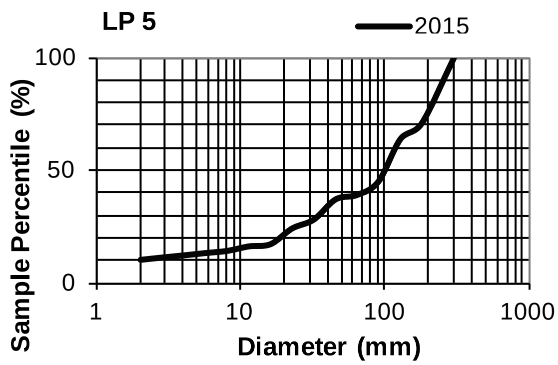
LP 5
2015
Sample Percentile (%)
100
50
0
1
10
100
1000
Diameter (mm)

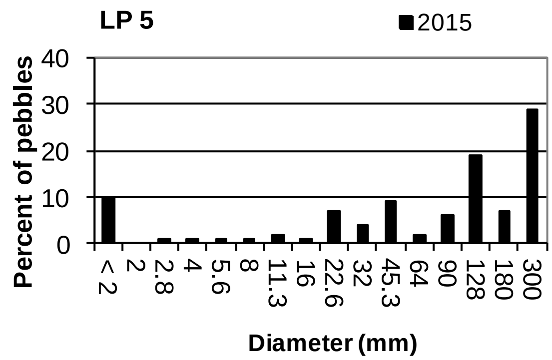
LP 5
2015
Percent of pebbles
40
30
20
10
0
< 2
2
2.8
4
5.6
8
11.3
16
22.6
32
45.3
64
90
128
180
300
Diameter (mm)

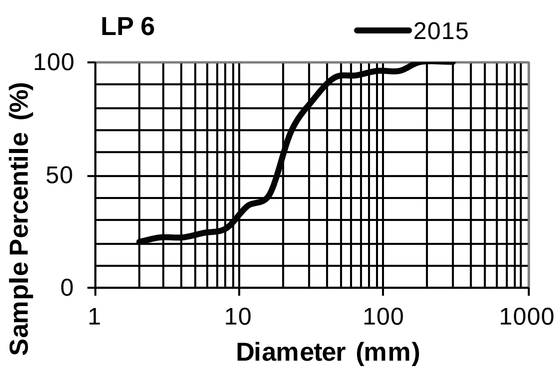
LP 6
2015
Sample Percentile (%)
100
50
0
1
10
100
1000
Diameter (mm)

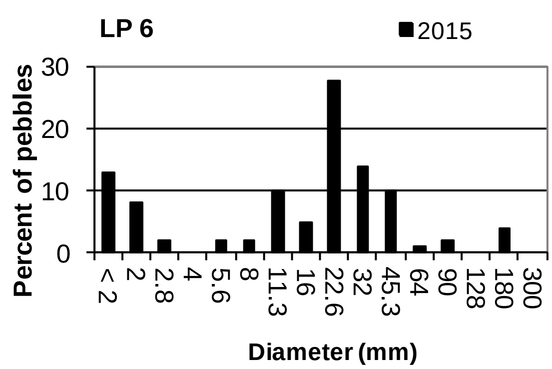
LP 6
2015
Percent of pebbles
30
20
10
0
< 2
2
2.8
4
5.6
8
11.3
16
22.6
32
45.3
64
90
128
180
300
Diameter (mm)

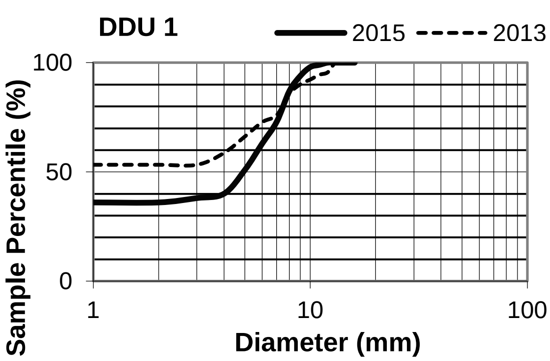
DDU 1
2015
2013
Sample Percentile (%)
100
50
0
1
10
100
Diameter (mm)

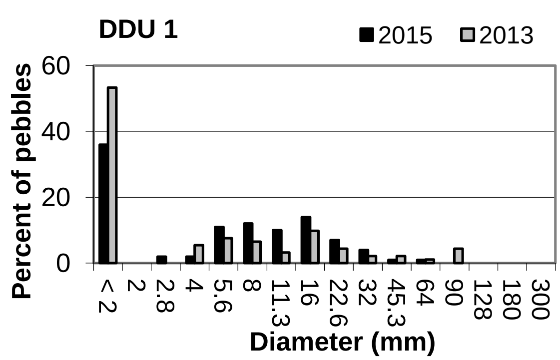
DDU 1
2015
2013
Percent of pebbles
60
40
20
0
< 2
2
2.8
4
5.6
8
11.3
16
22.6
32
45.3
64
90
128
180
300
Diameter (mm)

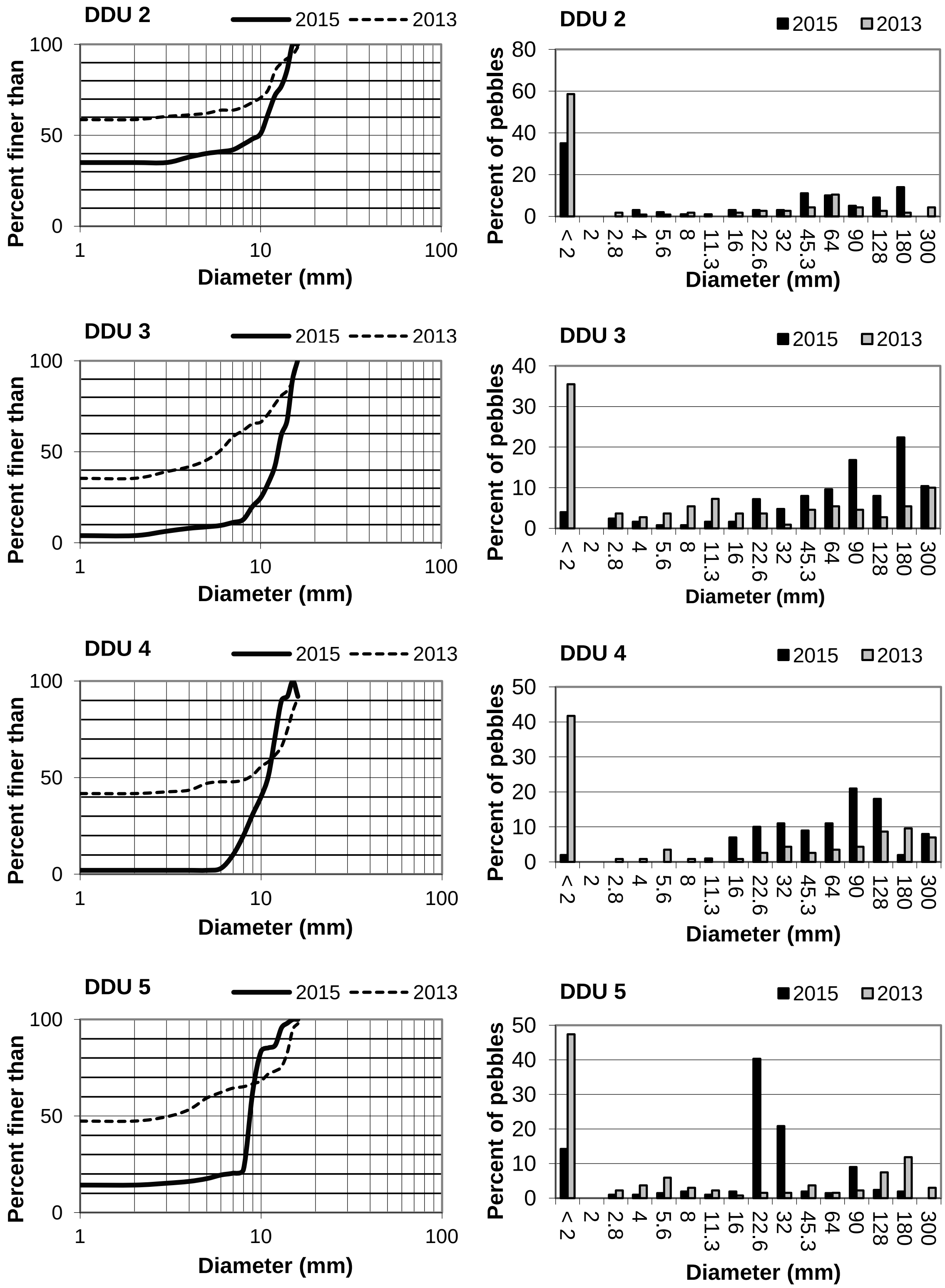
DDU 2
2015
2013
Percent finer than
Diameter (mm)
Percent of pebbles
DDU 3
DDU 4
DDU 5
< 2
2
2.8
4
5.6
8
11.3
16
22.6
32
45.3
64
90
128
180
300

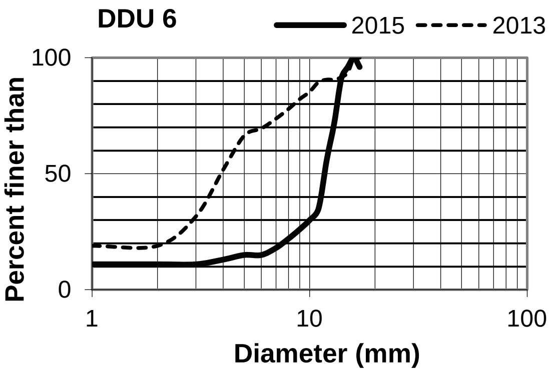
DDU 6
2015
2013
Percent finer than
100
50
0
1
10
100
Diameter (mm)

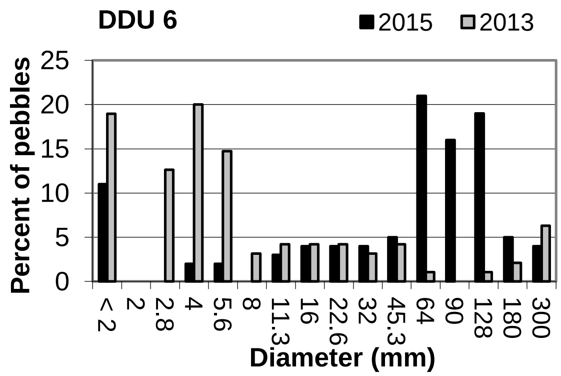
DDU 6
2015
2013
Percent of pebbles
25
20
15
10
5
0
< 2
2
2.8
4
5.6
8
11.3
16
22.6
32
45.3
64
90
128
180
300
Diameter (mm)

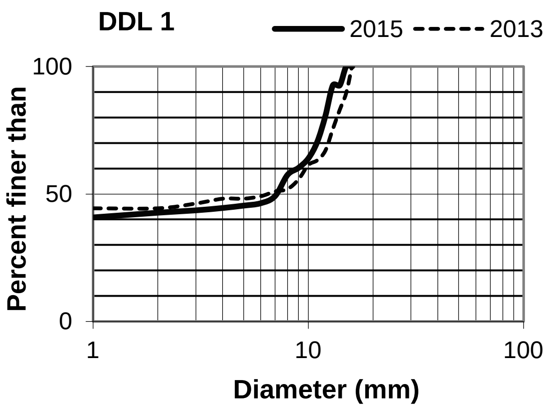
DDL 1
2015
2013
Percent finer than
100
50
0
1
10
100
Diameter (mm)

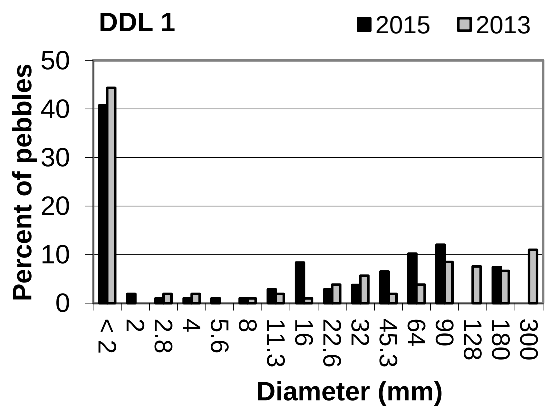
DDL 1
2015
2013
Percent of pebbles
50
40
30
20
10
0
< 2
2
2.8
4
5.6
8
11.3
16
22.6
32
45.3
64
90
128
180
300
Diameter (mm)

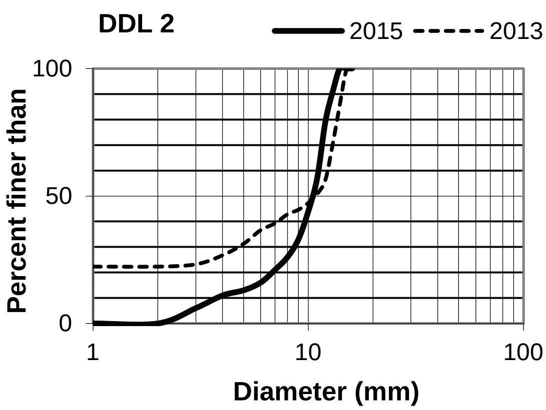
DDL 2
2015
2013
Percent finer than
100
50
0
1
10
100
Diameter (mm)

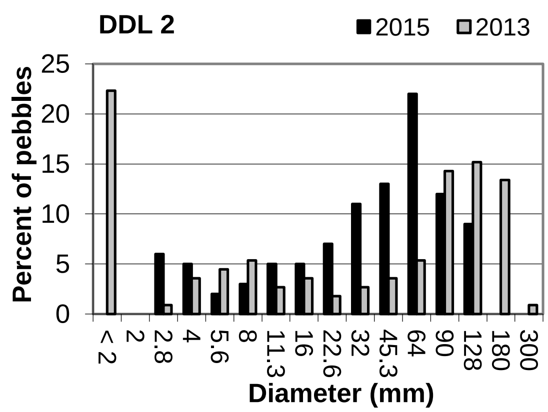
DDL 2
2015
2013
Percent of pebbles
25
20
15
10
5
0
< 2
2
2.8
4
5.6
8
11.3
16
22.6
32
45.3
64
90
128
180
300
Diameter (mm)

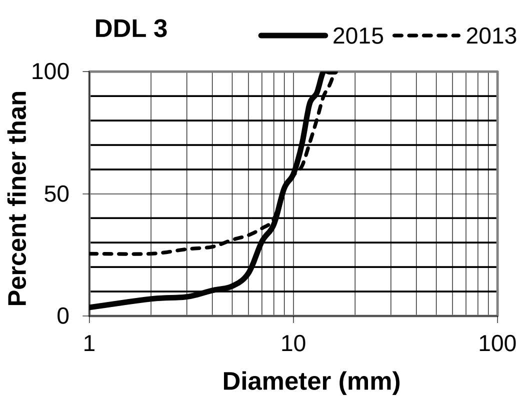
DDL 3
2015
2013
Percent finer than
100
50
0
1
10
100
Diameter (mm)

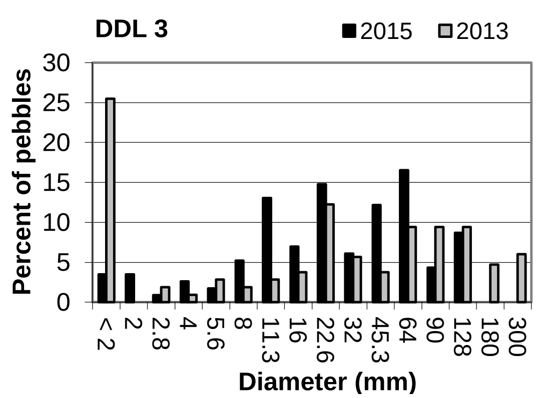
DDL 3
2015
2013
Percent of pebbles
30
25
20
15
10
5
0
< 2
2
2.8
4
5.6
8
11.3
16
22.6
32
45.3
64
90
128
180
300
Diameter (mm)

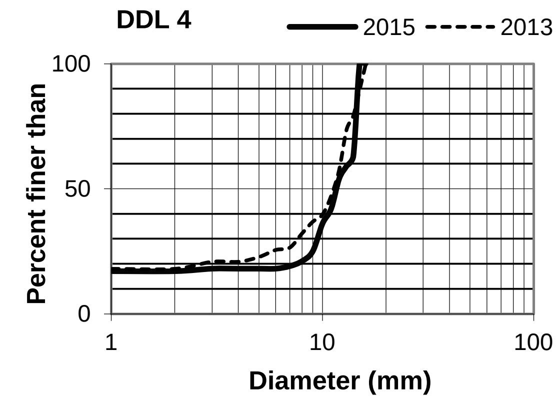
DDL 4
2015
2013
Percent finer than
Diameter (mm)

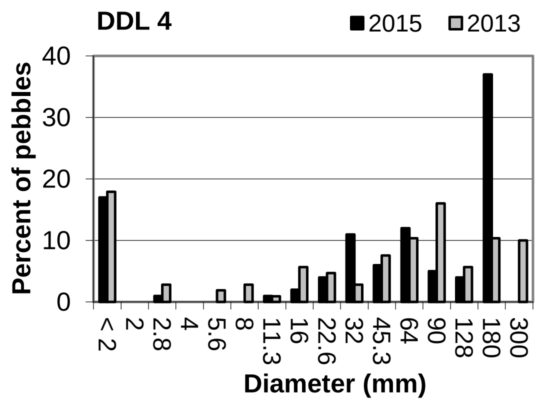
DDL 4
2015
2013
Percent of pebbles
Diameter (mm)

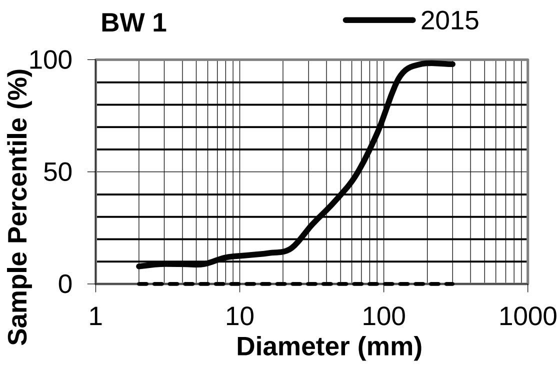
BW 1
2015
Sample Percentile (%)
Diameter (mm)

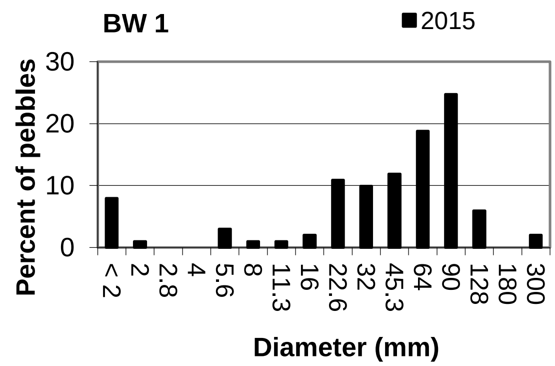
BW 1
2015
Percent of pebbles
Diameter (mm)

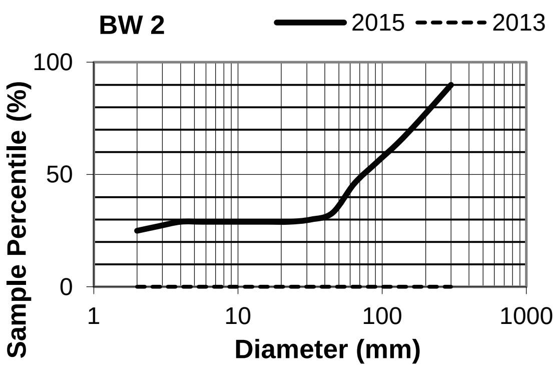
BW 2
2015
2013
Sample Percentile (%)
Diameter (mm)

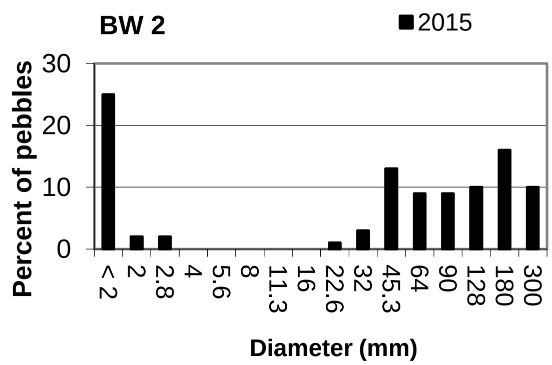
BW 2
2015
Percent of pebbles
Diameter (mm)

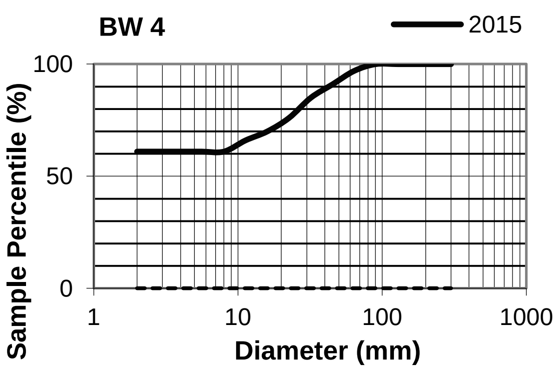
BW 4
2015
Sample Percentile (%)
Diameter (mm)

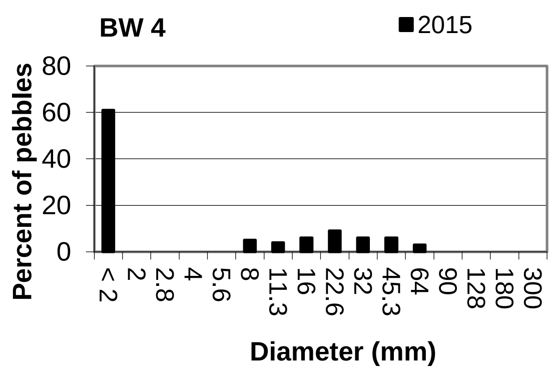
BW 4
2015
Percent of pebbles
Diameter (mm)

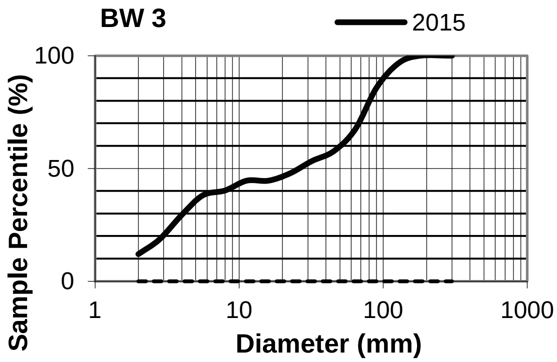
BW 3
2015
Sample Percentile (%)
100
50
0
1
10
100
1000
Diameter (mm)

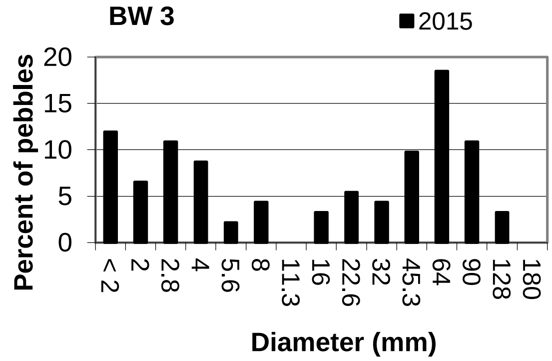
BW 3
2015
Percent of pebbles
20
15
10
5
0
< 2
2
2.8
4
5.6
8
11.3
16
22.6
32
45.3
64
90
128
180
Diameter (mm)

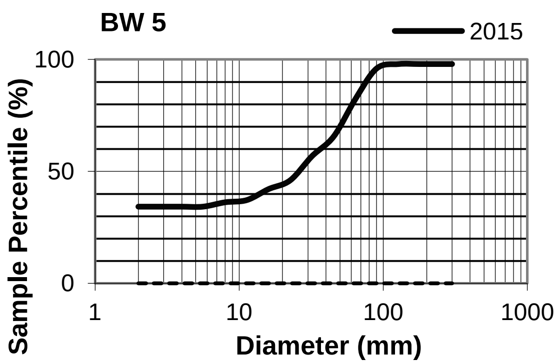
BW 5
2015
Sample Percentile (%)
100
50
0
1
10
100
1000
Diameter (mm)

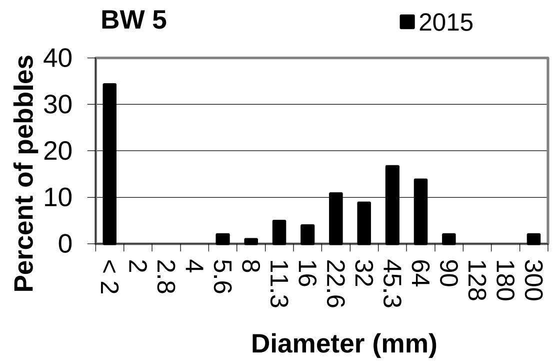
BW 5
2015
Percent of pebbles
40
30
20
10
0
< 2
2
2.8
4
5.6
8
11.3
16
22.6
32
45.3
64
90
128
180
300
Diameter (mm)

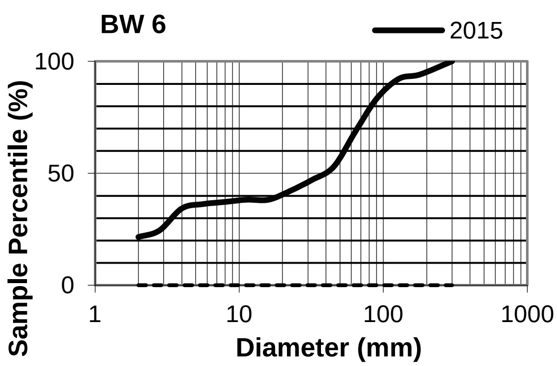
BW 6
2015
Sample Percentile (%)
100
50
0
1
10
100
1000
Diameter (mm)

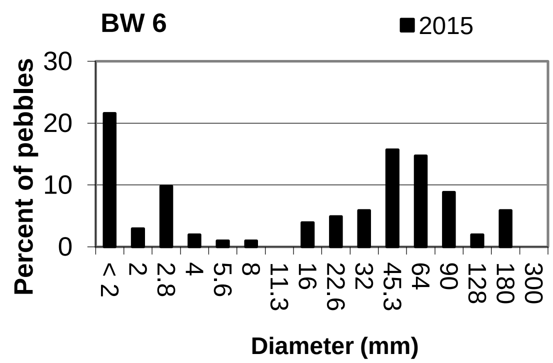
BW 6
2015
Percent of pebbles
30
20
10
0
< 2
2
2.8
4
5.6
8
11.3
16
22.6
32
45.3
64
90
128
180
300
Diameter (mm)

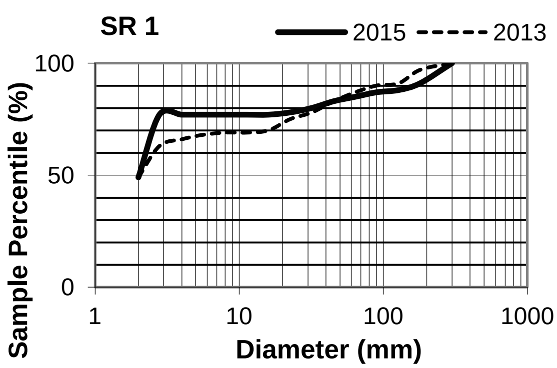
SR 1
2015
2013
Sample Percentile (%)
100
50
0
1
10
100
1000
Diameter (mm)

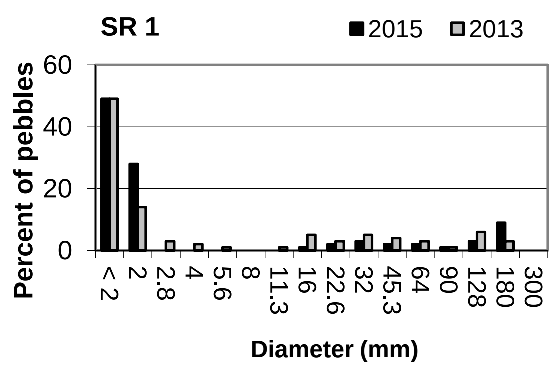
SR 1
2015
2013
Percent of pebbles
60
40
20
0
< 2
2
2.8
4
5.6
8
11.3
16
22.6
32
45.3
64
90
128
180
300
Diameter (mm)

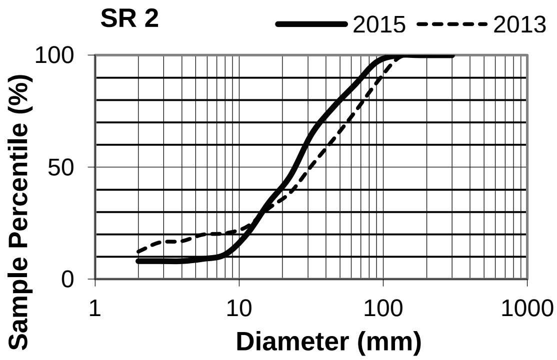
SR 2
2015
2013
Sample Percentile (%)
100
50
0
1
10
100
1000
Diameter (mm)

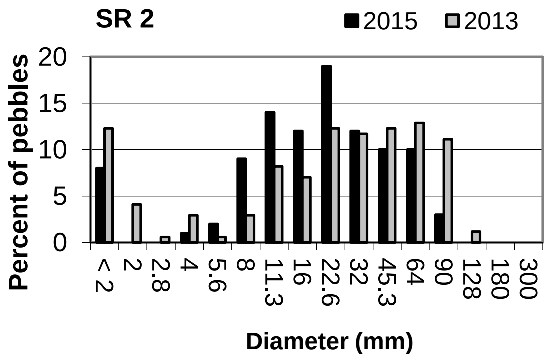
SR 2
2015
2013
Percent of pebbles
20
15
10
5
0
< 2
2
2.8
4
5.6
8
11.3
16
22.6
32
45.3
64
90
128
180
300
Diameter (mm)

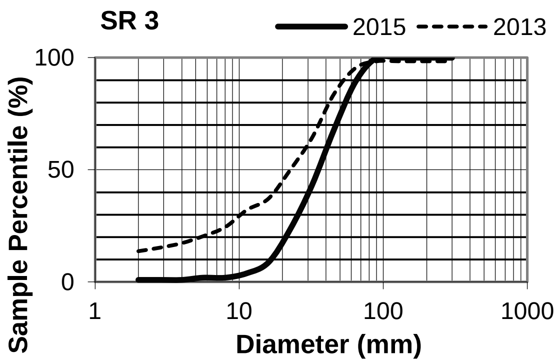
SR 3
2015
2013
Sample Percentile (%)
100
50
0
1
10
100
1000
Diameter (mm)

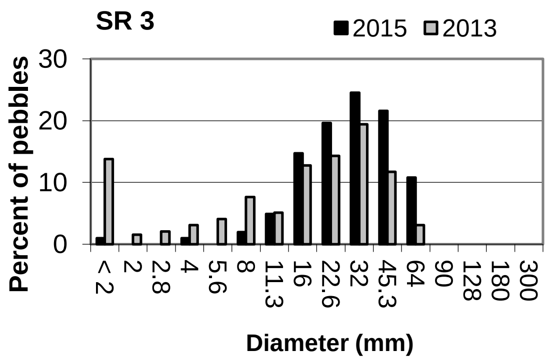
SR 3
2015
2013
Percent of pebbles
30
20
10
0
< 2
2
2.8
4
5.6
8
11.3
16
22.6
32
45.3
64
90
128
180
300
Diameter (mm)

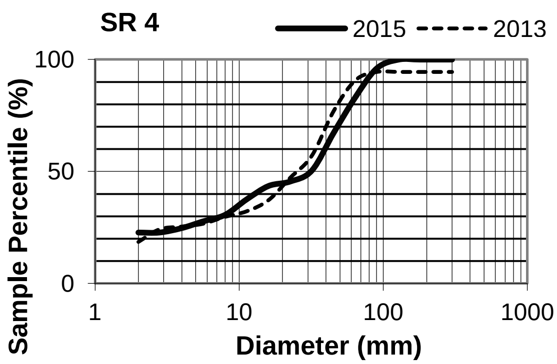
SR 4
2015
2013
Sample Percentile (%)
100
50
0
1
10
100
1000
Diameter (mm)

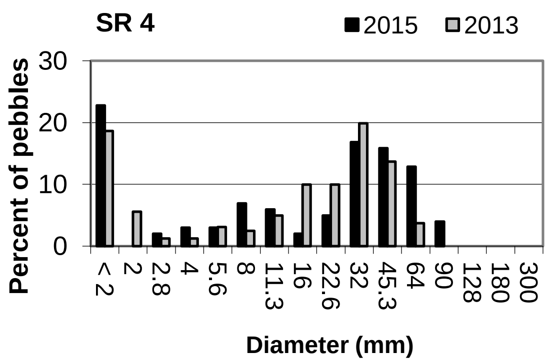
SR 4
2015
2013
Percent of pebbles
30
20
10
0
< 2
2
2.8
4
5.6
8
11.3
16
22.6
32
45.3
64
90
128
180
300
Diameter (mm)

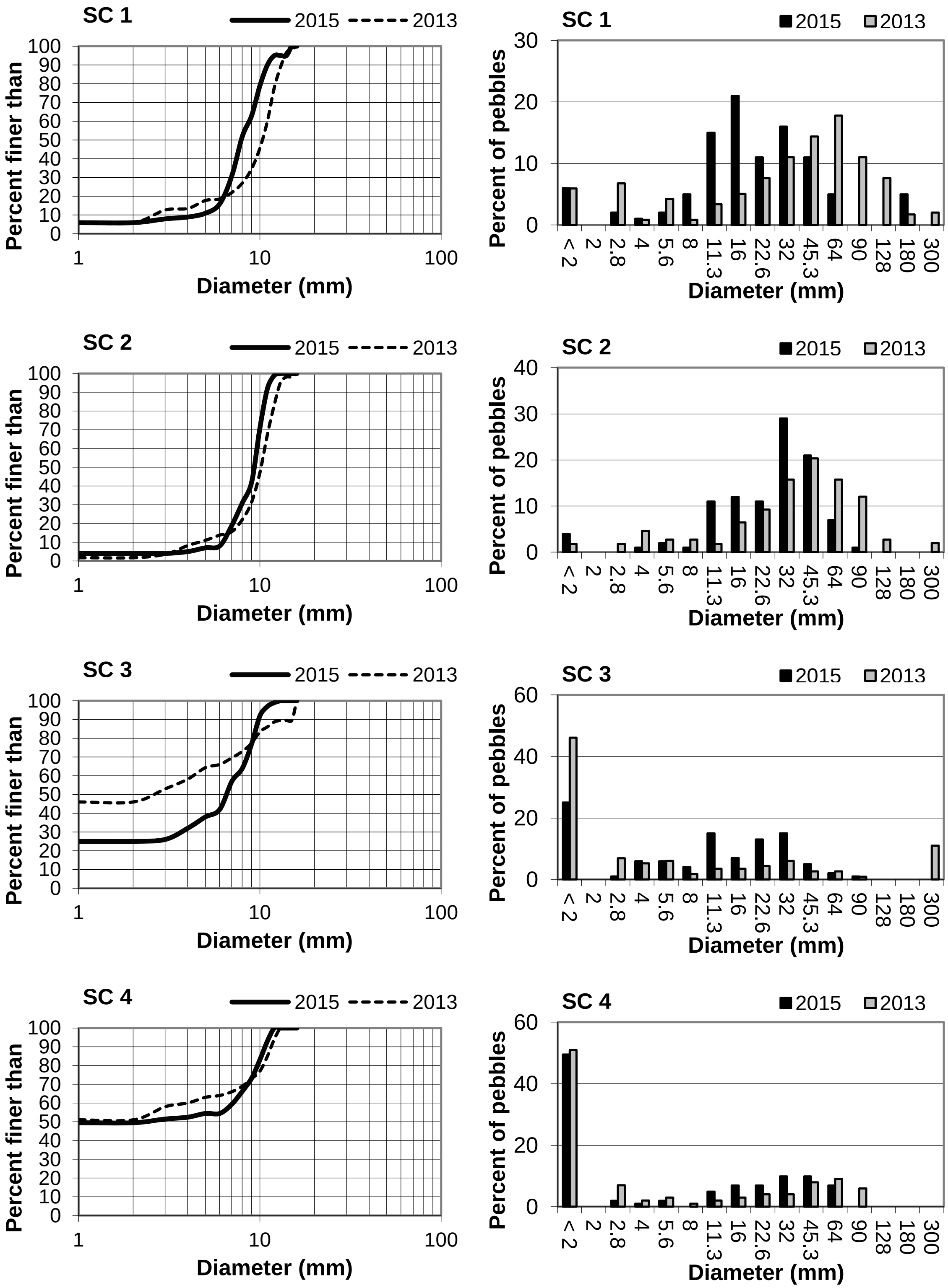
SC 1
2015
2013
Percent finer than
Diameter (mm)
Percent of pebbles
SC 2
SC 3
SC 4
< 2
2
2.8
4
5.6
8
11.3
16
22.6
32
45.3
64
90
128
180
300

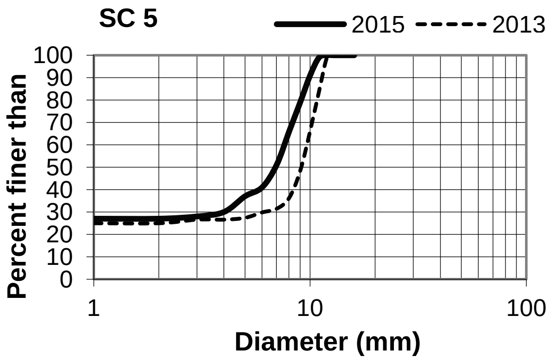
SC 5
2015
2013
Percent finer than
100
90
80
70
60
50
40
30
20
10
0
1
10
100
Diameter (mm)

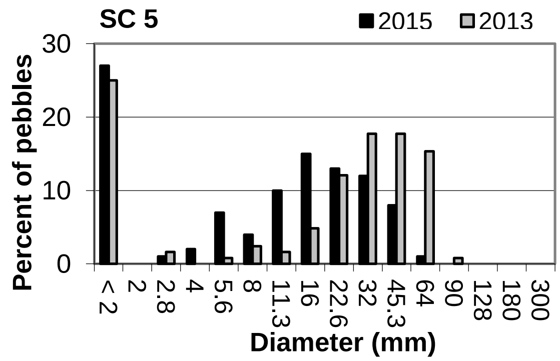
SC 5
2015
2013
Percent of pebbles
30
20
10
0
< 2
2
2.8
4
5.6
8
11.3
16
22.6
32
45.3
64
90
128
180
300
Diameter (mm)

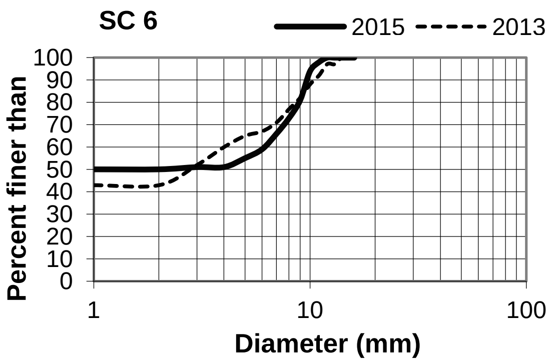
SC 6
2015
2013
Percent finer than
100
90
80
70
60
50
40
30
20
10
0
1
10
100
Diameter (mm)

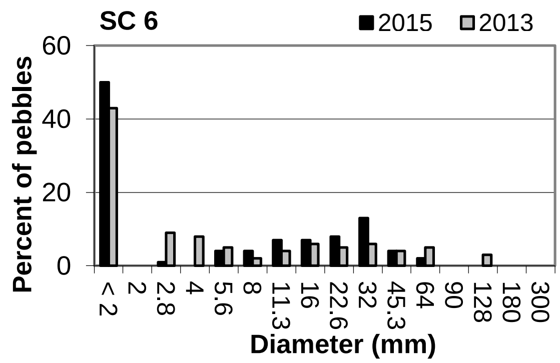
SC 6
2015
2013
Percent of pebbles
60
40
20
0
< 2
2
2.8
4
5.6
8
11.3
16
22.6
32
45.3
64
90
128
180
300
Diameter (mm)

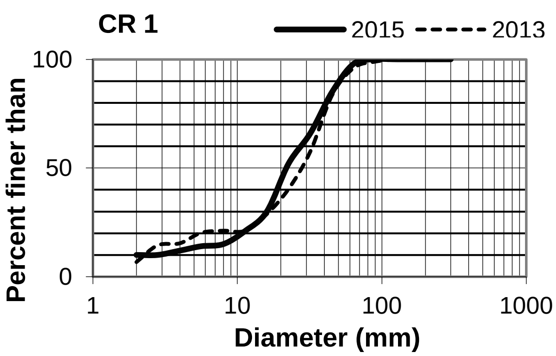
CR 1
2015
2013
Percent finer than
100
50
0
1
10
100
1000
Diameter (mm)

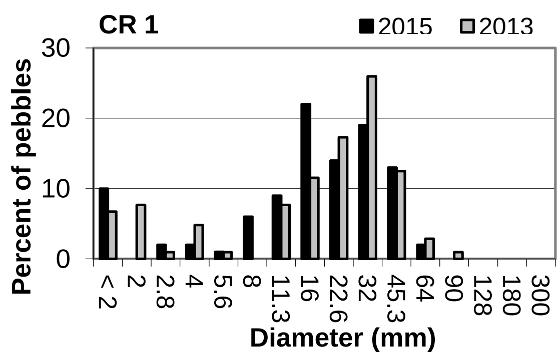
CR 1
2015
2013
Percent of pebbles
30
20
10
0
< 2
2
2.8
4
5.6
8
11.3
16
22.6
32
45.3
64
90
128
180
300
Diameter (mm)

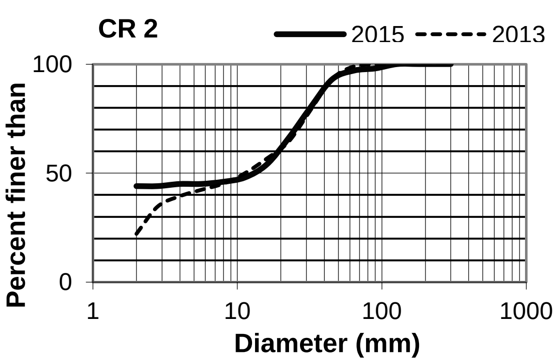
CR 2
2015
2013
Percent finer than
100
50
0
1
10
100
1000
Diameter (mm)

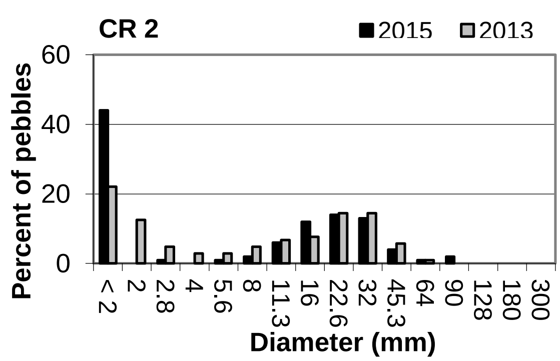
CR 2
2015
2013
Percent of pebbles
60
40
20
0
< 2
2
2.8
4
5.6
8
11.3
16
22.6
32
45.3
64
90
128
180
300
Diameter (mm)

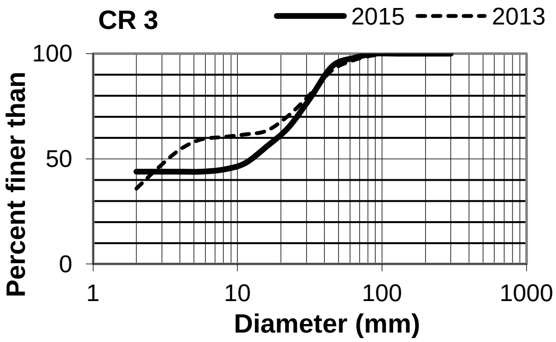
CR 3
2015
2013
Percent finer than
100
50
0
1
10
100
1000
Diameter (mm)

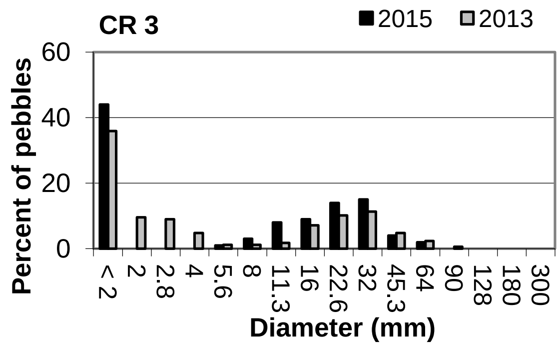
CR 3
2015
2013
Percent of pebbles
60
40
20
0
< 2
2
2.8
4
5.6
8
11.3
16
22.6
32
45.3
64
90
128
180
300
Diameter (mm)

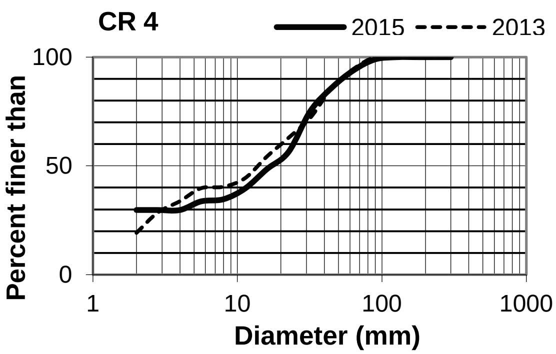
CR 4
2015
2013
Percent finer than
100
50
0
1
10
100
1000
Diameter (mm)

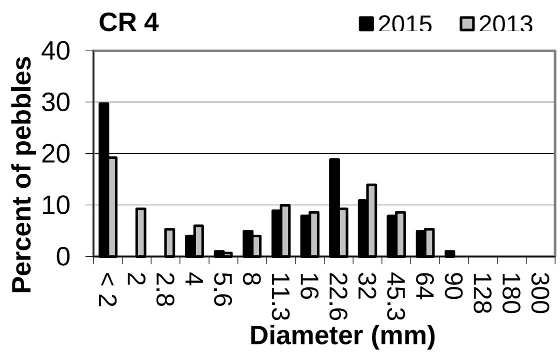
CR 4
2015
2013
Percent of pebbles
40
30
20
10
0
< 2
2
2.8
4
5.6
8
11.3
16
22.6
32
45.3
64
90
128
180
300
Diameter (mm)

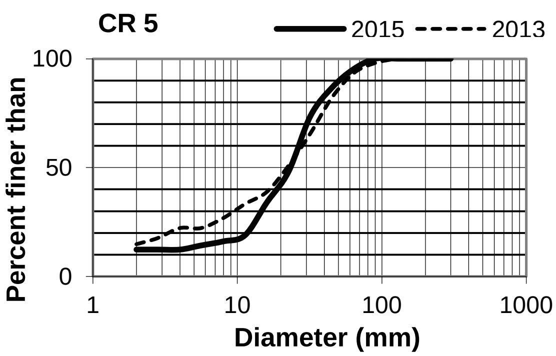
CR 5
2015
2013
Percent finer than
100
50
0
1
10
100
1000
Diameter (mm)

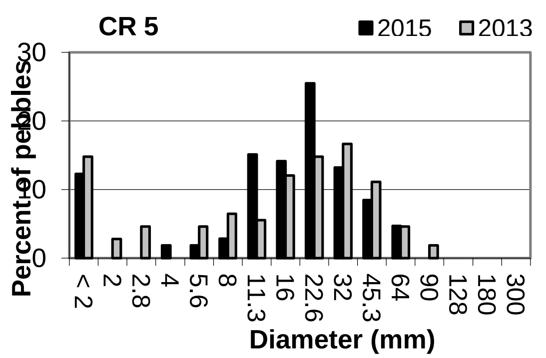
CR 5
2015
2013
Percent of pebbles
30
0
< 2
2
2.8
4
5.6
8
11.3
16
22.6
32
45.3
64
90
128
180
300
Diameter (mm)

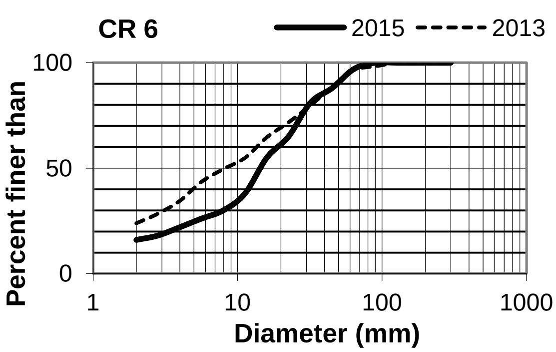
CR 6
2015
2013
Percent finer than
100
50
0
1
10
100
1000
Diameter (mm)

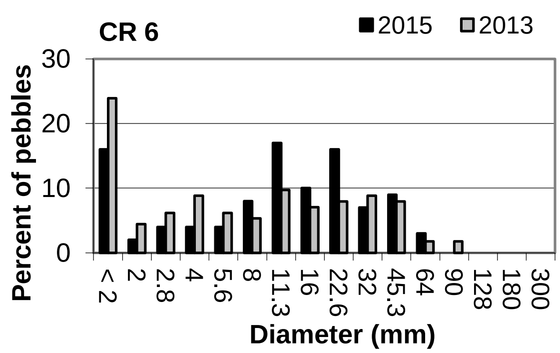
CR 6
2015
2013
Percent of pebbles
30
20
10
0
< 2
2
2.8
4
5.6
8
11.3
16
22.6
32
45.3
64
90
128
180
300
Diameter (mm)

ANALYSIS OF THE CARMEL VALLEY ALLUVIAL GROUND-WATER BASIN, MONTEREY COUNTY, CALIFORNIA

U.S. GEOLOGICAL SURVEY
Water-Resources Investigations
Report 83-4280

Prepared in cooperation with the
MONTEREY PENINSULA WATER MANAGEMENT DISTRICT

ANALYSIS OF THE CARMEL VALLEY ALLUVIAL GROUND-WATER BASIN,

MONTEREY COUNTY, CALIFORNIA

By Glenn W. Kapple, Hugh T. Mitten, Timothy J. Durbin, and Michael J. Johnson

---

U.S. GEOLOGICAL SURVEY

Water-Resources Investigations Report 83-4280

Prepared in cooperation with the

MONTEREY PENINSULA WATER MANAGEMENT DISTRICT

4024-06

Sacramento, California
June 1984

UNITED STATES DEPARTMENT OF THE INTERIOR

WILLIAM P. CLARK, Secretary

GEOLOGICAL SURVEY

Dallas L. Peck, Director

For additional information
write to:

District Chief
U.S. Geological Survey
Federal Building, Room W-2235
2800 Cottage Way
Sacramento, CA 95825

Copies of this report
can be purchased from:

Open-File Services Section
Western Distribution Branch
U.S. Geological Survey
Box 25425, Federal Center
Denver, CO 80225
Telephone: (303) 236-7476

CONTENTS

ILLUSTRATIONS

TABLES

CONVERSION FACTORS

The inch-pound system of units is used in this report. For readers who prefer International System of Units (SI), the conversion factors for the terms used in this report are listed below:

Multiply	By	To obtain
acres	0.4047	ha (hectares)
acre-ft (acre-feet)	0.001233	hm^3 (cubic hectometers)
acre-ft/yr (acre-feet per year)	0.001233	hm^3/a (cubic hectometers per year)
(acre-ft/acre)/yr (acre-feet per acre per year)	0.30402	m/a (meters per year)
ft (feet)	0.3048	m (meters)
ft^2/d (feet squared per day)	0.0929	m^2/d (meters squared per day)
ft/d (feet per day)	0.3048	m/d (meters per day)
ft/mi (feet per mile)	0.1894	m/km (meters per kilometer)
ft/yr (feet per year)	0.3048	m/a (meters per year)
ft^3/s (cubic feet per second)	0.02832	m^3/s (cubic meters per second)
$(ft^3/s)/mi^2$ (cubic feet per second per square mile)	0.01093	$(m^3/s)/km^2$ (cubic meters per second per square kilometer)
$(gal/d)/ft^2$ (gallons per day per square foot)	0.04047	m/d (meters per day)
gal/min (gallons per minute)	0.003785	m^3/min (cubic meters per minute)
(gal/min)/ft (gallons per minute per foot)	0.2070	m^2/s (meters squared per second)
inches	25.4	mm (millimeters)
in/yr (inches per year)	25.4	mm/a (millimeters per year)
kWh/acre-ft (kilowatthours per acre-foot)	2,919	J/m^3 (joules per cubic meter)
mi (miles)	1.609	km (kilometers)
mi^2 (square miles)	2.590	km^2 (square kilometers)

Degree Fahrenheit is converted to degree Celsius by using the formula:
$°C = (°F-32)/1.8$.

The use of firm, brand, or trade names in this report is for identification purposes only and does not constitute endorsement by the U.S. Geological Survey.

ANALYSIS OF THE CARMEL VALLEY ALLUVIAL GROUND-WATER BASIN,

MONTEREY COUNTY, CALIFORNIA

By Glenn W. Kapple, Hugh T. Mitten, Timothy J. Durbin,
and Michael J. Johnson

ABSTRACT

A two-dimensional, finite-element, digital model was developed for the Carmel Valley alluvial ground-water basin using measured, computed, and estimated discharge and recharge data for the basin. Discharge data included evapotranspiration by phreatophytes and agricultural, municipal, and domestic pumpage. Recharge data included river leakage, tributary runoff, and pumping return flow. Recharge from subsurface boundary flow and rainfall infiltration was assumed to be insignificant. From 1974 through 1978, the annual pumping rate ranged from 5,900 to 9,100 acre-feet per year with 55 percent allotted to municipal use principally exported out of the valley, 44 percent to agricultural use, and 1 percent to domestic use. The pumpage return flow within the valley ranged from 900 to 1,500 acre-feet per year. The aquifer properties of transmissivity (about 5,900 feet squared per day) and of the storage coefficient (0.19) were estimated from an average alluvial thickness of 75 feet and from less well-defined data on specific capacity and grain-size distribution. During calibration the values estimated for hydraulic conductivity and storage coefficient for the lower valley were reduced because of the smaller grain size there. The river characteristics were based on field and laboratory analyses of hydraulic conductivity and on altitude survey data.

The model is intended principally for simulation of flow conditions using monthly time steps. Time variations in transmissivity and short-term, high-recharge potential are included in the model. The years 1974 through 1978 (including "pre-" and "post-" drought) were selected because of the extreme fluctuation in water levels between the low levels measured during dry years and the above-normal water levels measured during the preceding and following wet years. Also, during this time more hydrologic information was available. Significantly, computed water levels were generally within a few feet of the measured levels, and computed flows were close to gaged riverflows for this simulation. However, the nonuniqueness of solutions with respect to different sets of data indicates the model does not necessarily validate the correctness of the individual variables. The model might be improved with additional knowledge of the distribution of confining sediments in the lower end of the valley and the aquifer properties above and below them. The solution algorithm could account for confinement or partial confinement in the lower end of the valley plus contributions from the Tularcitos aquifer.

INTRODUCTION

Background

The Monterey Peninsula and Carmel Valley obtain a large part of their water supply from ground water in Carmel Valley. During an extended period of drought their water supply is obtained almost entirely from pumping wells in the Carmel Valley. This increased pumping imposes a severe stress on the ground-water system. Such a drought occurred during 1976-77, and water-use and pumping restrictions were imposed during 1977. Because of a lack of knowledge of the aquifer system and the uncertainty of the water supply, the Monterey Peninsula Water Management District requested the U.S. Geological Survey to evaluate the ground-water resources in Carmel Valley.

Purpose

The purposes of this study were to provide a better understanding of the geohydrology of the Carmel Valley alluvial ground-water basin as an aid toward effective management of that basin and to identify areas of inadequate data in the ground-water basin.

Scope

The scope of this study included conceptualizing the geohydrology of the ground-water drainage basin based on existing information. Physical properties of the drainage basin were translated into mathematically usable numerical values, which in turn were used to develop and calibrate a digital flow model based on historical water-level, pumpage, and riverflow data.

Acknowledgments

The authors appreciate those persons and agencies who assisted in developing the data base for this project. Particular acknowledgment is given to Bruce Buel, Monterey Peninsula Water Management District; Dick Meffley, California Department of Water Resources; and personnel with the Monterey County Flood Control and Water Conservation District, California American Water Co. and Water West Corp., and the Monterey branch of the Pacific Gas and Electric Co.

DESCRIPTION OF THE STUDY AREA

Physical Setting

The Carmel basin is a small intermontane basin in the central coastal region of California, southeast of Monterey (fig. 1). The drainage basin has an area about 250 mi^2, but the valley floor containing the alluvial ground-water basin covers only about 6 mi^2. Urban and agricultural activities are confined primarily to the valley floor, which is long in comparison to its width--about 16 mi long and from 300 to 4,500 ft wide. Altitudes on the valley floor range from sea level at Carmel Bay to about 350 ft in the upper parts of the valley.

The drainage basin is bounded on the northeast by the Sierra de Salinas range with altitudes as high as 4,470 ft, and on the southeast by the Santa Lucia Range with altitudes up to 4,850 ft. Both ranges have steep slopes and dense foliage. North slopes rising from the valley floor average about 430 ft/mi, and south slopes average about 350 ft/mi. Slopes in the upper part of the drainage basin rise about 360 ft/mi. The Sierra de Salinas range, in the lower 7 or 8 mi of the drainage basin, has less vegetation and is characterized by a chaparral environment.

Carmel Valley has the typical coastal California wet-dry seasonal patterns; about 80 percent of the annual precipitation falls during January through April. Mean annual precipitation over the drainage basin ranges from 14 to 40 in/yr and averages about 17 in/yr at Carmel Valley (California Department of Water Resources, 1974, p. 5). Nonrecording rain gages are currently maintained at Monterey and at three sites in Carmel Valley--Carmel Valley, San Clemente, and Los Padres (fig. 2). Measured pan evaporation ranges from about 40 in/yr at Carmel to 60 in/yr at Carmel Valley. Mean monthly temperatures near the coast range from 54°F in the winter to 60°F in the summer; farther inland near Carmel Valley mean monthly temperatures range from 51°F to 64°F.

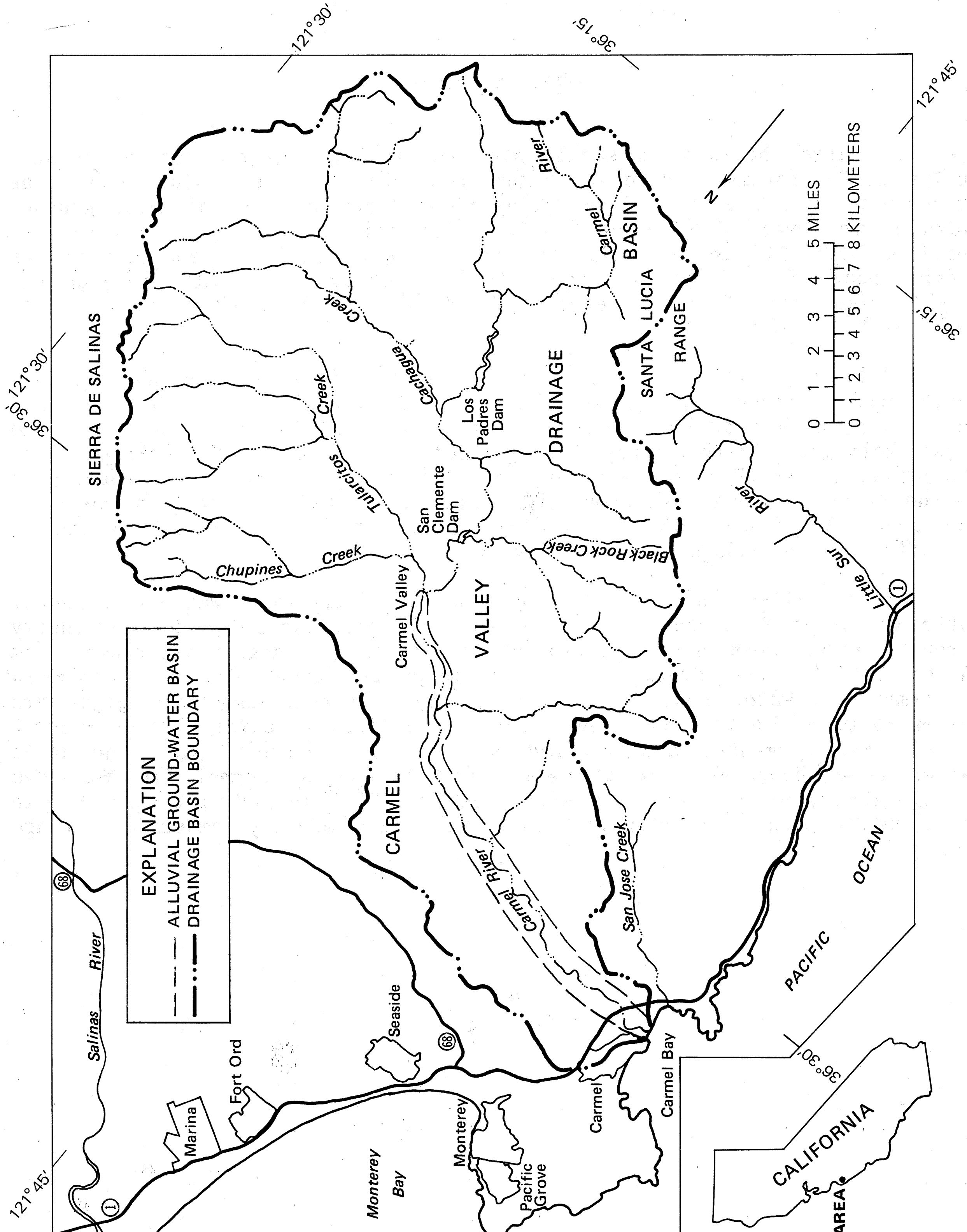

FIGURE 1. — Carmel Valley drainage basin and alluvial ground-water basin.

Surface-Water Hydrology

Drainage basin runoff occurs via the Carmel River. This runoff is gaged by the Geological Survey at Robles Del Rio in the upper part of the drainage basin and near Carmel near the coast (fig. 2, pl. 1A). The drainage basin rapidly reacts to rainfall with a high rate of discharge per unit area--peak discharge of record (1963-79) from the drainage basin was 8,620 ft^3/s (Jan. 26, 1969), and mean discharge was about 98 ft^3/s. The mean discharge represents an average runoff per unit area of about 0.4 $(ft^3/s)/mi^2$. For comparison, the Salinas basin just north of Carmel Valley with a drainage area of about 4,200 mi^2 has an average runoff per unit area of $0.1(ft^3/s)/mi^2$.

On an annual average, the river gains over its course through the valley as additions from adjacent tributary streams exceed the amount of induced river leakage. During 1963 through 1979, the average inflow at Robles Del Rio was 80.8 ft^3/s, and outflow at Carmel was 97.4 ft^3/s. Monthly records indicate that, in general, the river gains during the first half of the year and loses during the second half--a response that would be expected on examination of seasonal pumping and rainfall patterns. Mean monthly flows from the two river gages for 1974 through 1978 are shown in figure 3. Inflow to the valley is regulated slightly by the Los Padres and San Clemente Reservoirs, which have a combined capacity of 4,600 acre-ft.

Recent river-channel degradation has occurred and, if it continues, needs to be considered in any long-range projections of future ground-water conditions. Over most of its 18-mi course, the Carmel River flows in a well-defined channel ranging from 20 to 150 ft in width through mostly unconsolidated alluvial deposits. Significantly, bank altitudes are as much as 30 ft below adjacent terraces, indicating a downcutting stream undergoing a cycle of headward erosion and river channel sediment removal. The most recent sediment transport in the river channel has been significantly altered by man, principally by the complete removal of sediment load by upstream reservoirs. The rate of channel degradation downstream from reservoirs is increased as the stream loses its sediment load and increases its tractive force to begin movement and removal of materials in the river channel through the valley floor. Man's extraction of sand and gravel from the channel floor further accelerates this lowering of river-channel altitudes. Carlson and Rozelle (1978) reported that from 1966 through 1974 the lower 10 mi of the river channel underwent degradation at a rate of 0.25 ft/yr. Declines in river-channel altitudes would directly lower natural water levels in the alluvial aquifer, and, consequently, some riparian vegetation would be deprived of water because maximum water-table altitudes during the dry season are controlled principally by recharge from the river.

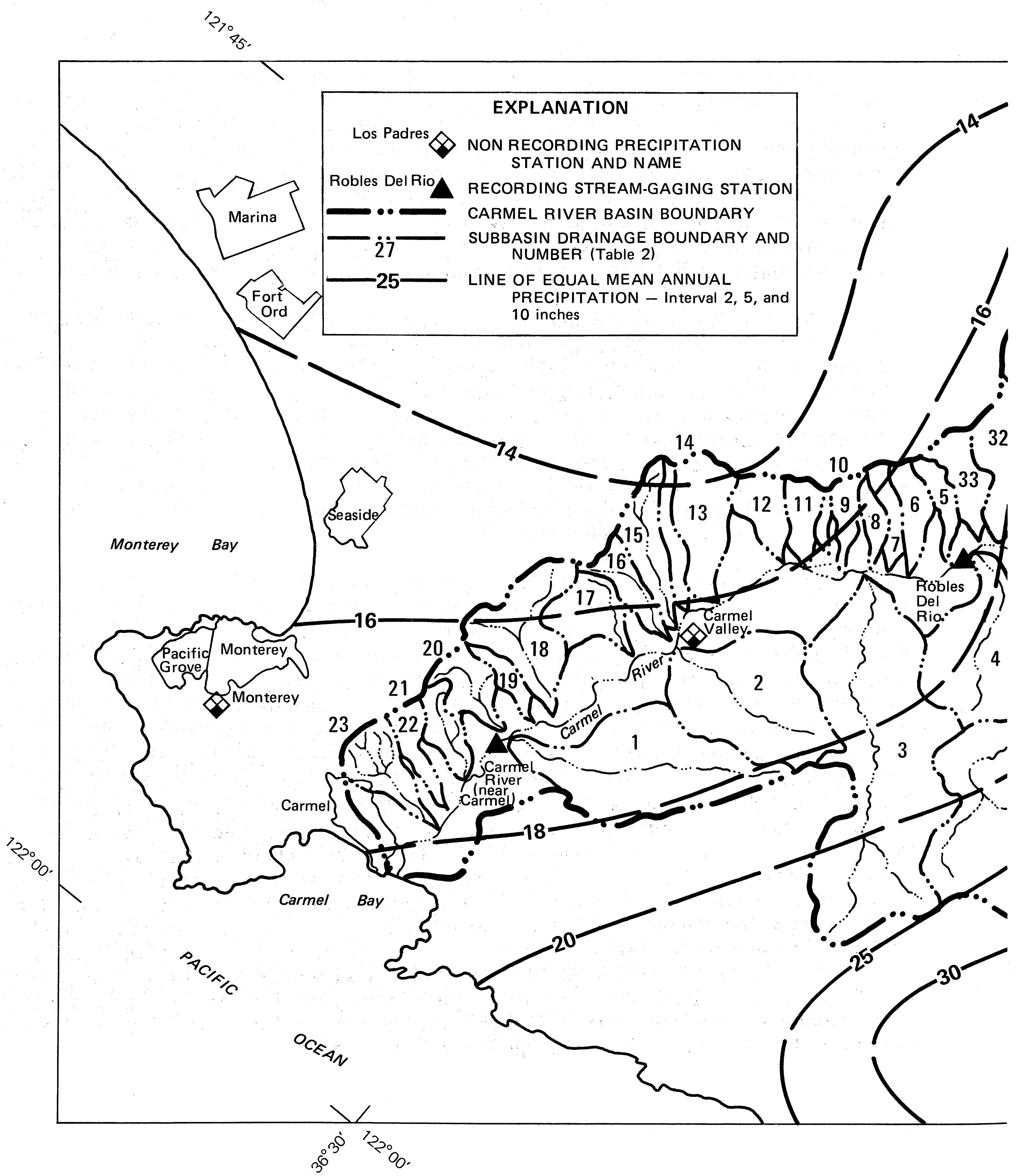

FIGURE 2. — Subbasin drainage areas and mean annual

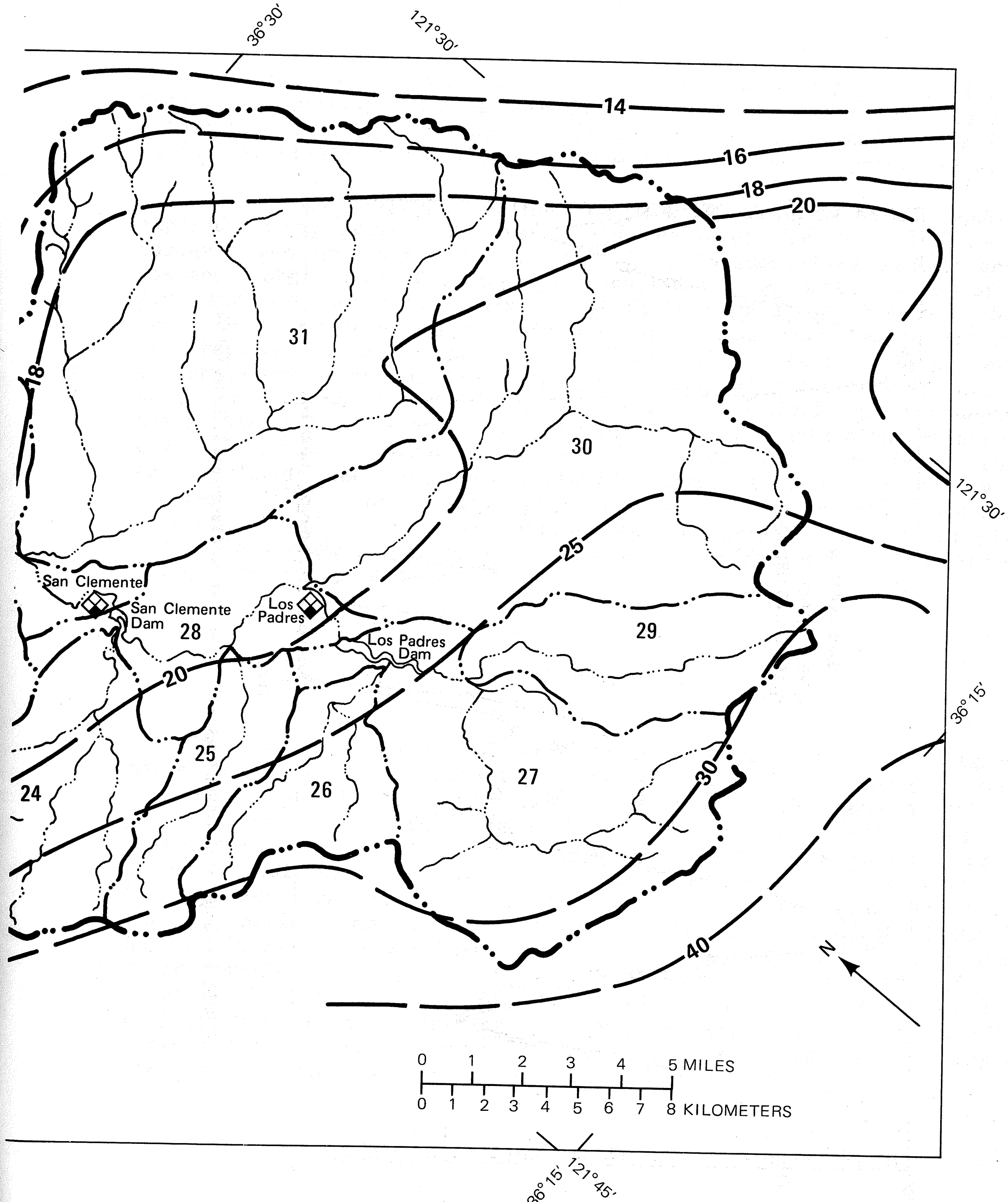

precipitation in the Carmel Valley drainage basin.

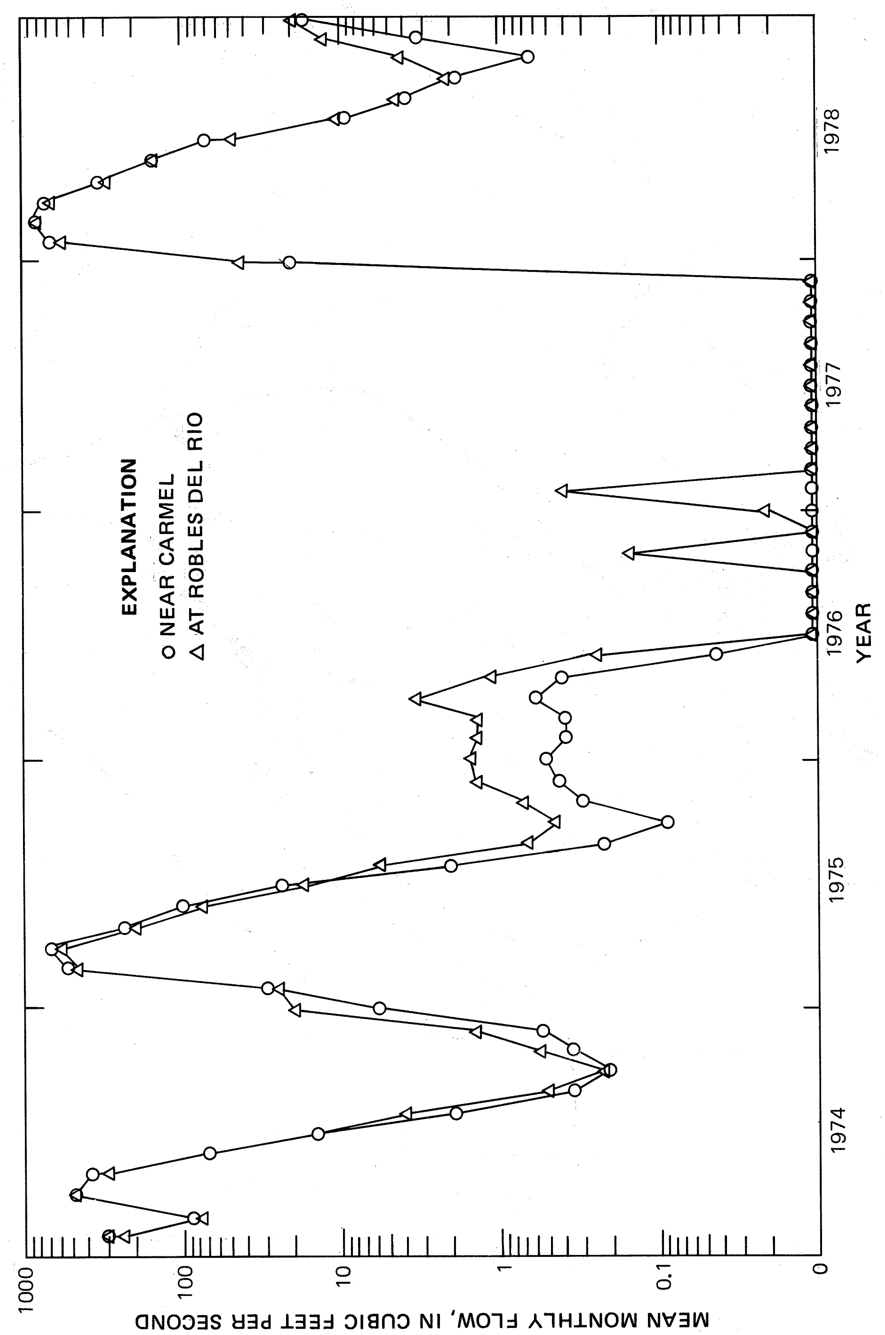

FIGURE 3. – Gaged mean monthly flows in the Carmel River near Carmel and at Robles Del Rio.

Geology

For modeling purposes the geology of the Carmel Valley was simplified to reflect its principal geologic features (pl. 1A). Those readers interested in detailed surface geology mapping are referred to Clark and others (1974) and to Fielder (1944), from which plate 1 was composited and generalized.

The Carmel River carved its valley while draining an erosional surface exposed during periods of uplift and sea-level decline. The complex and variable geologic units within the valley include three significant units: Basement rocks of pre-Tertiary age, consolidated sedimentary rocks of Tertiary age, and unconsolidated sediments of Quaternary age (table 1). The oldest rocks beneath the drainage basin are crystalline rocks of pre-Tertiary age that form the basement complex of the area. The basement rocks are exposed in a northwestward-trending belt, paralleling the major strike-slip faults of the area. They occur in the subsurface at a progressively greater depth toward the northeast. Successively younger Tertiary rocks have been deposited on the crystalline rocks. Although considerably folded into a series of anticlines and synclines that trend more westward, oblique to and truncated by regional faults, their general dip is also to the northeast. Southwesterly, successively older rocks are exposed at the surface. The Carmel River cuts across this sequence of folded Tertiary rocks offset by faulting and deposits younger Quaternary sediments.

Basement Rocks

The basement rocks of pre-Tertiary age are composed of igneous and metamorphic rocks. The metamorphic rocks are the Sur Series of Trask (1926) and consist mainly of biotite schist and gneiss. The igneous rocks are the Santa Lucia granites of Lawson (1893) and consist mainly of porphyritic granodiorite and quartz diorite. The basement rocks have a very uneven erosional surface upon which the younger Tertiary rocks rest unconformably. The basement complex is extensively exposed to the south and east of the drainage basin, with isolated outcrops north and at the mouth of the drainage basin. It is deeply weathered locally, and, where weathered and saturated, it could supply minor quantities of water to wells, sufficient for limited domestic and stock use. Only a few wells on the valley floor have been drilled through the overlying materials and penetrate the granite. Except where weathered, the basement rocks are considered non-water-bearing and are treated as a ground-water barrier.

TABLE 1. - Generalized geologic units of the Carmel Valley

Age	Geologic units	Maximum thickness (feet)	General lithologic character	Water-bearing properties
Quaternary	Younger alluvium and river deposits (Holocene)	180	Boulders, gravels, sand, silt, and clay.	Major water-bearing unit in the valley. Sufficient yields to supply municipal, agricultural, and domestic wells. Municipal wells yield from 200 to 2,000 gal/min. Domestic wells yield from 3 to 200 gal/min. Hydraulic conductivity assumed to be 30 to 64 ft/d.
	Older alluvium and terrace deposits (Pleistocene)	50	Gravel, sand, and clay.	Transmits water freely but generally lacks summer storage. In favorable places, may supply individual domestic wells.
Tertiary	Monterey Shale (Miocene)	700-1,000	Siliceous marine shale interbedded with sandstone in lower part.	Some domestic wells yield 15 to 30 gal/min from sandstone stringers and silicified fractures. Mudstone facies yield virtually no water.
	Tertiary sandstone units (Miocene and Paleocene)	900	Mostly marine sandstones; includes some beds of siltstone, conglomerate, and volcanic rock.	Limited well penetration and great variations in rock character limit knowledge of water-bearing properties. Locally, domestic supplies of generally less than 5 to 10 gal/min have been obtained from wells with reports of some well yields exceeding 100 gal/min. Hydraulic conductivity assumed to be 1 ft/d.
Pre-Tertiary	Basement complex		Igneous and metamorphic rocks.	Locally, wells yield small quantities from fractures or weathered zones. Supplies may be limited and unreliable.

Consolidated Sedimentary Rocks

The consolidated sedimentary rocks, several thousand feet thick, consist of Tertiary sandstone units of Paleocene and Miocene age and the overlying Monterey Shale of Miocene age. Within these units, only the Miocene sandstone beds and silicified fracture zones in the lower part of the Monterey Shale have any hydrologic significance (Thorup, 1979).

The Tertiary sandstone units of Paleocene age, referred to as the Carmelo Formation by Bowen (1965), consist of sandstone, siltstone, conglomerate, and shale. Erosion has removed most of these sediments from the present Carmel Valley; the small occurrences, known to be present only along the coastal part of the drainage basin, have no hydrologic significance.

The Tertiary sandstone units of Miocene age consist of a lower terrestrial unit of sandstone, siltstone, and conglomerate termed the red beds of Robinson Canyon (Robinson Canyon Member of the Chamisal Formation of Bowen, 1965), and a middle and upper sequence of marine sandstone with basaltic flows termed marine sandstone by Clark and others (1974). These sandstone units comprise what Thorup (1976) defines as the Tularcitos aquifer and include most of the strata lying between the basement complex and the Monterey Shale within the Carmel Valley. Outcrops of the sandstone units are numerous along the southern side of the drainage basin and in places are in direct contact with the alluvium. The character of these sandstone units varies greatly from one place to another and from one layer to another within the drainage basin. This variability, along with minimal well penetration, restricts our knowledge of the sandstone units' true water-bearing properties. The Tertiary sandstone units are assumed to have a hydraulic conductivity of about 1 ft/d, even though in some areas their hydraulic conductivity may be higher due to a higher degree of sediment sorting or fault-related fracturing. Because the hydraulic conductivity of these rocks probably is considerably less than that of the alluvium, the exchange of water between them and the alluvium is assumed to be limited. However, these sandstone units are believed to underlie one-third of the entire drainage basin with an average thickness of about 250 ft and therefore may contain considerable water in storage (Thorup, 1976). Most wells drilled into the unit yield at least enough water for domestic use, and a few wells yield considerably more.

The Monterey Shale of Miocene age consists of siliceous marine deposits occasionally interbedded with fine-grained sandstone that increases in abundance toward the base of the formation. Extensively exposed along the northern side of the drainage basin, it directly underlies the alluvium and conformably overlies the lower Miocene marine sandstone units. Although some domestic wells obtain water from sandstone stringers and fractures within the formation, the Monterey Shale is generally considered non-water-bearing and is treated in the model as a ground-water barrier.

Unconsolidated Sediments

The unconsolidated sediments include older alluvium and younger alluvium. The older alluvium of Pleistocene age generally consists of gravel and sand terrace deposits exposed on the north side of the river. Individual patches are small and typically situated on well-drained bluffs. Although this unit transmits water readily, its distribution is limited and erratic; therefore, it is not considered a significant aquifer in this study.

The younger alluvium of Holocene age along the valley floor is composed of poorly consolidated boulders, gravel, sand, and silt deposited by the Carmel River. Clay layers are thin and uncommon. Silt becomes more abundant downvalley. The basal part of the alluvium from Meadows Road to the ocean may contain water confined by a layer of nearly impermeable silt at depths of 30 to 40 ft (Greenwood, 1978). The younger alluvium is the most significant water-bearing unit in Carmel Valley, with hydraulic conductivities assumed to be 30 to 64 ft/d (see section on "Aquifer Properties").

Structure

A series of high-angle faults trends northwestward across the Carmel Valley area (principally strike-slip faulting that strikes N. 40° W). Oblique to the trend of these faults is a series of anticlines and synclines that trends westward and is truncated by faults. Strata north of the river are folded into several synclines and anticlines; those south of the river are folded into one predominant syncline. The important faults in the Carmel Valley are the Cypress Point fault, the Navy fault, and the Tularcitos fault (pl. 1A).

The Cypress Point fault extends across the mouth of the valley with an uplifted granite basement to the west. The Carmel River has cut through the uplifted western block of the basement rock to a depth of more than 86 ft below sea level. Thus, the uplifted granite is not an effective barrier to seawater intrusion at the river's mouth (California Department of Water Resources, 1974). However, the thinning of the unconsolidated sediments across the fault zone could have some effect on limiting seawater intrusion to the basal part of the alluvium and underlying formations just east of the fault.

The Navy fault cannot be traced through the alluvial deposits of the Carmel Valley. However, its near-alinement with the mapped Tularcitos fault to the southeast and its similarity in trends strongly suggest that these two faults are continuous (Clark and others, 1974). The alluvium is noticeably thinner in sec. 19, T. 16 S., R. 2 E., east of the fault alinements where the underlying formations are mostly granitic; west of the fault alinements the underlying rocks are mostly sedimentary, principally Monterey Shale.

Ground-Water System

The extent and thickness of the younger alluvium--the unconfined aquifer modeled in this study--is shown on plate 1B. This map is based almost entirely on an isopach map previously published by the California Department of Water Resources (1974) with minor modifications made by the Department in 1977 from post-1974 drillers' log information. Aquifer thickness ranges from about 30 ft at the drainage basin narrows in the upper basin to about 180 ft 1 mi from the mouth of the drainage basin.

At the mouth of the drainage basin, the aquifer thins due to an uplifted fault block west of the Cypress Point fault. This uplift impedes but does not stop ground-water movement across the fault. Seismic-refraction surveys (California Department of Water Resources, 1974) indicated that the depth of the alluvium across the mouth ranged from 32 ft north of the river to 86 ft at the river's edge. These data were confirmed within a few feet by an unpublished resistivity and seismic-refraction survey done by the Geological Survey in 1979 (J. C. Tinsley III and M. J. Johnson, oral commun., 1979). Because the alluvium is still in direct contact with saline waters to depths of at least 75 ft below sea level, the uplift is not an effective barrier to seawater intrusion.

Recharge to the aquifer is derived mainly from river infiltration which composes about 85 percent of the net recharge. The potential recharge rate from the river to the aquifer is high, perhaps 100 ft^3/s or more (Dames and Moore, 1973), and during normal or above-normal flow years, the water table recovers completely from the dry-season low. After the 2-year drought of 1976-77, precipitation that began in January 1978 caused water levels to recover by February 1978. Thus, it appears that the aquifer recovers in a month or less even after severe stressing. Water levels after recovery are often a few feet above the riverbed, indicating that additional and significant recharge occurs, mostly from tributary stream infiltration.

Ground-water flow is, generally, downvalley, with gradients ranging from about 50 ft/mi in the upper drainage basin to about 10 ft/mi toward the lower end. After recovery, water-table depths range from about 5 to 30 ft below land surface with an average of about 15 ft. During normal rainfall years, water-level fluctuation is about 5 to 15 ft; during drought years, water levels decline as much as 50 ft. Previous estimates of the aquifer's storage potential (California Department of Water Resources, 1974) indicate a total storage in the springtime of about 50,000 acre-ft. The report also estimates subsurface discharge to the ocean at about 140 acre-ft/yr.

DIGITAL MODEL

Conceptual Model

To develop a digital model of a complex ground-water system, a conceptual model of the system must be established on the basis of simplified geohydrologic assumptions. For Carmel Valley, the younger alluvium is considered to be the sole water-bearing formation and is conceptualized as a single-layer, unconfined, horizontal unit. The model was developed by making the following assumptions:

1. All ground-water movement is horizontal.
2. Changes in storage occur instantaneously.
3. Physical characteristics of the aquifer vary with time.
4. The aquifer is isotropic.
5. Recharge occurs instantaneously.
6. The underlying Monterey Shale and sandstone units are impermeable.
7. Hydraulic gradients equal the slope of the free surface and do not vary with depth.

Mathematical Model

Ground-water flow in a conceptual model can be described by the mathematical equation (Bear, 1972):

$$\frac{\partial}{\partial x}\left(bK\frac{\partial h}{\partial x}\right)+\frac{\partial}{\partial y}\left(bK\frac{\partial h}{\partial y}\right)=S\frac{\partial h}{\partial t}+W,$$

where

b=aquifer thickness, which varies with x, y, and t;
K=hydraulic conductivity, which varies with x and y;
S=specific yield, which varies with x and y;
h=hydraulic head, which varies with x, y, and t;
W=composite of source-sink terms; and
t=time; x=abscissa; and y=ordinate.

For this study, the source-sink terms include components representing discharge from pumping, evapotranspiration, and the river; and recharge from river infiltration, pumpage return flow, and tributary stream infiltration.

River leakage is computed internally by the computer program as a function of the head differential between the river stage and ground-water level at the midpoint of each river reach length and the river flow width. The functional relation for river leakage rate (Q_R) derived from Durbin and others (1978, p. 49-50) is:

$$Q_R=C_R(h_R-h)W_RL,$$

where C_R is a proportionality constant (analogous to channel-bed hydraulic conductivity), h_R is the river stage, h is the ground-water level, W_R is the flow width, and L is the reach length.

The river stage is the channel-bed altitude plus the depth of flow in the river which may be approximated as a power function of inflow to each river reach. Thus, the stage is expressed functionally as:

$$h_R=H_R+a_dQ^{b_d},$$

where H_R is the channel-bed altitude, Q is the river discharge, and a_d and b_d are numerical coefficients. The flow width also was estimated by a power function:

$$W_R=a_wQ^{b_w},$$

where a_w and b_w are numerical coefficients.

Combining these equations produces the generalized leakage equation used in the model:

$$Q_R=C_R\left(H_R+a_dQ^{b_d}-h\right)a_wQ^{b_w}L.$$

The use of the functional relation for river leakage rate was described by Durbin and others (1978, p. 53-62). To use this relation in the model, the river was first divided into subreaches. The length of each subreach is equal to the sum of one-half the distance to each of the adjacent river nodes (pl. 1C). Then, for each subreach the continuity equation is:

$$Q_{IN}+Q_T-Q_R=Q_{OUT},$$

where Q_{IN} is the river inflow to the reach, Q_T is the tributary inflow, Q_R is the leakage rate, and Q_{OUT} is the river outflow from the reach. The computer program does not allow the leakage rate to exceed the sum of the river and tributary inflows at any reach.

The model includes calculations for each time step of the net quantity of water in storage and the rate of aquifer discharge to the ocean. Storage is calculated for each element on the basis of the element area, saturated thickness, and storage coefficient. Aquifer discharge is the flow through the eight elements adjacent to the ocean and is calculated on the basis of the water-table gradients and transmissivities for these elements.

Computer Code

The computer code used for this project is similar to that used previously by Durbin (1978). Modifications were made to the input-output sections, but the computational sections of the program remain unchanged. The Galerkin finite-element procedure with triangular elements was used. The program was executed on the U.S. Geological Survey's IBM compatible AMDAHL system in Reston, Va., and required about a half-second of execution time per time step.

Element Configuration

The element configuration used for the model and the location of river nodes are shown on plate 1C. This configuration consists of 832 elements and 525 nodes, designed such that each "line" of 5 nodes (or 8 elements) across the drainage basin is generally perpendicular to downgradient flow. Each line across the drainage basin was subdivided into four equal lengths such that the configuration across the drainage basin consists of five nodes and eight elements throughout the length of the drainage basin. Nodes and elements are numbered consecutively as illustrated on plate 1C, which shows the configuration of the first 32 elements in the lower part of the drainage basin and selected elements elsewhere.

The finite-element technique adapts well to areas with irregular geometry, such as Carmel Valley, as opposed to the finite-difference technique which must conform to straight-line configurations of rows and columns. Data input to the model is supplied either by node or element, and water levels are computed at each node location.

Model Input Data

The data used to develop this model, either measured, computed, or estimated, are outlined below:

1. Aquifer properties
2. Tributary-stream characteristics
3. River-channel characteristics
4. Evapotranspiration losses
5. Pumpage and pumpage return flow
    a. Municipal pumpage
    b. Agricultural pumpage
    c. Domestic pumpage.

As discussed in the following sections, some of these data are coded into the model by node and others by element. The model computes water levels and drawdowns at all nodes.

Aquifer Properties

Initial estimates of aquifer hydraulic conductivities and storage coefficients used in the model were based on specific-capacity test data and assumptions concerning the nature of the granular materials. Available specific-capacity test data show a high degree of divergence, even for repeated tests made on the same well, perhaps because tests made during wet periods are influenced by induced leakage from the river. Reliable dry-period data were available for seven wells in the drainage basin. Specific capacities from those tests ranged from 14.8 to 44.1 (gal/min)/ft, averaging 22 (gal/min)/ft. The average specific capacity converts to a transmissivity of 5,896 ft^2/d. The derived transmissivity data, though inconclusive, were used in conjunction with alluvial thickness data to initially estimate hydraulic conductivity for the model. Assuming an aquifer thickness of 110 ft for the test sites, hydraulic conductivity ranged from 30 to 64 ft/d and averaged about 60 ft/d.

The model-derived transmissivities reflect the assumption of time variance; the model recomputes transmissivity for changes in saturated thickness of the aquifer. For calibration, initial estimates of hydraulic conductivity were modified to obtain the best match between observed and computed water levels during the 1974-78 period.

Values for specific yield, also derived from calibration, ranged from 0.09 to 0.20 and averaged about 0.19. A specific yield of 0.20 was initially assumed as representative of sand-and-gravel-type materials such as those found in Carmel Valley (Davis and DeWiest, 1966).

Examination of drillers' logs did not reveal any discernible lithologic patterns in the drainage basin. These logs typically indicate a large amount of sand and gravel with intermixed sequences of clay, silt, shale, and boulders. There are a few logs available for the lower part of the drainage basin that indicate some increase in silt and clay. For the model, it was assumed that the lithologic properties of the aquifer were homogeneous, except in the lower drainage basin where the increase in silt and fine sand content presumably would decrease the hydraulic conductivity and the storage coefficient. The values used for these characteristics are shown in figure 4. Hydraulic conductivity was increased from a value of 30 ft/d near the river mouth to 64 ft/d about 3.5 mi up the drainage basin. Storage coefficients over this distance were increased from 0.09 to 0.20.

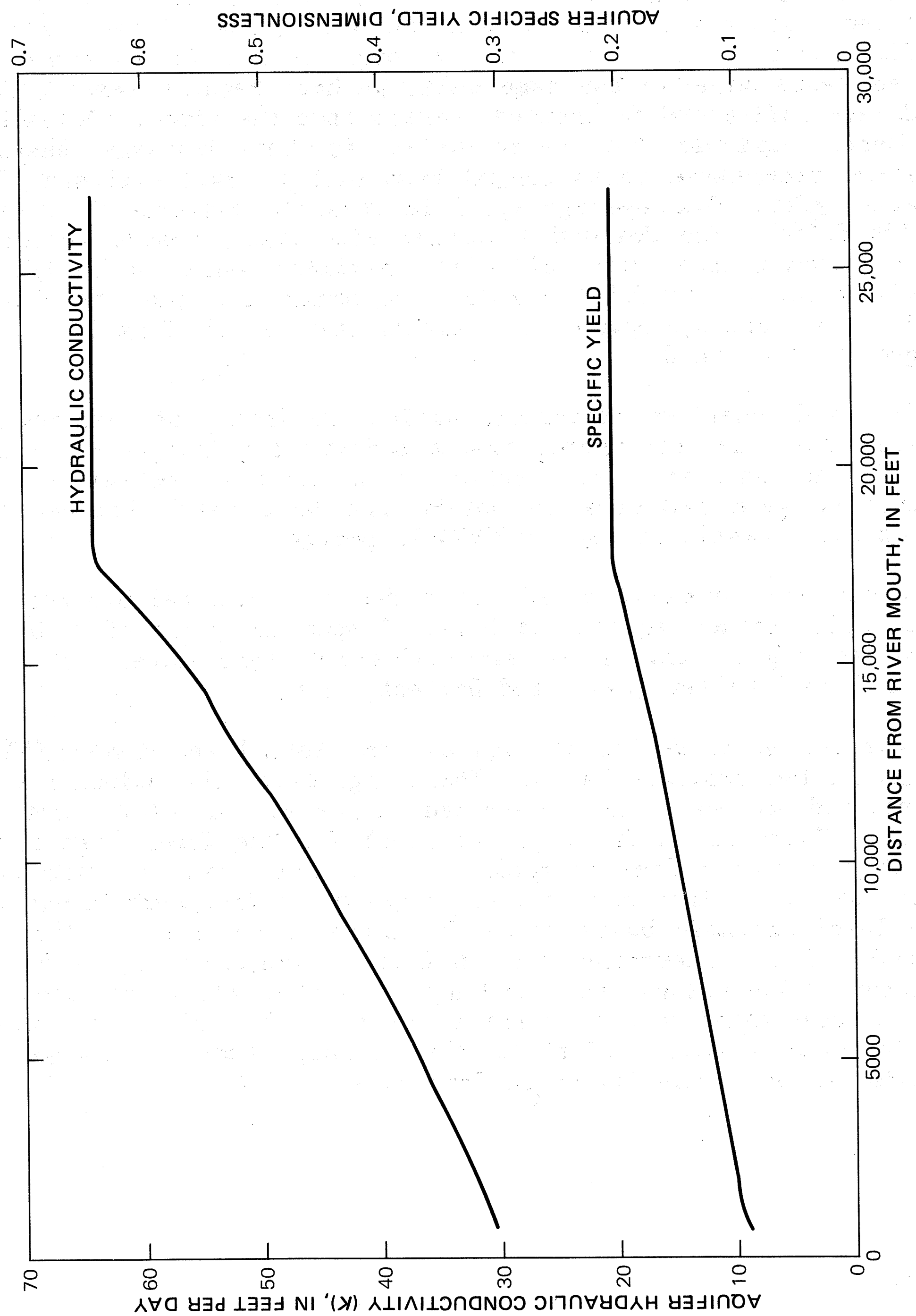

FIGURE 4. — Aquifer hydraulic conductivity and specific yield for a selected reach upstream of the mouth of the Carmel River.

Tributary-Stream Characteristics

The aquifer receives recharge from sources other than river leakage because ground-water levels in parts of the drainage basin are several feet higher than river-bed altitudes. Most of this recharge can be attributed to infiltration from tributary-stream channels. Tributary runoff that does not infiltrate to the water table contributes to riverflows and accounts for most of the 15-percent increase in annual discharge between the Robles Del Rio and Carmel gages (pl. 1D). The additional inflow from tributaries below the Robles Del Rio station increases the river's capability to recharge the aquifer. As a result, the runoff from ungaged tributary streams and the parts of this runoff that contribute to aquifer recharge and riverflows were estimated.

Monthly tributary runoff for 1974 through 1978 was estimated by correlating tributary subbasin areas, mean annual precipitation, and the streamflow records from the Robles Del Rio gage. First, the drainage basin was divided into subbasins and overlaid with mean annual precipitation contour lines taken from Rantz (1969) (fig. 2). Second, the area and mean annual precipitations were determined for each subbasin, and the percentage of tributary flow--based on subbasin areas and precipitation--was calculated for each tributary below the Robles Del Rio gage (table 2). Third, total monthly runoff for the tributaries below Robles Del Rio was estimated using the equation:

$$Q_T = Q_G \; \frac{\Sigma A_b P_b}{\Sigma A_a P_a},$$

where Q_T is the monthly tributary runoff, Q_G is the monthly gaged runoff at Robles Del Rio, and A_a, A_b, P_a, and P_b are the individual subbasin areas and mean annual precipitations above and below the Robles Del Rio gage. This computation indicates that tributary runoff is about 20 percent of the gaged runoff from the drainage basin upstream from Robles Del Rio.

The runoff computation and the previously calculated runoff percentages also provide an estimate of the monthly runoff from each tributary to the valley floor. To apportion this runoff accurately between the infiltration and river-inflow components would require either detailed information pertaining to the individual tributary-channel infiltration characteristics or field measurements of tributary flows. Such information was not available, and obtaining it is probably not warranted. For the purpose of this model, an estimate of tributary infiltrations was made by assuming that up to 15 percent of the net withdrawal from pumping could be replaced by tributary-stream infiltration. If the monthly tributary runoff was less than 15 percent of the withdrawal, then only the amount available was applied in the model as infiltration; if not, the excess was added to the riverflows. The total estimated monthly tributary infiltrations and river inflows for the period 1974-78 are shown in figure 5. During months in which the tributary runoff was less than 15 percent of the net withdrawal, the infiltration data represent the total tributary runoff (fig. 5); otherwise, the sum of the infiltration and inflow represents the total tributary runoff. In this model, tributary infiltration was applied at the nearest node to the tributary along the edge of the alluvium, and tributary inflows were applied at the nearest river node to the tributary confluences for each of the 23 subbasins.

TABLE 2. - Tributary subbasin areas, mean annual precipitation, and percentage of mean tributary flow

Subbasin No. (fig.2)	Tributary subbasin[1]	Area (square miles)	Mean annual precipitation (inches)	Percentage of mean tributary flow[2]
1	Potrero-------------	5.20	18.2	11.2
2	Robinson------------	5.43	17.9	11.5
3	Las Gazas-----------	13.20	19.7	30.7
4	Hitchcock-----------	4.60	18.8	10.2
5	-- ------------	.61	17.0	1.2
6	-- ------------	.68	16.6	1.3
7	-- ------------	--	--	--
8	-- ------------	.58	16.5	1.1
9	-- ------------	.62	16.1	1.2
10	-- ------------	.10	16.2	.2
11	-- ------------	.85	15.6	1.6
12	Juan de Matte-------	1.01	15.5	1.8
13	Coyote--------------	1.78	14.9	3.1
14	Meadows-------------	.62	15.7	1.1
15	Buckeye-------------	1.78	15.1	3.2
16	Berwick-------------	1.16	16.0	2.2
17	De la Ordena--------	1.35	16.4	2.6
18	-- ------------	2.91	16.4	5.6
19	-- ------------	.54	17.0	1.1
20	Roach---------------	1.33	17.1	2.7
21	Martin--------------	.78	17.4	1.6
22	-- ------------	.81	17.6	1.7
23	Hatton--------------	1.35	17.7	2.8
24	San Clemente--------	15.6	23.6	--
25	Pine----------------	7.8	25.2	--
26	Danish--------------	8.1	27.5	--
27	Carmel River upstream from Los Padres Dam----	25.3	29.7	--
28	Carmel River upstream from San Clemente Dam--	12.9	20.1	--
29	Miller--------------	10.4	28.0	--
30	Cachagua------------	46.3	22.3	--
31	Tularcitos----------	56.3	18.3	--
32	Klondike------------	2.1	18.0	--
33	-- ------------	1.41	17.2	--

[1]Some tributary subbasins are not named.

[2]Percentage of tributary flow is given only for tributaries downstream from Robles Del Rio.

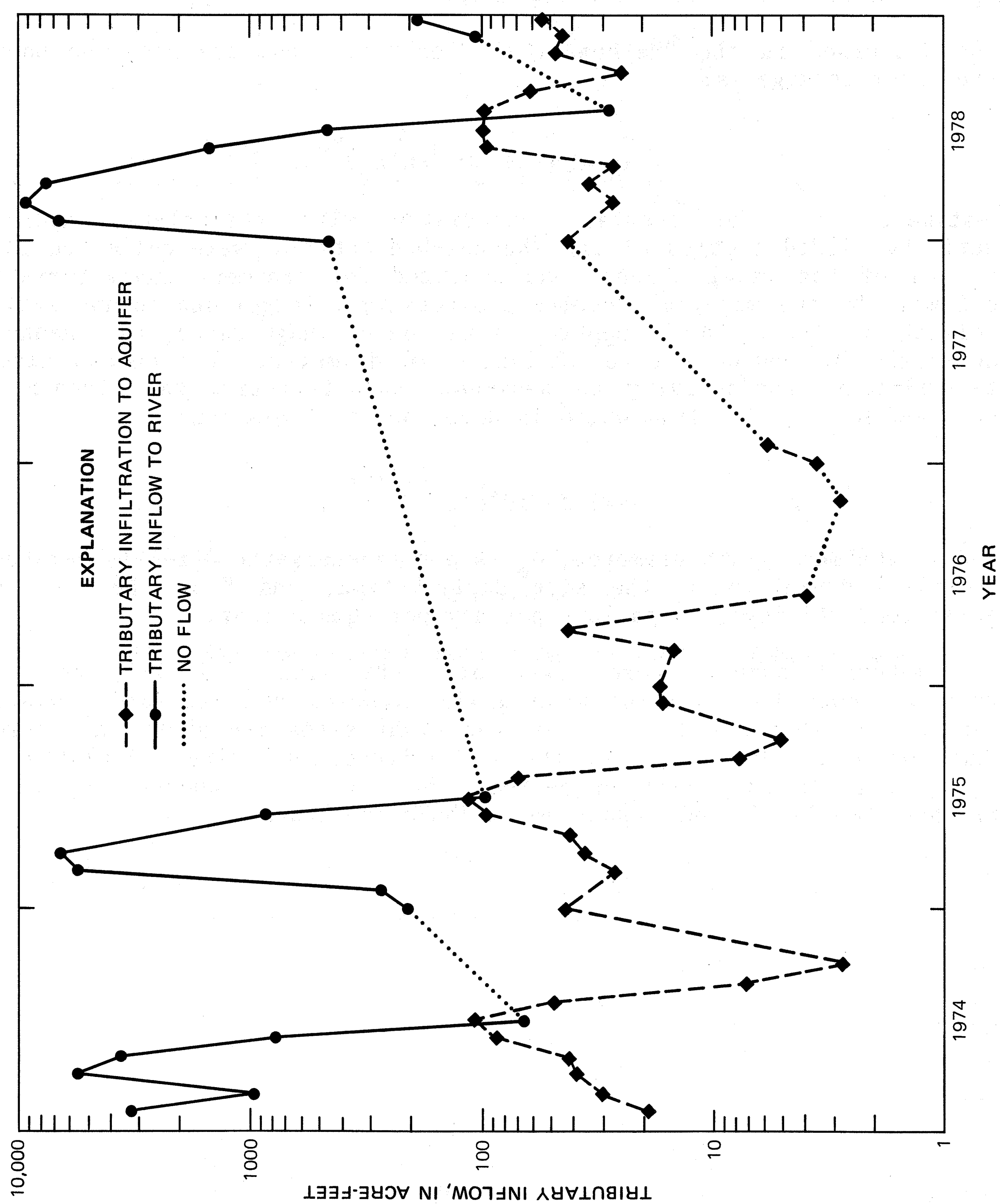

FIGURE 5. — Estimated monthly tributary infiltrations and inflow to Carmel River, 1974 through 1978.

Model calculation of river leakage requires estimates of channel-bed hydraulic conductivity, channel width, and river stage. As would be expected, a cursory field examination of the channel bed indicated a decrease in grain size of the bed materials toward the mouth of the river. As hydraulic conductivity depends mostly upon the median grain size of porous material (Corey, 1969), the channel-bed conductivity and, consequently, the river-leakage potential will decrease downvalley.

As discussed in the "Mathematical Model" section, the equation used to compute river leakage is:

$$Q_R=C_R\left(H_R+a_dQ^{b_d}-h\right)a_wQ^{b_w}L.$$

To estimate C_R, the constant associated with channel-bed hydraulic conductivity, field samples of the channel-bed material were collected in the lower 5 mi of the river channel and analyzed for sediment characteristics. Above 5 mi, the bed material becomes progressively larger and is not amenable to sediment analysis. In the upper part of the drainage basin, the channel is characterized by boulders 6 to 12 inches in diameter. The method used to relate hydraulic conductivity to sediment characteristics was discussed by Krumbein and Monk (1942) from which is developed the relation:

$$K=1.38\times10^4\bar{d}^2e^{-1.31\sigma_\phi},$$

where $\bar{d}$ is the mean grain diameter, σ_ϕ is a characteristic directly related to the standard deviation of the size distribution, and K is the laboratory hydraulic conductivity[1], in gallons per day per square foot.

Bed-material samples were taken at eight sites (pl. 1E), and sieve analysis was done to determine mean grain diameter and standard deviation. Grain-size distributions for each of the eight sites are shown in figure 6, and the extracted data used in the hydraulic-conductivity calculation are shown in table 3; the relation between the hydraulic conductivity of the channel bed and the distance upstream is shown in figure 7.

---

[1]Laboratory hydraulic conductivity (K) in Darcy units, which does not include viscosity effects of water, equals 18.2 times the specific hydraulic conductivity (C_R), in gallons per day per square foot, at a water temperature of 60°F (Davis and DeWiest, 1966).

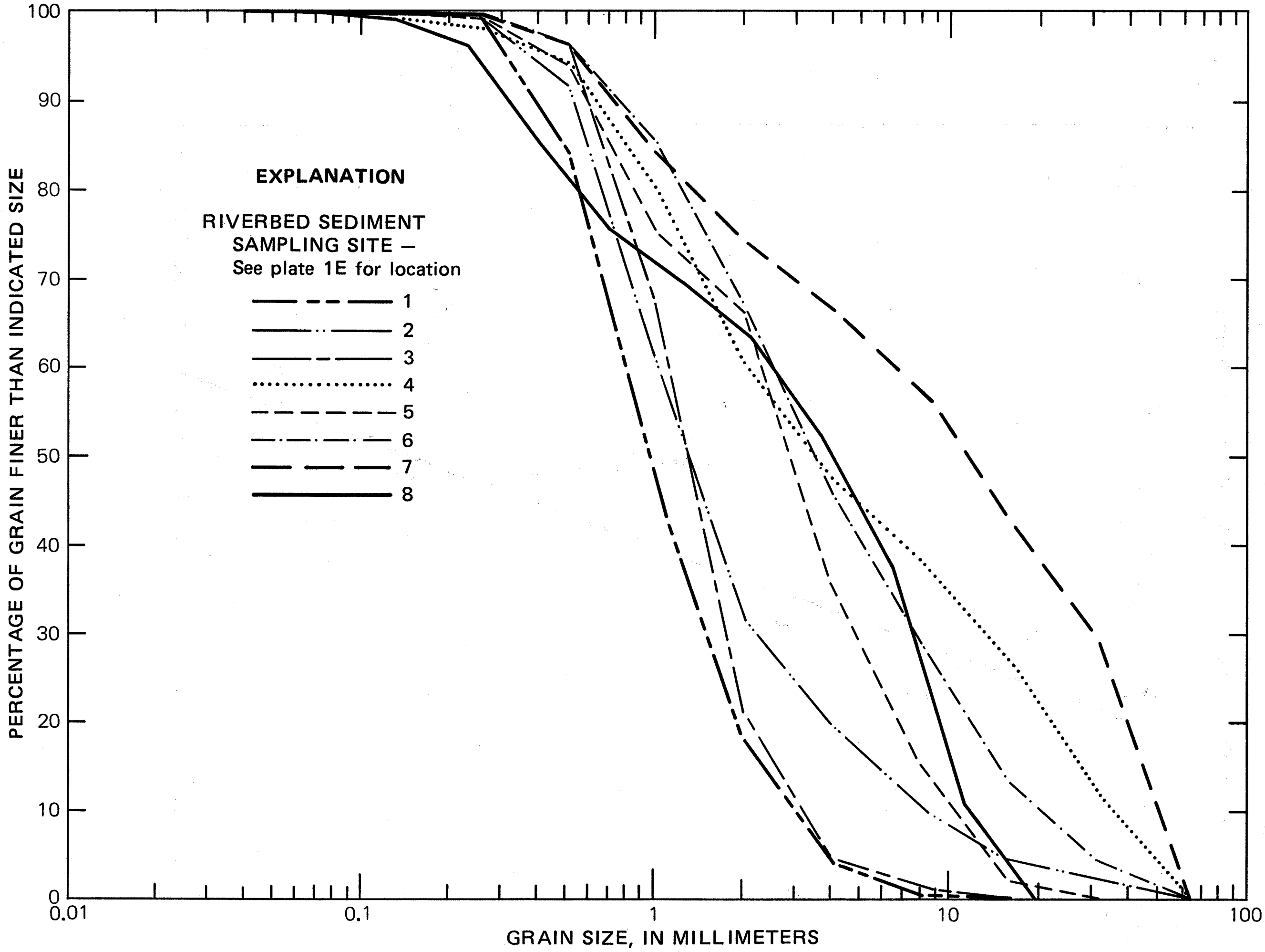

FIGURE 6. — Channel-bed grain size distribution at sites in the lower Carmel Valley river channel.

TABLE 3. - Data used to compute channel-bed hydraulic conductivity

[$\bar{d}$, mean grain diameter; σ_ϕ, characteristic directly related to the standard deviation of the size distribution; K_R, laboratory hydraulic conductivity. Location of sample sites is shown on plate 1E]

Sample No.	$\bar{d}$ (millimeters)	σ_ϕ (phi units)	K_R (gallons per day per square foot)	Upstream distance (thousands of feet)
1	0.58	1.10	1,040	0
2	.99	1.64	1,580	3.15
3	.74	1.60	940	6.20
4	1.40	2.16	1,610	10.25
5	1.13	.96	5,020	17.00
6	1.80	1.55	5,830	21.05
7	2.90	1.88	9,910	24.85
8	3.95	2.10	12,950	24.85

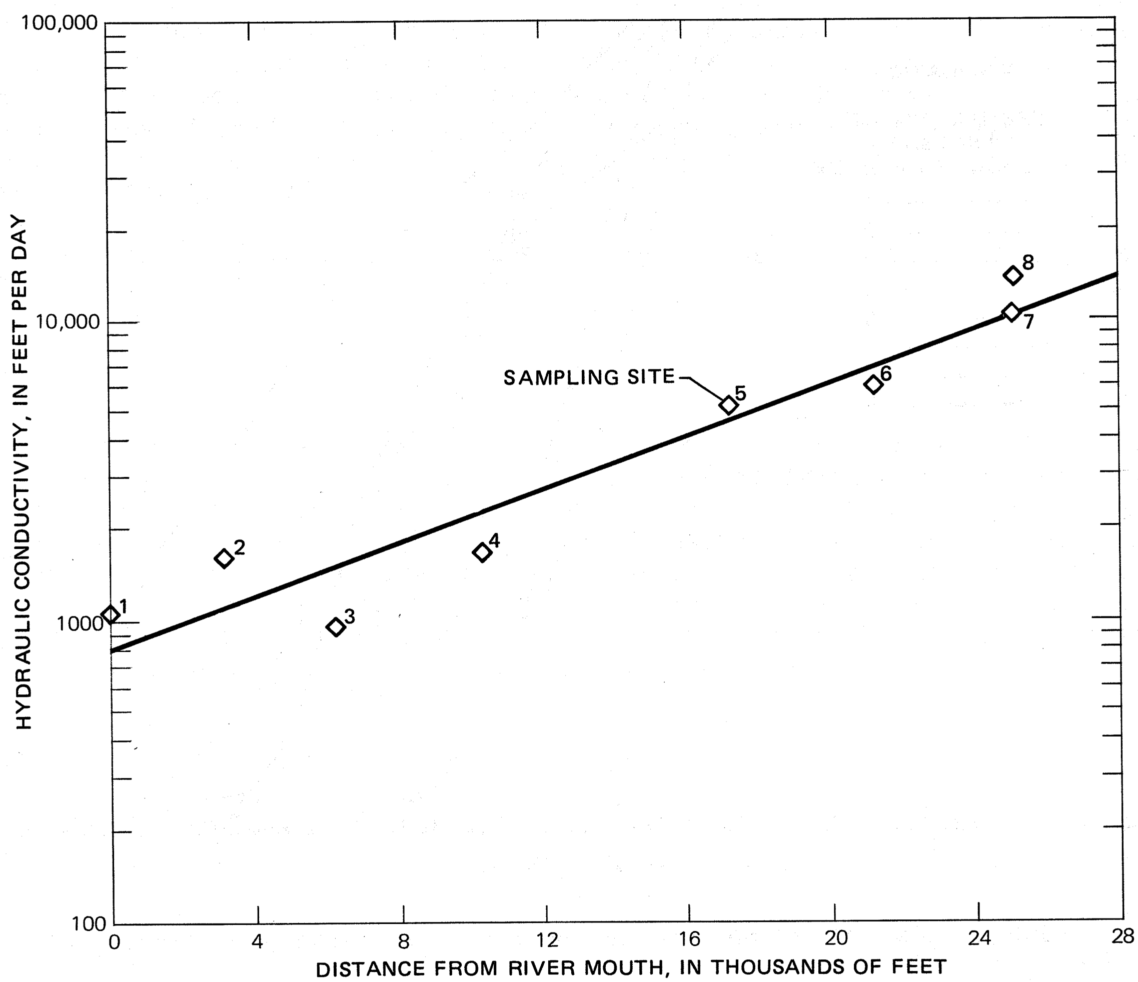

FIGURE 7. — Channel-bed hydraulic conductivity versus upstream distance from mouth of river, computed from the Krumbein-Monk relationship.

Information on the altitude of the channel bed (H_R) was obtained from George Nolte and Associates, San Jose, Calif., who made an evaluation of altitudes throughout the drainage basin using aerial photographs. Altitudes across the drainage basin were determined at more than 300 locations, with distances of several hundred feet between cross sections. These data were used to interpolate channel-bed altitudes for the model at each of the 103 river nodes (fig. 8). This information is currently being used in a flood-insurance study by George Nolte and Associates and is, at this time, (1983) unpublished.

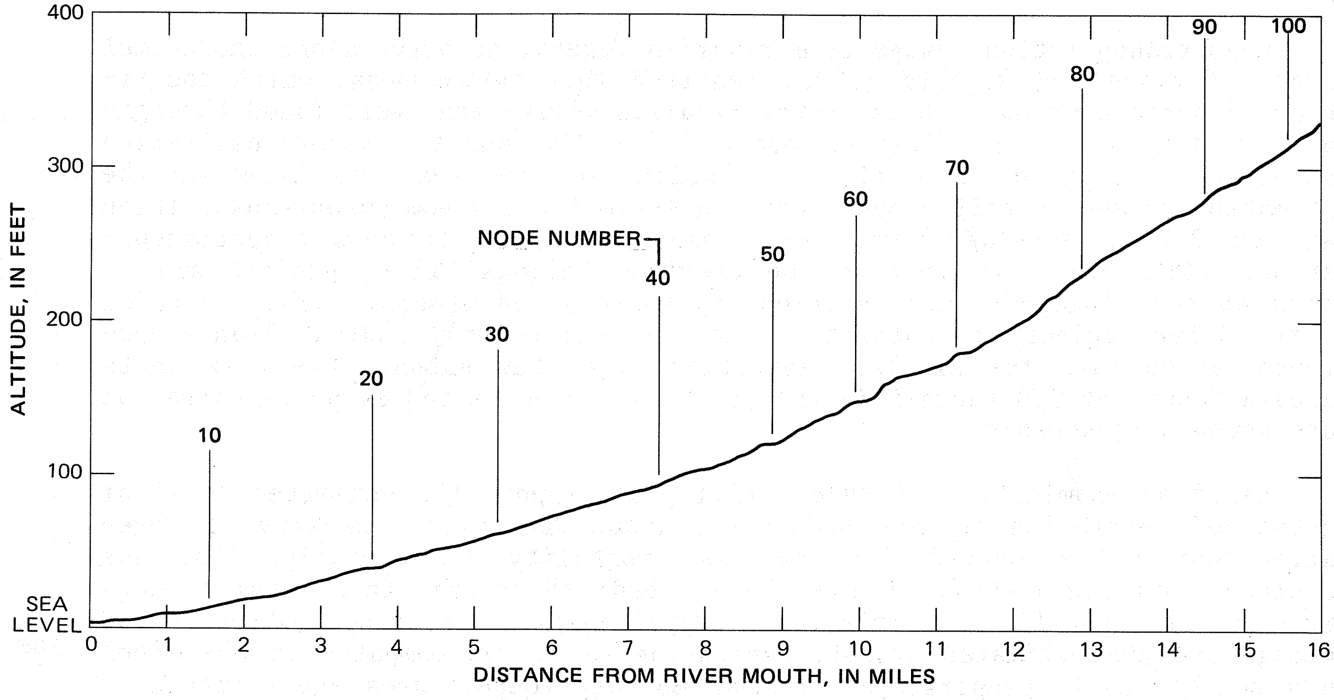

FIGURE 8. – Channel-bed altitude versus upstream river distance, with selected river node numbers for the Carmel River.

Characteristics for the flow-dependent river stage and width components of the leakage equation (a_d, b_d, a_w, and b_w) were derived from the channel geometry. The values thus obtained were a_d=0.3, b_d=0.38, a_w=1.0, and b_w=0.40. The model is not particularly sensitive to these characteristics because of the rapid recovery potential of the aquifer at normal to high riverflows and the relatively large time steps (monthly) used in the model. A more refined model analysis of river leakage would require considerably shorter time steps.

Evapotranspiration Losses

Evapotranspiration loss is the amount of ground water lost through transpiration of plants and evaporation. The rate at which this loss occurs declines from a maximum when the water table is at or near land surface to almost zero as the water table approaches the maximum depth penetrated by roots. Between this maximum depth and the water table there may be a point chosen (depending on the problem) at which the rate is considered insignificant.

Evapotranspiration losses from riparian vegetation occur along the Carmel River. Carlson and Rozelle (1978) reported that cottonwoods, which constituted 85 percent or more of the total riparian vegetation, were found throughout the length of the drainage basin. For the model, evapotranspiration losses were computed by a linear relation to head that was based on the estimated acreage of cottonwood trees, an estimated maximum evapotranspiration rate of 2.7 (acre-ft/acre)/yr, and a depth of 15 ft to zero evapotranspiration. This rate was used in the previous Salinas Valley project and is based on the Blaney-Criddle relationship (Durbin and others, 1978). Studies in the drier regions of southern California (Muir, 1964) indicated an evapotranspiration rate for similar vegetation along San Antonio Creek in Santa Barbara County of 3.0 (acre-ft/acre)/yr; thus the estimated evapotranspiration rate appears reasonable.

Based on examination of 1978 aerial photographs, the estimated total of cottonwood vegetation in the valley was about 200 acres. Density of vegetation was not accounted for, nor was mortality of vegetation that has resulted from degradation of the channel bed; therefore, this total acreage figure may be significantly in error. Evapotranspiration, based on cottonwood acreage and the estimated evapotranspiration rate, was computed in the model on a monthly basis proportional to mean monthly temperatures and altitude of the water table. The monthly distribution of evapotranspiration losses is shown in figure 9, and generated evapotranspiration rates for the entire drainage basin are shown in figure 10. The cycle shown in figure 9 is reflected in figure 10. Maximum evapotranspiration rates were about the same during the 1974-75 predrought years, decreased during the 1976-77 drought, and then increased in 1978, after the drought.

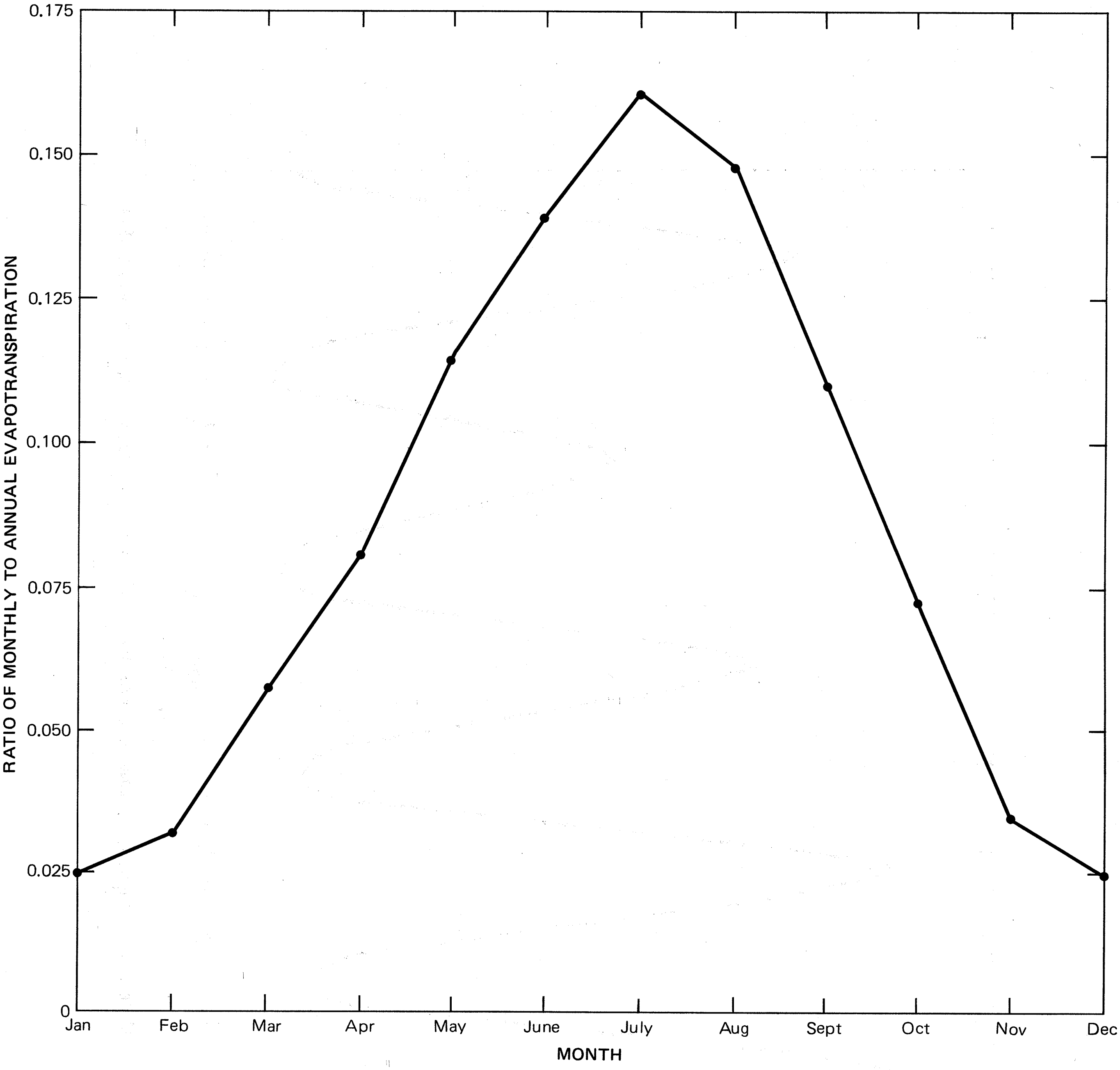

FIGURE 9. – Monthly distribution of phreatophyte evapotranspiration losses used in the digital model.

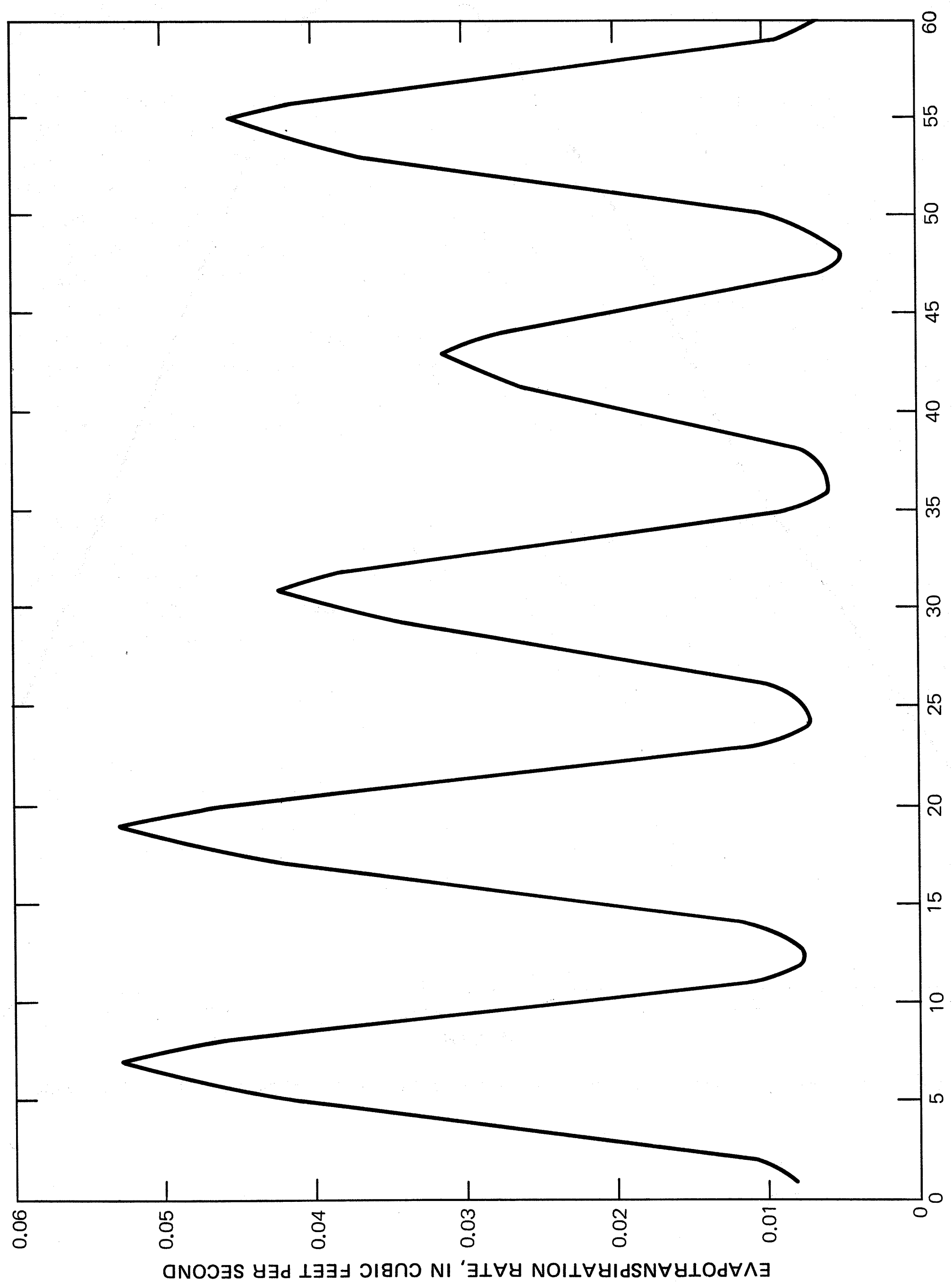

FIGURE 10. — Model computed total evapotranspiration rates for the 60 monthly time steps beginning in January 1974.

Pumpage and Pumpage Return Flow

Pumpage and pumpage return flow were calculated on a monthly basis for 1974 through 1978. For the model, pumpage was subdivided into three categories: municipal, which was tabulated from pumpage records obtained from the California American Water Co. and California Department of Water Resources; agricultural, which includes farmland and golf-course irrigation water estimated on the basis of electrical power use and pump-efficiency factors; and domestic, which includes estimates of pumpage from private wells for domestic use. The annual totals and net percentages for each category are summarized in table 4. During the 5 years, municipal use accounted for 55 percent of the pumpage, agricultural use accounted for 44 percent, and domestic use accounted for 1 percent. Return flows by type are disproportional to the pumpages by type, principally because much of the municipal water is diverted from the drainage basin. From 1974 through 1978 of the total return flow, that from municipal pumpage was 25 percent, that from agricultural pumpage was 72 percent, and that from domestic pumpage was 3 percent. The methods used to compute each total are described below.

TABLE 4. - Annual pumpage and return flow, in acre-feet per year, for 1974-78

Calendar year	Municipal		Agricultural		Domestic		Total	
	Pumpage	Return	Pumpage	Return	Pumpage	Return	Pumpage	Return
1974---------	2,879	259	1,823	601	53	27	4,755	887
1975---------	3,052	294	2,752	908	64	32	5,868	1,234
1976---------	5,772	401	3,280	1,083	89	42	9,141	1,526
1977---------	3,035	157	3,556	1,173	33	14	6,624	1,344
1978---------	3,368	991	2,843	938	119	58	6,330	1,487
Total-----	18,106	1,602	14,254	4,703	358	173	2,718	6,478
Percentage[1]	55.3	24.7	43.6	72.6	1.1	2.7		

[1]Figures represent the percentage of the total 5-year pumpage or return for each type of pumpage.

Municipal Pumpage.--California American Water Co. supplies more than 90 percent of the municipal pumpage. The company's distribution system consists of a single main pipeline that carries ground water as well as water diverted from the San Clemente Reservoir. More than 90 percent of the combined water is exported out of the drainage basin. Monthly meter records of pumpage for individual municipal wells, reservoir diversions, and water piped out of the drainage basin were obtained from California American Water Co. Net monthly deliveries to the drainage basin were calculated by subtracting the quantities diverted from the drainage basin via the pipeline from the sum of pumpage and reservoir diversions supplied to the pipeline. Unpublished monthly pumpage records also were available from Water West Corp., which does not pipe water out of the basin and services a smaller area of Carmel Valley.

Municipal return flow was calculated by first distributing the deliveries throughout the drainage basin according to a service-connection map obtained from the Monterey Peninsula Water Management District. All the drainage basin, except for a small area in the lower part serviced by the Carmel Sanitary District, uses soil-absorption systems. There are approximately 980 unsewered connections out of a total of 1,500 on the valley floor; for the model the monthly deliveries were apportioned equally among the 980 units. Return flow from municipal pumpage was calculated using a net 70 percent of the water supplied from each connection to a soil-absorption system and a net 70 percent of the water leached from each absorption system to the water table (Kennedy Engineers, 1979). Thus, the amount of return flow from municipal deliveries for each unsewered connection, estimated to be 50 percent, was distributed on the basis of unit usage per month.

Agricultural Pumpage.--Agricultural pumpage was calculated from monthly electrical-usage data and pump-efficiency tests obtained from the Pacific Gas and Electric Co. in Monterey. About 20 available pump tests were considered to be representative of the efficiency of the production wells, with energy factors ranging from 100 to 220 kWh/acre-ft. The average from these tests was 150 kWh/acre-ft and, except for the wells that had specific pump tests, the factor of 150 kWh/acre-ft was used to compute pumpage for all agricultural wells that did not have pump-efficiency tests.

Domestic Pumpage.--Domestic pumpage, which accounts for only about 1 percent of total pumpage, was estimated on a unit basis, assuming the same unit usage and return as for the municipal pumpage. There are about 110 domestic wells in the drainage basin.

The agricultural pumpage, the sum of municipal and domestic pumpage, and the total monthly pumpage from the drainage basin during 1974 through 1978 are shown in figure 11. The 1978 distribution of pumpage and recharge in the valley is shown by subsection on plate 1D.

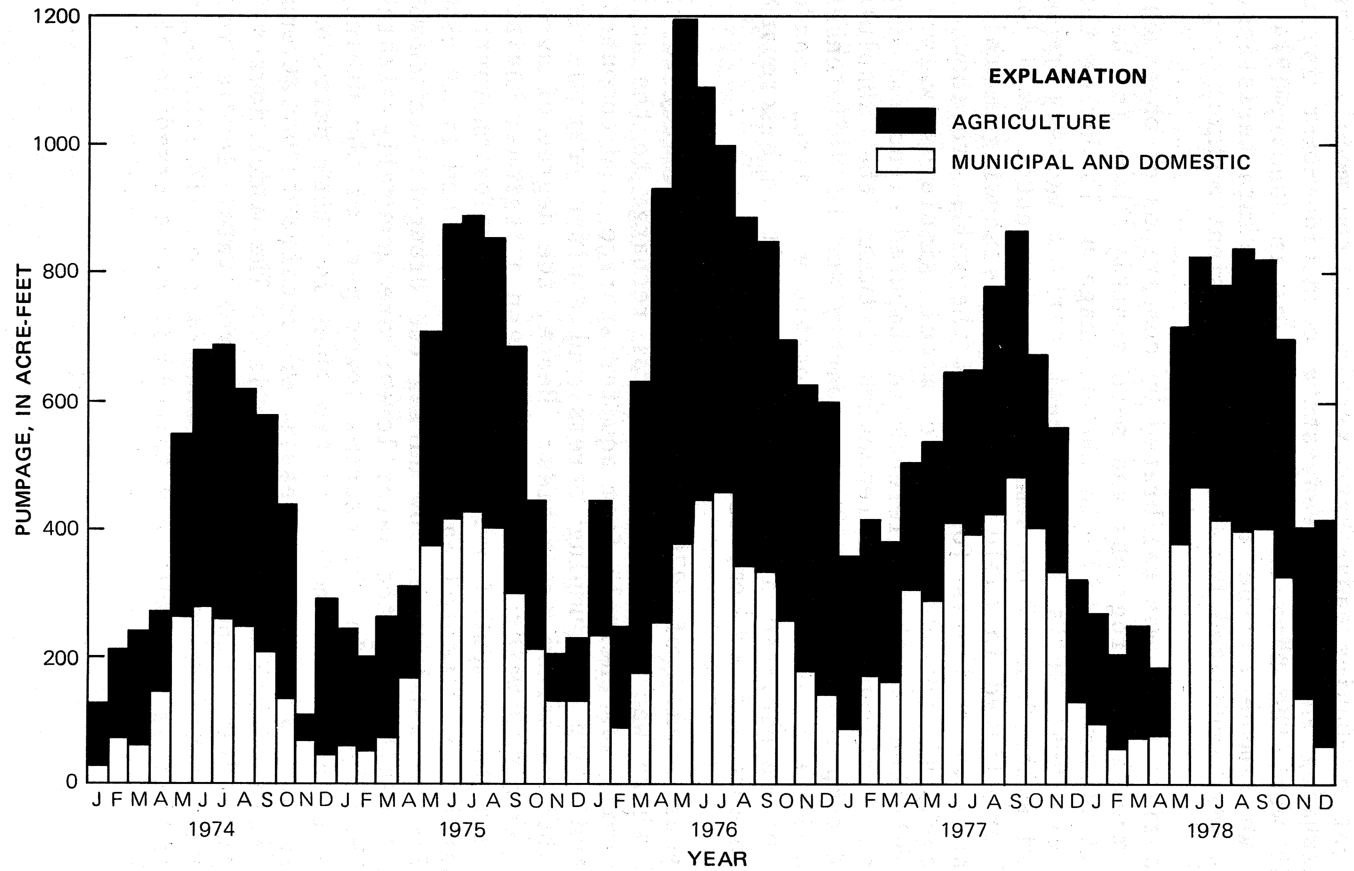

FIGURE 11. – Monthly pumpage from the Carmel Valley drainage basin, 1974 through 1978.

Model Calibration

The model was calibrated for calendar years 1974 through 1978 with monthly time steps and input data discussed in the previous section. During this process, adjustments were made of the aquifer hydraulic conductivity and storage coefficients and the river-channel characteristics. Recharge and discharge data were not changed. The first stage of the calibration involved development of a quasi-steady-state version of the model, using 1974 stress data and assuming an annual steady-state condition--that is, assuming that water levels were the same in January 1975 as in January 1974. Preliminary adjustments were made on the aquifer and river characteristics, and initial water levels were generated for use in the transient model.

The transient model was calibrated by comparison of observed and computed water-level maps and hydrographs and mean monthly flows in the Carmel River. There were 29 observation wells in the drainage basin during the calibration period; 12 of these wells had at least partial monthly records, and the remainder had either annual or semiannual measurements. Well locations shown on plate 1E are listed in table 5. Hydrographs showing monthly measured and model-generated water levels for seven of the wells are shown in figure 12. These hydrographs indicate that the model simulates water-level trends reasonably well because the difference in computed highs and lows agrees with the observed difference. Discrepancies between the absolute values of observed and computed water levels are partly due to differences in altitude between nodal and observation-well locations. Also, inadequate nodal definitions of channel-bed altitudes could result in discrepancies of 5 and 10 ft between observed and computed water levels.

The 2-year drought of 1976-77 provided an opportunity to simulate water levels when there was virtually no natural recharge to the aquifer. During this time pumping was entirely from aquifer storage, and computed water levels were dependent only on pumping stress and aquifer characteristics, not on river or tributary stream properties. Hence, the degree of agreement between observed and computed water levels, at least on a regional basis, is a measure of accuracy for the computed net discharge and aquifer characteristics during drought conditions. Computed water-level contours and field observations for December 1977--the water-level low during the drought--are shown on plate 1E. On a regional basis, computed water levels are generally within 10 ft of the measured water levels. In the extreme lower part of the drainage basin, the observed water levels are more erratic than in other parts of the drainage basin. This may occur as a result of localized variations in aquifer properties due to lenticular silt and clay. The model does not accommodate these irregularities. Computed and observed water levels for April 1978, after the aquifer had recovered, are shown on plate 1E. During this time the computed water levels were always within 13 ft of observed levels.

TABLE 5. - Element and nearest node locations of selected items used in the model

[Elements and nodes are shown on plate 1C]

Item	Elements or range	Nearest node or range
Gaging stations		
Near Carmel----------	142	94
At Robles Del Rio----	704	440
Wells		
16S/1W-13R1----------	58	37
16S/1E-18F2----------	87	54
16S/1E-17L3----------	126	84
16S/1E-22E2----------	228	148
16S/1E-22J1----------	267	167
16S/1E-25B1----------	363	227
16S/2E-32A1----------	548	348
Discharge-recharge subsections[1]		
1-----------------	1-32	1-25
2-----------------	25-72	26-50
3-----------------	65-112	51-75
4-----------------	105-152	76-100
5-----------------	145-192	101-125
6-----------------	185-232	126-150
7-----------------	225-272	151-175
8-----------------	265-312	176-200
9-----------------	305-352	201-225
10-----------------	345-392	226-250
11-----------------	385-432	251-275
12-----------------	425-472	276-300
13-----------------	465-512	301-325
14-----------------	505-552	326-350
15-----------------	545-592	351-375
16-----------------	585-632	376-400
17-----------------	625-672	401-425
18-----------------	665-712	426-450
19-----------------	705-752	451-475
20-----------------	745-792	476-500
21-----------------	785-832	501-525

[1]Subsection boundaries pass through elements and nodes.

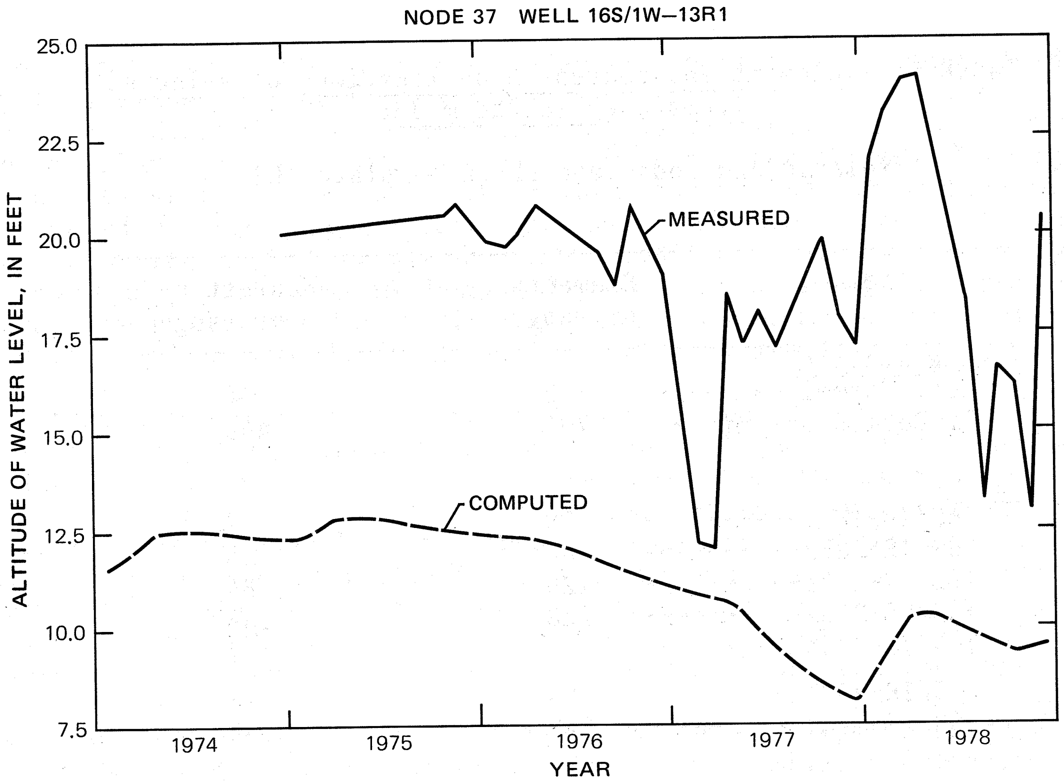

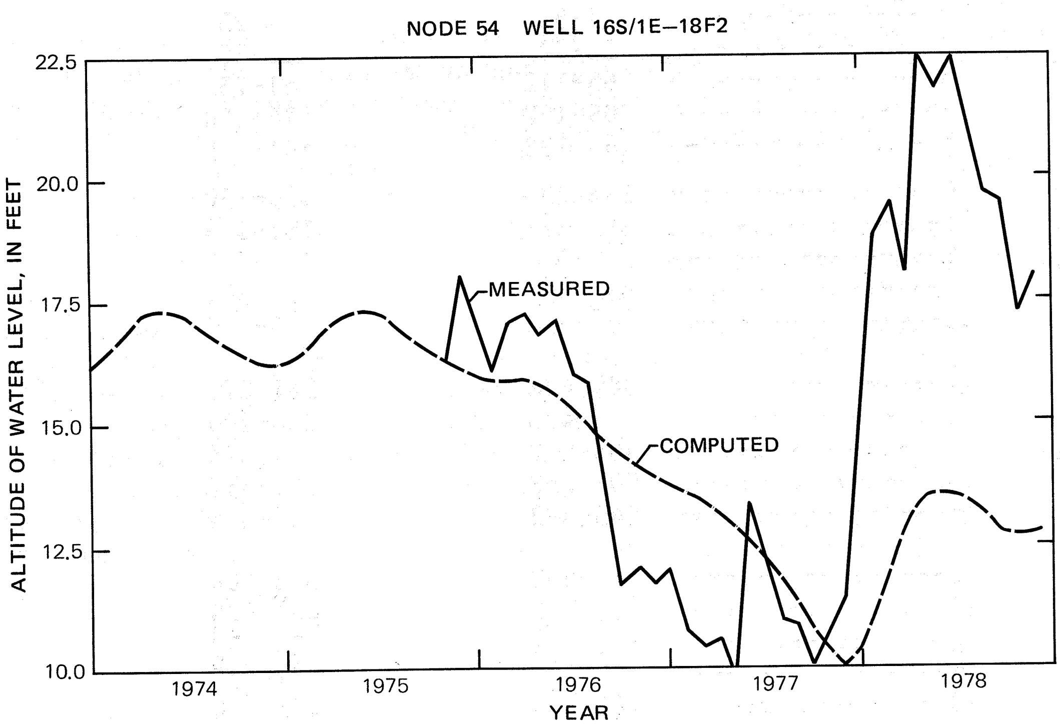

FIGURE 12. – Hydrographs showing monthly measured and model-generated water levels in seven wells in the Carmel Valley drainage basin.

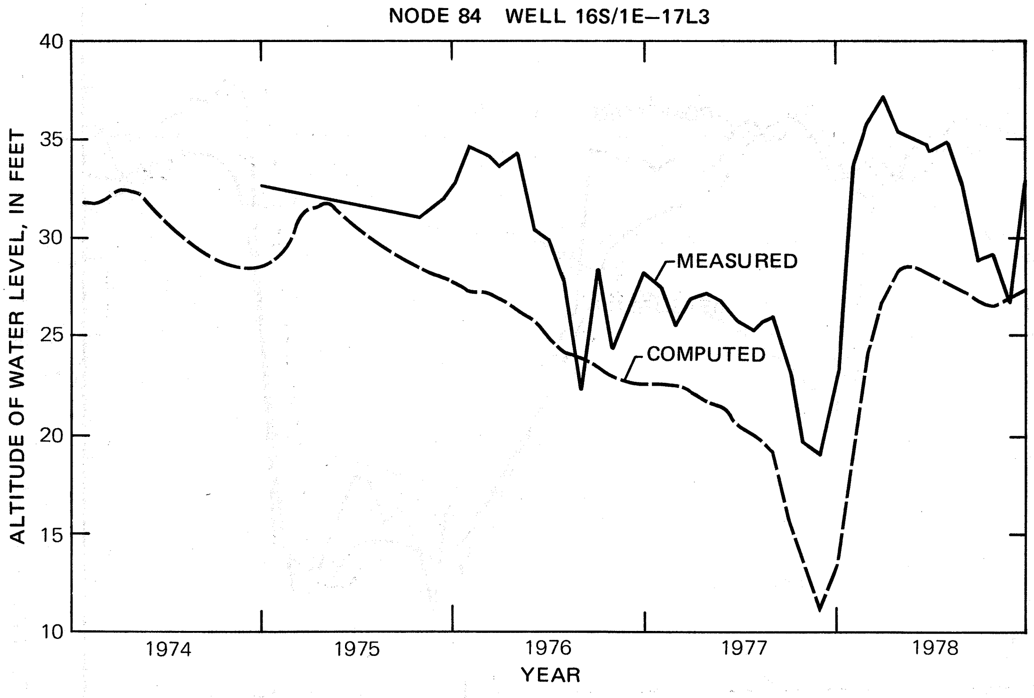

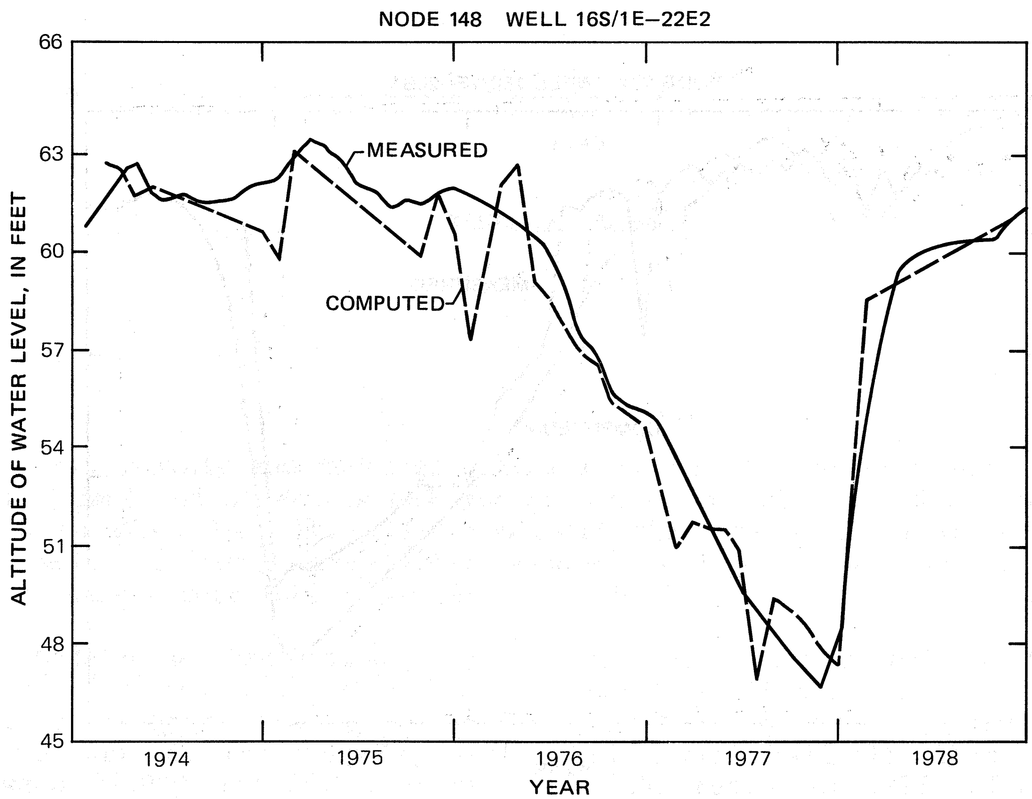

FIGURE 12. – Continued.

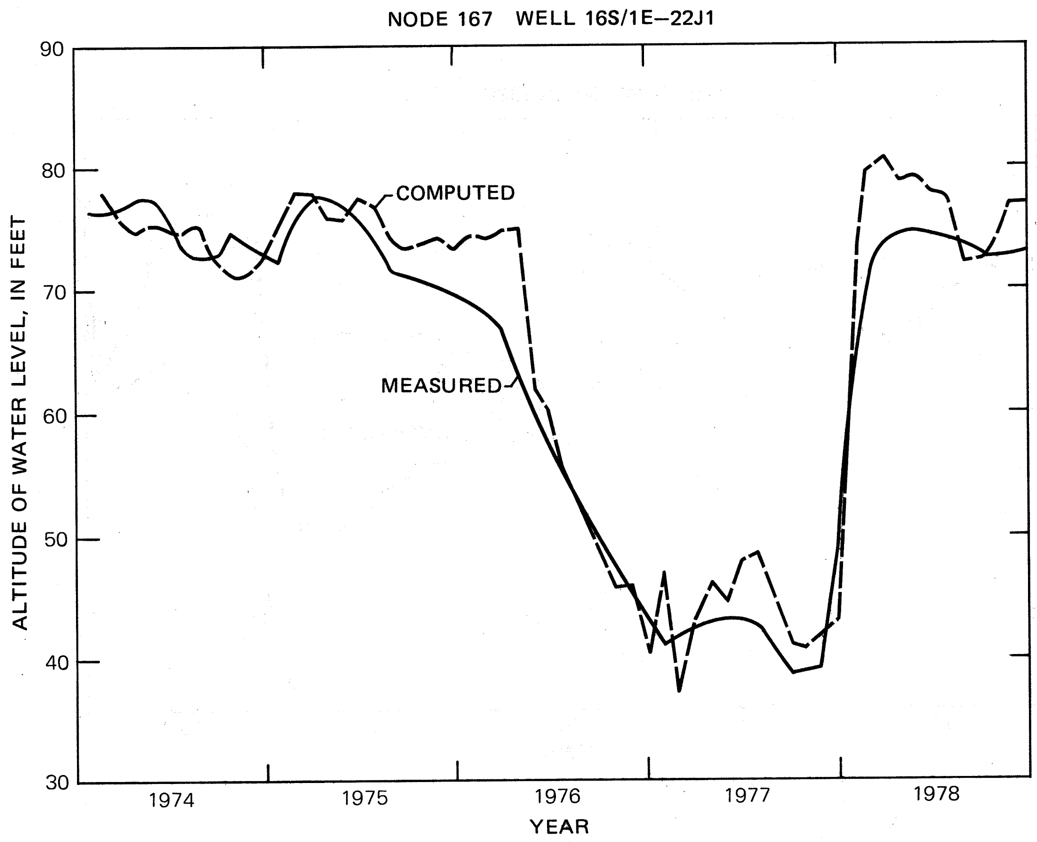

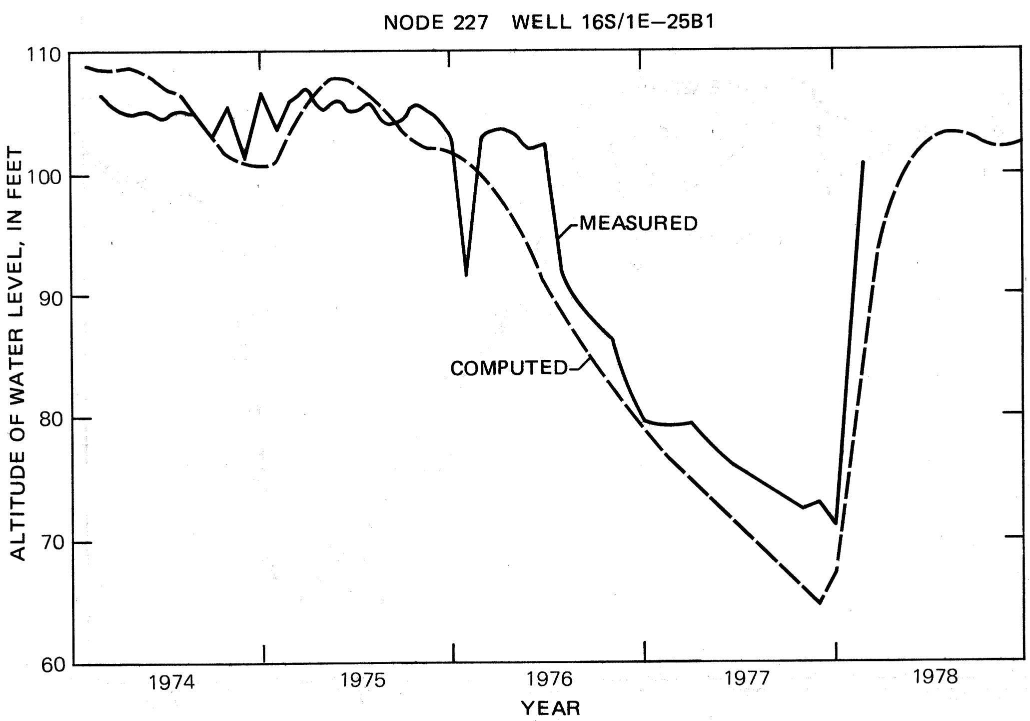

FIGURE 12. – Continued.

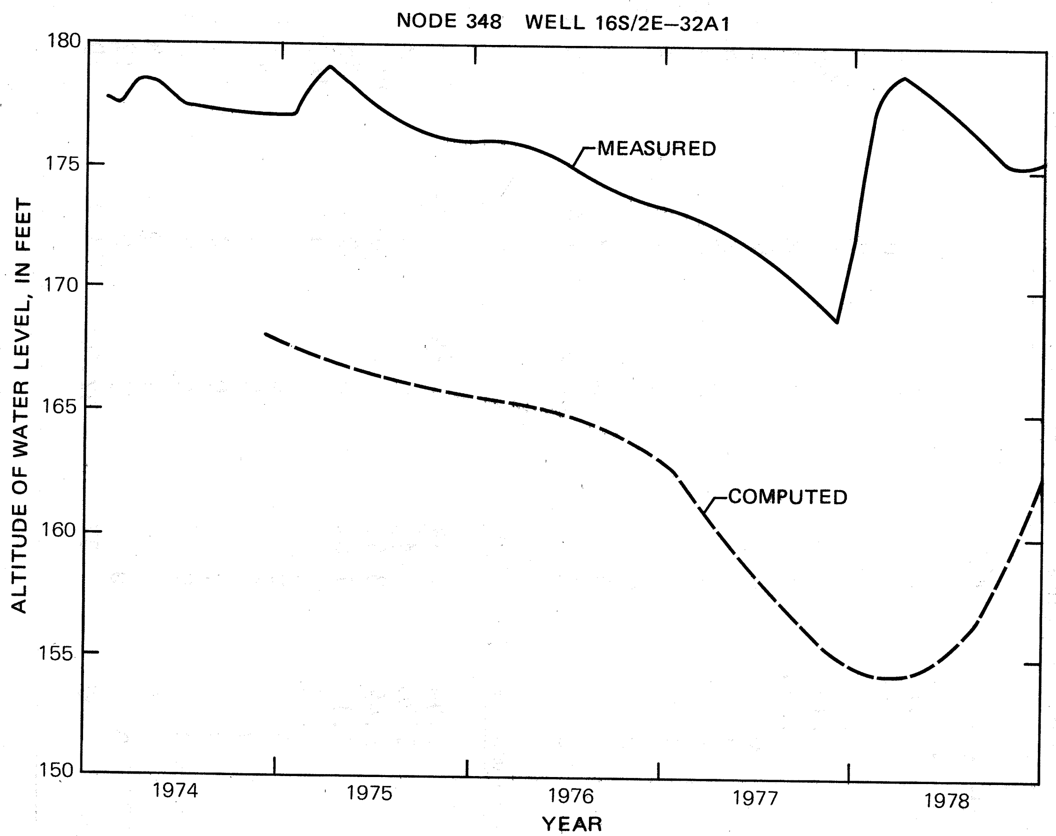

FIGURE 12. – Continued.

Mean monthly and model-generated flows in the Carmel River at the gages near Carmel and at Robles Del Rio are shown in table 6. Gage locations are shown on plate 1A. The table indicates that the model simulates riverflows very well. Differences in flows between the gages for measured and generated values have a correlation coefficient of 0.81.

Model-Generated Results.--In the spring, during normal rainfall years, the model computed a net storage of about 40,000 acre-ft (fig. 13) and an aquifer discharge rate to the ocean of about 215 to 230 acre-ft/yr (fig. 14). In the autumn, the computed storage of normal rainfall years declined to between 37,000 and 38,000 acre-ft. In the autumn of 1977, after a 2-year drought, storage was reduced to 32,000 acre-ft, and the discharge rate decreased to 156 acre-ft/yr. Imposed pumping restrictions lessened the effect of the drought on aquifer conditions. Had the 1976 pumping rates continued through 1977, the quantity of storage probably would have been reduced to less than 30,000 acre-ft and the aquifer discharge rate probably would have decreased to less than 100 acre-ft/yr.

TABLE 6. - Measured and computed flows, in cubic feet per second, in the Carmel River

	1974		1975		1976		1977		1978	
	Measured	Computed	Measured	Computed	Measured	Computed	Measured	Computed	Measured	Computed
Near Carmel (nearest node 94)										
January------	302	292	28.5	24.7	0.37	0	0	0	650	619
February-----	86.4	88.4	534	536	.38	0	0	0	789	855
March--------	479	559	672	674	.58	.26	0	0	698	743
April--------	375	363	233	226	.40	0	0	0	324	325
May----------	70	83.4	98.5	86.7	.044	0	0	0	145	158
June---------	14.7	14.4	23.0	16.6	0	0	0	0	66.1	48.9
July---------	1.97	2.80	2.01	3.53	0	0	0	0	8.81	7.11
August-------	.35	.11	.22	0	0	0	0	0	3.58	1.29
September----	.21	0	.09	0	0	0	0	0	1.79	0
October------	.35	0	.30	0	0	0	0	0	.59	.47
November-----	.56	.10	.41	0	0	0	0	0	3.09	7.71
December-----	5.68	17.8	.50	0	0	0	20.5	2.4	16.4	15.8
At Robles Del Rio (nearest node 440)										
January------	253	258	26.1	26.6	1.44	1.44	0.40	0.21	574	586
February-----	77.6	78.9	465	476	1.36	1.34	0	0	754	771
March--------	479	490	577	591	3.49	3.41	.01	0	647	662
April--------	310	317	194	199	1.11	1.03	0	0	285	292
May----------	72.7	74.2	77.0	78.8	.25	.19	0	0	142	145
June---------	14.7	14.8	17.6	17.9	0	0	0	0	48.0	48.8
July---------	4.10	4.10	5.88	5.95	0	0	0	0	10.4	10.4
August-------	.51	.52	.68	.73	0	0	0	0	4.29	4.29
September----	.22	.23	.45	.50	0	0	0	0	2.15	2.16
October------	.58	.58	.72	.76	.16	.05	0	0	4.14	4.14
November-----	1.48	1.47	1.43	1.46	0	0	0	0	12.7	12.8
December-----	20.4	20.7	1.51	1.53	.02	.07	42.3	41.2	19.8	20.8

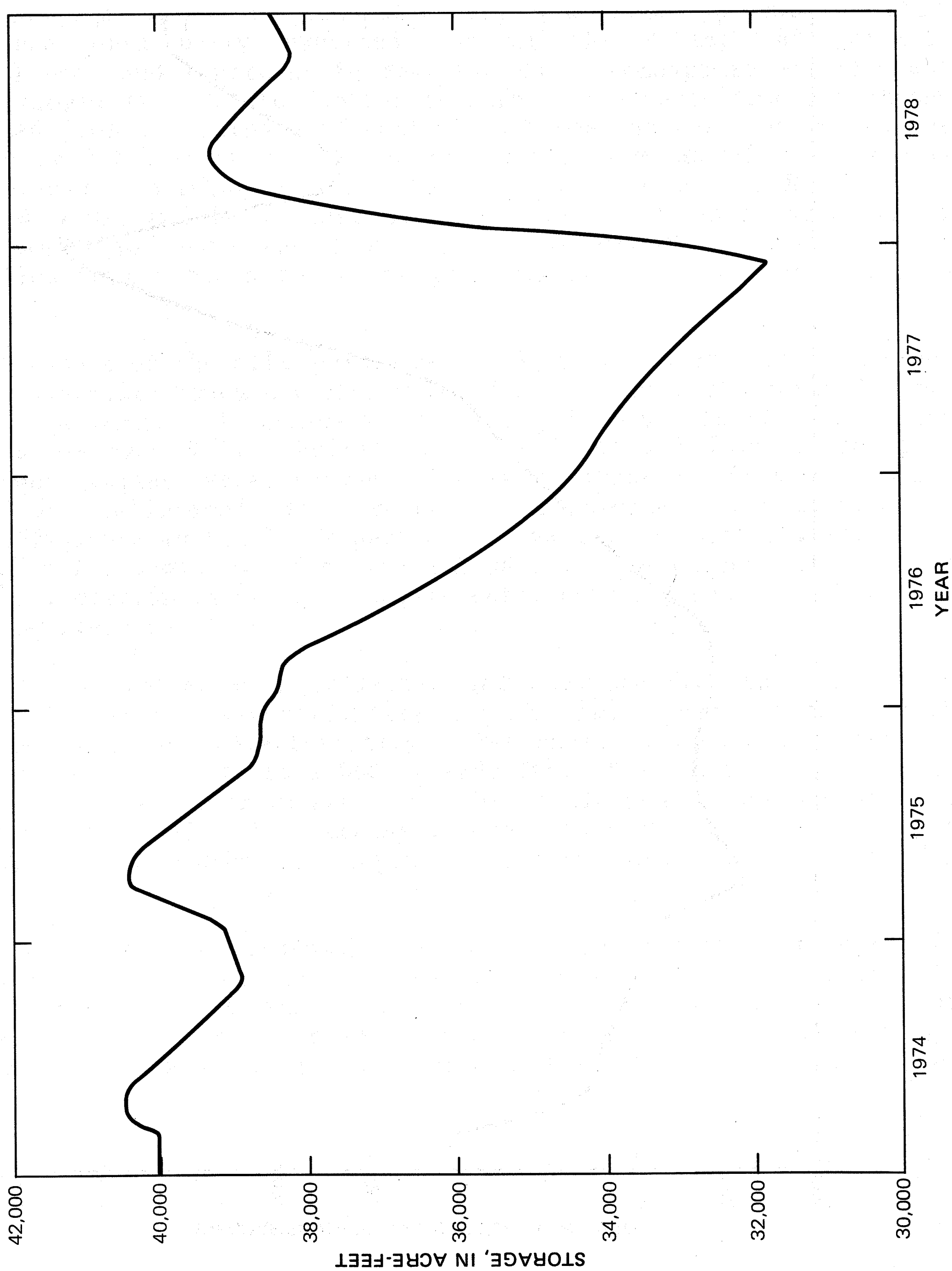

FIGURE 13. — Total aquifer storage in the modeled area.

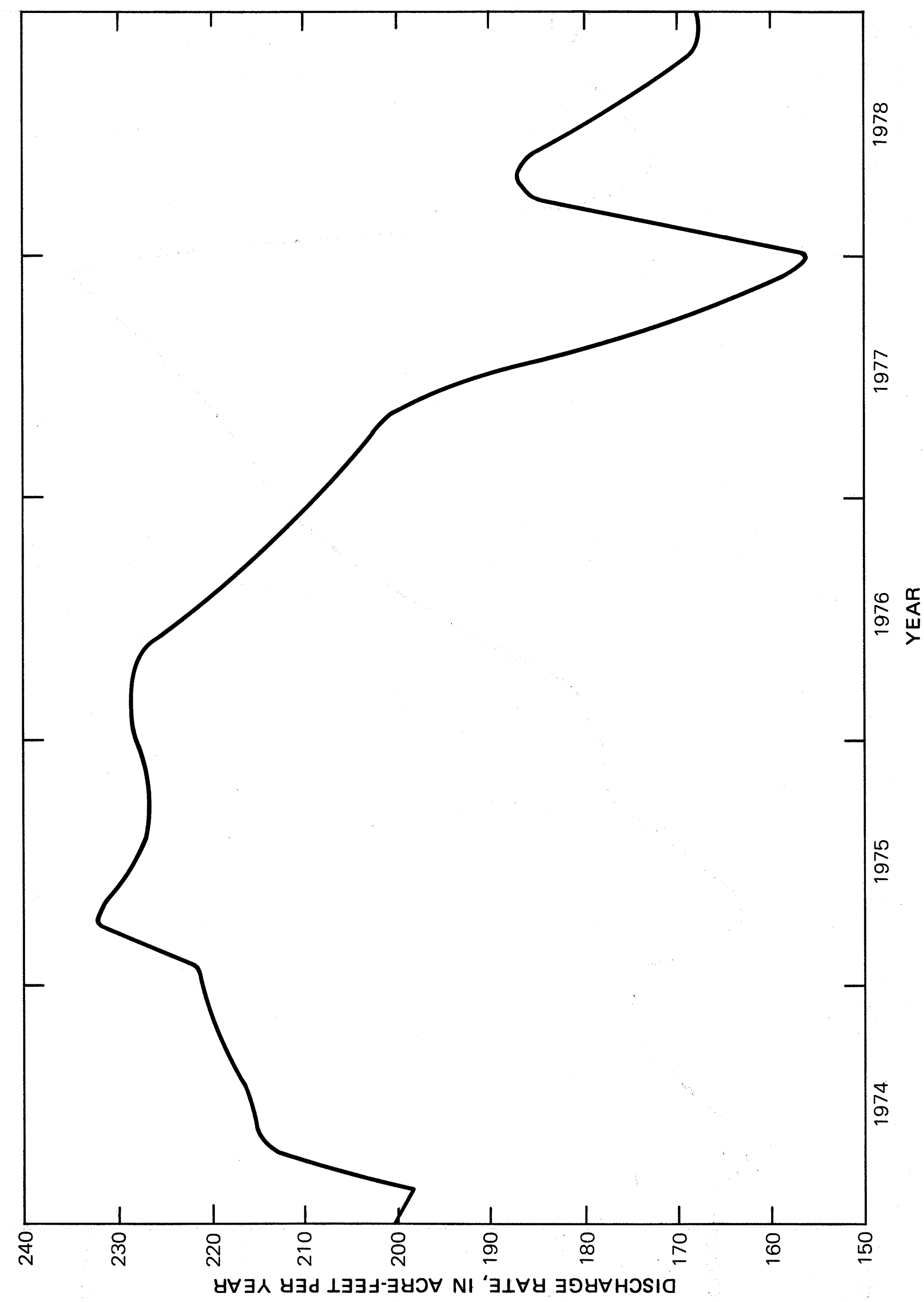

FIGURE 14. — Aquifer discharge to ocean.

SUMMARY AND CONCLUSIONS

Rapid urban growth and droughts cause stress on the ground-water system in the Carmel Valley drainage basin. A two-dimensional, digital, ground-water flow model was developed and calibrated using available data from 1974 through 1978 to provide a better understanding of the geohydrology of the drainage basin, and to identify areas of inadequate data. Pumping rates during those years ranged from 5,900 to 9,100 acre-ft/yr, with 55 percent allotted to municipal use principally exported out of the valley, 44 percent to agricultural use, and 1 percent to domestic use. Pumpage return flow within the valley ranged from 900 to 1,500 acre-ft/yr. Discharge from phreatophytes was estimated from the acreage of cottonwood trees, assuming an evapotranspiration rate of 2.7 acre-ft/yr. Tributary runoff from the 23 major subbasins was calculated by correlation from the gaged inflows at the Robles Del Rio station, and above and below that station from the drainage areas and mean annual precipitation over the subbasins. This calculation indicates that tributary flow to the basin below the gage was about 20 percent of the gaged inflow.

The thickness of the alluvium averages 75 ft and is adequately defined by well logs. Hydraulic conductivities were, for the most part, derived from the calibration process. Transmissivity averaged 5,900 ft^2/d, and storage coefficients averaged 0.19. Hydraulic conductivity and storage coefficients in the lower valley were reduced during calibration from the original estimates. The calibrated model produced lower hydraulic conductivities and storage coefficients in the lower part of the valley and probably reflects the presence of silt, clay, and fine-grained sand in the younger alluvium found there. The reduction in storage coefficients, however, was not indicative of a confined aquifer condition.

Channel-bed samples were collected and analyzed from the lower 5 mi of the river, and hydraulic conductivities for the channel bed were determined on the basis of sediment characteristics. The analysis indicated a downstream decrease from about 10,000 to 1,000 $(gal/d)/ft^2$. These data were used in the model as part of the river-leakage calculation along with aerial-survey data defining altitude of the river channel. Other characteristics, pertaining to flow-dependent flow widths and depths, were estimated and adjusted during calibration.

Model calibration is reasonable except in the extreme lower part of the drainage basin. Discrepancies in this area could result from localized and undefined lenticular silt and clay. On a regional basis, computed water levels were within a few feet of observed levels. Toward the end of the 1976-77 drought, computed water levels were within 13 ft of the measured water levels.

The model is intended principally for simulation of flow conditions using monthly time steps. The data base used to develop this model is adequate for present purposes, but the nonuniqueness of solutions with respect to different sets of data indicates the model does not necessarily validate the correctness of the individual variables. For example, an error in net pumpage could be counterbalanced by an error in the storage coefficients. Possible improvements of the data and the computational algorithm might include:

1. Samples could be collected from small-diameter wells drilled in the lower end of the valley. Drilling would provide knowledge of the distribution of confining sediments and aquifer properties above and below them.
2. Additions could be made in the solution algorithm used for future modeling studies with a more refined data base. The model could account for confinement or partial confinement in the lower end of the valley. The model also might include contributions from the Tularcitos aquifer.

In the process of defining a conceptual model and building and running the mathematical model, it became apparent that the single most important source of recharge to the alluvial ground-water basin is the Carmel River. Not only does the Carmel River with its tributary flows account for most of the recharge to the alluvial aquifer, but its sustained flow into the pumping season helps to moderate the lowering of water levels. The Carmel Valley alluvial aquifer is a river-channel aquifer composed of deposited river sediments; water levels in these river sediments are principally maintained by the altitude of the bottom of the river's present channel when there is riverflow.

Construction of reservoirs upstream from the alluvial valley has removed most of the river's sediment load previously used to build the alluvial aquifer and maintain the altitude of the river channel. Although regulated flow may have made the Carmel River more effective as a recharging source throughout a larger part of the year, the loss of upstream sediment transported to the alluvial valley coupled with the river's removal and man's extraction of sand and gravel from the river channel in the alluvial valley has caused declines in river-channel altitudes. Declines in river-channel altitudes directly cause lower water levels in the alluvial aquifer even if no pumping stress were present. With or without pumping stress, the water table during the dry season can be no higher than the altitude of the adjacent river channel. Consequently some riparian vegetation on adjacent banks or terraces would be partially or completely deprived of water during the dry season.

Superimposed on this hydrogeologic system is a considerable dry-season pumping stress. Given the present river-channel geometry, the model addresses the effects of increased pumping stress throughout a severe drought cycle when the Carmel River ceases to be an effective source of recharge during a 2-year drought. It appears that after severe stressing the aquifer will recover to its natural water level, defined by river-bed altitude, within a month or less of sustained riverflow.

SELECTED REFERENCES

Bear, Jacob, 1972, Dynamics of fluids in porous media: New York, American Elsevier, 764 p.

Bowen, O. E., 1965, Stratigraphic structure and oil possibilities in Monterey and Salinas quadrangles, California, in American Association of Petroleum Geologists: 40th Annual Meeting Pacific Section, Bakersfield, Calif., p. 48-67.

______1969, Geologic map of the Monterey quadrangle, California: California Division of Mines, scale 1:24,000.

California American Water Co., Monterey Peninsula District, 1976, Canada de la Segunda pipeline, and Begonia Iron Removal Plant: Monterey, Calif., Draft environmental impact report, 90 p.

California Department of Water Resources, 1969, Carmel River basin water quality investigation: San Joaquin District, A water-quality investigations memorandum report prepared for the Central Coastal Regional Water Quality Control Board, 46 p.

______1974, Zone 11 Investigation - Carmel Valley and seaside ground water basins, Monterey County: San Joaquin District, 25 p.

______1977, Carmel Valley - thickness of alluvium: San Joaquin District, letter to Monterey County Flood Control and Water Conservation District, December 16, 1977, plates 2A and 2B.

California State Public Utilities Commission, 1974, A summary report of facts, analysis and conclusions relating to the Monterey Peninsula water supply problems: California State Public Utilities Commission Case 9530.

Carlson, F. R., and Rozelle, K. D., 1978, Carmel Valley vegetation study: San Francisco, Calif., CH2M Hill, Inc., Report to the Monterey County Flood Control and Water Conservation District, 52 p.

Carmel Valley Master Plan Study Committee, 1978, Technical analysis planning recommendations for the Carmel Valley Master Plan: Carmel Valley, Calif., 25 p.

Clark, J. C., Dibblee, T. W., Jr., Greene, H. G., and Bowen, O. E., Jr., 1974, Preliminary geologic map of the Monterey and Seaside 7.5-minute quadrangles, Monterey County, California, with emphasis on active faults: U.S. Geological Survey Miscellaneous Field Studies Map MF-577, scale 1:24,000, 2 sheets.

Clayton, C. J., 1978, Zone 11 Monterey County Flood Control and Water Conservation District--Review of studies and reports for supplemental water supply for Zone 11 compiled: various pagination.

Corey, A. T., 1969, Flow in porous media: Fort Collins, Colorado State University, Agricultural Engineering Department Pub. AEP68-69ATC42, 259 p.

Dames and Moore, Consulting Engineers, 1973, Yield of alluvial aquifer in Carmel Valley near Carmel-by-the-Sea, California: Los Angeles, Report to California American Water Co., 37 p.

Davis, S. N., and DeWiest, R. J. M., 1966, Hydrogeology: New York, John Wiley, 463 p.

Dibblee, T. W., 1974, Geologic map of the Jamesburg quadrangle, California: U.S. Geological Survey open-file map, scale 1:62,500.

Durbin, T. J., 1978, Calibration of a mathematical model of the Antelope Valley ground-water basin, California: U.S. Geological Survey Water-Supply Paper 2046, 51 p.

Durbin, T. J., Kapple, G. W., and Freckleton, J. R., 1978, Two-dimensional and three-dimensional digital flow models for the Salinas Valley ground-water basin, California: U.S. Geological Survey Water-Resources Investigations 78-113, 134 p.

Earth Metrics, Inc., Consulting Engineers, 1977, Aquifer recharge case study technical report: Report for the Association of Monterey Bay Area Governments, 68 p.

Esmaili and Associates, Inc., 1978, Nonpoint sources of ground-water pollution in Santa Cruz and Monterey Counties, California: Berkeley, Calif., various pagination.

Fiedler, W. M., 1944, Geology of the Jamesburg quadrangle, Monterey County, California: California Division of Mines Report 40, p. 177-250, pl. 9: Geologic map of the Jamesburg quadrangle, Monterey County, California, scale 1:62,500.

Graham, S. A, 1976, Tertiary sedimentary tectonics of the central Salinian Block of California: Stanford, Calif., Stanford University Geology Department, Doctoral dissertation, 443 p.

Greene, H. G., 1977, Geology of the Monterey Bay Region: U.S. Geological Survey Open-File Report 77-718, 347 p.

Greene, H. G., and Clark, J. C., 1979, Neozene paleogeography of the Monterey Bay Area, California, in Cenezoic paleography of the western United States: Pacific Coast Paleography Symposium, 3d, San Francisco, 1979, 335 p.

Greene, H. G., Lee, W. H., McCulloch, D. S., and Brabb, E. E., 1973, Fault map of the Monterey Bay Region, California: U.S. Geological Survey Miscellaneous Field Studies Map MF-518, scale 1:200,000, 4 sheets.

Greenwood, R., 1978, Water supply for Carmel Valley Master Plan Study Commission: Monterey, Calif., 15 p.

Hood, A. G., 1973, Sanitary engineering investigation of water quality, Carmel River and Carmel Valley ground water, Monterey County, Water Sanitary Section, California State Department of Health: Monterey, Calif., 3 p.

Kennedy Engineers, 1979, Carmel Valley/Highlands study, Carmel Sanitary District areawide facilities plan: San Francisco, Project report, various pagination.

Krumbein, W. C., and Monk, G. D., 1942, Permeability as a function of the size parameters of unconsolidated sand, in Transactions of the American Institute of Mining and Metallurgical Engineers: v. 151, p. 153-163.

Lawson, A. C., 1893, The geology of Carmelo Bay: University of California Publications in Geological Sciences, v. 1, no. 1, p. 1-59.

Lee, E. B., 1978, Background for consideration of expanding water extraction from the Carmel Valley aquifer: Report prepared for Monterey County Board of Supervisors, 6 p.

Monterey County Flood Control and Water Conservation District, 1968-75, Ground water and climatology: Monterey, Calif., annual issue.

Monterey Peninsula Water Management District, 1979, Report to the California Coastal Commission: Monterey, Calif., various pagination.

Muir, K. S., 1964, Geology and ground water of San Antonio Creek Valley, Santa Barbara County, California: U.S. Geological Survey Water-Supply Paper 1664, 53 p.

Neill Engineers and Hahn, Wise and Associates, Inc., Consulting Engineers, 1969, Public service and facilities element of the General Plan -- Carmel Valley-Carmel Highlands study area: Carmel, Calif., various pagination.

Pinder, G. F., and Frind, E. O., 1972, Application of Galerkin's procedure to aquifer analysis: Water Resources Research, v. 8, no. 1, p. 108-120.

Planning Collaborative, Inc., Consulting Engineers, 1978, Recommended management guidelines--Aquifer recharge protection, AMBAG 208 Program: Report for the Association of Monterey Bay Area Governments, 26 p.

Rantz, S. E., 1969, Mean annual precipitation in the California region: U.S. Geological Survey open-file map, scale 1:1,000,000.

Simpson, J. P., III, 1972, The geology of Carmel Bay, California: Monterey, Calif., Naval Postgraduate School thesis, 74 p.

Thorup, R. R., 1976, Ground-water study of the Carmel Valley Ranch and Carmel River watershed, Monterey Peninsula, Monterey County, California: Monterey, Calif., Consultant's report for the Monterey County Planning Commission hearing on Carmel Valley Ranch, March 31, 1976, 24 p.

______1979, Ground-water report on the Carmel Valley Ranch and Carmel River watershed, Monterey County, California: Monterey, Calif., Consultant's report for the Carmel Valley Ranch, 22 p.

Trask, P. D., 1926, Geology of Point Sur quadrangle, California: University of California Publications in Geological Sciences, v. 16, M.S. thesis, 74 p.

U.S. Army Corps of Engineers, 1977, Carmel River, Monterey County, California, Progress report for water resources development: Monterey, Calif., various pagination.

______1979, Feasibility report for water resources development for Carmel River, Monterey County, California: Monterey, Calif., 111 p.

U.S. Department of Agriculture, 1977, Soil survey of Monterey County: Monterey, Calif., Soil Conservation Service, 90 p.

Waananen, A. O., and Crippen, J. R., 1977, Magnitude and frequency of floods in California: U.S. Geological Survey Water-Resources Investigations 77-21, 96 p.

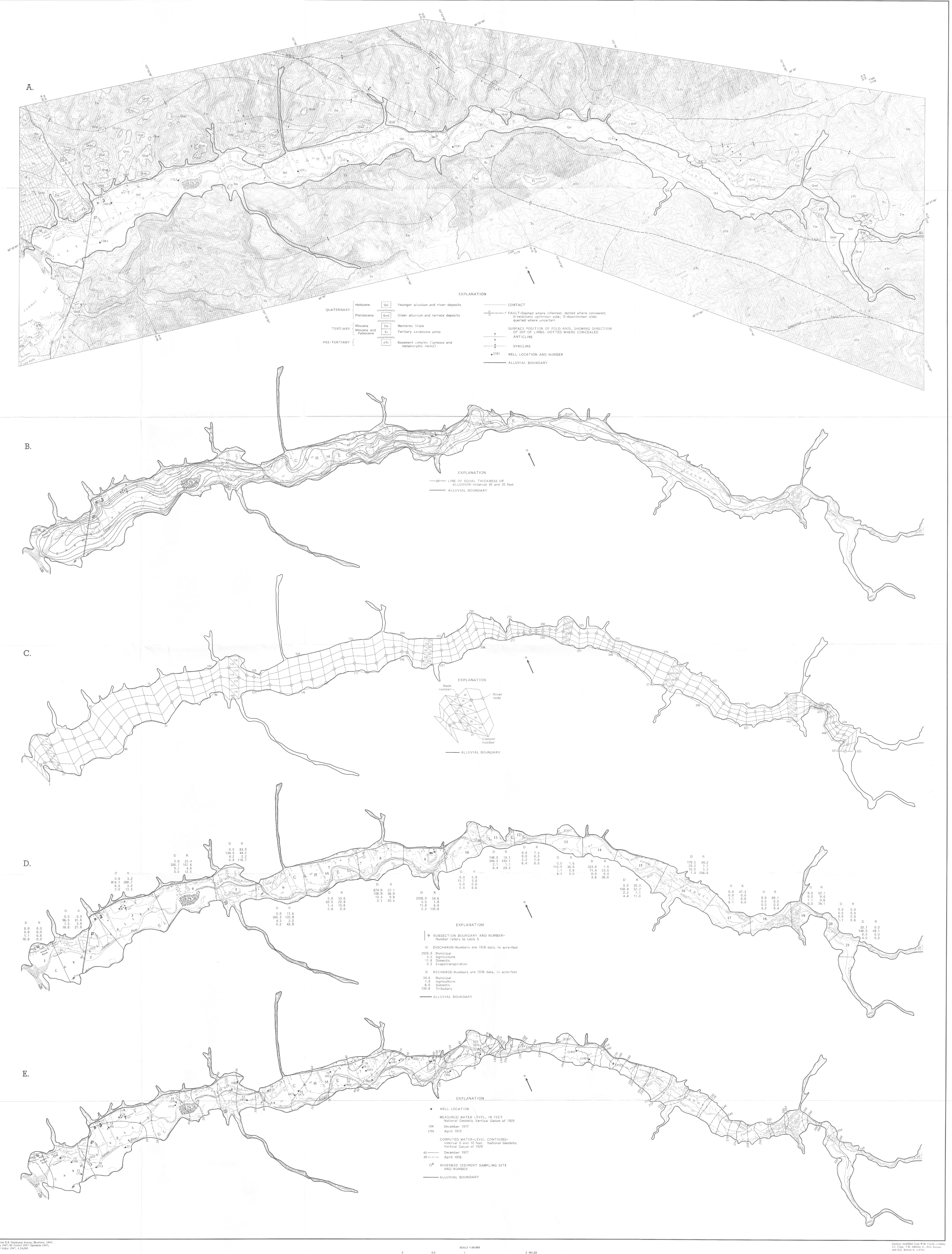

Base from U.S. Geological Survey, Monterey, 1947; Seaside 1947; Mt Carmel 1947; Spreckels 1947; Carmel Valley 1947, 1:24,000

SCALE 1:24,000
0 0.5 1 2 MILES
0 0.5 1 2 3 KILOMETERS
CONTOUR INTERVAL 20 AND 40 FEET
NATIONAL GEODETIC VERTICAL DATUM OF 1929

Geology modified from W.M. Fiedler (1944); J.C. Clark, T.W. Dibblee Jr., H.G. Greene and O.E. Bowen Jr. (1974)

MAP SHOWING SIMPLIFIED GEOLOGY, THICKNESS OF ALLUVIUM, NODES AND ELEMENTS, DISCHARGE AND RECHARGE DISTRIBUTION, AND COMPUTED AND MEASURED WATER LEVELS FOR CARMEL VALLEY, MONTEREY COUNTY, CALIFORNIA